

2nd ANSA & μETA INTERNATIONAL CONGRESS

June 14-15, 2007

Olympic Convention Center
Porto Carras Grand Resort Hotel
Sithonia, Halkidiki, Greece

Proceedings





2nd ANSA & μETA International Congress

June 14-15, 2007

Olympic Convention Center

Porto Carras Grand Resort Hotel

Sithonia, Halkidiki, Greece

Proceedings

Contents

Proceedings	7
Session H2.1	9
Building discipline specific FE-models based on the "Common Model" concept	9
G. Nikolaidis [▲] , D. Zafeiropoulos [▲] , Konstantinos Ntamagkas BETA CAE Systems S.A., Greece	
Structural FE-model of thin adhesive layers well suited for implicit and explicit analyses	27
T. Brandt ¹ , H. Friese ¹ , B. Heydt ^{2▲} , Dr. U. Hindenlang ¹ ¹ LASSO Ingenieurgesellschaft mbH, Germany, ² METABOWERKE GmbH, Germany	
Session H2.2	29
Capturing the best practices for the organization and analysis of crash-test simulation load-cases	29
I. Makropoulou [▲] , K. Kiouptsidis, K. Skolarikis BETA CAE Systems S.A., Greece	
Crashworthiness design of ANSALDOBREDA light metro vehicle	49
L. Lenzi [▲] , S. Raiti AnsaldoBreda S.p.A., Italy	
A CAE tool for processes optimization according to FMVSS201U	59
P. Williamson ^{1▲} , L. Rorris ² ¹ P+Z Engineering GmbH, Germany, ² BETA CAE Systems S.A., Greece	
Session H3.2	67
Automated build-up and analysis of NVH models with ANSA/μETA package	67
V. Pavlidis [▲] , M. Tryfonidis [▲] BETA CAE Systems S.A., Greece	
δYNAMIS: A new solver for linear and nonlinear finite element models	85
D. Giagopoulos ¹ , Prof. S. Natsiavas ^{2▲} ¹ DYNAMical Systems TechnologY, Greece, ² Aristotle University, Greece	
Automated process deployment for NASTRAN SOL200 optimization analysis, using ANSA/ μETA package	97
G. Korbetis [▲] , K. Marmaras BETA CAE Systems S.A., Greece	

An efficient re-analysis methodology for optimization of large-scale vibration systems 107Z. Mourelatos¹▲, E. Nikolaidis²¹Oakland University, Rochester MI, USA, ²The University of Toledo OH, USA**Session H2.3** 121**Case study on the FE-model and geometry morphing in Structural Analysis** 121

G. Panagos, Dr.-Ing. N. Drivakos▲

BETA CAE Systems S.A., Greece

Applications of shape optimization with LS-OPT and ANSA 135¹Heiner Müllerschön¹, ¹Marko Thiele, ²Wolfram Mühlhuber, ²Uwe Gerlinger¹DYNAmore GmbH, Germany, ²AUDI AG, Germany**Analysis of component joints in Finite-Element models of car bodies** 149

Dr.-Ing. H. Wüstenberg▲

Volkswagen AG, Germany

Session H2.5 153**Overview on optimization methods** 153

I. Nitsopoulos▲, B. Lauber

FE-DESIGN GmbH, Germany

Optimization of a vehicle front part structure at AUDI using ANSA morphing and Optimus 159M. Kaufmann¹, B. Lauber²▲, Dr. C. Katzenschwanz²¹AUDI AG, Germany, ²FE-DESIGN GmbH, Germany**A new approach for the preprocessing of TOSCA optimization tasks in ANSA** 169¹Lauber, Boris▲, ²Korbetis, George, ²Marmaras, Dinos,¹FE-DESIGN GmbH, Germany, ²BETA CAE Systems S.A., Greece**Session H3.5** 177**ANSA for CFD - overview and outlook** 177

M. Lanfrit▲, T. Lehnhäuser

ANSYS Central & Eastern Europe - FLUENT Deutschland GmbH, Germany

Combining quality, performance & efficiency in CFD pre-processing 197

E. Skaperdas▲, C. Kolovos

BETA CAE Systems S.A., Greece

Automatic optimization of automotive designs using Mesh Morphing and CFD 217F. Campos¹▲, P. Gerenia², E. Skaperdas³¹ICON, United Kingdom, ²ESTECO, United Kingdom, ³BETA CAE Systems S.A., Greece

Session H2.6	229
Definition and parameterization of a process workflow, applied on modeling for ABAQUS	229
Dr.-Ing. S. Seitani [▲] , M. Giannakidis BETA CAE Systems S.A., Greece	
Using submodeling technique to understand passivation cracks in microelectronic devices - Preprocessing with ANSA	241
Dr. E. Barti [▲] , Dr. M. Stecher ² ¹ SIEMENS AG, Germany, ² Infineon Technologies AG, Germany	
Crack propagation in various 3-D shell structures, application of special software-tool using ANSA/μETA with standard ABAQUS solver	257
D. Dreissig, B. Weisser [▲] , Dr. U. Hindenlang LASSO Ingenieurgesellschaft mbH, Germany	
Orthotropic material of bones generated by means of clinical CT-data, applied to FE models for the nonlinear simulation of one-leg stand with pelvis, femur and lower leg	259
R. Schneider ^{1▲} , P. Helwig ² , G. Faust ³ , Dr. U. Hindenlang ¹ ¹ LASSO Ingenieurgesellschaft mbH, Germany, ² University of Freiburg, Germany, ³ University of Stuttgart, Germany	
Session H3.6	261
Prediction of e-coat voids and puddles during automotive painting using ANSA	261
P. D. Hanumalagutti ¹ , Y.-N. Liu ¹ , R. Mothukuri ^{2▲} ¹ Research and Advanced Engineering, Ford Motor Company, USA, ² BETA CAE Systems USA Inc., USA	
Usage of ANSA's automated volume meshing-methods in the rapid product development process of diesel engines	269
G. Pessi [▲] , Dr. R. Ehart, G. Bumberger BMW Motoren GmbH, Austria	
Pre-processing of lighting heat analysis at Visteon-Autopal	279
T. Havlik [▲] , R. Malucha VISTEON-AUTOPAL s.r.o, Czech Republic	
Thermal judder on drum brakes due to mounted radial run out	285
D. Suryatama [▲] , R. P. Uhlig, S. Vallurupalli, R. M. Lundgren, F. J. Zweng DaimlerChrysler NA, USA	
Session H2.7	297
The development of the 2007 formula SAE by the ART-7 team	297
D. Perperidis [▲] Prepared by the ART-7 team members	

2nd ANSA & μETA International Congress

June 14-15, 2007 Olympic Convention Center, Porto Carras Grand Resort Hotel, Halkidiki Greece

Proceedings

Session H2.1

BUILDING DISCIPLINE SPECIFIC FE-MODELS WITH THE COMMON MODEL CONCEPT

George Nikolaidis*, Dimitrios Zafeiropoulos*, Konstantinos Ntamagkas
BETA CAE SYSTEMS S.A., Greece

KEYWORDS - FE Simulations, Discipline Models, Data Management, Batch Mesh, Representation Manager, CAE process workflow

ABSTRACT - The research and development in the automotive industry is faced with a continuously increasing number of FE simulations. Almost 75% of the total time required for the model building of a vehicle for 5 different disciplines, is spent until the engineer is able to apply all kinds of load cases to the analysis model. Therefore, the big challenge is to establish a pre processing workflow, which ensures that the different kind of requirements are met by these models, with a high reliability and reduced time and cost effort.

This paper presents the Common Model concept, introduced by BETA CAE Systems S.A towards the creation of Discipline Models starting from CAD data. A centralized Data Management system is proposed, to store, retrieve and provide engineers with all necessary data for the generation of the different models requested. The combined use of a Batch Mesh and Representation Managers will fully exploit the storing advantages of the proposed Data Management structure, keeping the overall CAE process cost efficient and error proof.

TECHNICAL PAPER -

1. BUILDING THE DISCIPLINE MODELS

1.1. Introduction to the CAE process workflow

The recent advances in parametric design and new CAD tools that have been introduced helped CAD departments not only to improve design work, but also to greatly reduce the amount of time required to produce large number of vehicle variations. Thus, it has been made equally important that the CAE engineering teams are equipped with the appropriate toolkit to deal with the increased number of model versions and load cases that should be analysed in an error proof, time and cost efficient way.

The basic concept on which the proposed way of dealing with the increased CAE work load is based, is that the creation of all Discipline Models that are to be analysed by the specified solver afterwards, depends on a pure geometric form of the model under consideration. The latter, also referred to as the Common Model, will have the correct Engineering data applied, such as Material and Property Thickness, as well as the welding information between parts. As soon as the CM has been freed of all possible design errors, it is ready to be meshed based on different scenarios in order for the requested Discipline Models to be produced.

All requests are passed through the Representation Manager, which will, in turn, coordinate the Batch Meshing process. The resulting model can be considered as the Discipline specific Common Model, which will serve as the starting point for all the appropriate load cases to be applied. The final analysis models are then sent to the specified solver for further analysis. As depicted in figure 1, the procedure proposed, is highly supervised by an integrated workflow manager, a tool where all the individual tasks of the development of a vehicle simulation model are included.

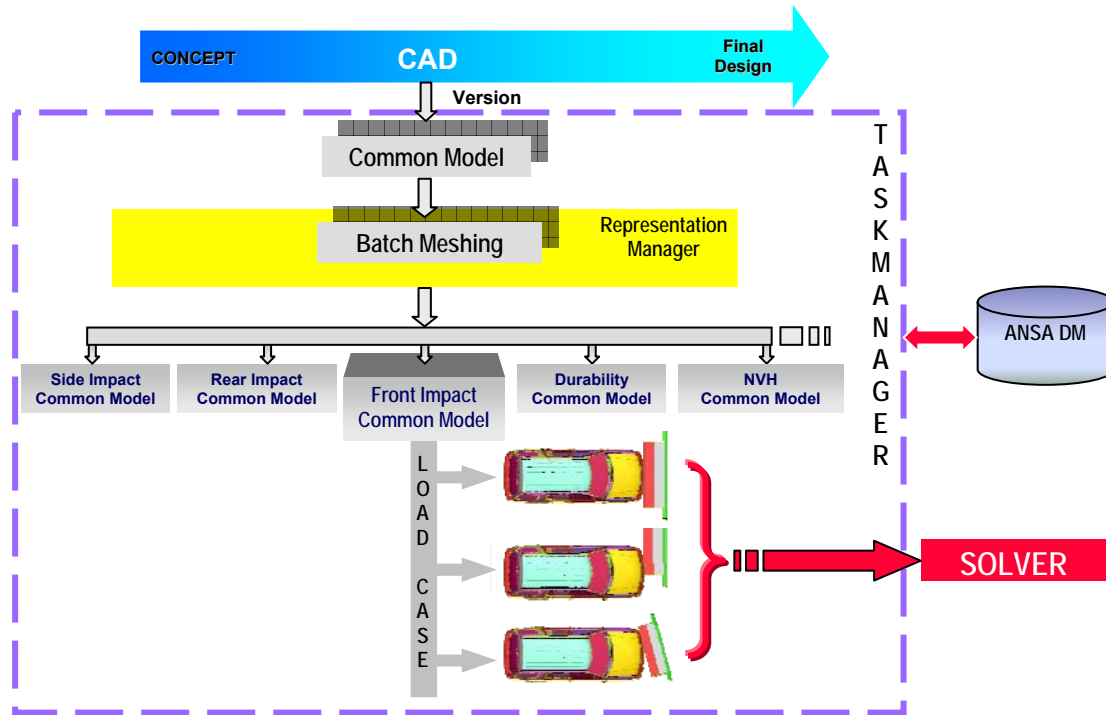


Figure 1

To facilitate and precipitate the CAE analysis, the Task Manager is in constant communication with a centralised data management system called ANSA DM, used to store, retrieve and monitor model components for potential CAD updates (1). The previously described procedure, assures that all CAD engineers work on the same and up-to-date components, the whole process workflow is error-proof and highly automated and that no time is wasted on performing the same tasks twice. The complete process as well as ANSA DM and the different parts of the Task Manager are described in more detail in the paragraphs to follow.

1.2. ANSA Data Management (ANSA DM)

ANSA DM is a structured and centralized Data Management System. It assures that all engineering data, which are used during the building process of a vehicle simulation model, are securely stored and can be retrieved at any time by all CAE engineers, working on various fields of development, (2). Typical data residing in DM are:

- The individual sub-systems, such as seats/dummies, walls/barriers, in their FE representations.
- Library items, such as connectors, boundary conditions and output requests.
- Files containing engineering, connection and trim data.
- Load cases, such as Front, Side and Pedestrian impacts.
- Material data and
- A number of different custom items.

In the case of Part and the Subassembly Data, information is organised in a structured way, corresponding to the output format of the CAD departments. Different CAD versions are stored in such a way, so as to follow the release sequence of the designing departments, (3). At the beginning, each version contains the part's pure geometric description, as produced in the design phase of the vehicle development, also known as the part's Common Representation (CM). The latter will be the basis for the creation of all Discipline dependant mesh variations, which in turn will be used for the production of all requested Reduced FE Representations, such as Lumped Mass or Trim.

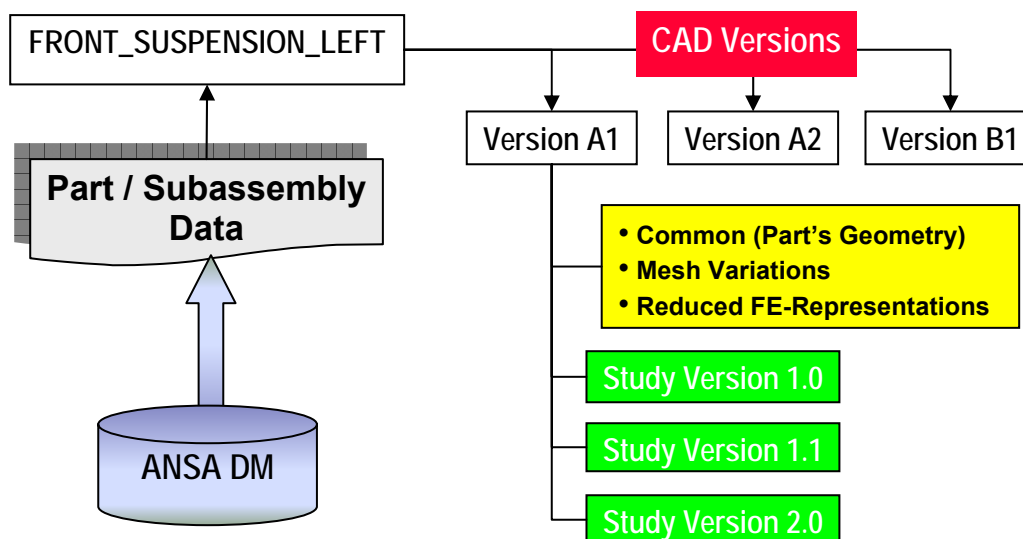


Figure 2

The first FE representation files to be produced in this way can be considered to form the First Study Version of each part. The Optimization Process uses the first Study Version as starting point. All other representation models that are to be developed constitute optimized variations of the first study version. They will thus be stored accordingly as later study versions of the same part, as depicted in figure 2 above. Once saved in ANSA DM all part versions and study versions are available to engineering teams for reference and further optimisation. Through DM, CAD version changes are effectively monitored, while CAE teams are notified the moment component updates are available, thus greatly facilitating all optimization work.

1.3. Building the Common Model

The designing output of the CAD department constitutes the model's pure geometric form. In order for the CAE engineers to begin working on it, this form must first undergo a certain translation process, which will lead to the production of the Common Representation, as previously mentioned.

The first action to be performed is the Definition of the Model as described in the VPM tree, a file exported by the CAD system and handled over to the CAE department. The VPM Tree Editor, (figure 3), will not only distinguish all different parts but also recognise the Symmetry and the Multi-Instantiated ones, as parts being at different locations. Translated parts that have already been saved in ANSA DM are also recognized. As a result, from the group of parts forming the model, only the newly added ones are exported to a Download List (D/L-list) to be translated.

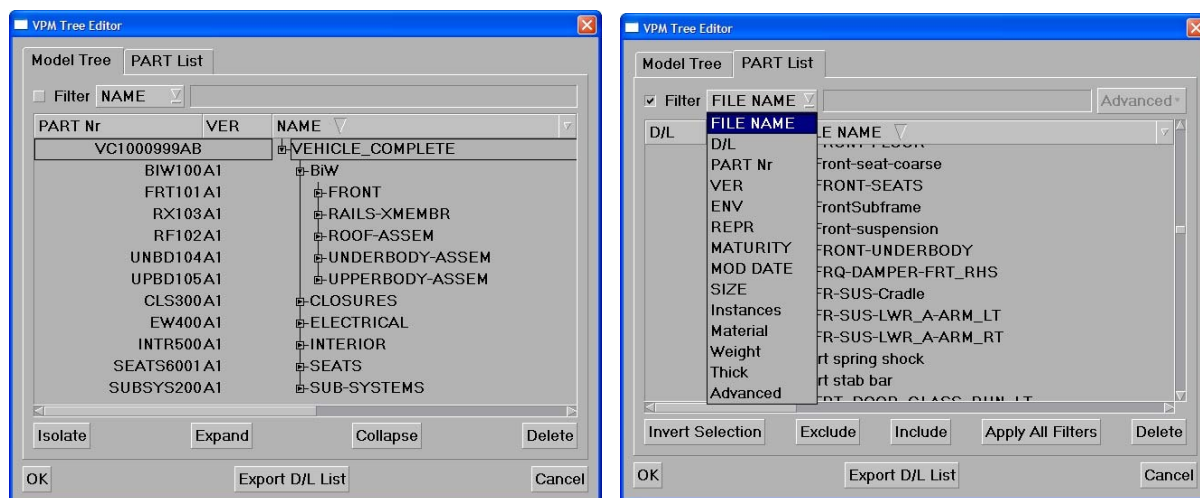


Figure 3

The next Step to be taken is the translation of the CAD data, for which the D/L – list works as an input. A significant number of issues is taken under consideration, to ensure that all parts are correctly translated. To begin with, the part offset can be performed directly in the case of sheet metal parts in a thin description, if the Part's Offset Rules are included in the CAD file. To continue, the middle-surface will be extracted in the case of sheet metal parts in a solid description. As far as solid parts are concerned, a volume can be defined automatically. Also, correct Engineering Data, retrieved from the D/L - list can be applied during the Translation. It is also worth mentioning that any arising errors and any missing-information will be noted as comments and will accompany the translated part in the outputted file. Comments can be later reviewed, and help with the detection and correction of errors.

After translation has been completed, the imported parts are positioned as described in the VPM tree to form the complete model. Parts that had been previously translated are retrieved from DM, in their latest CAD version and are positioned along with the new ones. All Welding Information will be imported at the end, to conclude the model's assembly process. The last step of building the CM consists of checking the model in order to fix any translation or assembly errors. ANSA automatically detects all wrongly positioned parts and the in-accurate welding information and offers all the proper tools to deal with them.

As soon as any errors are resolved, the Common Representation of the new parts is stored in ANSA DM and can be used further on for the creation of all FE representations. At this point it should be made clear that if possible errors are not fixed at this moment, engineers will come across them in each Discipline Model. The error free Common Model, once built, can be used as a starting point for the creation of each Discipline Specific Model.

1.4. Representation Manager

Once the Common Model has been built, all needed Representations can be constructed through the Representation Manager (RM), which handles all Representation requests for each Part or Subassembly, (3).

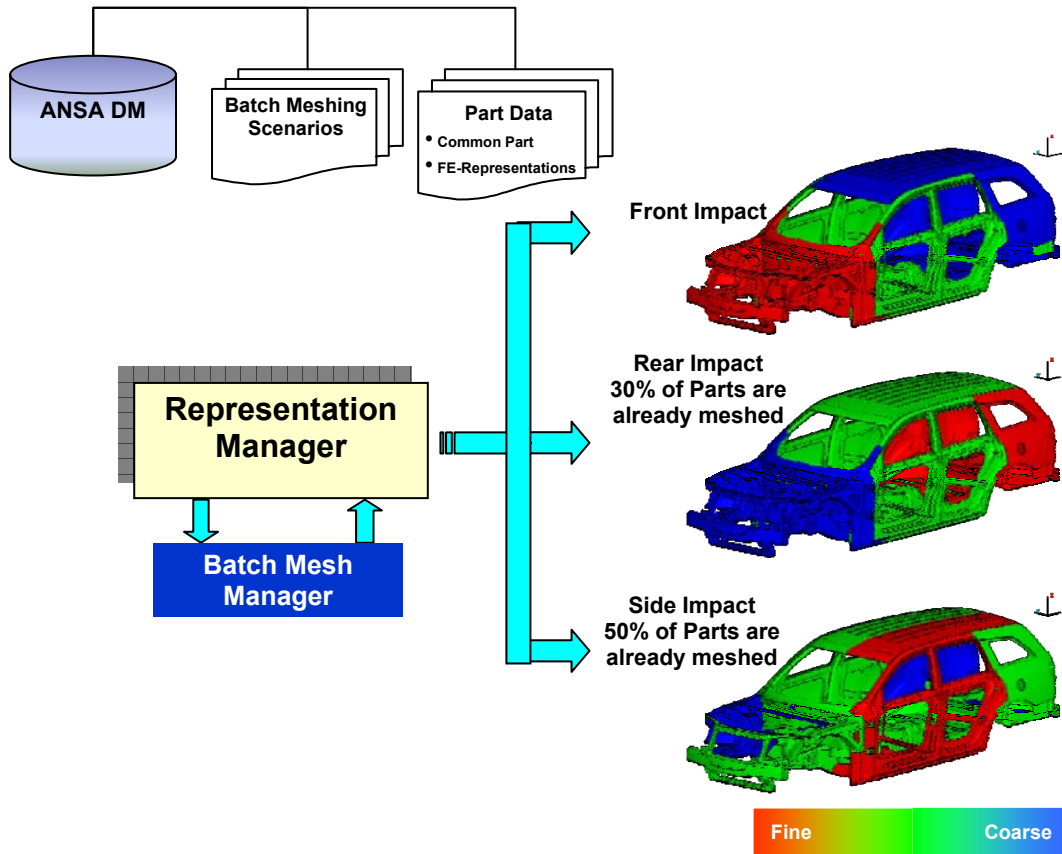


Figure 4

The moment a specific Discipline FE Representation will be requested, a search is carried out in DM. In case no such Representation has been saved, RM will retrieve the common representation and the respective meshing scenario and will send the job to the Batch Mesh Manager (BMM), which is designed to execute the different Discipline Meshing Scenarios. Each BM Scenario consists of a set of Meshing Rules. Parts according to their characteristics, such as location and name, will be meshed using the predefined Mesh Parameters. This concept can be applied either on the whole model or on single parts. RM will commit each FE-Representation in ANSA DM, and at the same time will record the specific Discipline this mesh was created for and the meshing rules that were used. This procedure assures that no meshing scenario is executed twice

In the example illustrated in figure 4, the Representation Manager will return upon request, the Front Impact Model. One should notice that the mesh size in the front region of the model is smaller than in the rear one. In the case where the Rear Impact model is requested, meshing will not be performed in all parts. Since 30% of parts have been already meshed with the same scenario for the Front Impact representation, they will be directly retrieved from ANSA DM. Only the remaining parts will be sent to the BMM to be meshed. The same principle applies in the case of the Side Impact Model, where due to the common meshing rules applied, 50% of the parts have already been meshed in the execution of different representation scenarios.

1.5. Dealing with new CAD versions

As soon as a specific Representation is stored in DM, all CAE engineers working in the particular project can be notified of the existence of a newer file of a part/subassembly, which is currently under work. In case of Minor Updates from CAD (which means that a new CAD Version is released for some of the parts) the translation Process will be executed only for the new parts. Queries to the DM, concerning the existence of new versions and study versions, can be executed through the “Check DM Updates” Tool.

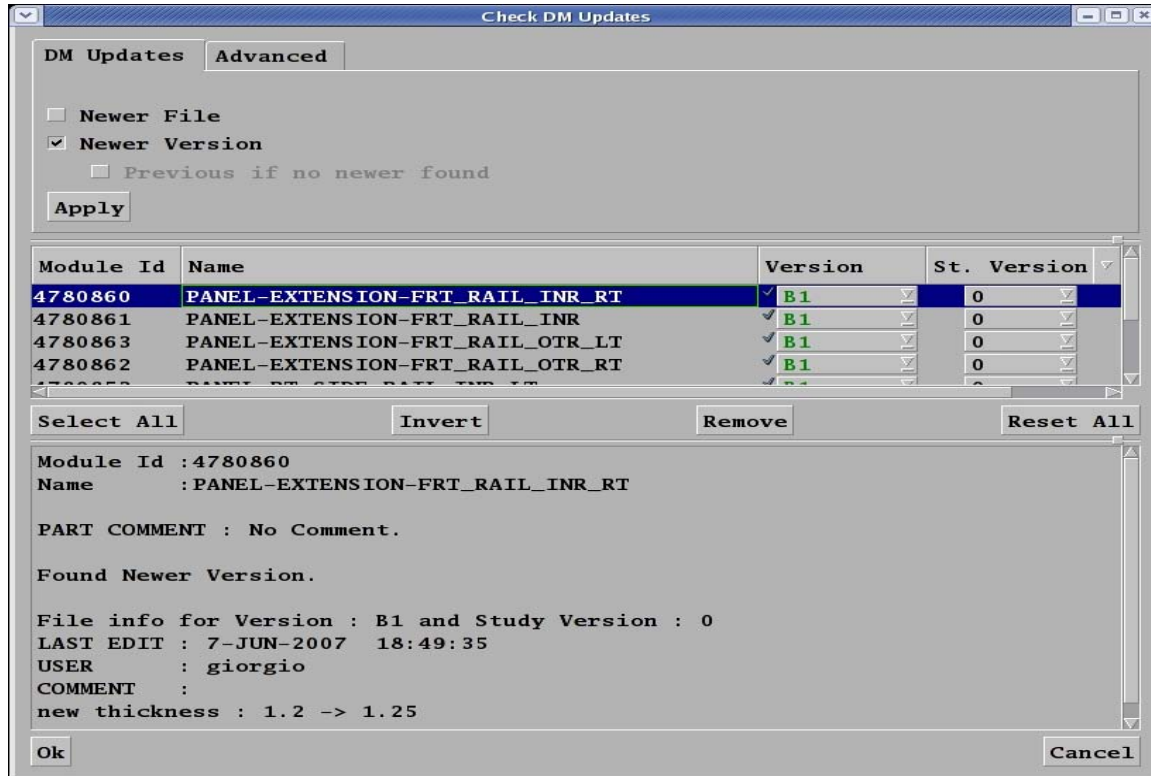


Figure 5

Parts of interest can be isolated and engineers can decide whether to import the new versions or not after having checked each part’s information and comments, as depicted in figure 5 above. All requested parts will be automatically integrated to the Models, while at the same time important information regarding the Connections, the Boundary Conditions and the Output Requests will be updated. It’s important to mention, that the Representations of the new parts can be created with the Representation Manager either before use or on a “just in time” request.

In the case of Major updates, where some of the previous parts have been deleted and new parts have been added in the model’s part list, the whole process will be repeated as previously described, starting with the translation of a new VPM-tree.

2. ANSA BATCH MESHING CAPABILITIES

2.1. The Batch Mesh tool

As mentioned above, when the Common Model's construction has finished, CAE engineers can continue working on the different FE Representations required to fully analyse the model/subassembly under consideration. The meshing tasks required for each Discipline are different and the recommended way to deal with them is through the Batch Mesh Manager.

Batch Mesh is the tool, available within ANSA, which performs automatic mesh generation on geometrical surfaces, (4). Its main characteristic is the ability to define several Batch Meshing Sessions, in order to mesh various parts of a model having set different meshing parameters. Two main sets of parameters are defined, when setting up a Batch Mesh scenario. The first one consists of the Mesh Parameters needed for the mesh generation, the several feature treatment tools as well as for quality improvement tasks. The second one contains all quality requirements and provides the ability to define threshold ranges. Batch Mesh also gives the ability to control a large number of features during mesh generation, such as dealing with fillets, flanges, holes, defeaturing and volumes, which will be explained in more detail in the paragraphs to follow.

At the end of the Batch Mesh procedure a report is generated, which presents general statistics regarding the mesh process and the quality achieved, based on the criteria and parameters that were set.

2.2. Batch Mesh scenario creation

For the purpose of demonstration, a vehicle model is considered, where Front, Side Rear and NVH analysis are requested. Figure 6 depicts such a model, where different colours are used to paint parts of the vehicle which belong to different scenarios. Obviously, several groups of parts need to be meshed using different parameters. In other words, a number of different mesh sessions must be introduced to meet the rules and requirements of the representation scenarios mentioned above. Through the Batch Mesh Manager tool, sessions can be fully customised and further subdivided to include sub sessions, where different meshing rules must be applied.

Consider the Front Impact case as shown in figure 7. The initial session has been partitioned according to each part's location in the vehicle. As a result three new sub sessions have been created, which are named the front, middle and rear section. The front section where the impact area is located, should have a small element size, the middle area a mid element size and at the rear a coarse one. This partitioning can be performed with the use of the ANSA Batch Mesh filters.

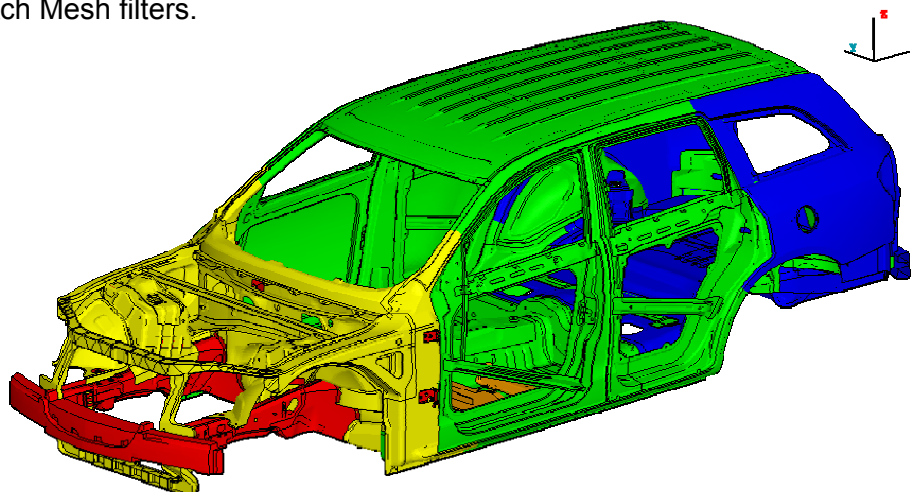


Figure 6

After the initial sectioning we need to identify some parts that need to follow different meshing rules from the rest. First of all we have to separate all the small parts of the structure. These parts need to be meshed with a finer element length and can be identified from their small area size, using the appropriate filter. At the next stage we have to identify all the important parts of the structure. These parts also need to be meshed with a finer element length from the rest of the area and can be recognized by a keyword in their name. In our example this way of filtering was applied for the front rails, the bumper and the cross members of the structure. Finally we have to separate the solid parts of the model that need to be meshed using volume elements.

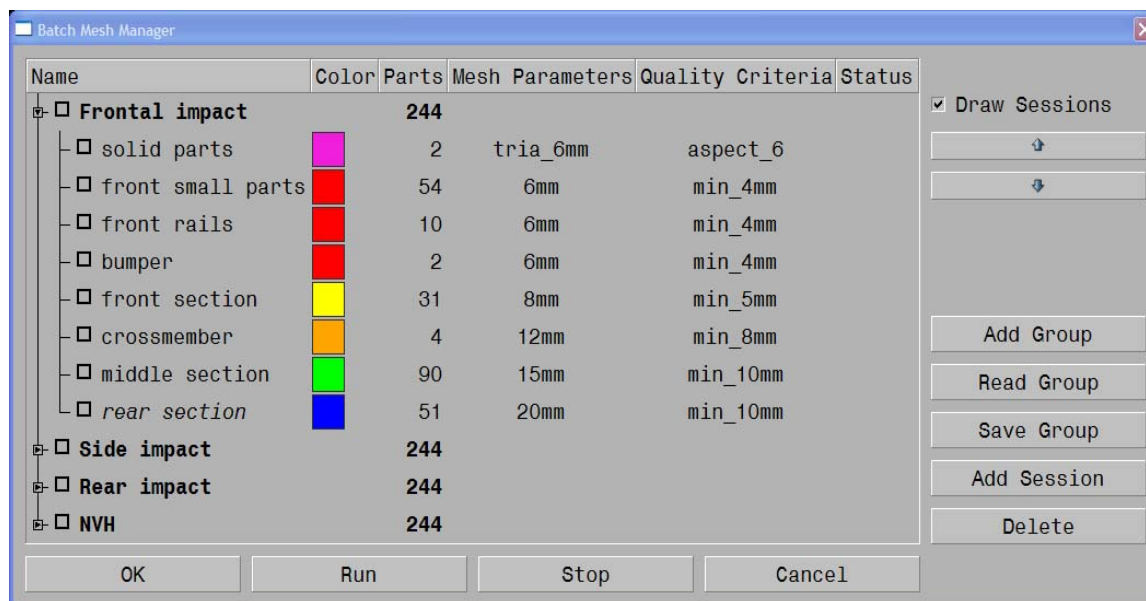


Figure 7

At this stage we have identified and partitioned our model in 8 different areas of interest. The next step is to define all the meshing rules for each area. These meshing rules consist of the mesh parameters and the quality criteria. Both of them can be set through Batch Mesh Manager. The meshing parameters are categorized in such a way that the meshing result of each session can be easily supervised.

2.3. Mesh Parameters

2.3.1 Shell Mesh properties

The first step in setting the mesh parameters is to define the shell mesh properties, depicted in figure 8. The available mesh types which can be selected from are Mixed, Quad, Tria, CFD and STL mesh, (4). Each of them has its own set of parameters so as to control the mesh size and the distortion rules of each session. The Distortion Distance is the maximum allowed normal distance between the nodal chord of a perimeter segment and the underlying CAD that defined it. Distortion Angle is the maximum allowed angle, measured in degrees, between the tangents of a perimeter segment at two consecutive nodes. The element order can also be defined, whereas an option is offered as to whether work should be done on existing mesh or any existing mesh should be erased before a new one is created. Options are also provided in order for triangular shell elements to be removed from Spots, Internal Single Bounds and Feature Lines.

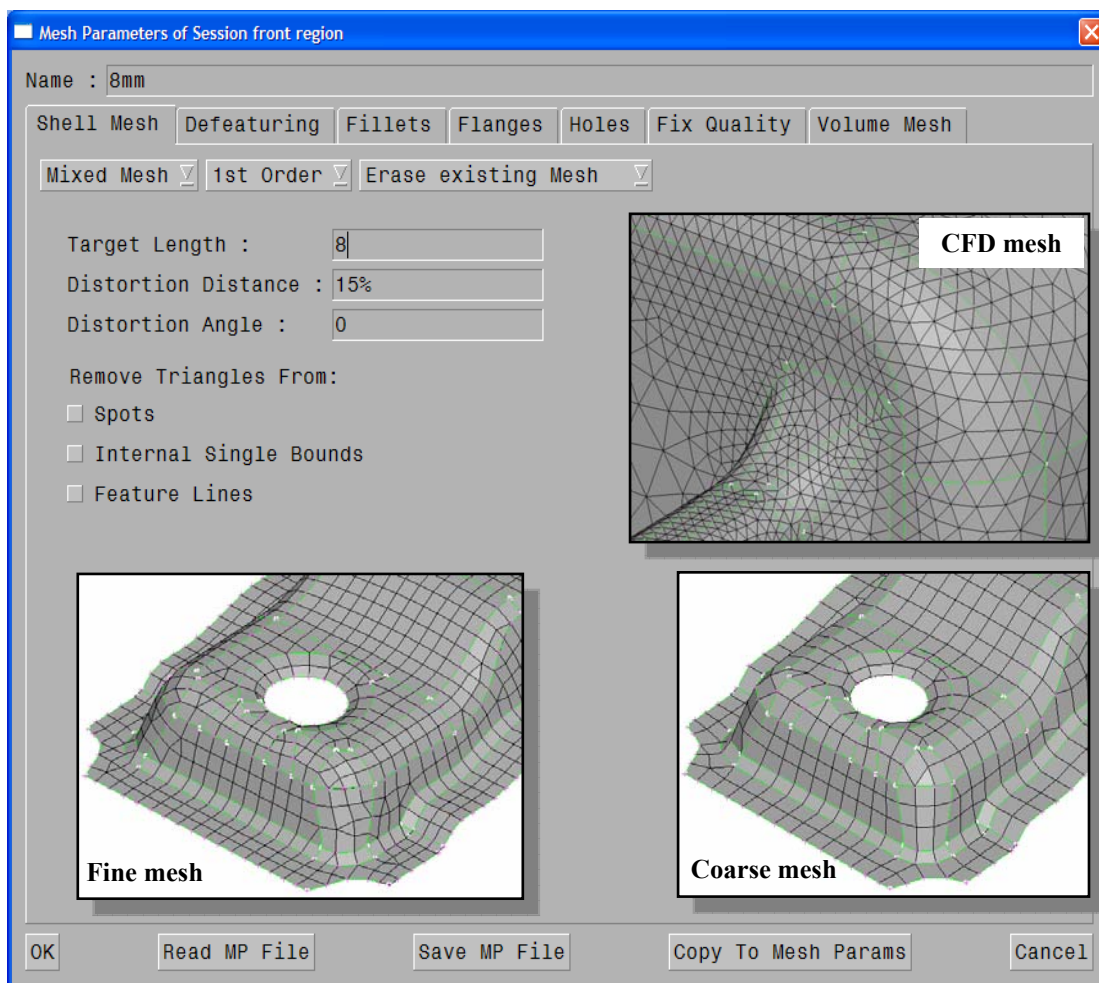


Figure 8

2.3.2 De-featuring

Moving on to the de-featuring section, (figure 9), in order to achieve the desired mesh result, several parameters can be set so as to define on which occasions perimeters should be joined or not and on which parts of the model Hot points should inserted or deleted. Feature Line Angles are very important as they determine which perimeters should be considered as important ones during the meshing procedure. The automatic identification of such perimeters is achieved through the use of the Feature Line Angle (4), which is defined as the supplementary of the angle formed between two adjacent surfaces on a common Perimeter.

Equally important is the use of the Feature Line's Corner Angle, in order to determine which corners between two Feature Lines are important. It is defined as the supplementary of the angle formed between two consecutive Feature Lines. The batch mesh tool also provides the ability to maintain characteristic perimeters during the meshing process, such as the symmetry plane and cuts which are used for model splitting.

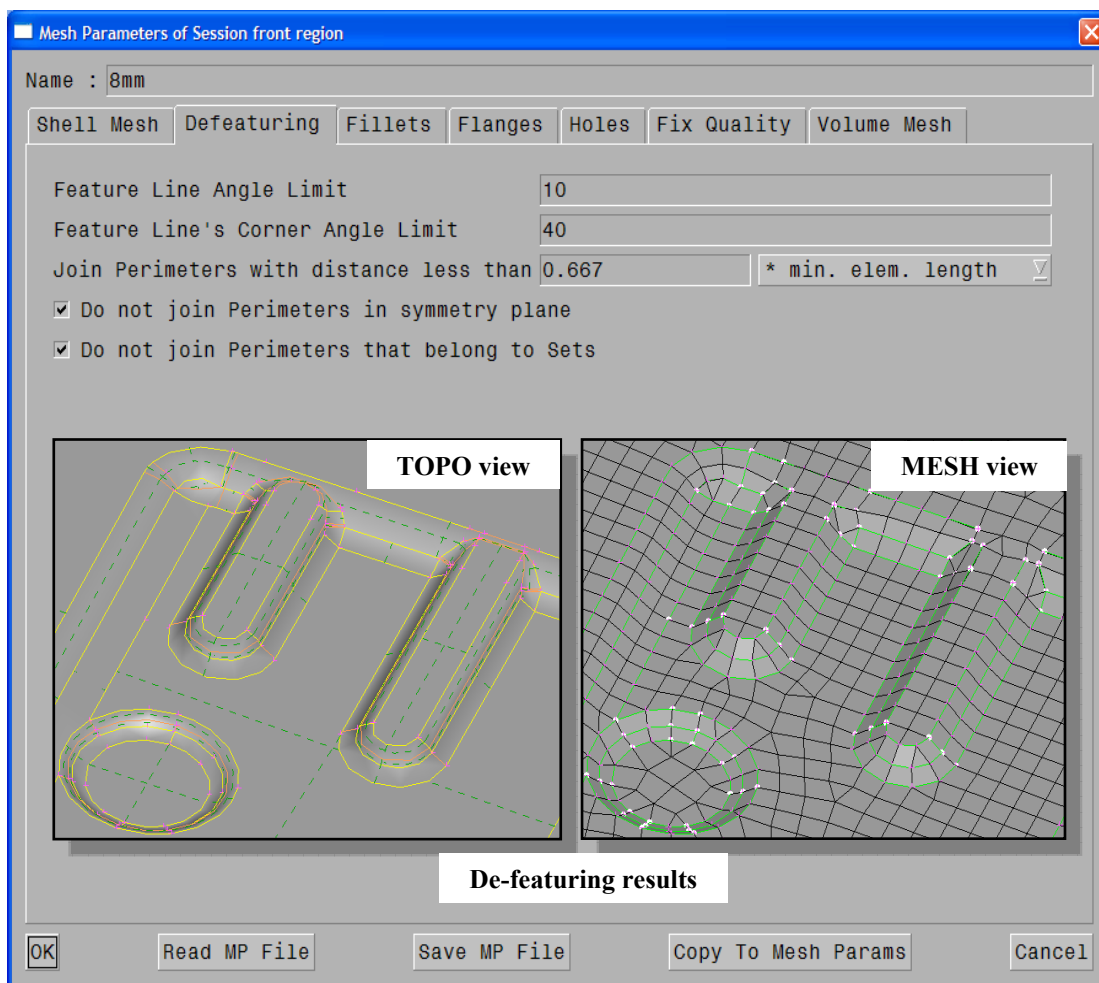


Figure 9

2.3.3. Fillet treatment

As far as fillets are concerned, their detection by the Batch Mesh tool, (figure 10), is based on their width and radius. The range of values is inputted, based on which they will be recognized and sets the desired method for treating them, (4). To be more specific, there are three ways available to deal with fillets, a) sharpening, b) splitting and c) creating element rows. The first one replaces fillets with the respective corner faces, while following the second one, fillets are cut in half iso-parametrically. Should the third way is selected all fillets will be meshed in order to create the requested rows of elements.

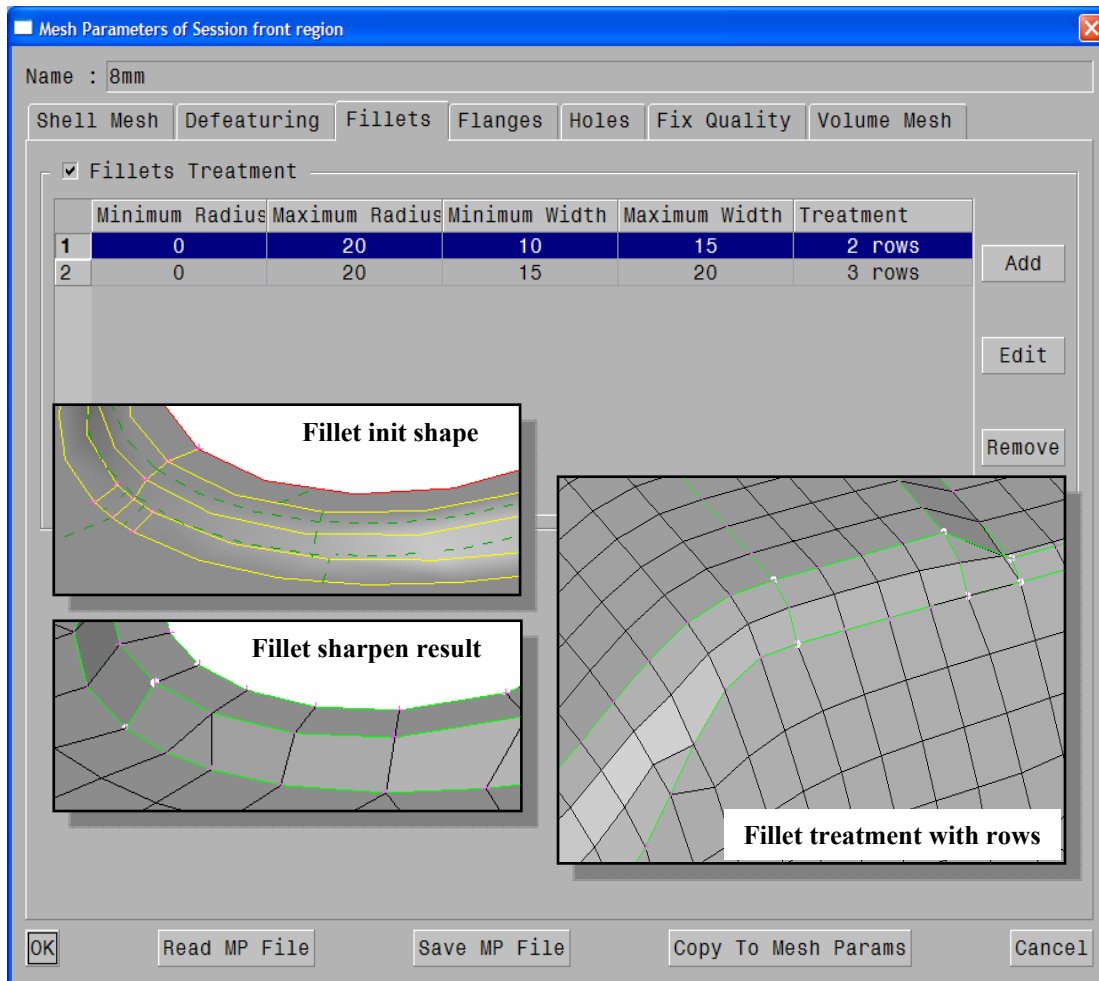


Figure 10

2.3.4. Flanges

Through the mesh parameters the treatment of flanges can also be set. The Batch Mesh tool, (figure 11), provides the ability to define the number of rows of elements that will be created during meshing. Flanges can be recognized in three different ways.

The first one is implemented with the use of faces proximity, (4). Flanges are detected by locating faces that lie opposite each other. Two variables are used, the distance and angle formed between normal vectors. The second way to recognize flanges is by studying the faces' shape. Faces that have at least one red bound and their width is in the range set in the flanges parameters section are identified. This algorithm is recommended in the case where each part is meshed separately and there are no connections available. Lastly, if there is connection data available, Batch Mesh can recognize faces close to connections based on the specified distance and identify flanges.

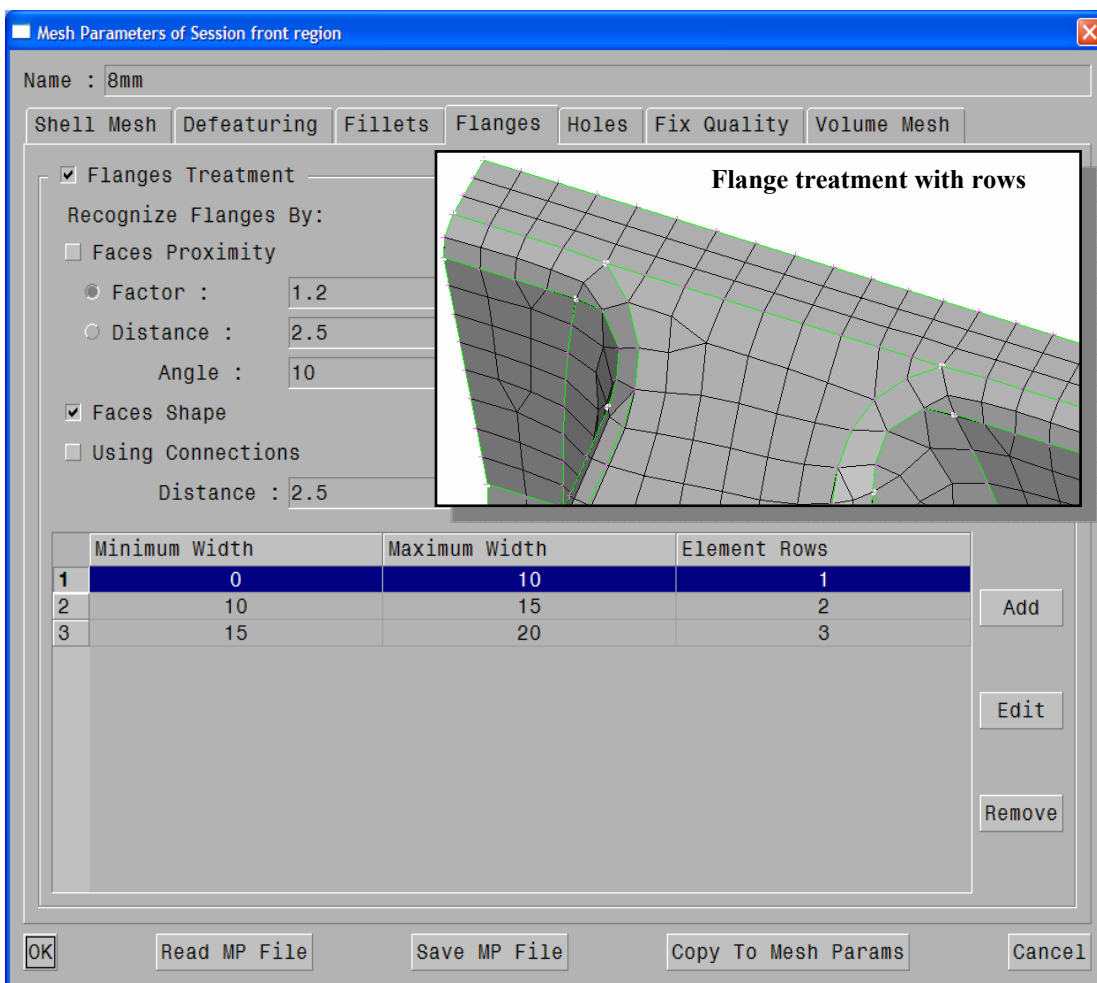


Figure 11

2.3.5. Holes treatment parameters

Batch Mesh also allows for the control of meshing generated around holes. Bolt holes parameters can be set separately from the rest and can be identified in three different ways in addition with the specified diameter range, as shown in figure 12. To begin with bolt holes are recognized by means of proximity, using the distance and angle formed between the normal vectors of the holes' centers, (4). Secondly, in the case connection information being available, the distance of the bolt connection to a center of a hole can be used to identify one. Lastly, all holes with specified shapes will be considered to be bolt holes.

Once holes have been recognized, certain options are given to set the holes' node number, fill holes and optionally mark the center point, resize the holes' diameter and/or created a specific number of zones around them. For holes falling within a certain diameter range a new diameter value can be defined. Additionally, the number of nodes in the holes' perimeter can be set, either as a stand alone number or given as a factor multiplied by the diameter. Last but not least, the number and width of quad zones, which will be introduced around holes, can be optionally defined.

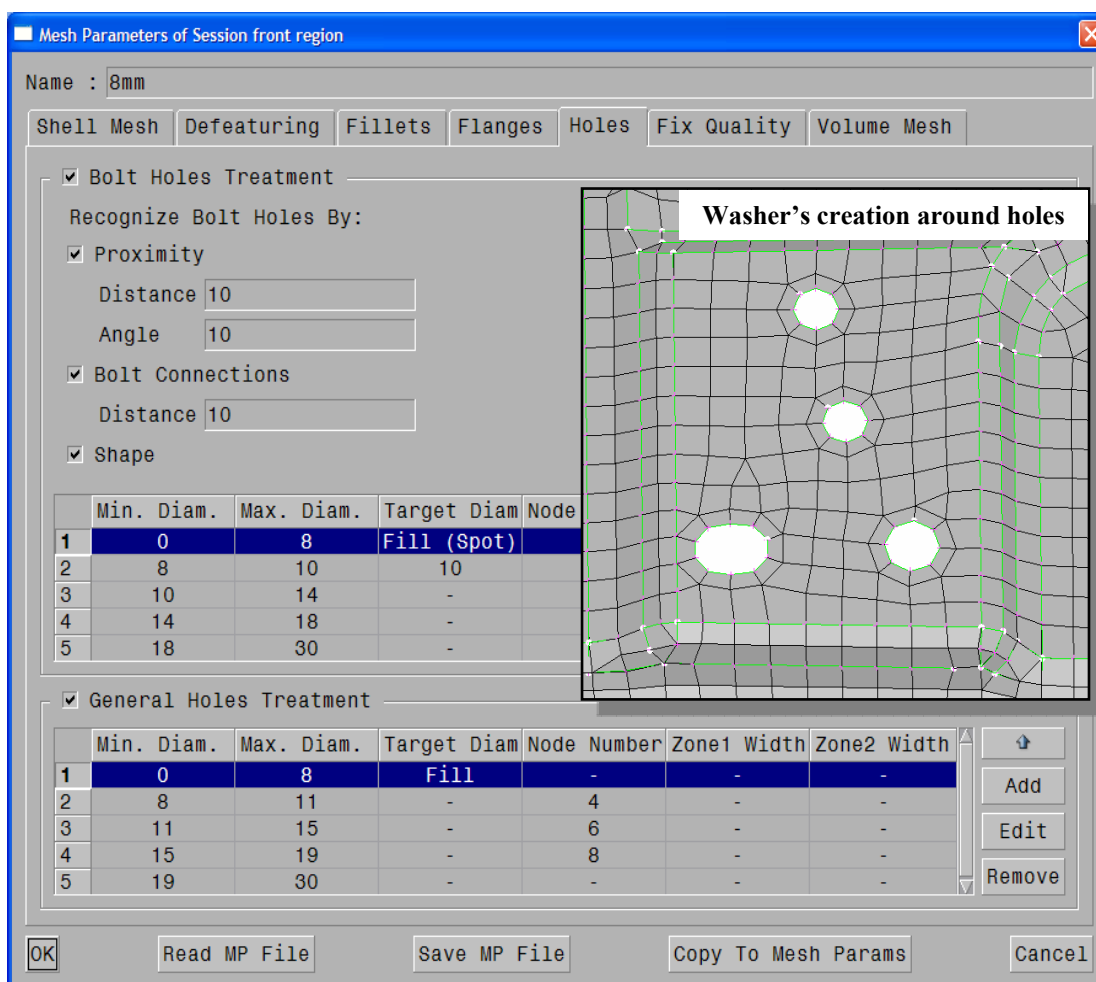


Figure 12

2.3.6 Fix Quality algorithm

Violating elements, which are generated as a result of the meshing process, can be dealt with a quality improvement algorithm that lies within the Batch Mesh tool. Fixes are applied according to quality criteria set, such as minimum element length, warping, skewness, taper and mid point deviation. Certain options are also included to specifically address quality violations and deal with them as requested, as depicted in figure 13 below.

First of all, a selection is offered as to whether the remaining violating quads, once the fix quality tool has been applied, should be split or not. Secondly, one can define whether minimum element length should be corrected on rows of elements created in fillets, (4). The same option exists for the case of element rows generated in flanges, where its correction is not always desirable. In this way, a larger number of rows can be requested than those allowed by the minimum length criterion. To continue an option is also given to allow for some small hole shape deformation in order to fix potential washer's creation problems. In order for violations to be dealt with, elements must be moved in several directions and distances, which are controlled constrains that define the maximum allowed movement from the surface or perimeter. Finally, it should be pointed out that all movements are performed as close to the original geometry as possible.

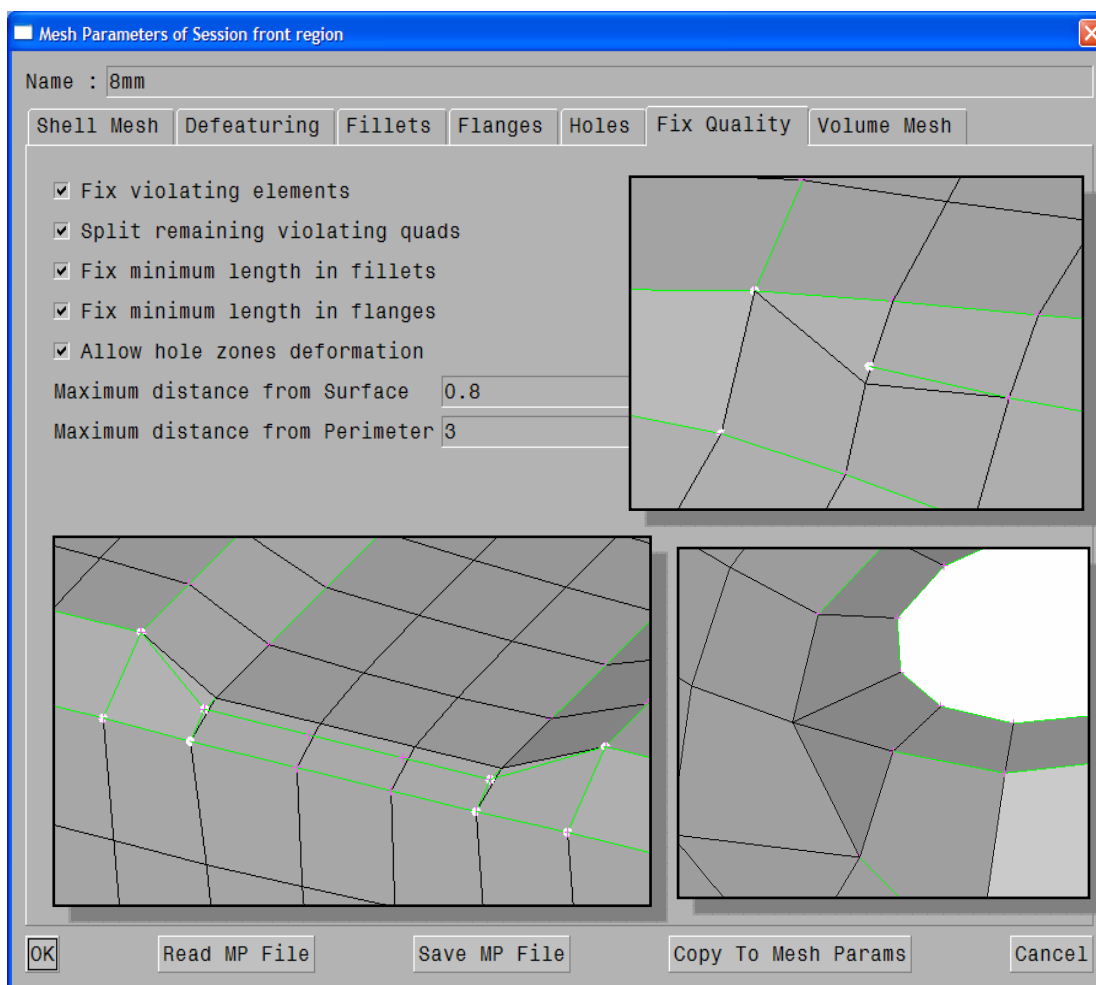


Figure 13

2.3.7 Volume meshing parameters

The last set of parameters to be set prior to batch meshing is the one regarding the meshing of closed volumes. Volume meshing can be achieved with the application of Tetra algorithm, while Layers and Hexa Interior creation are also supported, figure 14.

The Tetra algorithm is mainly suited for geometries of fairly thin volumes and nearly uniform surface element length, (4). As such it is applicable to most structural cases and some CFD scenarios. The generation of such elements is controlled by size and growth rate parameters. Layers support, allows for the creation of tetra elements which are surrounded by layers of hexas or pentas, which grow from all surfaces in a single step. Finally, with the set of Hexa Interior parameters a volume mesh can be created, which constitutes of a combination of hexa mesh inside the main volume and a transition zone to the surface mesh.

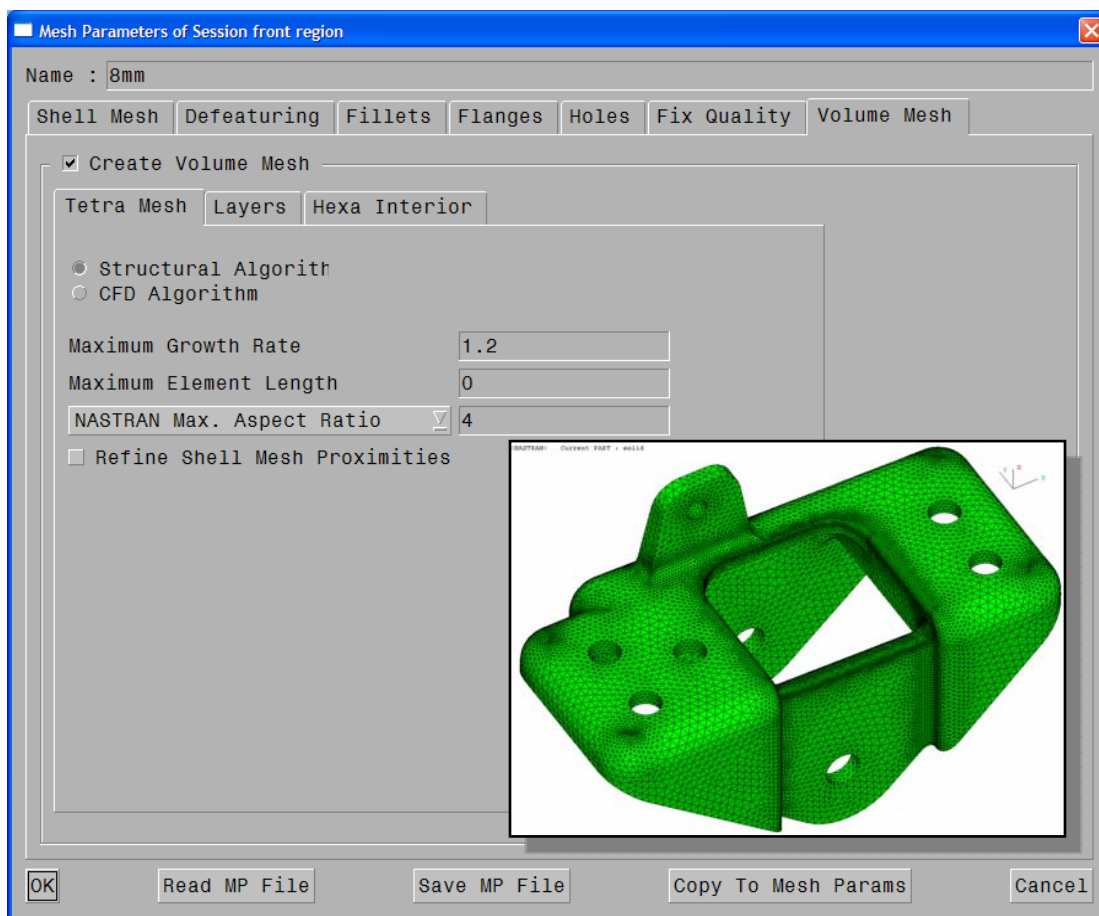


Figure 14

2.4 Mesh generation and further optimization

Once all mesh sessions have been defined for a specific Discipline scenario and all mesh parameters and quality requirements have been set, the Batch Mesh tool can continue with the requested mesh generation. Mesh parameters and quality criteria can be saved in ANSA DM so that they can be reused in different meshing scenarios where despite the fact that different sessions are to be executed the parameters to be set remain the same. As soon as the mesh generation has been completed, a statistics report is generated, figure 15, providing information on the results' status of each session that has been processed, (4).

Using the previously mentioned Batch Mesh Report Tool, the model's mesh quality can be thoroughly examined and any possible problems will be outlined. At the end it will be determined whether further improvement is required. Possible problems are considered to be quality violations and unmeshed macros. Once violating areas have been identified, fixing tasks can be scheduled to improve the meshed outcome. CAE engineers are then assigned different parts of the work to be done, which are handled in parallel so that the overall optimization process achieves the time saving and cost efficient goals that have been set at beginning of the project

After each part that has been checked and fixed is then published to the rest of the engineering group, simply by saving the representation in ANSA DM. The submitted part is then available for use by all potential meshing scenarios which might require the specific representation. The two most important aspects of the process described above, job subdivision and parallel working, are essential not only to meshing applications but also to other time consuming operations, such as the initial geometry clean up and are incorporated within the organizational capabilities of ANSA DM.

ANSA												
STATISTICS REPORT												
PARTS				STATISTICS			VIOLATING SHELL ELEMENTS					
Name	Module ID	Version	Session	Aver. Length	Unmeshed	Triangles %	Total	Aspect	Skewness	Warping	Crash	Min. Len.
CrossMember - LowerRad	60001	A1	front region	8.1429	0	1.21581	0	0	0	0	0	0
FRT-WHEELHOUSE_FRONT_RIGHT	60006	A1	front region	9.50528	0	8.98004	0	0	0	0	0	0
FRT-WHEELHOUSE_FRONT_LEFT	60005	A1	front region	9.46653	0	8.56354	0	0	0	0	0	0
EL COUPLER INNER LEFT	60004	A1	front region	8.42572	0	5.94724	23	0	4	17	0	10
LR JOINT LOAD BEAR OUTER LEFT	60002	A1	front region	8.3755	0	3.13117	7	0	0	5	0	2
R JOINT LOAD BEAR OUTER RIGHT	60003	A1	front region	8.39837	0	3.31633	4	0	0	2	0	2
TOTAL				8.58385	0	4.71725	34	0	4	24	0	14

Figure 15

3. CONCLUSIONS

Latest developments in the CAD process have made it very hard for the CAE engineers to keep up with the large number of model designs that are outputted by the design departments. Thus the overall meshing process, analysis and verification of the several component alternatives have become time consuming and error prone. Different model releases require the generation of several discipline scenarios, analysing the same or different model parts, with the use of a wide range of meshing parameters and quality criteria. At the same time it is extremely complex for CAE analysts to make sure that they work and compare results for the same models, since different alternatives may be used for the same part by different departments.

The proposed highly automated CAE workflow contributes to the robust developing of several discipline models, which follow specific guidelines and share common requirements. ANSA Data Management provides engineering teams with the latest model data versions, exhibiting effective communication methods and central organisation skills. DM drastically reduces developing time and cost, maintaining high process reliability, while at the same time allows for job subdivision and parallel working. Time consuming processes like geometry clean-up and meshing routines are performed only for newly arrived versions, while the joint use of the Representation Manager and Batch Meshing Tool guarantees that no task is performed twice, thus substantially reducing meshing time up to 90%. By implementing the suggested methodology CAE becomes faster and more flexible, allowing for better communications not only between CAE engineers working on the same project but also between the CAE and CAD departments, reducing the possibility of errors.

REFERENCES

- (1) BETA CAE Systems, "ANSA Task Manager Users Guide", ANSA v12.1.2 Documentation, 2007
- (2) Dimitrios Angelis, Stylianos Seitanis, "Efficient CAE DATA and process management, for virtual product development and verification, in LS –DYNA simulations", LS –DYNA Anwenderforum, Ulm 2006
- (3) BETA CAE Systems, "ANSA Data Management Users Guide", ANSA v12.1.2 Documentation, 2007
- (4) BETA CAE Systems, "ANSA Users Guide", ANSA v12.1.2 Documentation, 2007

STRUCTURAL FE-MODEL OF THIN ADHESIVE LAYERS WELL SUITED FOR IMPLICIT AND EXPLICIT ANALYSES

¹Thomas Brandt, ¹Holger Friese, ²Boris Heydt, ¹Dr. Ulrich Hindenlang

¹LASSO Ingenieurgesellschaft mbH, Germany, ²Metabowerke GmbH, Germany

KEYWORDS -

ABSTRACT - Structural stiffness properties of assemblies are affected to a considerable degree by coupling conditions of construction units. More and more adhesives replace welding and other techniques for joining parts. This kind of connections is a high challenge for a realistic representation in FE-analyses. By the method presented here it is shown how such an adhesive layer can be represented in a simply handled way. Additionally it is still possible to use already existing FE-models of assemblies without modifications of the way of discretisation generally applied.

Starting from a volume representation of the connected parts as well as the adhesive layer, the transition to a shell representation of the parts is performed. Here the adhesive layer is inserted in between the parts as an automatically generated network of rod elements. For this purpose there are nearly no extraordinary demands to the connected shell mesh. There is no need of an identical mesh topology of the connected regions. Also, it is possible to couple structures with shell meshes of different element sizes.

For a correct representation of stiffness properties the cross-sections of the rod elements have to be calibrated with respect to the element sizes and the thickness of the connected parts. Also this process of calibration is automated. The calibration itself has been analysed and tested in a study of convergence.

This FE-representation of adhesive layers has a large variety of applications. There are simple stiffness analyses and crash simulations. For crash simulations an additional failure criterion, which still has to be determined, can be defined. Furthermore it can be used in thermo mechanical analyses and in simulations of the adhesive's hardening process in course of fabrication. For this specific application a particular material description has to be defined. Here it is necessary to consider that the adhesive does not show a non-negligible stiffness from the beginning but only when re-cooling the assembly. Influences of different thermal expansion coefficients as well as an inhomogeneous development of the temperature field have to be taken into account and can be visualized by this simulation.

The suitability of the developed FE-representation was tested at samples of simple geometry. Subsequently this technique was validated at a car door in hybrid design.

Up to now this simulation of the manufacturing process is the main application of this method, where it has been used frequently and very successfully.

Session H2.2

CAPTURING THE BEST PRACTICES FOR THE ORGANIZATION AND ANALYSIS OF CRASH-TEST SIMULATION LOAD-CASES

Irene Makropoulou, Konstantinos Kiouptsidis, Konstantinos Skolarikis
BETA CAE Systems S.A., Greece

KEYWORDS - Simulation model robustness, process repeatability, crash-test simulation, Data Management, Task Manager

ABSTRACT - The current tendencies of modern automotive industry impose the reduction of the CAE turnaround cycle, promoting at the same time the requirement for the generation of robust simulation models. Currently, slight changes in model parameters may result in a great scatter in simulation results. The robustness of the simulation models also suffers from the incorporation of changes that originate from the product evolution process. To develop accurate models, the CAE engineers have a great necessity for pre- and post-processing tools able to safeguard and capture the best practices used for the simulation model build-up and evaluation, reducing the error-prone procedures involved in the CAE-cycle while ensuring the repeatability and versatility of the complete process.

This paper will present the means provided by BETA CAE Systems S.A. towards the development of robust, repeatable and realistic crash and safety simulation models and the evaluation of the analysis results. ANSA Data Management facilitates the "replace-include-exclude" procedures that constantly arise during the model build-up, while ANSA Task Manager guides the generation of the simulation models, identifying the dependencies among modeling actions. The simulation model set-up becomes a repeatable and user-independent procedure, safeguarding the model quality and fidelity.

TECHNICAL PAPER -

1. INTRODUCTION

In the framework of virtual prototype development, a great number of discipline models must be built and analyzed for the validation of a new vehicle model design. In the presently CAE-driven design process, the increasing number of vehicle model variants further increases the number of the load-cases that must be studied. With the aid of powerful and “intelligent” batch meshing capabilities, the bottleneck of the CAE turnaround cycle tends to move from the model discretization to the actual discipline model build-up.

The build-up of crash-test simulation models is a process complex and time-consuming, vulnerable to model parameter changes and error-prone. Furthermore, despite of the very detailed specifications provided by OEMs for the set-up of simulation models, the overall model quality is always user-dependant. Thus, the “weak” points in the current crash-test simulation models set-up process can be roughly outlined as follows:

- Organization: there is a great difficulty in gathering all necessary data
- Flexibility: in most cases, CAE engineers have a hard-time incorporating component updates at the late stages of the model build-up
- Repeatability: the simulation model build-up process requires great expertise and cannot be reproduce by inexperienced engineers
- Robustness: small changes in the model parameters may lead to a great scatter in the simulation results
- Model validation: there are incomplete model checks prior to the output

All these deficiencies maintain the CAE productivity at low level.

In this paper, the capabilities of ANSA Task Manager in combination with ANSA Data Management are explored, having as target the elimination of the physical drawbacks that arise during the crash-test simulation models build-up. ANSA Task Manager is used to capture the best practices for the crash simulation models set-up, as these are determined by the CAE analysis expert, scoping to the increase of CAE teams flexibility, efficiency and productivity.

The whole procedure is demonstrated using the full vehicle model shown in Fig.1.

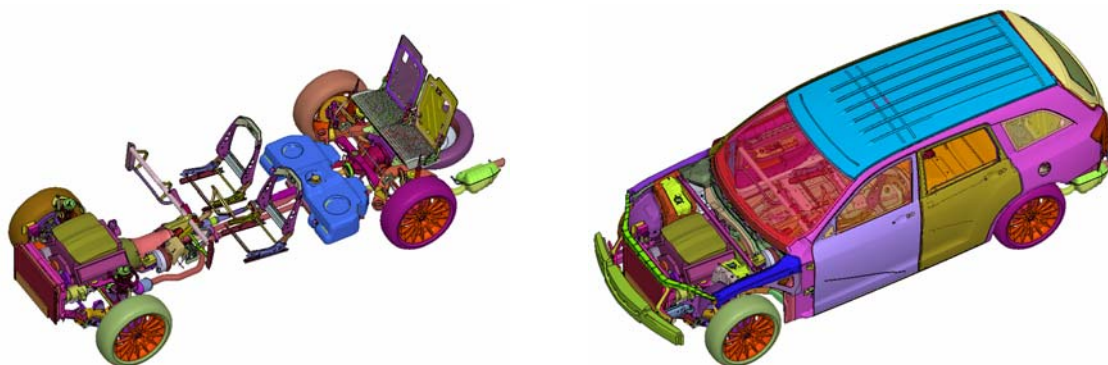


Fig.1. Full vehicle model

From this model, two load-cases input deck files are extracted. The first is a front-impact 40% offset analysis, with an initial velocity of 64km/h (FMVSS 208), to be conducted with LS-DYNA solver, while the second is a side-impact analysis, with an initial velocity of the barrier of 50km/h (EURO-NCAP 2004), to be conducted with PAM-CRASH. The use of two different explicit codes for the analysis of two crash-test simulation models is for demonstration purposes only.

2. ANSA DATA MANAGEMENT AS A DATA POOL

ANSA DM collects and stores in a structured and hierarchical form all engineering data that are necessary during the development process of a vehicle simulation model (1). Tasks created in ANSA Task Manager are saved in ANSA DM as template processes in order to guide the model build-up of model assemblies. These processes are built once by the CAE analysis expert, who must take into account and include in the tasks all distinct modeling actions that need to be performed during the simulation model build-up.

The great variety of data that will be incorporated in the analysis models studied are gathered under ANSA DM. Such data are:

- Mesh representations of components
- Material databases
- Barrier models
- Custom-made templates for Connector Entities, Mass Trim items, Boundary Conditions and Output Requests Generic Entities

ANSA Task Manager is perfectly combined with ANSA DM in all cases where data storage or data retrieval is necessary. Thus, all templates and auxiliary components referenced by the process items can be automatically invoked and incorporated in the model according to the rules specified in the Tasks.

3. CONCEPTUAL ORGANIZATION OF THE CRASH-TEST SIMULATION MODEL BUILD-UP IN ANSA TASK-MANAGER

ANSA Task Manager considers the model build-up consisting of three distinct stages: The *Common Model*, the *Solver Common Model* and the *Solver Load-case*. Each stage groups several *task items* which represent certain modeling actions. During the *Task* execution, the actions implied by the *task items* are realized and verified. Possible dependencies among modeling actions are automatically detected and treated appropriately.

The *Common Model* contains all modeling actions which are common for all the discipline analyses that will be conducted on the model (i.e. NVH analyses, front impact, side impact, rear impact analyses, durability analyses etc.). Thus, the *Common Model* is stripped of any solution dependant entities and it is ready to be “transformed” in a form suitable for the analysis that follows.

The *Solver Common Model* contains those modeling actions which are not common for all the discipline analyses, but are certainly common for all the load-cases that will follow. The *Solver Common Model* also plays another significant role: It dictates the “transformation” of the *Common Model* into a form suitable for the analysis that will follow.

Finally, the *Solver Load-case* contains the modeling actions that are load-case dependent.

For the build-up of a front-impact and a side-impact analysis, regardless of the solver where the analysis will be conducted, the *Common Model* needs to adopt two different mesh representations. This automatically implies that there must be two *Solver Common Model* groups created, one for the front- and one for the side-impact load-case. Under the *Solver Common Model* items, there may be one or more load-cases, varying on the initial conditions, boundary conditions and output requests e.g. initial velocity and barrier position.

4. THE COMMON MODEL IN ANSA TASK-MANAGER

The *Common Model* defines the model that will participate in the analysis. It consists of all the components, BiW connections, connectors and mass trim items that are common to all disciplines (Fig.2).

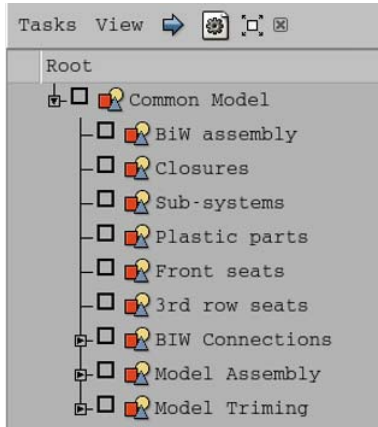


Fig.2. The Common Model task item

The *Common Model*, in the same manner as all other ANSA Task Manager groups, represents a process that must be followed exactly as dictated by the sequence of *Task Items*. This sequence, once defined is saved as a template process in ANSA Data Management system and can be directly retrieved for its application on the assembly model.

Gathering the components that comprise the model

ANSA Task Manager allows for a model grouping suitable for the discipline models build-up. This grouping simplifies the assembly hierarchy tree coming from VPM systems, enables easy access to the actual sub-assemblies and eases the communication of ANSA Task Manager with ANSA Data Management system.

The model grouping created for the goals of this study consists of six sub-models:

- BiW assembly
- Closures
- Sub-systems
- Plastic parts
- Front seats
- 3rd row seats

These sub-models are reflected in the Parts Manager as ANSA groups. These groups initially appear as empty. By simply *linking* the actual model assembly components in the respective Task Manager sub-model groups, ANSA Task Manager becomes aware of the model that it is placed under its control (Fig.3).

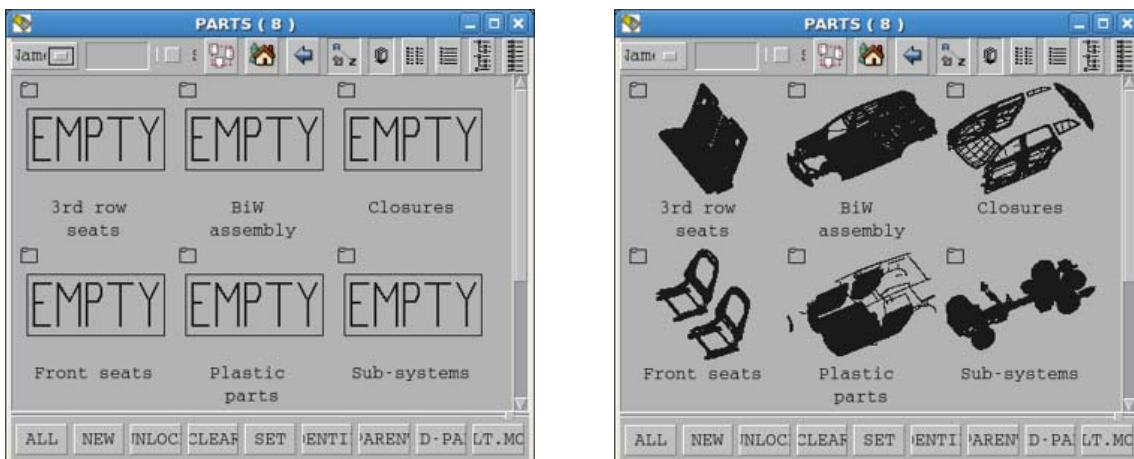


Fig.3. Task Manager sub-models before and after the interfacing with the model assembly

Furthermore, all the capabilities of ANSA Data Management with respect to parts management can be directly accessed from within Task Manager. Most important:

- The retrieval of suitable mesh representations for front- and side-impact analyses
- The notification for part updates and their incorporation in the model assembly.

During the execution of the *Common Model*, ANSA Task Manager verifies that there are no empty parts among the ones referenced by the sub-models. The assembly up to this point is not meshed. The mesh is a discipline-dependent feature.

BiW Connections

After the validation of the sub-model items, comes the BiW assembly. The BiW is assembled using connection points and curves. The welding information will be input at this point. ANSA Task Manager will verify the connectivity specified in each connection entity, with respect to the availability of the parts and properties referenced.

The welding information neutral file is retrieved from ANSA DM. During the execution of the *BiW Connections* group of items and with the aid of the Connection Manager, Task Manger validates every single connection entity (Spot weld points, Spot weld lines, Adhesive lines, Bolts).

The connection entities do not take an FE-representation at this stage. The FE-representation is a discipline-dependent feature.

Model Assembly: The Connector Entities

In order to impose the kinematic constraints that physically exist between parts and sub-assemblies Connector Entities are used (Fig.4). A Connector Entity can carry information regarding:

- Its location in space and orientation.
- Connectivity. Which components are connected?
- Representation. What FE-representation should be used?
- Interface. Which is the interface entity between the representation entities and the connected components?

These entities can apply rigid interface between the connected components or even use template, parameterized entities to model the kinematic constraints. During the execution of the *Model Assembly* group of items, Task Manager validates every single Connector Entity with respect to the availability of the parts and properties referenced in its connectivity information.



Fig.4. Connector Entity Symbol

At this stage, the Connector Entities do not take any FE-representation. The FE-representation is a discipline-dependent feature.

Model Trimming: The Mass Trim items

Mass trimming takes place either with the addition of lumped mass on certain components or with the addition of distributed mass on components. All cases where mass addition is common for all discipline models are collected under the *Mass Trimming* group in the form of *Mass Trim* items (Fig.5). A Trim Item can carry information regarding:

- Its location in space.
- Connectivity. On which components should the mass be added?
- Representation. What FE-representation should be used?
- Interface. Which is the interface entity between the representation entities and the components?



Fig.5. Mass Trim item Symbol

During the execution of the *Model Trimming* group of items, Task Manager validates every single Mass Trim item with respect to the availability of the parts and properties referenced in its connectivity information.

At this stage, the Mass Trim items do not take any FE-representation. The FE-representation is a discipline-dependent feature.

The characteristic features of the model assembly after the validation of all *Common Model* contents are summarized below:

- There are no parts missing among the sub-models that comprise the model assembly
- The welding information exist in the form of connection entities (connection points and connection curves) which verified with respect to their connectivity information
- The locations where kinematic constraints exist between parts and sub-assemblies are marked with Connector Entities. These entities are verified with respect to their connectivity information.
- The locations where mass trimming takes place for all discipline models are marked with Mass Trim items. These entities are verified with respect to their connectivity information.
- There are no intersections between components. All possible intersections were resolved prior to the population of the model geometry into ANSA Data Management¹.

This error free assembly model (Fig.6) comprises the base for the creation of any discipline model, since it is ready to be “transformed” into any suitable form.

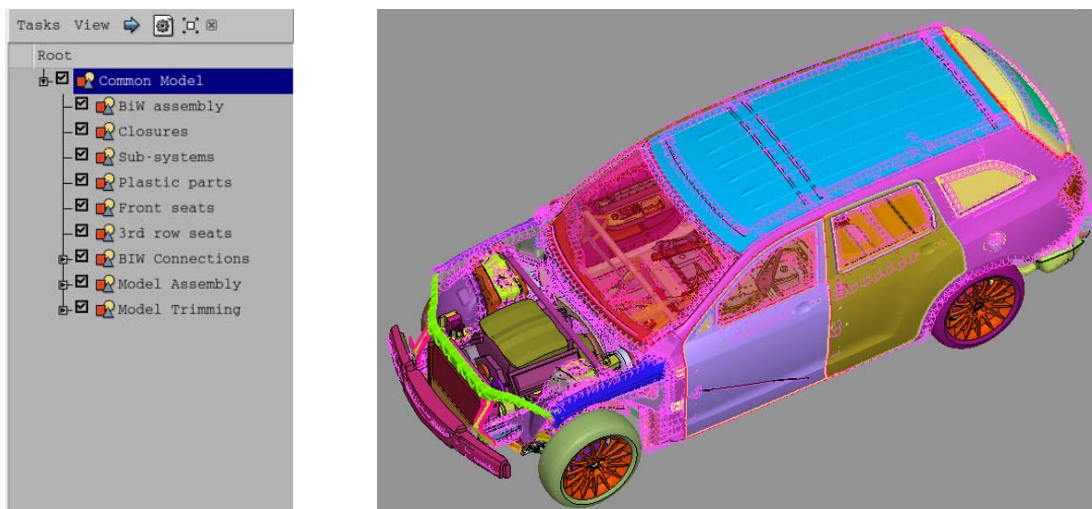


Fig.6. Common Model completed

5. THE SOLVER COMMON MODEL

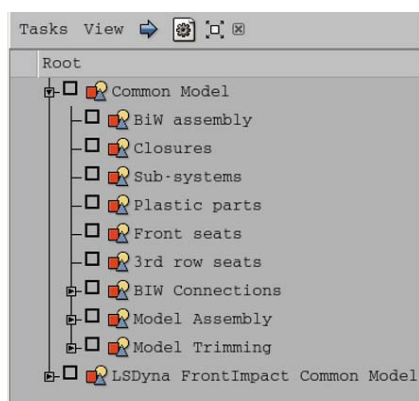
The significance of the *Solver Common Model* group of items lies in the fact that it is the linkage between the *Common Model* and the *Solver Load-case*. It is the *Solver Common Model* that dictates the “transformation” of the *Common Model* in a form suitable for the analysis to be conducted.

The *Solver Common Model* safeguards a part of the model build-up process in the form of a sequence of modeling actions. Once built by the CAE analysis expert, it is saved as a process template in ANSA Data Management system so that it can be easily retrieved and re-used for several applications.

In this study, an *LS-Dyna Common Model* is used for the build-up of the front-impact load-case and a *Pam-Crash Common Model* for the side-impact one.

LS-Dyna Common Model

As soon as the *LS-Dyna Common Model* is invoked, ANSA Task Manager is notified that the actual model built within the *Common Model* must adopt a form suitable for the LS-Dyna analysis. All the *Common Model* task items that will be affected by the “transformation” of the *Common Model* become automatically un-checked, (Fig.7). Thus, the user is forced to execute them again, this time with the conditions dictated by the *LS-Dyna Common Model*.



During the re-execution of the *Common Model*, the components referenced by the sub-model items must adopt a suitable for front-impact analysis mesh representation, the BiW connections must be “realized”, connecting the parts they reference by suitable for the LS-DYNA analysis entities, the Connector Entities and the Mass Trim items must be also “realized”, using built-in or custom template representations.

Fig.7. Addition of the LS-Dyna Front-impact Common Model

Sub-model items: FE-representation

With the *LS-Dyna Common Model* present, ANSA Task Manger does not validate any sub-model item unless the components it references do not contain any unmeshed macro areas or volumes. Therefore, for each sub-model the proper representation is retrieved from ANSA DM, with the aid of the *Part Representation Manager* (Fig.8). All functionality related to the communication of the Task Manager model with ANSA DM is directly accessed from within Task Manager.

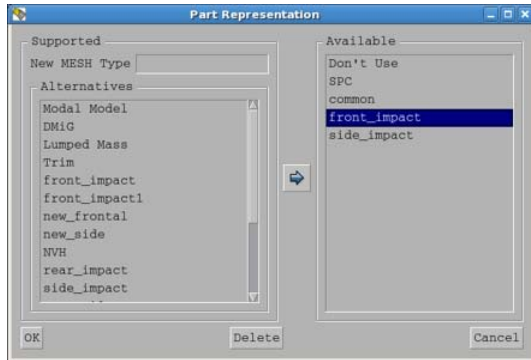


Fig.8. Retrieving the front-impact mesh representation from ANSA DM

After the retrieval of the front-impact mesh representation for each sub-model item (Closures, Sub-systems, Plastic parts, Front seats, 3rd row seats), ANSA Task Manager validates their definition with respect to the existence of unmeshed areas and volumes (Fig.9).

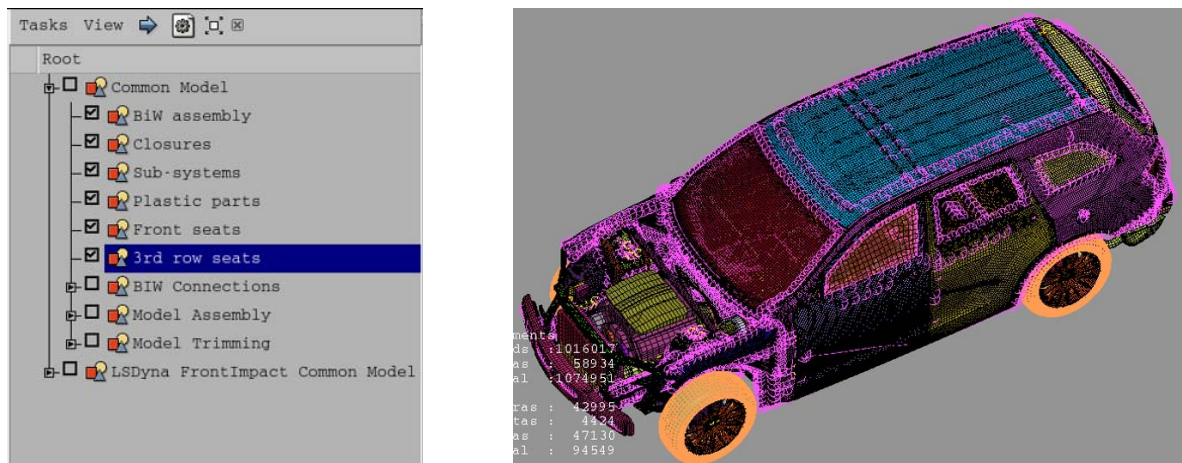


Fig.9. Front-impact mesh representation for *Common Model* sub-models

BiW Connections: Realization of welding information

With the *LS-Dyna Common Model* present, ANSA Task Manger does not validate any BiW connection entity type item unless all the entities of this type are “realized” with suitable FE-representations. For each connection entity type, annotations created by the CAE analysis expert guide the realization pattern (Fig.10).

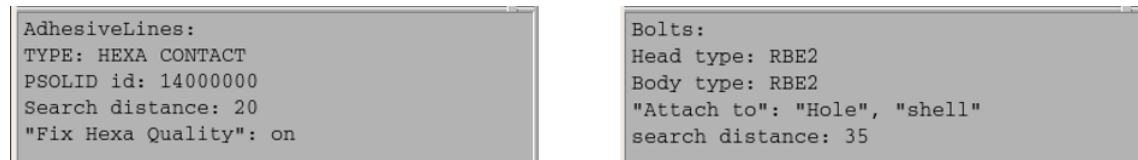


Fig.10. Annotations for the realization of Adhesive Lines and Bolts

Table 1 shows examples of connection entities realization patterns.

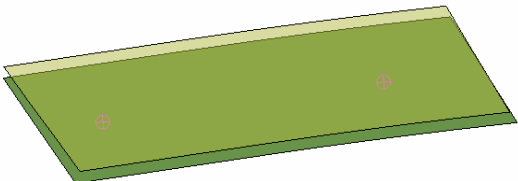
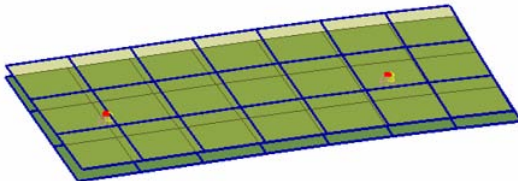

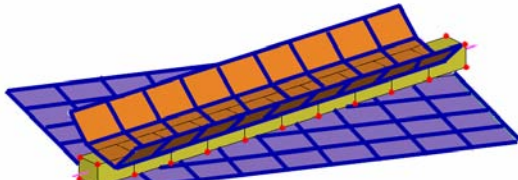
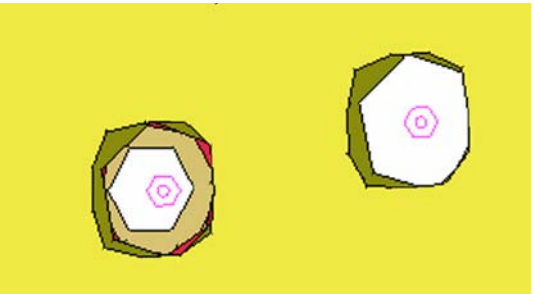
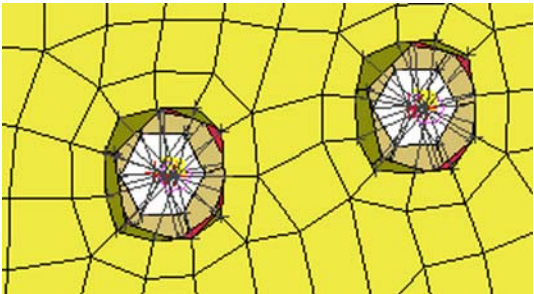
Before the LS-Dyna Common Model	After the LS-Dyna Common Model
 <p>Spot weld point connection entities</p>	 <p>DYNA SPOTWELD pattern</p>
 <p>Adhesive line connection entity</p>	 <p>HEXA CONTACT pattern</p>
 <p>Bolt connection entity</p>	 <p>Rigid interface, rigid body pattern</p>

Table 1. Realization patterns of BiW connections

After the realization of all connection entities, ANSA Task Manger validates their definition.

Model Assembly: Realization of Connector Entities

With the *LS-Dyna Common Model* present during the execution of the *Model Assembly* group of items, ANSA Task Manger applies the Connector Entities FE-representation. Some characteristic features of the Connector Entities realization are:

- The Connector Entities are defined using *mesh density independent* patterns for the identification of connected entities. Thus, a connector can be applied on a hole, a circular feature, a certain number of nodes or elements in a pre-defined search domain
- Connector Entities that connect a rigid with a deformable component with rigid interface automatically detect the case and create *CONSTRAINED_EXTRA_NODES instead of *CONSTRAINED_NODAL_RIGID_BODY entities
- Connector Entities that connect rigid components together with rigid interface, automatically detect the case and create *CONSTRAINED_RIGID_BODY entities
- The Connector Entities can use the built-in representations (i.e revolute and spherical joints) or even custom made ones, retrieved as templates from ANSA DM libraries, promoting the model robustness

Table 2 summarizes the custom templates used for the representation of Connector Entities. Such templates once created, are saved in ANSA DM libraries so that they can be re-used for various applications.

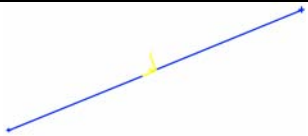


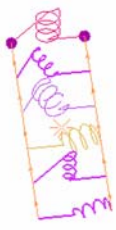

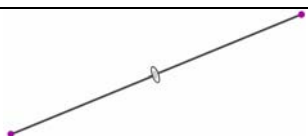
Template in ANSA DM	Description
	*ELEMENT_BEAM_ELFORM_1 Parameters: diameter, length and orientation according to application
	*CONSTRAINED_JOINT_SPHERICAL Parameters: Value of added mass on both ends
	*CONSTRAINED_JOINT_REVOLUTE Parameters: Value of added mass on both ends, orientation according to application
	*ELEMENT_DISCRETE for 6 dofs Predefined: *DEFINE_SD_ORIENTATION vectors, *SECTION_DESCRETE Parameters: Value of added mass on both ends
	*CONSTRAINED_JOINT_UNIVERSAL Parameters: Value of added mass on central nodes, orientation according to application
	*CONSTRAINED_JOINT_CYLINDRICAL Parameters: Value of added mass on both ends, orientation according to application
Table 2. Parameterized templates for connectors retrieved from the ANSA DM library	

Figure 11 shows an example of connector entities realization.

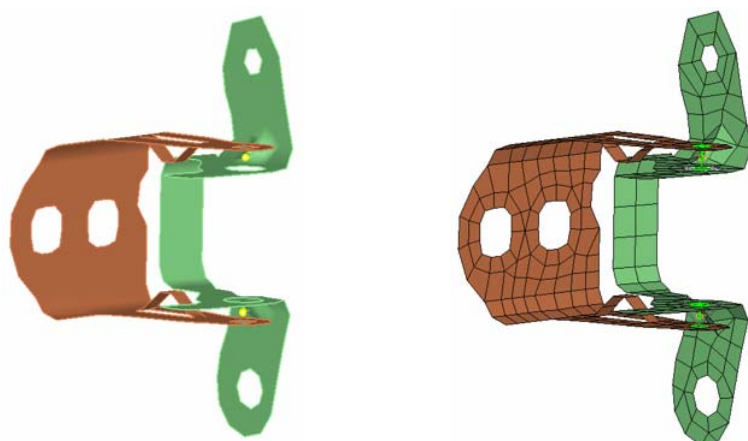


Fig.11. Connector entities before and after their realization

Model Trimming: Realization of Mass Trim items

With the *LS-Dyna Common Model* present during the execution of the *Mass Trimming* group of items, ANSA Task Manger applies the Mass Trim items FE-representation. The FE-representations of Mass Trim items for LS-Dyna can be:

- Certain amount of added mass distributed over pre-defined components in the form of **ELEMENT_MASS*
- Certain amount of added mass attached on pre-defined components at specified locations in the form of *lumped mass*
- Certain amount of added mass distributed over pre-defined components in the form of a skin of **MAT9_MAT_NULL*. The density of the material is automatically calculated so as to result to the desired total weight
- The substitution of the detailed FE-representation of a component by an equivalent amount of mass distributed over the nearby components

After the realization of Mass Trim items with the pattern dictated by the *LS-Dyna Common Model* the *Common Model* has adopted a form suitable for the front-impact analysis.

Front-impact related items

The items added by the *LS-Dyna Common Model* are common for all the front-impact load-cases that may follow. Such items can be additional components, boundary or initial conditions, output requests and of course model checks. In this study, the first items to be added by the *LS-Dyna Common Model* are the additional components and the change of the detailed representation of certain components into a reduced one, suitable for the front-impact analysis:

- Passengers' mass: These mass elements of pre-defined value are added in the form of *lumped masses* and are attached specified components (i.e. seats, rear floor) with the aid of Mass Trim items.
- Instrumentation mass: This mass of pre-defined value is added in the trunk in the form of *lumped mass* and is attached to specified components, again using the Mass Trim items.
- Closures interior plastic components: The detailed FE-representation of these components is substituted by a *Trim representation*, spreading mass elements of an equivalent total weight over the nearby inner panel components (Fig.13)

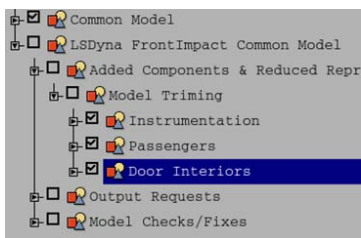


Fig.12. Front Impact added components

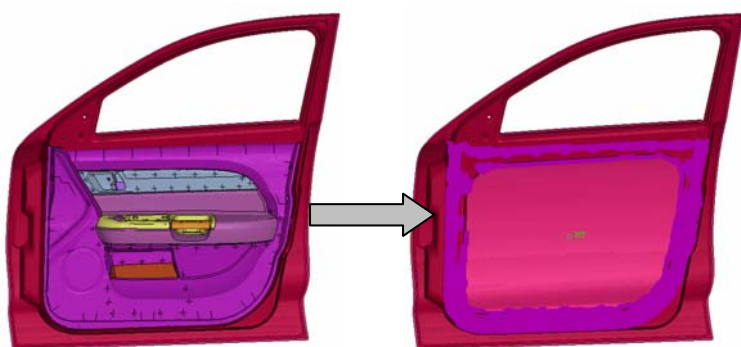


Fig.13. Trim representation created with the aid of Mass Trim items

The creation of section forces output requests, a tedious and time-consuming procedure, becomes really flexible and efficient with the use of Output Request Generic Entities. The positions, cutting planes and the components cut are pre-defined in the Output Request Generic Entities by the CAE analysis expert. Once defined, they can be applied during the Task execution with no extra input.

Output Request Generic Entities are also used for the positioning of accelerometer sensors at pre-defined locations. The representation of accelerometer sensors, again pre-defined by the CAE analysis expert, is stored as custom template in ANSA DM library (Table 3). Each output request definition contains information for the location and the connectivity of the accelerometer sensor to be created. Figure 14 shows the accelerometers and sections created by Output Request Generic Entities.

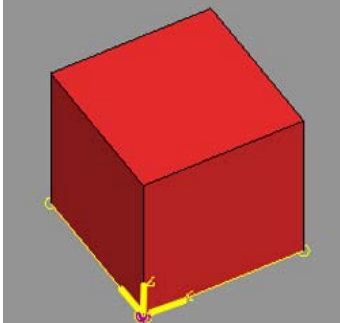
Template in ANSA DM	Description
	<p data-bbox="608 1610 1209 1641">*ELEMENT_SEATBELT_ACCELEROMETER</p> <p data-bbox="608 1713 1369 1809">Each accelerometer is attached on a 10x10x10 rigid hexa element. A mass element is attached to the accelerometer reference node.</p>
<p data-bbox="204 1937 1348 1960">Table 3. Custom template for accelerometer sensor retrieved from the ANSA DM library</p>	



Fig.14. Accelerometers and sections created by Generic Entities

After the addition of output requests, the model integrity is checked. Among the various available checks, the CAE analysis expert is flexible to add custom checks with the aid of user scripts. ANSA Task Manager does not proceed until all checks are successfully implemented. The checks performed at this stage for this study are summarized in Table 4.

Model check	Fix options
Rigid dependency	After the identification of rigid dependency errors, they can be automatically fixed from within ANSA Task Manager
Connectivity	Loose components are directly identified
Joints	The validity of joints definition is directly checked
Number of integration points	This custom made check assigns 5 IPs in case there are properties that reference less
Undefined materials	Material properties are automatically updated from the LS-Dyna material database retrieved from ANSA DM

Table 4. Model integrity checks in *LS-Dyna Common Model*

After the implementation of model checks and the correction of possible errors the *LS-Dyna Common Model* is ready (Fig.15). The model built up to this stage can be used for the creation of any LS-Dyna front-impact load-case.

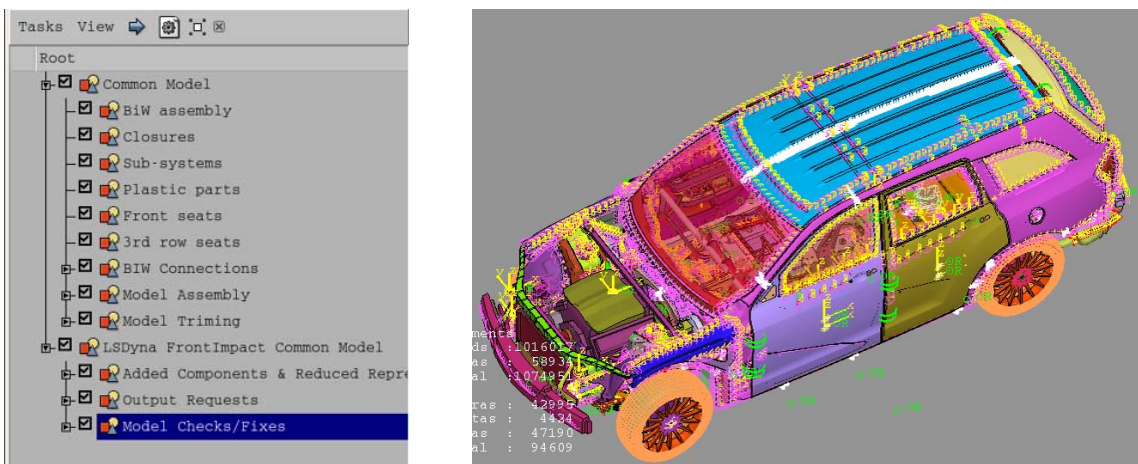


Fig.15. LS-Dyna front-impact common model completed

PAM-CRASH Common Model

The *Pam-Crash Common Model* for the side-impact load-cases is very much alike the *LS-Dyna Common Model* with respect to the work-flow. At a first step, the *Pam-Crash Common Model* “transforms” the *Common Model* in a form suitable for side-impact analysis. Then, it adds to the model certain solver dependant entities that are common for all the side-impact load-cases that may follow.

As soon as the *Pam-Crash Common Model* is invoked, the *Common Model* gets un-updated so that the user executes it again, with the conditions dictated by the *Solver Common Model*.

“Transformation” of the Common Model

With the aid of the Part Representation Manager, the *Common Model* sub-models adopt a mesh representation suitable for side-impact analysis, as shown in figure 16. The mesh representation of each component is invoked from ANSA DM.

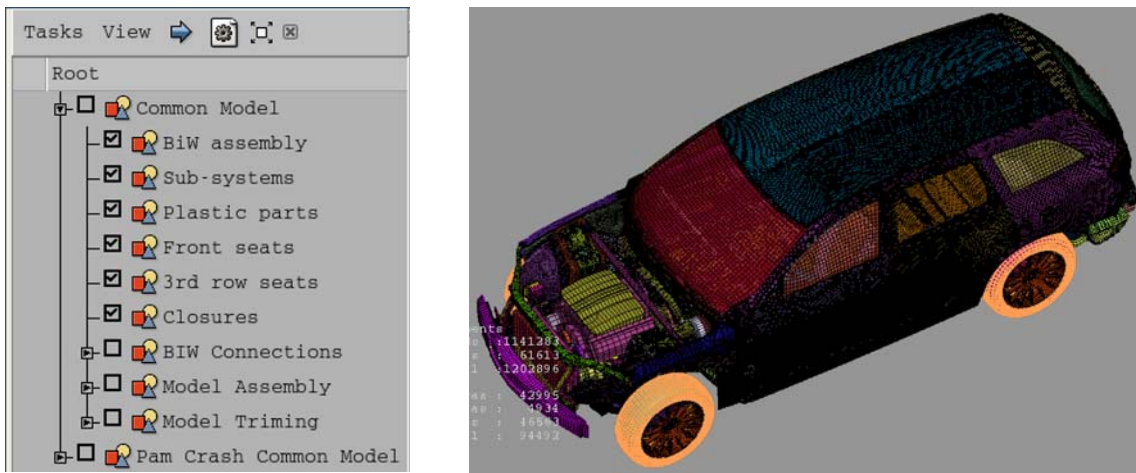


Figure16. Side-impact mesh representation for Common Model sub-models

The BiW Connections are “realized”, getting a suitable FE-representation. Again, the user is guided by annotations for the attributes of the connection elements that will be created by the Connection Manager. The spot weld points and curves are realized as PLINK elements (Fig.17), the adhesive lines as HEXA-CONTACT and finally the bolts with rigid interface and rigid body.

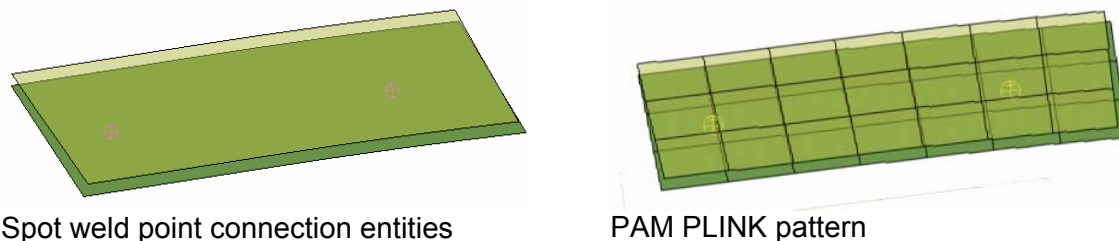


Fig.17. Realization pattern of BiW connections: Spot weld points

For the Connector Entities, which take care of the kinematic constraints between components, proper templates are retrieved from the ANSA DM libraries. KJOIN, BEAM and SPRING elements with predefined properties are used this time.

Finally, the Mass Trim items are realized as ADMAS entities, either distributed over components or as lumped masses with RBODY interface.

Side-impact related items

The items added by the *Pam-Crash Common Model* are common for all the side-impact load-cases that may follow. Starting from the additional components, again the passenger's mass and the instrumentation mass are added with the aid of *Mass Trim* items. The closure inner plastic components are also turned into the reduced *Trim* representation.

Section forces output requests are created with the aid of pre-defined Output Request Generic Entities.

Finally, the integrity of the model is checked with the aid of built-in and custom checks. The CAE expert who built the task has pre-defined the checks that must be performed prior to the load-case dependant entities addition (Table 5).

Model check	Fix options
Rigid dependency	After the identification of rigid dependency errors, they can be automatically fixed from within ANSA Task Manager
Connectivity	Loose components are directly identified
PLINKs	The validity of PLINK elements definition is directly checked
Number of integration points	This custom made check assigns 5 IPs in case there are properties that reference less
Undefined materials	Material properties are automatically updated from the Pam-Crash material database retrieved from ANSA DM

Table 5. Model integrity checks in *Pam-Crash Common Model*

After the implementation of model checks and the correction of possible errors the *Pam-Crash Common Model* is ready (Fig.18). The model built up to this point can be used for the creation of any Pam-Crash side-impact load-case.

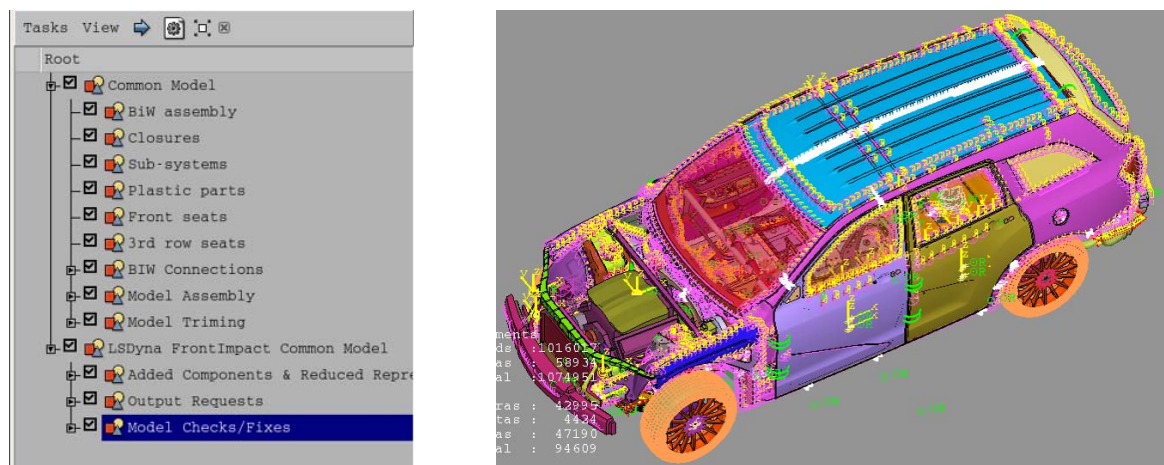


Fig.18. Pam-Crash side impact common model completed


6. THE SOLVER LOAD-CASE

All the entities that differentiate the front-impact load-cases from each other are added by the *Solver Load-case* group of items. This Task is again invoked from the ANSA DM data pool. The most important aspects of the *Solver Load-case* Task are outlined below:

- Solver controls: The solver controls are set-up once for each load-case by the CAE analysis expert and are safeguarded in the Task
- Contact interface cards: The contact interface cards, along with their parameters, are set-up once during the Task build-up. During the Task execution, Task Manager automatically fills the contact sets and there is no need for user-intervention in the contact definition.
- Barrier file definition and positioning: The barrier file to be used in each load-case is pre-defined in the *Barrier Positioning* item of ANSA Task Manager along with information for the positioning procedure. During the Task execution, the barrier is retrieved from the ANSA DM data pool and is automatically positioned and de-penetrated according to the load-case specifications.
- Rigid road: The attributes of the rigid wall used as the boundary road are saved along with the Task.
- Initial velocity and acceleration field: The solver cards parameters are defined once by the CAE analysis expert. There is no need for user intervention during the Task execution, since Task Manager automatically fills the sets referenced in these cards with the appropriate entities
- Model checks: The model is checked prior to the output with respect to load-case specific entities definition.

Front-impact 40% offset 64km/h with LS-DYNA

All the aforementioned *Solver Load-case* attributes find application in the front-impact load-case. Additionally, in this *LS-Dyna Load-case* nodal time history is requested at pre-defined locations with the aid of Output Request Generic Entities. The custom representation of these output requests is retrieved from the ANSA DM library (Table 6).

Template in ANSA DM	Description
	*DATABASE_HISTORY_NODE_SET
Table 6. Custom template for nodal time history retrieved from the ANSA DM library	

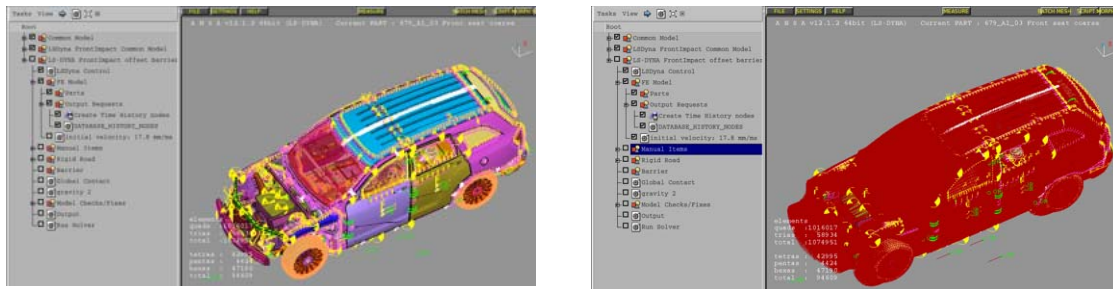


Fig.19. Addition of time history nodes and initial velocity

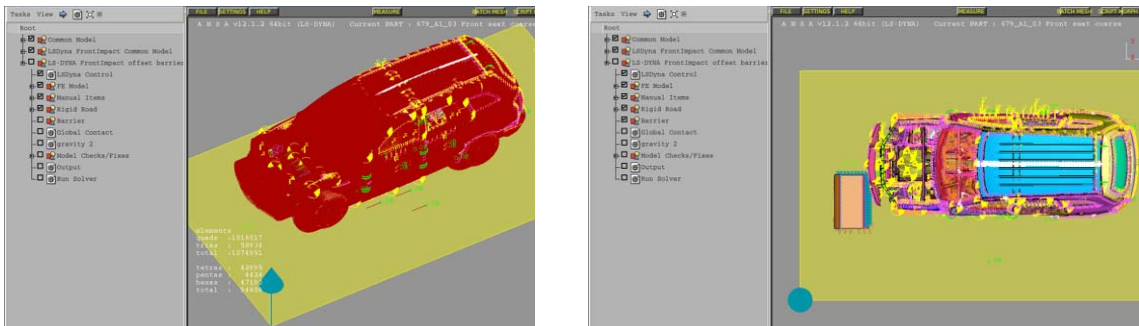


Fig.20. Addition of rigid-road and front barrier

Figures 19-20 show the items added sequentially by the *LS-Dyna Load-case*.

The *Barrier Positioning* tool assures that the barrier will be positioned properly relative to the vehicle body, with no penetration between them. Figure 21 shows the *Barrier Positioning* control card, which requires the minimum information for a front-impact load-case.

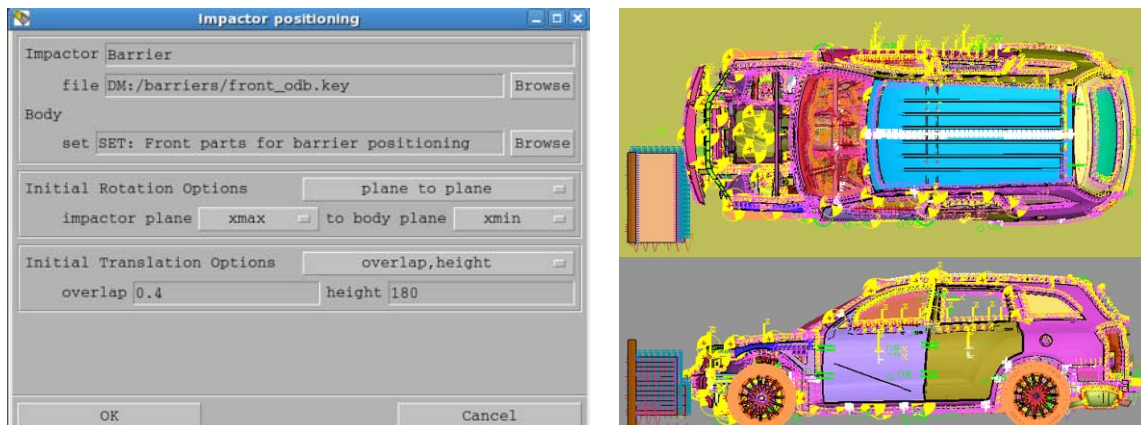


Fig.21. Barrier positioning: Pre-defined set-up of offset and height

Finally, the global contact definition and gravity are added and the model is checked with respect to load-case specific definitions. After the execution of model checks, the analysis model is ready for output. The complete model is shown in figure 22.

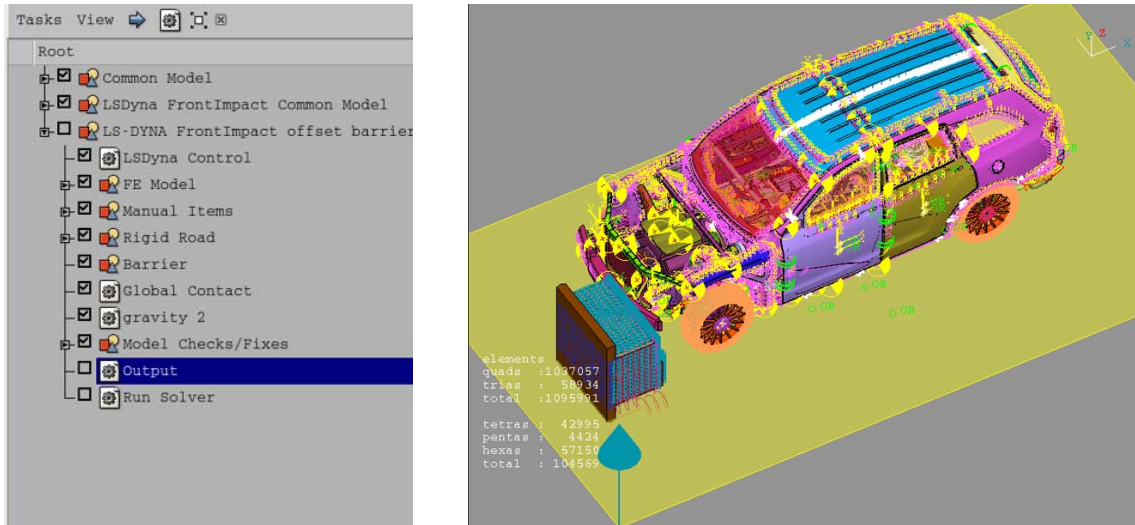


Fig.22. LS-Dyna Front-impact 40% offset 64km/h complete model

Side-impact 50km/h with Pam-Crash

Load-case specific entities are added in the *Pam-Crash Load-case*, in the same manner as in the front-impact case. The following images show the sequential addition of load-case specific entities.

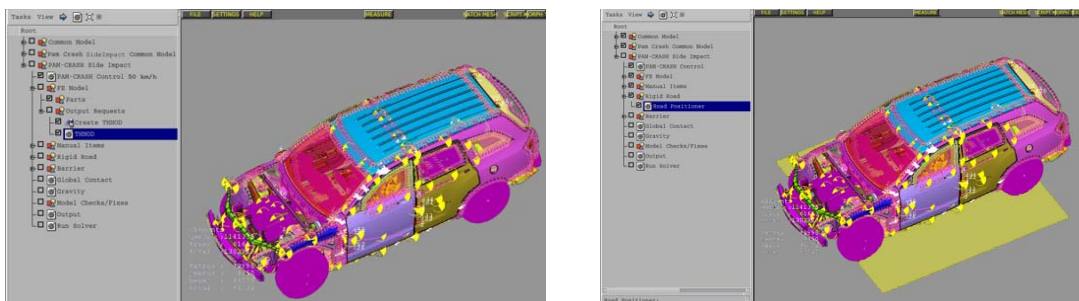


Fig.23. Addition of time history nodes and rigid-road

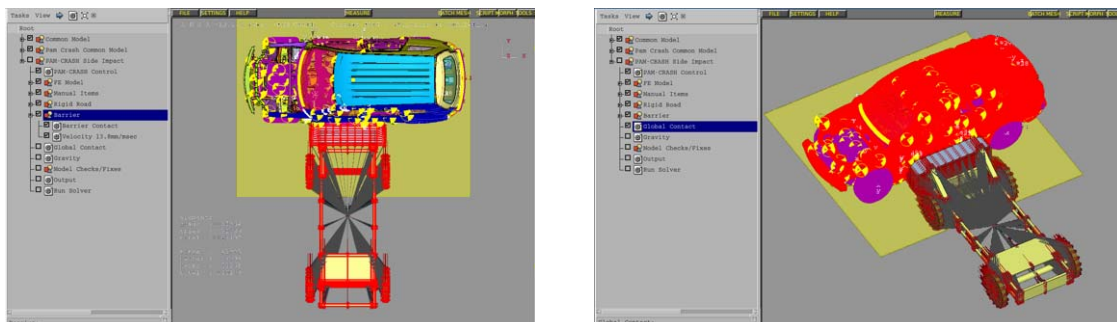


Fig.24. Positioning of the barrier and definition of the vehicle-barrier contact
Addition of vehicle global contact and barrier initial velocity

Finally, the gravity acceleration field is added and the model is checked with respect to load-case specific definitions. After the execution of model checks, the analysis model is ready for output. The complete model is shown in figure 25.

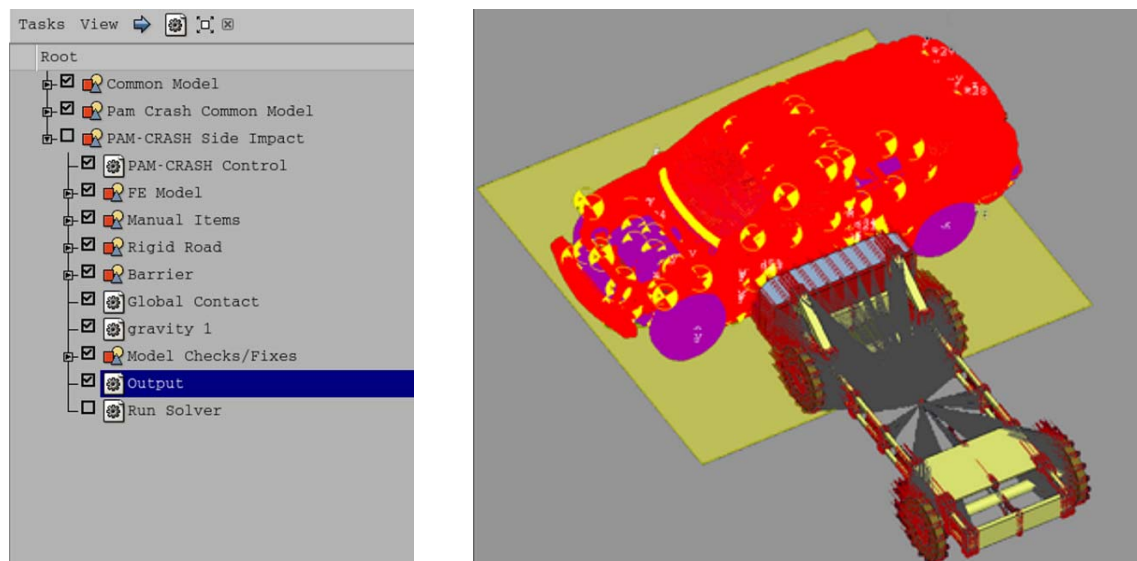


Fig.25. Pam-Crash Side-impact 50km/h complete model

7. CONCLUSIONS AND REMARKS

The data organization and process standardization necessary for the demanding task of crash-test simulation models build-up can be achieved with the use of ANSA Task Manager in combination with ANSA Data Management. With the aid of ANSA Task Manager, OEMs can safeguard the model quality and promote knowledge transfer, capturing the best-proven practices for the analysis model build-up as a sequence of modeling actions. ANSA Data Management assures the organization of all data, storing them in a structured form under a common location, enabling their easy retrieval by Task Manager.

Tasks in Task Manager are created by the CAE analysis expert, who collects all the modeling actions and considerations that must be taken into account during the model build-up and interprets them as distinct task items. The completed tasks are saved in ANSA DM as template processes and can be reused for application on the vehicle model assemblies.

ANSA DM libraries carry custom template definitions for connectors, output requests and boundary conditions, assuring that model entities are defined with the proper parameters. Multi-parametric solver cards (e.g. contact definitions, initial velocity, acceleration field, solver controls) are incorporated in ANSA Task Manager with parameter values set by the CAE analysis expert, eliminating error-prone procedures and promoting the model robustness.

During the execution of pre-defined Tasks, ANSA Task Manager makes sure that all task items are properly executed, considering at the same time possible dependencies between them. The validity of model entities definitions is checked prior to the output with the aid of various built-in check algorithms. The model quality is safeguarded and the build-up of crash-test simulation models becomes fast and efficient.

REFERENCES

- (1) Georgios Nikolaidis, Dimitrios Zafeiropoulos, Konstantinos Ntamagkas, "Building discipline specific FE-models with the Common Model concept", 2nd ANSA-μETA International Congress.

CRASHWORTHINESS DESIGN OF ANSALDOBREDA LIGHT METRO VEHICLE

¹Luca Lenzi*, ¹Stefano Raiti

¹AnsaldoBreda, Italy

KEYWORDS - crashworthiness, 15227, crumple, absorption, metro

ABSTRACT - The latest revisions of prEN15227 introduced new strong requirements related to the lifting of the axles mounted on the bogies of the impacting vehicles. This work describes the methodology applied by AnsaldoBreda to demonstrate the compliance of its new Light Metro Vehicle to all the prescriptions stated in prEN15227. Starting from the main idea of the train configuration, the passages needed to define the final layout of the adopted energy absorption devices have been illustrated. The whole model has been realized with BETA CAE Systems' ANSA and consists of a FEM description of the vehicle VS vehicle crash scenario, with initial vertical offset. The models of the leading cars, belonging to the two impacting metro units, embody the sacrificial crumple elements, the automatic coupler and the bogies. Due to the fundamental role covered by the bogies, both in the dynamic behaviour of the vehicle and in the analysis of the vertical movements of the axles, a special attention has been dedicated to the development of their models. The whole final model consists of about 1400000 elements, the simulations have been performed with LSTC LS-Dyna X64 solver and the post processing of results has been carried out with LSTC LS-Post and BETA CAE Systems' μETA PostProcessor.

TECHNICAL PAPER -

1. INTRODUCTION

A modern rolling stock must not only fulfil the traditional static load and fatigue requirements, but also the passive safety requirements. These crashworthiness requirements must be considered in the design of the coach structural part of the vehicle.

Sophisticated crashworthiness analysis are today a regular step in the engineering process of developing a new train, AnsaldoBreda has employed the explicit finite element to perform crashworthiness analysis for about ten years.

Vehicle crash is a dynamic phenomenon featuring a complex interaction between structural and inertial behaviour. It is generally recognised that in a typical collision the end structure first experiences the impact and only successively it may undergo some deformation in the impact region itself. The passengers experience later the effect of the impact. The first phenomenon is normally referred to as primary collision and the second type of events, related to the passengers, are normally referred to as secondary collision.

Due to geometrical complexities of rail vehicle structures and to the complicated behaviour of the materials when involved in large plastic deformation, finite element computer programs with elastic-plastic dynamic analysis capabilities have to be used.

The structures in the front end of the first car are located in the impact region thus they should deform so as to dissipate a large amount of crash energy through plastic deformation of its part. The axial load carrying capabilities and force-deflection curves for the end structure parts are also obtained by the use of a finite element code considering both geometrical's and material's non-linearities.

The crashworthiness behaviour in a crash event of the Thessaloniki Automatic Driverless Light Metro has been analysed by means of a Finite Element Model (FEM). This document explains the methodology used to achieve, on the various components of the metro unit, the desired results in terms of forces, energies and deformation patterns, in compliance to the crash safety requirements stated on the Technical Specification of Thessaloniki Metro (1) and on prEN 15227 (2).

Since the front ends of the leading motorcars undergo the very first impact, energy absorption devices have been placed directly on the train's fronts. These structures, which serve as energy absorbers, are the result of many calculations and experiences coming from earlier projects.

The Light Metro unit will have a maximum speed of 80 km/h, it consists of four cars arranged as follows: two end cars with cabin and two intermediate, supported by four motor bogies and one, in central position, trailer bogie.

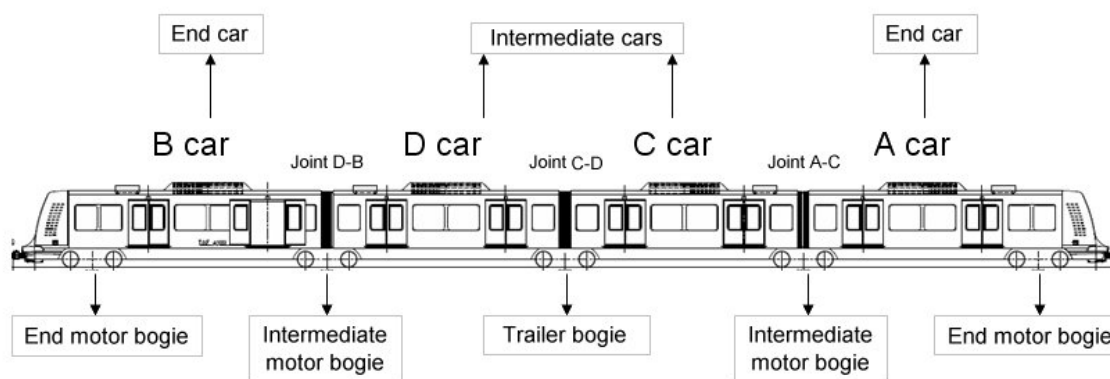


Figure 1 - Metro unit's layout

For the simulation the entire A motorcar has been modelled as deformable 1D, 2D and 3D elements, while the remaining cars have been simulated by means of lumped masses connected by springs of suitable stiffness; the connection between cars is obtained by the use of a rigid spherical joint whose upper and lower sides are mounted on the adjacent cars' ending beam.

The main conditions that shall be applied for the crash scenario object of this study are as follows:

- Frontal collision with initial vertical offset, between the two units, of 40 mm
- Straight track
- Relative speed of 25 km/h
- Two identical metro units impacting
- Considering the contribution, in term of masses, supplied by all seated passengers

Undergoing all the conditions written above, the cabin and the carbody of the cars belonging to the impacting metro units shall not be deformed.

1.1 DESCRIPTION OF THE MODEL

The FEM models have been prepared using the ANSA pre-processor by BETA CAE Systems, starting from the 3D CAD drawings. The whole model consists of about 1400000 elements of which more than 1,000,000 are deformable. To run such an analysis the LS-Dyna explicit code by LSTC has been used. This solves the dynamic equations of motion with a suitable numerical integration procedure and is able to perform a stress/strain analysis by taking into account the strain rate effects and the materials' failures and non-linearities. The analysis results provide information about force-time contact curves, decelerations, energies' levels. Moreover they give a qualitative evaluation of the collapse path of the sacrificial structures and of the dynamic and cinematic behaviour of the whole vehicle.

Considering the accuracy of the model, the articulated bogies which are not symmetrical and the expected not fully symmetrical and/or synchronized deformations between the left and right sides of the vehicles, it was impossible, to reduce calculation times, to perform the simulation using the symmetry along the entire vehicles. The size of the mesh has been chosen in agreement with the small or large deformations expected on the various elements. This means that the areas undergoing large deformations have a finer mesh than those ones where small or negligible deformations are expected. The deformable shell elements' side lengths are in the range between 5 and 30 mm.

The numerical model of the entire metro unit is composed by a certain number of subsets, of which the main are: the coupler, the energy absorbers, the bogies, the cabin and the carbody. FEM model is composed of:

- The leading's car carbodies
- The leading's car cabins
- The absorbers mounted on leading cars
- The automatic couplers mounted on leading cars
- The motor bogies
- The rail
- A series of beam elements with appropriate stiffness that play the role of the remaining train rake of each unit

The carbodies are light structures made of welded aluminium alloy's extrusions. The intermediate cars are symmetrical, while the ending cars have a front end designed to allow the mounting and the fastening of the cabin.

The cabin is a complex frame of high resistance steel tubes and plates. The cabin, in the chain of the transmission of the impacting loads, is the first structure that should not deform, due to that a lot of time was spent for its design and its optimization.

The automatic coupler can absorb energy thanks both to a regenerative device and to a not-regenerative device. Usually the regenerative device absorbs energy depending on the impacting speed: the more its characteristic curve becomes rigid the more the impacted speed grows. Consequently it is preferable not to take into account that element in the simulations of crash, because in real conditions, its contribution is very small in comparison to the levels of energy absorption.

The front couplers' heads are made of shell elements, that schematization was needed in order to simulate the contact one against the other. The draft gears, instead, have been simulated with beam elements, whose characteristic curves "stroke vs. force" are such that, after the absorption stroke related to the nominal compression force, there is a peak of force working as shear out and then a free stroke related to a zero value of force. That way of modelling the coupler, with its different phases of work, allows to describe in detailed way the cinematic and dynamic behaviours of the impacting vehicles.

The absorbers are sacrificial elements that are designed selecting the best compromise between shape and weight, in order to make them to deform in a controlled manner converting kinetic energy in deformation energy with high levels of efficacy and efficiency. The new requirements imposed by the latest draft of prEN15227 (2) are the reasons why a new generation of absorbers has been developed, to permit them to keep their stability not only under axial compression loads generated during an impact with vertical offset.

In the metro unit being studied there are two kinds of bogies: the motor bogie and the trailer bogie. Since it has been fully modelled only the leading A cars, were needed to study accurately only the motor bogie on which the A carbody is rested. Moreover, being the bogies very heavy and away from the impact point, they are very important for the calculation and above all for the cinematic and dynamic behaviour. Starting from these considerations, the bogies' FEM models are made up by a group of rigid parts with their right masses and inertial properties. Each part of the bogie is free to move with respect to the others, as it actually happens by the interposition of elastic and/or viscous elements.

Each bogie is composed of:

- Bolster beam simulated with rigid body
- Bogie frames simulated with rigid body
- Wheelset simulated with rigid body
- Traction Rod simulated with solid elements
- Motors and gearboxes simulated with rigid body
- Resilient wheels simulated with both rigid body and elastic spring
- Shock absorbers, primary suspension, secondary suspension, elastic elements between traction rods and chassis, gearbox's and motor's elastic supports, everyone simulated with elastic spring.

Since the latest versions of prEN15227's new requirements focused on the overriding risk linked to the lifting of the wheelsets during the impact, the anticlimbers and the bogies, have been simulate very carefully. A specific requirement in fact, imposes that: "the vertical displacement above the rail, of at least one wheelset on each bogie, shall be no more than 75% of the nominal flange height".

Main equipment contribute, in term of mass, has been spread on the vehicle structure, while the passenger's mass has been simulated with lumped masses placed on the frame of the car. Lumped masses have been also used to simulate the B, C, D cars and the remaining three bogies of each metro unit.

1.2 UNITS OF MEASUREMENT AND REFERENCE SYSTEMS

The units of measurement applied are:

Mass:	kilogram (kg)
Length:	meter (m,mm);
Time:	second (sec,msec)
Force:	Newton (N,KN)
Energy:	Joule (J,KJ,MJ)

Reference systems:

- Global Cartesian orthogonal for nodes;
- Local Cartesian orthogonal for elements.

1.3 CRASH SCENARIO

As required in the Technical Specification Thessaloniki Metro (1) the analysis are based on the assumption that a AW1-loaded Metro unit impacts against another one in standing conditions, with a relative speed of 25 Km/h (AW1 represents the sum of the vehicle's tare mass and of the all seated passengers' mass). The crash happens in a straight section of the track and, in order to respect the 40 mm of initial vertical offset as stated in prEN15227 (2), (due i.e. to different wheels' level of worn and/or dynamic effects), the standing unit have been placed 40 mm under the nominal height condition. The initialization of the velocity field of the impacting unit has also taken into account the rotational velocities of the wheelsets.

2. CHARACTERISTIC OF MATERIALS

The carbody structure is constituted of aluminum alloy, while the cabin and the absorbers are made of high resistance steel. For all structural material it has been used the “*MAT_PIECEWISE_LINEAR_PLASTICITY” from LSDYNA library. For the materials interested by large deformations, basically the sacrificial elements, the major accuracy is presented. That material has been characterized with the Cowper-Symonds parameters obtained by last AnsaldoBreda's test series.

3. DESCRIPTION OF THE CONTACTS

The types of contacts used in the analysis are:

- *CONTACT_AUTOMATIC_SURFACE_TO_SURFACE between the wheelsets and the rail
- *CONTACT_AUTOMATIC_SURFACE_TO_SURFACE between the couplers' heads
- *CONTACT_AUTOMATIC_SURFACE_TO_SURFACE between the two couples of absorbers
- *CONTACT_AUTOMATIC_SURFACE_TO_SURFACE between the interfacing plates cabins/carbodies
- *CONTACT_AUTOMATIC_SURFACE_TO_SURFACE secondary suspension's vertical stop
- *CONTACT_AUTOMATIC_SINGLE_SURFACE between the shell elements of the absorbers
- *CONTACT_AUTOMATIC_TIED_SURFACE between the solid modelled anticlimber plate and the shell modelled absorber

4. ANALYSIS RESULTS

The first absorption stage is provided by the automatic couplers' buffers, they absorb about 390 kJ; at the end of the not-regenerative stroke the force increases and when it is over the limit value of the shear out device it detaches from its plate. After the automatic coupler's extrusion the anticlimbers of the absorbers engage and the lateral crumple elements start their compression. The crumple elements work in series, it means that after an initial trigger the second one start to crush only when the first one reaches the total compression stroke. At the end of the crash phenomenon there is the elastic rebound of the involved structures and the anticlimbers disengage.

When the absorbers engage the vertical offset between their teeth is grown from the initial 40 mm (when there is the impact between coupler heads). This is due to the pitching movements of the leading cars originated by the forces acting on the coupler mounting plate in the first phase of absorbing.

4.1 ENERGY BALANCE

The initial kinetic energy has been transformed as shown:

$$E_{kin0} = E_{int} + E_{kin1} + E_{sd} + E_{sl} + E_h$$

where:

E_{kin0} = Initial Kinetic Energy (of the moving vehicle)

E_{int} = Internal Energy

E_{kin1} = Residual Kinetic Energy (of the two vehicles)

E_{sd} = Spring and damper energy

E_{sl} = Sliding energy

E_h = Hourglass energy

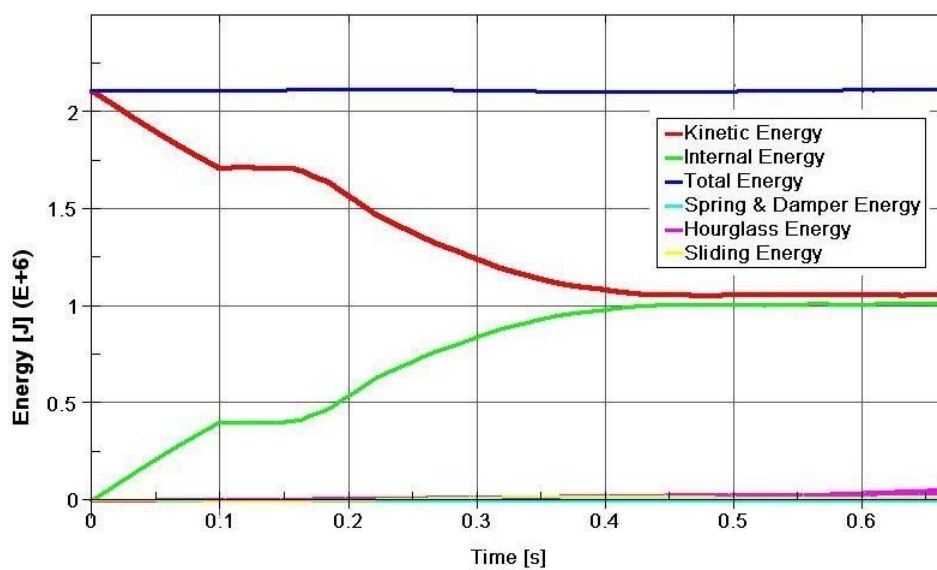


Figure 2 - Net accelerations

Here are reported the values of the energies.

We can consider that the crash phenomena regarding the front parts of the leading cars are ended after 500 ms.

$E_{kin0} \approx$	2.13 MJ	$t = 0$ ms
$E_{couplers} \approx$	388 KJ	$t = 500$ ms
$E_{absorbers} \approx$	566 KJ	$t = 500$ ms
$E_{kin1} \approx$	1.065 MJ	$t = 500$ ms

4.2 ACCELERATIONS

A fundamental parameter in crash analysis is the magnitude of the accelerations undergone by the vehicles (and their occupants) during the impact. Accordingly to prEN15227 (2) the method of determining the mean deceleration for the vehicle shall correspond to the time since when the net contact force on the vehicles exceeds zero, until when it falls again to zero. Notice that the net contact force shall be calculated as the algebraic sum of the longitudinal forces acting on opposite ends of the vehicle. The accelerations curves have been obtained as stated in (2) for the two leading cars (that are the ones experiencing the highest levels of acceleration), while for the 1D modelled remaining cars the accelerations on the joints' node have been plotted.

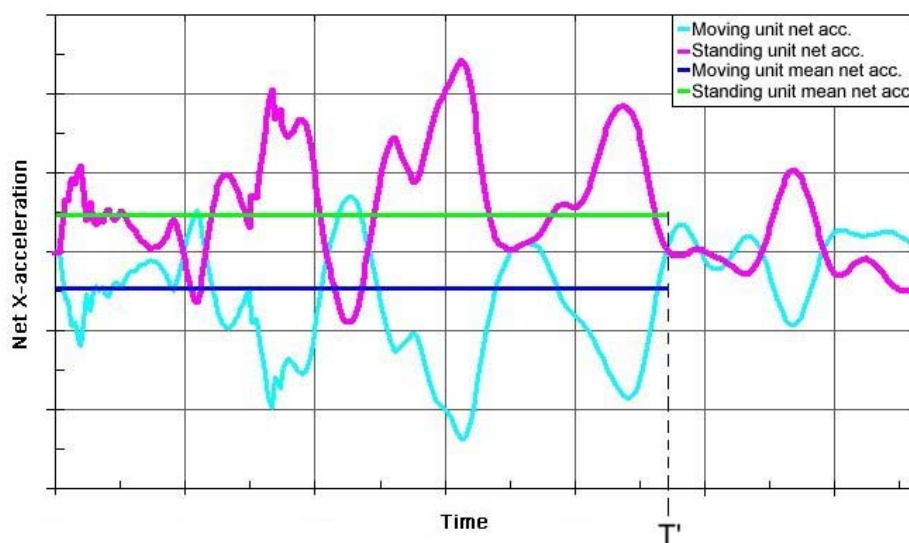


Figure 3 - Net accelerations

The accelerations undergone by the leading cars have been evaluated scaling the net contact forces with the masses of the respective cars. The masses considered are the sum of leading cars and of the first two bogies, because those are the elements that undergo the net force.

4.3 BOGIES

First the connection between bolster beam and chassis (provided by the traction rods) and the supports of bogies's equipments was investigated. The level of accelerations and forces prove that not failure or excessive deformations are reached.

The second goal to achieve was to demonstrate the compliance of the vehicle to the overriding requirements. Due to the design of the bogies, which have an articulated chassis, first the vertical displacement of each wheel had to be investigated. Then accordingly to (2), where only the complete wheelset is taken in to account, a mean value between the two wheels mounted on each axle of the bogies has been calculated. The vertical displacements, estimated as above, demonstrate that the wheelsets (and also the single wheels) undergo negligible liftings. The absence of large vertical displacement ensures that there are not derailment risks.

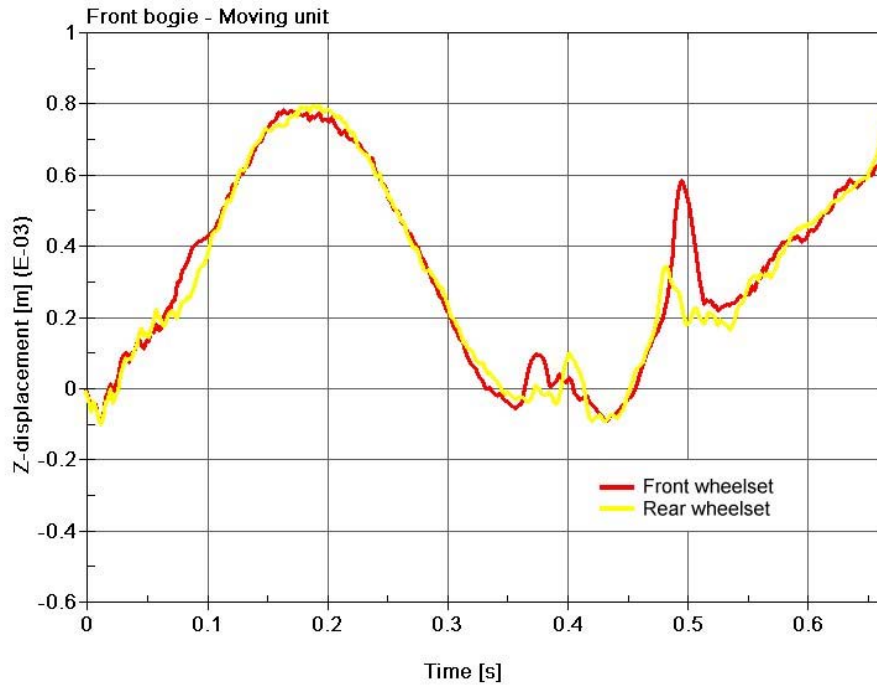


Figure 4 - Front bogie of moving unit

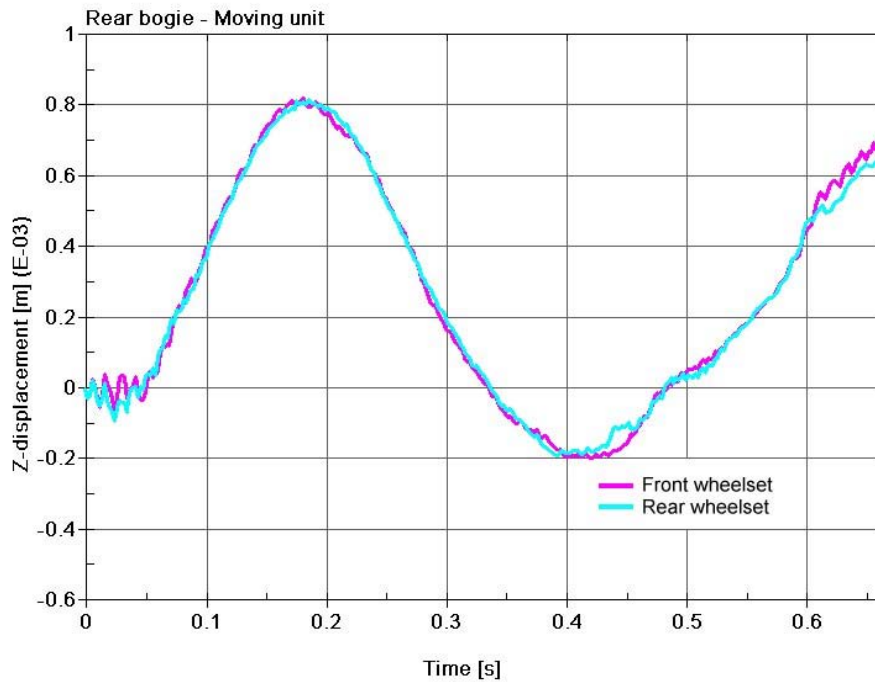


Figure 5 - Rear bogie of moving unit

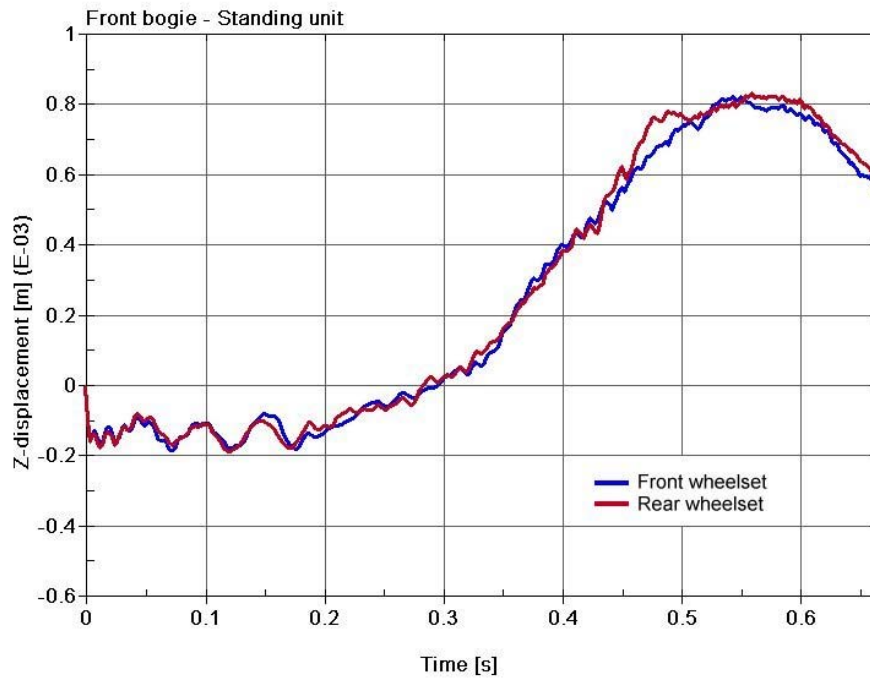


Figure 6 - Front bogie of standing unit

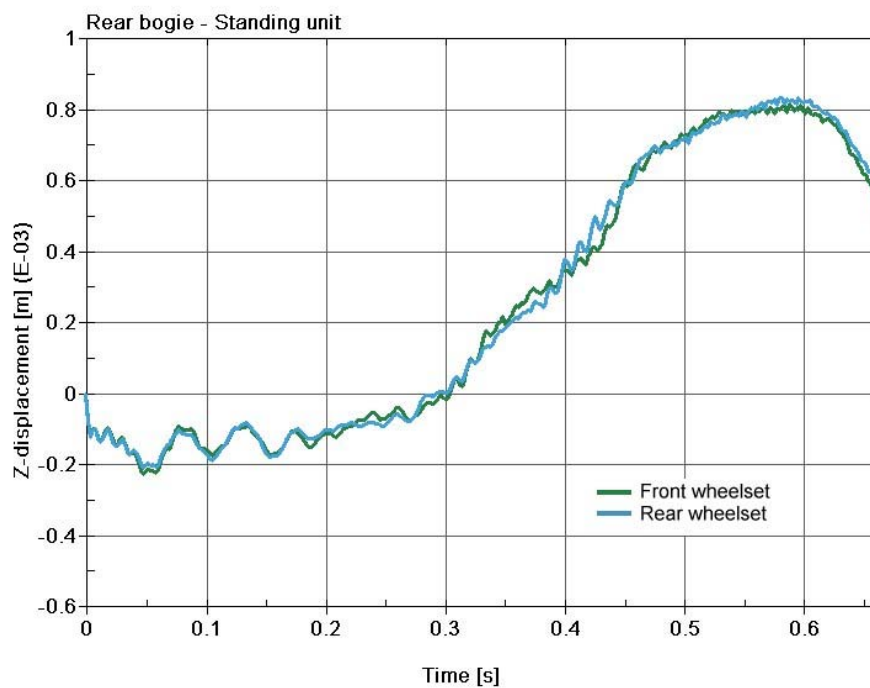


Figure 7 - Rear bogie of standing unit

5. CONCLUSIONS

The architecture of the front end results able to absorb the total amount of energy related to the crash scenario, without overloads on the cabin and on the carbody.

The cabin, the carbody and so the passengers involved in the collision undergo accelerations far minor than the maximum acceptable, while the structures of cars are affected by negligible deformations.

The anticlimbers devices placed on the absorbers first of all avoid the risks of overriding between cars, on the other hand they allow the remarkable fact that wheels keep in contact with the rail during all the event of crash.

Due to what is written above, the vehicle results compliant to the Technical Specification of Thessaloniki Metro (1) and the prEN 15227 (2).

REFERENCES

- (1) ATTIKO METPO A.E., "Technical specification Thessaloniki Metro", December 2004
- (2) European Standard - prEN 15227 - "Railway applications - Crashworthiness requirements for railway vehicle bodies" - Draft January 2007.

A CAE Tool for Processes Optimization According to FMVSS201U

¹Peter Williamson*, ²Lambros Rorris

¹P+Z Engineering GmbH, Germany, ²BETA CAE-Systems S.A., Greece

KEYWORDS – FMVSS201u, ANSA, ABAQUS Explicit, FMH

ABSTRACT – Project work being conducted at P+Z Engineering has resulted in the need to develop a tool to aid in the FE-Simulation in accordance with Federal Motor Vehicle Safety Standard 201u commonly known as FMVSS201u. The task was to automate the alignment process of the Free Motion Head Form. The Free Motion Head Form is the test body for the interior impact testing.

Due to the large number of impact points on the vehicles interior that are required for testing, the determination of the impact points and the correct alignment of the free motion head form are extremely time consuming tasks. Priority was placed on developing an efficient process accompanied by a reliable tool to aid in the automation of this process.

ANSA has been and is currently being delivered with features which automate the alignment of the Free Motion Head Form on the vehicle interior trim. Additionally solver interfaces that export the necessary transformation cards allowing for quick and easy implementation of the alignment information into a full scale finite element model have also been incorporated.

This paper aims to shed some light on the complexity of the FMVSS201u standard and what aspects also need to be considered when setting up simulation models before hardware testing has started. The new features added into the ANSA FMVSS201 Safety Tool will also be described.

TECHNICAL PAPER -

1. INTRODUCTION

At the start of the last decade leading up to the turn of the century it became apparent that unrestrained occupants in automobile accidents were suffering major head injuries as a result of the impact against the vehicles interior. In order to ascertain the cause of these injuries The National Highway Safety Administration (NHSTA) began its work.

Results of studies carried out showed that impact occurred on points of the upper roof, upper side rails and pillar areas. In order to reduce the risk of severe head injury a legal requirement was developed with the objective being to commit automobile manufactures to setup the car interior as “energy absorbing” as possible. The standard FMVSS201U (Federal Motor Vehicle Safety Standard, Upper Interior) began on 1. September 1998 and became law, with exceptions, in the USA on 1. September 2002.

The FMVSS201U test procedure TP201U-01 involves the use of a modified Hybrid III 50%ile head form commonly known as the FMH (Free Motion Head Form) for use in high impact testing against vehicle interior components. The procedures describe how to position the FMH, how to find the required impact points inside the test vehicle and the impact speed required for the desired impact point. An accelerometer in the FMH measures the acceleration during impact and rebound. The HIC(d), Head Impact Criteria - dummy, is then calculated in order to measure the severity of the impact.

$$HIC = \max_{t_1, t_2} \left[\left(\frac{1}{(t_2 - t_1)} \int_{t_1}^{t_2} a dt \right)^{2.5} (t_2 - t_1) \right]$$

$$HIC_{dummy} = 0.75446 HIC_{FMH} + 166.4$$

In order to increase efficiency and aid in the all phases of a vehicle development program simulation teams are called upon, using the Finite Element Method, to help optimise many aspects of vehicle structural behaviour. FMVSS201U tests are currently being successfully carried out on virtual near to full vehicle finite element models. Together Beta CAE Systems S.A. and P+Z Engineering GmbH have developed and are continuing to improve a CAE tool which aids in generating the necessary data required for the “worst case” alignment, highest HIC(d) value, during impact of the Free Motion Head Form. This paper aims to shed some light on the complexity of this problem and show how new developments continually being incorporated in ANSA aid in finding the “worst case” impact for the FMH.

Motivation

The change in crash code from PAM-Crash to ABAQUS Explicit resulted in the need for new innovative tools to aid the automated generation of CAE models, their submission and reporting. ANSA having already a comprehensive interface for the features offered in ABAQUS Explicit was suggested as a basis to build upon. Current project work at P+Z Engineering provided the perfect opportunity to work together with Beta CAE Systems.

Due to the variability of the HIC(d) value that can be encountered when testing at any one point it is often necessary to vary the parameters used and in turn increase the number of tests carried out ant any one point. Parameters such as horizontal angle, vertical angle, although often fixed, and impact position in the Free Motion Head Form Impact Zone (FIZ) on the FMH and or interior components play a decisive role in the severity of the HIC(d) value. As mentioned previously it is required that the worst case HIC(d) value be found and therefore the worst case combination of the previously stated parameters.

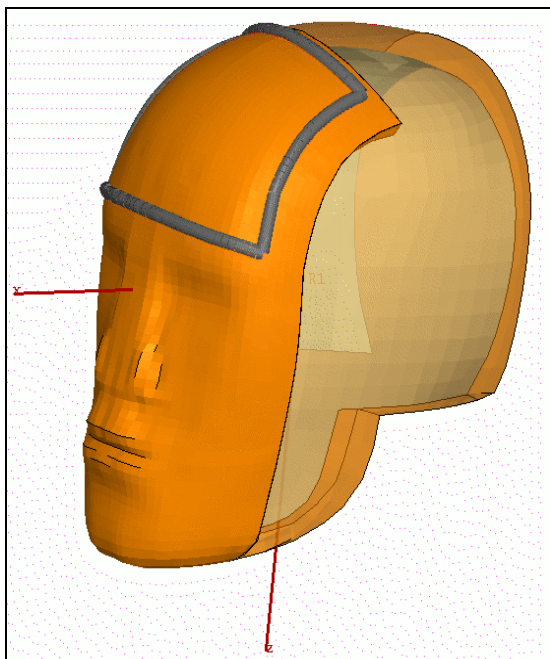


Figure 1.0 – Free Motion Head Form Front Impact Zone.

A standardised process was defined to increase efficiency during the creation of successive runs that are required to perform a full structural optimisation of the vehicle interior structure. Using this process it is possible to supply ANSA with the impact points on the interior vehicle trim surfaces and generate all required load cases and input decks. The user must not edit the input files himself.

Determination of the Impact Points in accordance with FMVSS201U

In order to generate complete documented procedure along with results, it is necessary to provide information gathered during the determination of the impact points. This information usually takes the form of a CATIA v5 / v4 format. Important is that the CG-F, CG-R and all impact points are clearly marked. The ANSA geometry engine currently possesses most of the features required for determination of the interior impact points. Work is currently being carried out in order to assess how much user input is required and how much of this input can be automated.

2. FMVSS201 SAFETY TOOL IN ANSA

FMH Alignment

Due to the complexity of modern motor vehicle interior structures the alignment procedure of the FMVSS201 Free Motion Head Form can become quite difficult and therefore needs to be described. The Figure below describes how to act when difficulties are encountered.

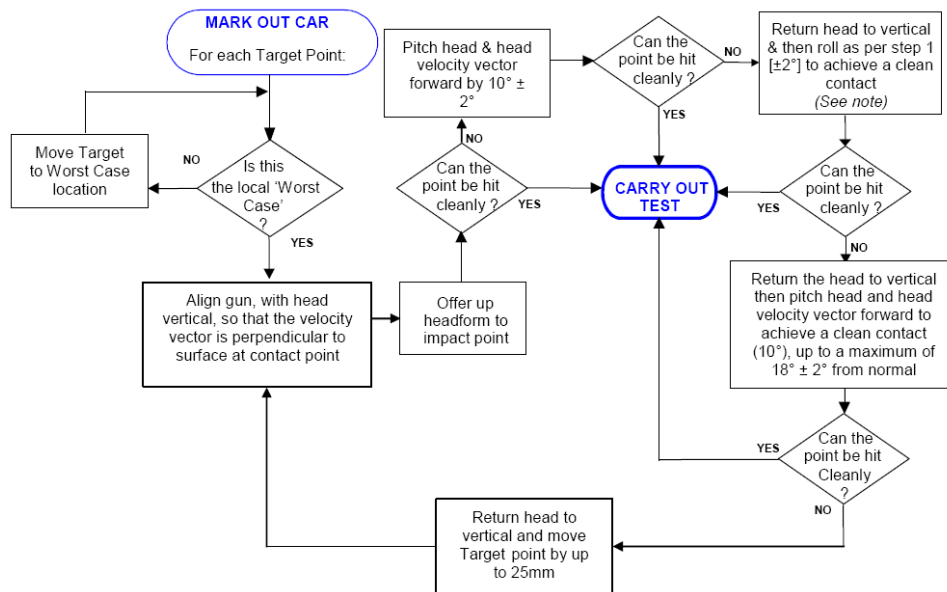


Figure 1.1: A free motion head form alignment procedure.

Finding the Horizontal Angle

As stated in table 1 of the FMVSS201U Laboratory Test Procedure seat belt mounting structures, door frame, A and B Pillars, the upper roof, rear most pillar all have predefined horizontal approach angle limits. The procedure defines a variable horizontal angle with an upper and lower limit. For the worst case HIC(d) value the corresponding horizontal angle must be found. The FMVSS201 Safety Tool developed and integrated in ANSA relies on an alignment algorithm to find the horizontal angle at which the midsagittal planes of the FMH and the interior trim surface line up. First contact between the Free Motion Head Form Impact Zone and the interior trim is, when combined with the previous step, also established. From this point onwards the vertical angle can also be calculated.

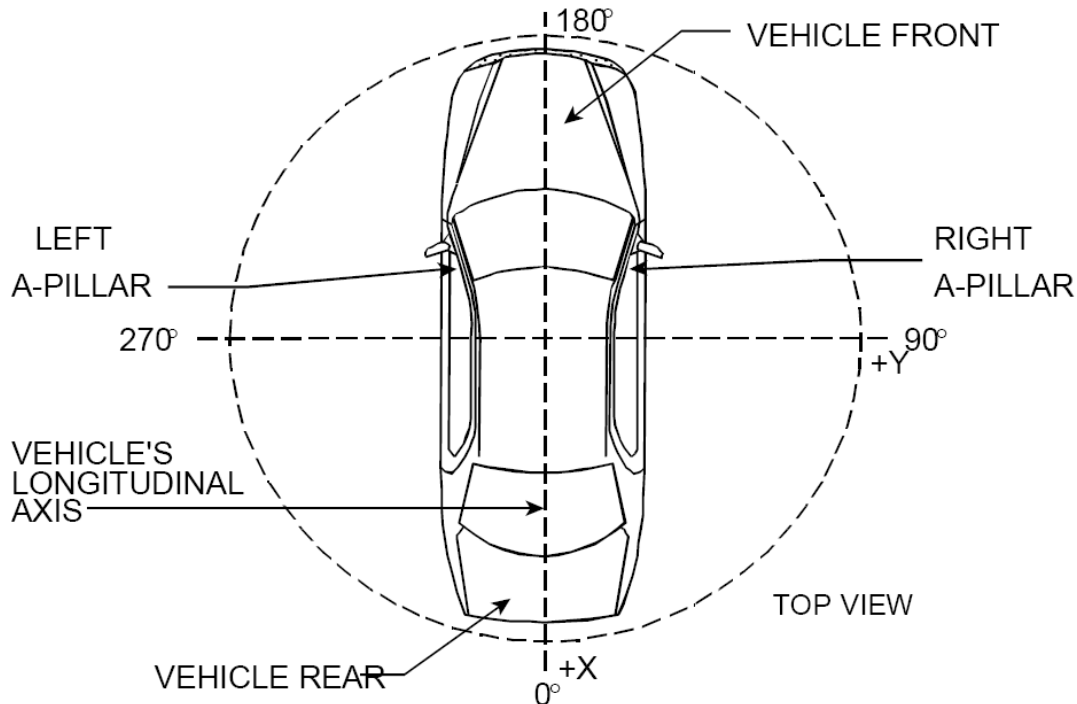


Figure 1.2: The vehicle horizontal angle reference frame.

Due to the complexity of the interior trim structure and the packaging behind, it is often required to use good “Engineering Judgement” in order to set the worst case for the horizontal angle. Based on the deformation of the trim structure and the subsequent impact against the BIW or packaging structure lining up the midsagittal planes of the FMH and trim at the impact point may not always represent the worst case. For this reason it is possible to manually set the limits of the horizontal angle so as to ensure good impact.

Finding the Vertical Impact Angle

The vertical angle at which the FMH is set to plays a key roll in influencing the HIC(d) value. As stated in the test procedure, the initial velocity of the Free Motion Head Form is always oriented in the positive local x-direction of the FMH, perpendicular to the skull base plate. The more the contact position is aligned with the initial velocity vector of the FMH the faster the interior trim structure will have to work in absorbing the energy during impact. Therefore it is imperative that the correct vertical angle be found. ANSA currently possesses the capability to find the vertical impact angle while staying contact with the impact surface.

Using Contact Algorithm

By setting the horizontal angle and moving the FMH from its original position to the impact point initial contact is made. From here it is necessary set the vertical angle so as to achieve the worst case HIC(d) value and adhere to the FMVSS201U standard. The vertical angle is taken about the local y-axis at the centre of gravity of the FMH. As a result of this rotation initial contact is lost between the FMH and the trim impact surface. It is easy to manipulate the FMH per hand however so as to hold the contact position. However in order facilitate automation and running in batch mode user intervention can be removed by allowing the software to generate a contact condition between the FMH front impact zone and the trim impact point surface. Using this method the software rotates the free motion head form about its local y-axis and adheres to a contact condition with the trim surface by translating the FMH in the local x-z plane. When a second contact is found between the trim surface and the nose or chin of the FMH of the vertical limit is reached the rebound angle is enforced.

Using Geometrical Relationships

Due to the complex geometry often encountered on the inner surface of modern automobiles it is quite often difficult to use a contact algorithm as the one and only criteria when determining the vertical impact angle. Using the impact position, the centre of gravity of the FMH and the desired arc along the FIZ (Front Impact Zone) it would be possible to set the vertical angle using the geometrical relationship if the contact algorithm were to fail. As an added function, to ensure quick and effective positioning of the Free Motion Head Form, work is currently being carried out in order to assess the feasibility of including such a feature.

Presetting the Vertical Angle:

As stated in the standard the horizontal angle is usually found first followed by the vertical angle. Whether or not the FMH be positioned in the vertical plane prior to finding the first contact must be left open to the user. It can quite often be the case that the geometry at the impact point is so complex that first contact with the FMH Impact Zone cannot be found. This option presents itself well when using automated positioning at the FH (Front Header) points. The FMVSS201 tool has an option that allows to user to set the vertical angle to an allowed value prior to finding first contact with the trim surface.

Initial Contact with other Interior Parts:

A common problem encountered when positioning the FMH is the collision between the FMH Impact Zone with other interior trim surfaces during alignment of the horizontal angle. This results in the FMH Impact Zone not being able to meet the desired impact point. Quite often the FMH can be obscured by other interior parts such as door trim, the sun visor or other interior trim surfaces. Although still in the experimental phase the version of ANSA used here is able to overcome these problems by recognising contact between other interior trim parts and the rest of the FMH. ANSA then attempts, in the correct order, different alignment angle combinations. When the FMH Impact Zone is able to make, in one step, contact with the impact point the vertical angle is set.

Outputting the Amount out of Position at the Impact Point:

Due to the geometrical form and complications encountered positioning the FMH it is often very difficult to ensure that the first point of contact between the FMH and the interior trim lies on the midsagittal plane of the FMH. For the purpose completeness it is required that the amount of “out of position” that occurs between the two points of contact be documented. For this reason an extra feature was built into the tool allowing contact based algorithm to output an exact value of the “out of position” that will occur during impact.

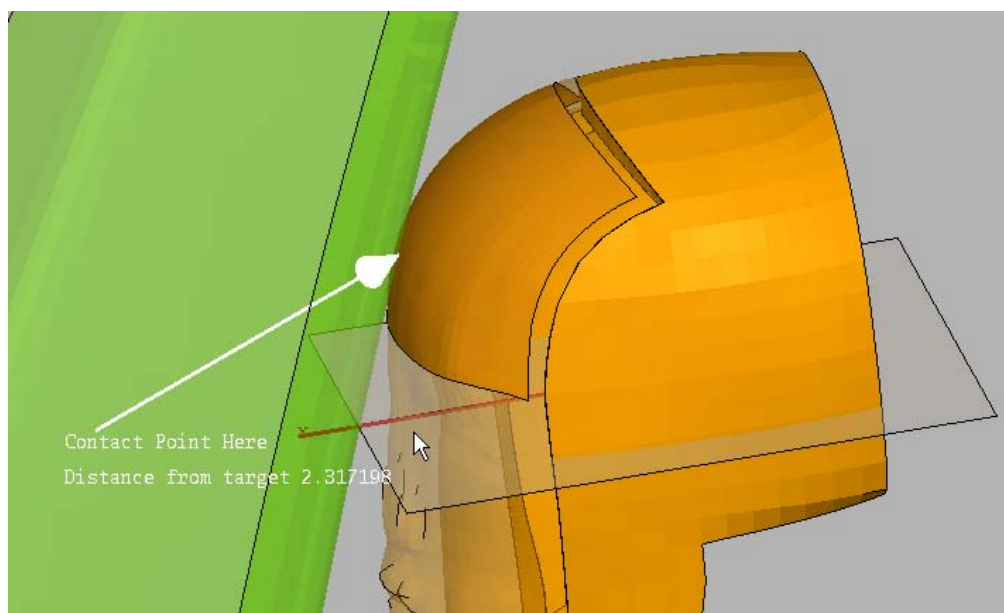


Figure 1.3: Determination of the “Out of Position” value.

Batch Mode

In order to assess the repeatability of the analysis inside the 1st and 2nd impact zones it is often required that several simulations at and around the same impact point of the interior trim be carried out. As it is clear that between 10 and 20 simulations will be required for each impact point an automated positioning process is required in order to save time. An automated feature using the FMH positioning process previously mentioned and template file defining the setup allows quick error free generation of the parameterised header files.

An ANSA_Transl file sets up the positioning data and recognises all associated FMH and interior trim data upon starting ANSA. The automated positioning is carried out using the “worst case” principal relying on lining up the midsagittal planes of the FMH and interior trim surfaces. Future versions will however allow the user to include their own horizontal and vertical angle limits. ANSA is able to run with the information regarding the impact points and the Free Motion Head Form. Batch mode produces the input decks ready for submission. The user interface of ANSA must not be opened and therefore no user interaction is required for this process. The input files can also be written back to their respective directory structure in order to avoid confusion.

Assessing the Vehicles Interior Structure

Additionally it may be necessary to relocate the desired impact point if the FMH impact zone, as a result of space problems and or the geometry of the interior trim surface, as it is unable meet with the desired impact point. In both cases creating a cross sectional view is necessary and will aid in finding the worst case position of the FMH. Therefore it is planned in a future version of ANSA to include this functionality.

3. CONCLUSION

To date ANSA's new Safety Tool, FMVSS201 incorporated has proven to be very useful when aligning the FMVSS201 Free Motion Head Form. Using the data generated the Occupant Safety project team within P+Z Engineering has been able to generate all data necessary without having to fall back on another tool. However, in order to achieve full automation extra work is still required.

REFERENCES

- (1) European Enhanced Vehicle-Safety Committee, EEVC Interior Side Impact and Head Protection, Figure 4 Method 1, head form alignment flow chart, page 20, Test Procedure Draft 3r, March 2005.
- (2) Department of Transportation, United States of America, Laboratory Test Procedure for FMVSS201U, TP201U-01, 1998.

Session H3.2

AUTOMATED BUILT-UP & ANALYSIS OF NVH MODELS WITH ANSA / μETA PACKAGE

Vassilios Pavlidis*, Michail Trifonidis*

BETA CAE SYSTEMS S.A., Greece

KEYWORDS – Process Automation, NVH Analysis, Data Management, Task Manager

ABSTRACT - Among the requirements of nowadays vehicles development, NVH defines one of the main attributes ensuring driving comfort with respect to the passenger's welfare. The use of the Finite Element Method (FEM) is becoming more and more important on this field, providing a means for simulating and improving the perceptions of a model, and thus, complementing efficiently the laboratory results.

The creation of reliable models that will deliver accurate results is a strenuous, time-consuming and error-prone process due to the particular requirements of NVH analysis and the communication bottlenecks, naturally existing between the different engineering teams that need to share information and be updated. Moreover, building such models efficiently implies that tedious tasks should be conducted fast, without errors and with the minimum user-interaction, assuring repeatability.

This paper presents an integrated process workflow using the ANSA/μETA Software Package, distributed by BETA CAE Systems S.A., for the development of NVH simulation models and the evaluation of the analysis results. The Data Manager tool imports and handles all different components with their suitable template-based representation and automatically looks after the versioning of parts, thus ensuring that the model will be always updated. The whole process of building up the model is controlled and monitored through the Task Manager, which includes all individual tasks of the workflow in a step-wise manner. Using the Data and the Task Managers, results in the NVH-simulation becoming a repeatable and cost-efficient procedure, assuring at the same time the high quality of the model.

TECHNICAL PAPER -

1. INTRODUCTION

The build up of an NVH model is a tedious and time-demanding task resulting in most time spent by the engineer for the preparation of the model instead for the analysis itself. This fact arises as a combination of various parameters such as:

- The large amount of CAE data that impose a need for their sufficient management.
- The data are collected from different sources. Different parts of the model are delivered to the NVH analyst from different departments. Thus, the demand for efficient management becomes more crucial.
- Data related to parts are not of the same type. It could be that for some parts the actual geometry exists (typical example could be the BiW) while for others only a pure FE mesh exists (this is the case with the power-train in many cases). Moreover, in some cases parts exist in the form of reduced models (e.g.: modal models, lumped masses, etc).

- Meshing requirements for NVH analysis differ significantly from other disciplines, thus prohibiting the use of the same model with other disciplines. Therefore, it is necessary that in any case, a model mesh dedicated to NVH should be built-up.
- Communication between engineers coming from different disciplines narrows even more the existing bottlenecks towards building up an NVH model.
- On top of the aforementioned issues, the quality of the model should be assured in any case and this imposes even more strict demands on the creation of the NVH model.

As a consequence of the high level of complication, the process is prone to errors, which in turn prolongs further the completion of the model and jeopardises its quality.

To address the increasing demands for better quality models completed in shorter time and with the minimum interaction from the engineer, BETA CAE Systems S.A. introduced two tools embedded within ANSA: the Data Manager and the Task Manager.

The Data Manager is a pool containing all necessary information and data used during the CAE-cycle:

- Parts are stored and retrieved based on their version and their different FE attributes (e.g. meshed with 10mm element size, 20mm element size, etc.). Consequently, the engineers can easily handle / modify the model and, on the same time, it is ensured that the model is always up to date.
- Predefined settings for the creation of different FE attributes for each part.
- Library items that can be considered as templates used for boundary conditioning, connecting subassemblies and application of output requests.
- Auxiliary Components added in particular load cases, like crash test dummies, impactors etc.

The Task Manager is the tool that automates the building up of the model. All individual tasks of the workflow are included in the Task Manager in a step-wise manner. In this way, the Task Manager is able to control the process through:

- Taking into account the order with which tasks should be accomplished.
- Taking into account the dependencies between tasks. Dependency between tasks means that if a last change in the model affects the result of a previously executed task, then the task stops and the user is notified by the Task Manager so as to take action.
- Running and checking automatically all tasks that can be run without user interaction.
- Notifying the user when a task fails to be executed due to modelling mistakes or lack of information.

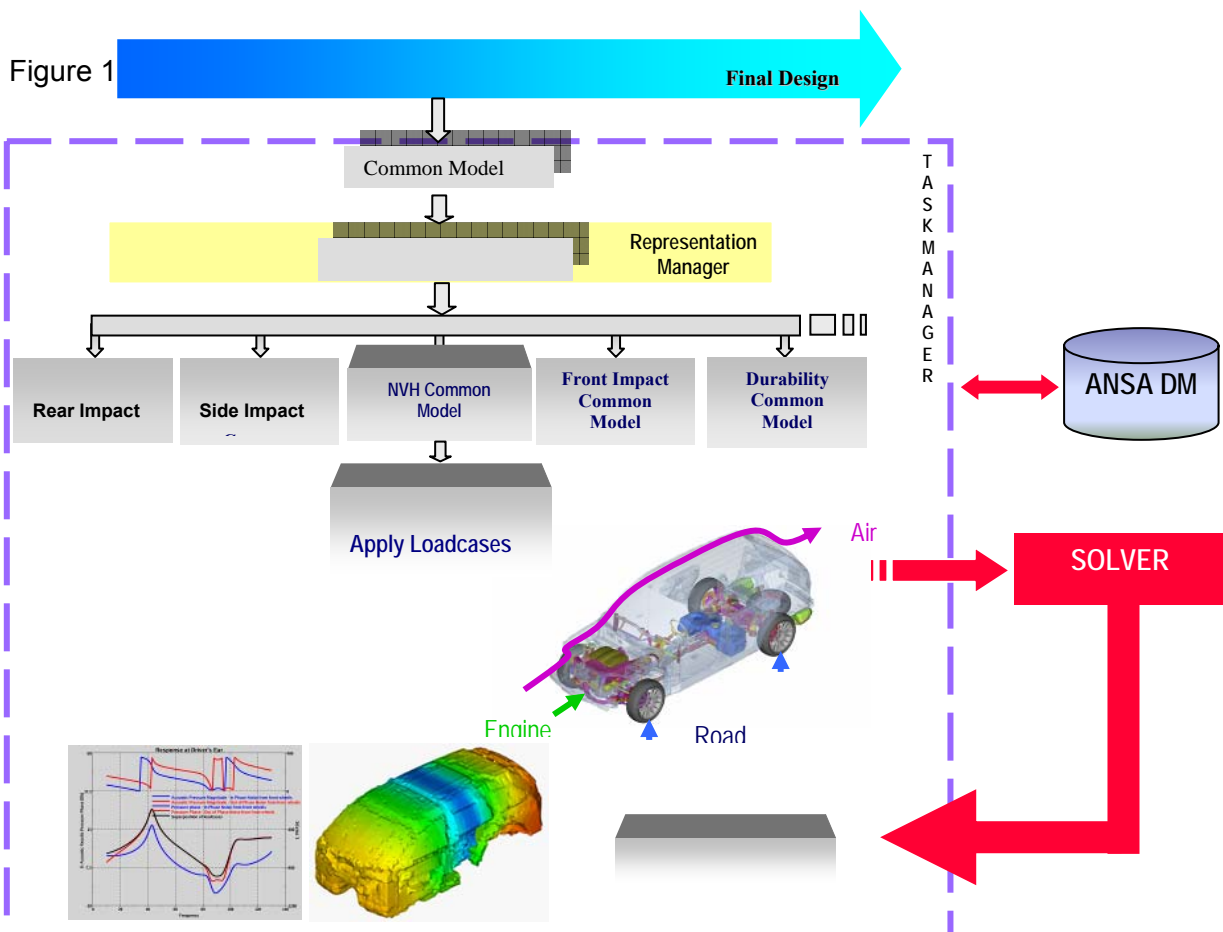
This paper outlines an integrated process workflow for the built-up and evaluation of results of an NVH model using the ANSA/μETA package. In this case, this process (the building-up of an NVH model) is looked upon as a part of a broader CAE process, which involves the deployment of both the Data and the Task Managers in cooperation. Therefore, in order to deliver a complete overview of the workflow, it is necessary to refer also to the preliminary work, which precedes the building-up of a discipline specific NVH model.

2. OVERVIEW OF THE COMPLETE PROCESS

Figure 1 displays schematically the overview of the complete simulation process workflow (1). It is evident from this figure that the build up of a model actually is comprised by three phases that are clearly reflected on the following respective groups of tasks of the Task Manager:

- The Common Model creation: this phase contains all information that is common to all disciplines.
- The Discipline Common Model creation: at the end of this phase, the model includes all information that is common to the specific discipline.
- The Load case definition: at the end of this phase, the model is ready to run. During this phase, all information that is related to a specific load case is added to the Discipline Common Model.

The core of this paper is related to the tasks involved in the build up of an NVH model therefore, it refers to the Discipline Common Model and the NVH Loadcase (which also includes running the solver and post-processing the respective results). However, prior to presenting the building-up of the NVH model, it is necessary to clarify issues related to the prerequisite work.



3. PREREQUISITE WORK

3.1. How to build a task (2, 3)

The tasks are built in an easy and simple way inside ANSA and are stored in the ANSA DM. Each task consists of task items, which reflect the steps of the workflow that should be executed. These tasks, when created, are model independent. All model related data are imported from the ANSA DM during the execution/update of each task item.

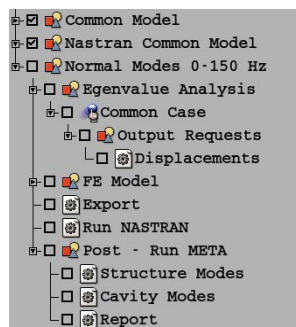


Figure 2 - Task items in ANSA's Task Manager

3.2. Preparation of the Common Model (CM) (2)

First the model hierarchy must be imported. The model hierarchy is read from the VPM tree file or any other source file that includes such information (2). This file (which is usually exported from CAD Systems) contains the model hierarchy and engineering information (like thickness, material, weight). A preview of this tree is given through the VPM Tree Editor, which furthermore allows filtering/modification activities. Through this editor a Download list (D/L-list) can be exported and this works as an input file for the CAD data import. Each part of the model that exists in a CAD format is translated into an ANSA database, which in turn is stored in the ANSA DM. During the translation procedure, engineering information is interpreted according to the D/L-list.

Other parts or subassemblies, which exist only in FE mesh, are also saved in corresponding ANSA databases stored again in the ANSA DM.

After all parts of the model have been stored in the ANSA DM, they are merged into an ANSA models.

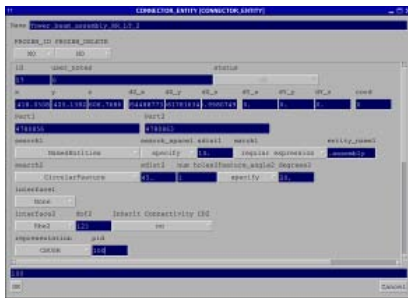
The task that should be used is also loaded into ANSA and now it is necessary to establish the association between the task items and the parts of the model.

3.3. The Common Model concept (2, 3)

The Common Model (CM) is the first phase towards the building up of the complete ready-to-run model. As its name implies, the CM includes all model data that are common to all disciplines. It is the common starting-point for the creation of any specific discipline model.

A CM consists of the following entities, which also correspond to respective task items in the Common Model task group:

- **Sub models:** These can be as many as necessary depending on how it is decided to split the model into sub-assemblies. As described in the previous paragraph, the association of the Task items with the Model entities is based on the sub-models. The sub-models can include either geometry of parts as they are translated from the CAD files or complete sub-assemblies in FE-Mesh that will be used as they are in the analyses (eg: power-train that comes as a complete assembly to be included in the analysis).
- **BiW Connections:** The connection information is read from an XML, VIP, VIP2 or any other ASCII file.
- **Model Assembly data (Generic Connectors):** These data include information for the connectors between sub-assemblies. The means to pass this information is the definition of Generic Connectors. These are ANSA entities, created by the CAE expert once for each model and are mesh-density independent. A Generic Connector is defined through the following card (Figure 3) and contains information about:



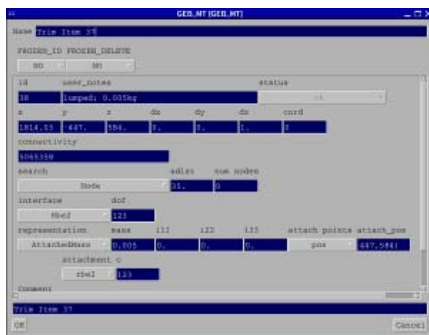
WHERE it is located

WHAT to connect

HOW to connect (this information is not included in the Common Model – this is the information that should be specified at a later phase, when the Discipline Common Model is created, since this information is discipline dependant).

Figure 3

- **Model Trimming data (Generic Mass Trim Items):** These data include information about the added mass that should be applied on parts. The means to pass this information is the definition of Generic Mass Trim Items. These are ANSA entities, created by the CAE expert once for each model and are discipline-independent. A Generic Mass Trim Item is defined through the following card (Figure 4) and contains information about:



WHERE it is located

WHICH entities affects

HOW to apply the mass: (this information could be included either during the Common Model phase or, in case it is discipline dependant, during the Discipline Common Model phase).

HOW MUCH mass to apply

Figure 4

3.4. How to establish the association between the model and the task items (3)

The association between the model and the task items is based on the names of the sub-models and is achieved through the ANSA Part Manager. Each sub-model of the Common Model Task group corresponds to one Group of the Part Manager with the same name. Therefore, when the Common Model Task group is loaded in ANSA, Empty groups corresponding to the sub-models task items, are created in the Part Manager with the same names. Then, when all parts of the model have been merged into ANSA, the user links inside the ANSA Part Manager the existing Parts and Groups to the respective Empty sub-models groups.

The association between task items and the model entities is established. Figure 5 depicts this process.

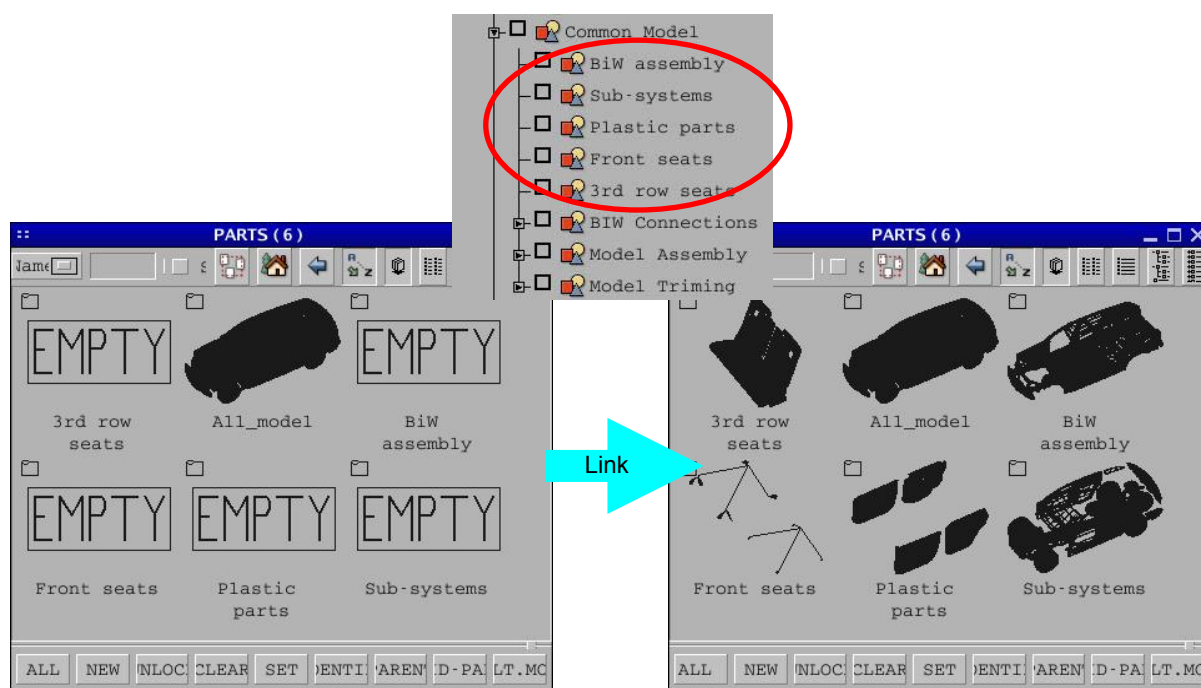


Figure 5

As soon as all the above data have been imported / specified in ANSA and the association between the task items and the model entities has been set-up, the Common Model definition phase is accomplished.

This Common Model can now be saved as an ANSA database and this will constitute the starting point for the build up of any Discipline Specific Common Model.

3.5. The Representation concept (2, 3)

The term “representation” for parts in ANSA defines the actual modelling characteristics attributed to a part within a complete model.

The solving time for an analysis depends on the number of elements / degrees of freedom that appear in the model. Thus, to keep the solving time to the minimum required without risking the accuracy of the results, the model is represented with fine mesh in areas of interest and with coarsen mesh in areas indifferent to the particular analysis (in between there are areas with transition mesh). Areas of interest are the components of a model, for which their behaviour is important to be captured with high accuracy. This is the concept behind the representation management of parts.

For example, one part could be meshed with element size 20 when included in an NVH model, while the same part could be meshed with element size 10 when included in a crash model. It could also be the case that the same part could be included within a model only as a lumped mass. All these modelling variations of the same part are called “representations”. Figure 6 shows two possible representations for a door.

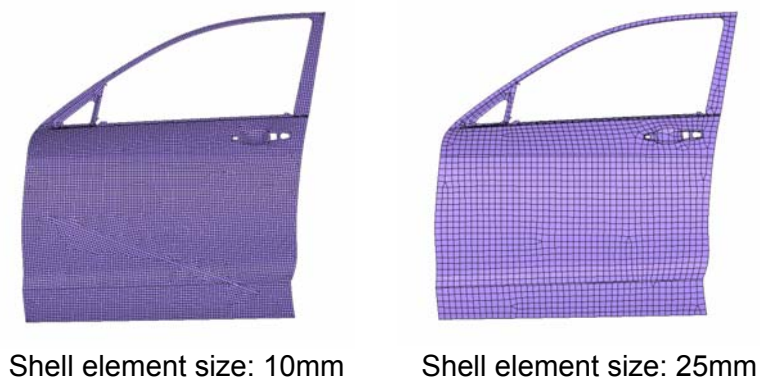


Figure 6

All possible meshing representations of each part can be created once and in an automatic way using the ANSA Batch Meshing features and saved in the ANSA DM through the ANSA Part Manager.

4. BUILDING THE NASTRAN NVH COMMON MODEL

4.1. General

The Common Model database is opened in ANSA and the build up of the Discipline Common Model (in this case the NASTRAN NVH Common Model) commences.

Two distinctive sections can be identified during this phase.

The first section is related to applying the proper modelling attributes to the already existing entities according to the NASTRAN NVH discipline. That is the application of the proper representation on each existing sub-model and the realisation of the existing connections, connectors and mass trim items according to NASTRAN NVH specifications.

The second section of this phase is related to importing any other sub-models, connections, connectors or trimming items that are specific only to NASTRAN NVH (e.g.: Heavy Air Seats) as well as to include actions related to NASTRAN NVH such as the creation of Acoustic Cavity, the execution of Model checks, the creation of a report etc.

All actions and entities that are related to this second section are reflected on the task items of the Nastran Common Model task group. This Task group is also saved in the ANSA DM and it is loaded when the building of the NASTRAN NVH Common Model begins.

4.2. Apply Representations

The application of representations on the parts / sub-models of the model is controlled through the Representation Manager. This process is depicted in Figure 7.

As the Task Manager starts running one by one the task items, the user applies for each sub-model task item the appropriate representation through the Representation Manager. Examples of several types of representations are shown below:

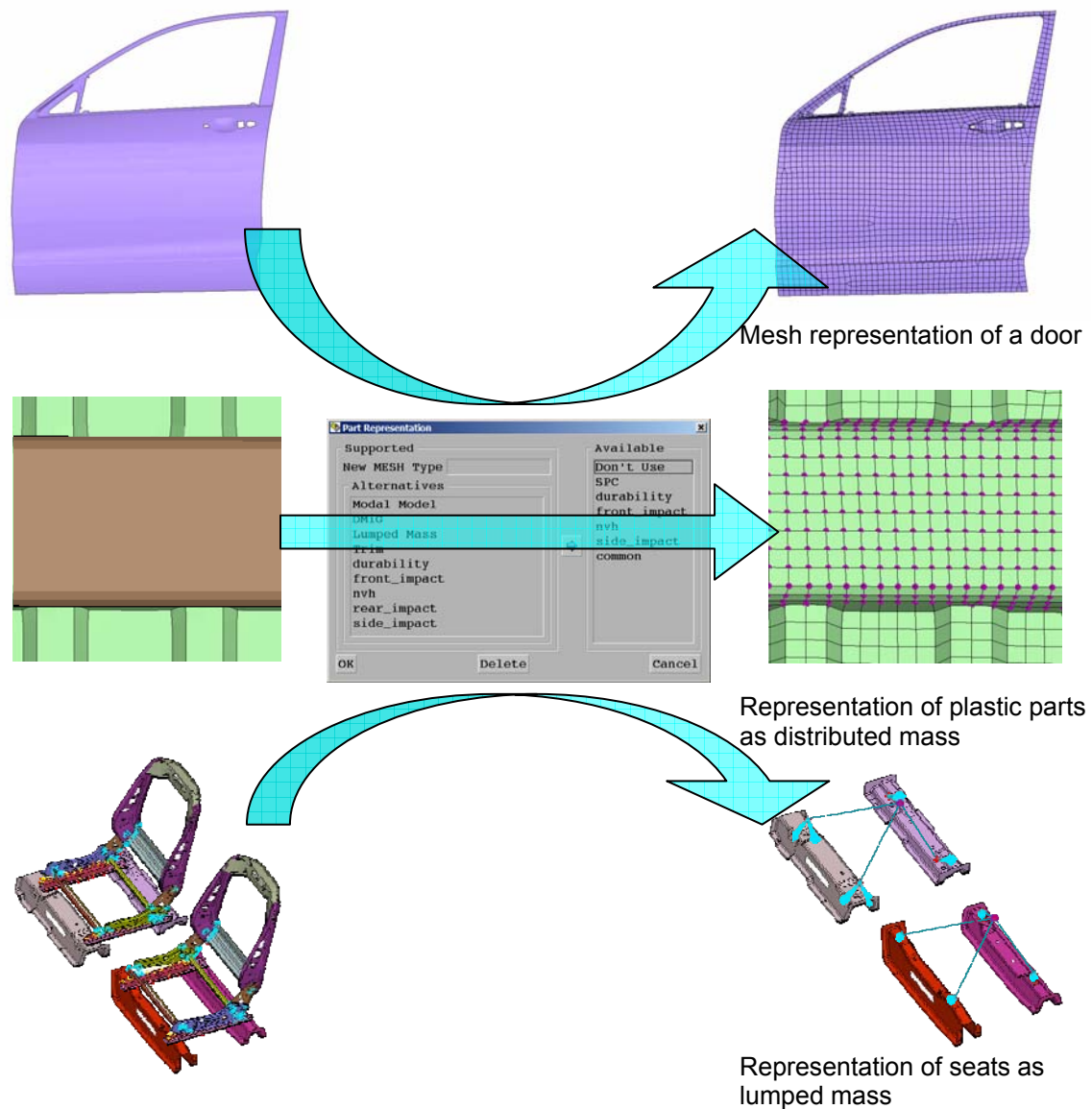


Figure 7 - Application of representations

4.3. Realisation of connections

As soon as the Task Manager reaches the task items that are related to connections, the Connection Manager is invoked and the user may select how each connection type should be realised. Typical examples of the realisation of several connection types are depicted in Figure 8.

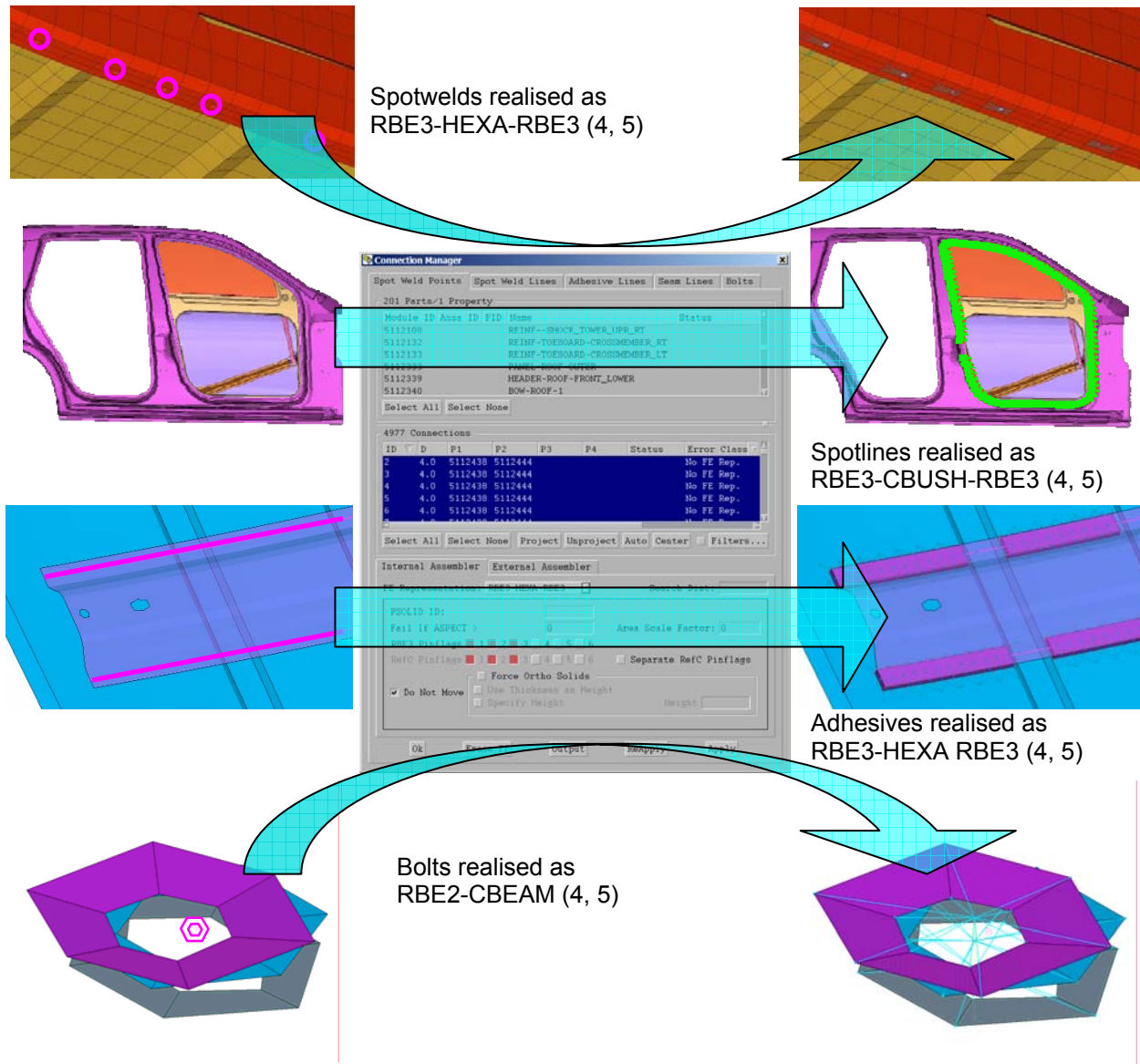


Figure 8

4.4. Realisation of Connectors

After the connections have been applied, the task continues with the realisation of Connectors. The realisation of connectors does not request user interaction and it is done automatically according to the definition of each connector. User interaction is necessary only if the realisation of a connector fails. In this case the task is stopped and the user is notified to take action. Only after the connector is realised, the Task shall continue.

The definition of connectors can be achieved either through one of the standard options, that exist within the Generic Connector card or through a library item. A library item is created once, stored in the ANSA DM and can be used as a template for a similar case (2).

As an example, Figure 9 shows 2 connectors that are realised with CBUSH elements. The library item is a simple CBUSH, which has parameterised properties, therefore, can be easily adjusted to different cases. This library item has unit length and should be aligned with the Ox axis. The interfacing of the CBUSH to the connected parts, in this case, is achieved with RBE2's and this information is also included within the definition of the Connector.

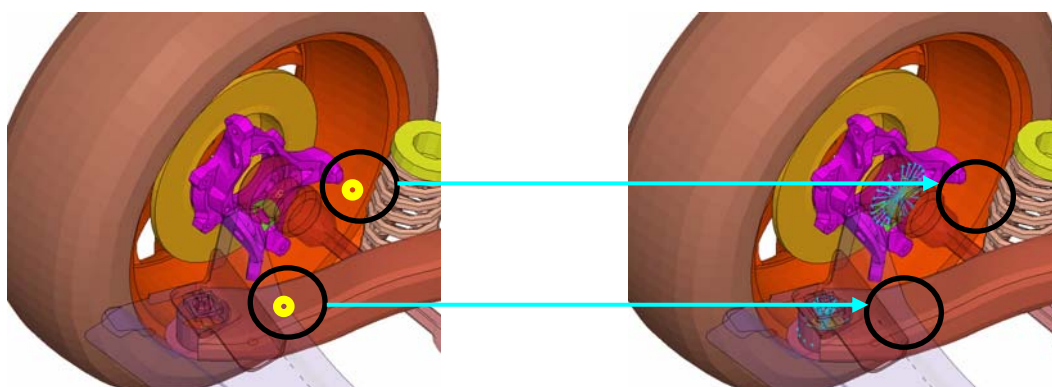


Figure 9

4.5. Realisation of Mass Trimmings

Next, the Mass Trim task items are realised. Similar to the connectors case, the realisation of the Mass Trim items does not request user interaction and it is performed automatically according to the definition of each Mass Trim item. User interaction is necessary only if the realisation of a Mass Trim item fails. In this case the task is stopped and the user is notified to take action. Only after the Mass Trim item is realised, the Task shall continue.

The realisation of Mass Trim items can be achieved either through one of the standard options that exist within the Generic Connector card or through a library item. A library item is created once, stored in the ANSA DM and can be used as a template for any similar case (2).

As an example, Figure 10 shows a Mass Trim item that is realised as a non-structural mass representing the mass of the paint of a part.

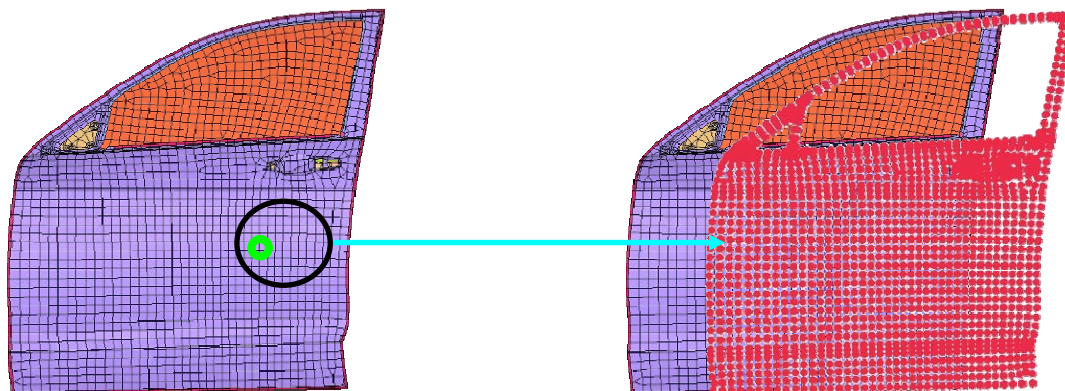


Figure 10

At this stage, the first section of the NVH Common Model phase is finished. The respective task items are checked in the Task Manager (Figure 11) indicating that the tasks were executed successfully.

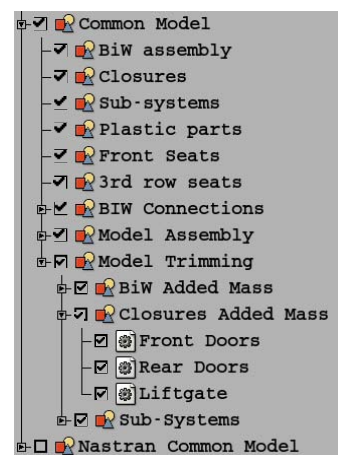


Figure 11

4.6. Importing NVH added components

At that point, the second section of the NVH Common Model commences. The Nastran NVH Common Model group of tasks includes additional sub-model task items. In this way, components specific only to NVH, such as the Heavy Air seats (Figure 12), are added for the needs of the Acoustic cavity analysis.

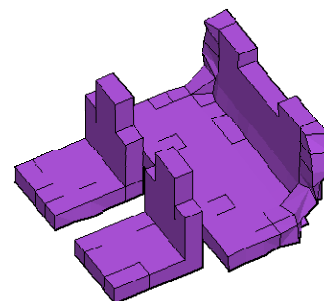


Figure 12

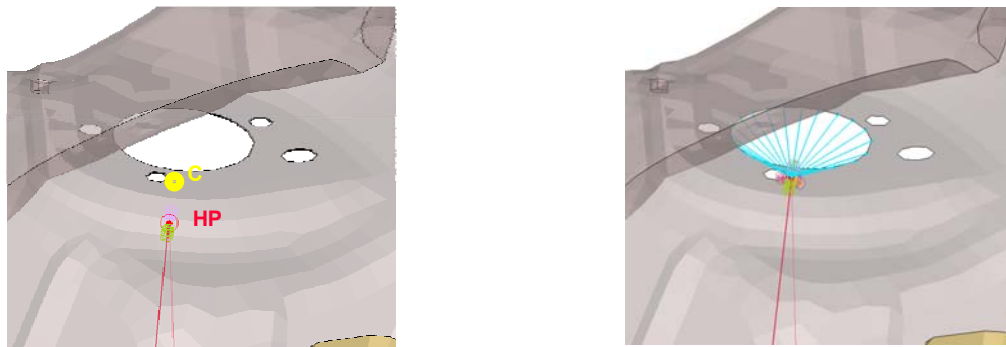
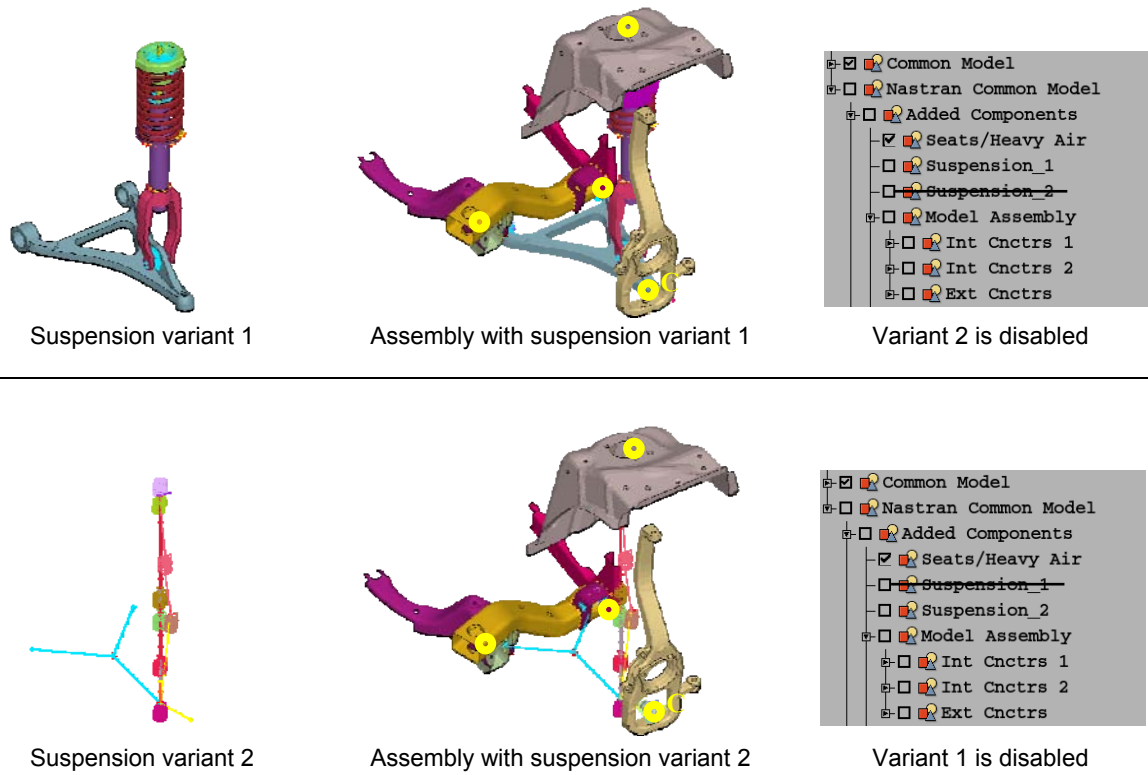
4.7. Using sub-modelling variants

One of the merits deriving from the use of the Task Manager is the easy and fast inclusion / exclusion of sub-model variants within the same model. A typical example that is depicted in Figure 13 is the suspension.

The suspension variant 2 replaces the suspension variant 1. Both suspension variants are included in the Task Manager as different sub-models but only one is enabled at any time. Both suspensions are connected to the rest of the model through the 4 connectors also appearing in Figure 13.

The substitution is achieved by simply disabling variant 1 in the Task Manager and enabling variant 2. The Task Manager automatically identifies variant 1 and excludes it from the visibility as well as from the model but it does not delete it. That means that this variant can be retrieved later if necessary. At the same time, variant 2 is brought to visibility and included in the model.

The variant suspension 2 is automatically connected to the rest of the model through the connectors. At that point, it should be mentioned that it is possible to connect the new suspension automatically even if its original dimensions do not fit to the connecting locations. This is possible with the use of Hard Points which are actually entities defined in ANSA and having several nodes assigned to them. These assigned nodes are dependent from the Hard Point therefore they follow the movement of the Hard Point as a rigid body.



Detail of the top section of the suspension. Originally, variant 2 did not fit to the connector's location. This problem is resolved by using Hard Points that actually stretch the variant suspension so that to reach the connector's location.

Figure 13

4.8. Preparation of Output locations

The next step towards the completion of the Nastran NVH Common Model is the preparation of the output locations. This is achieved through the following three task items:

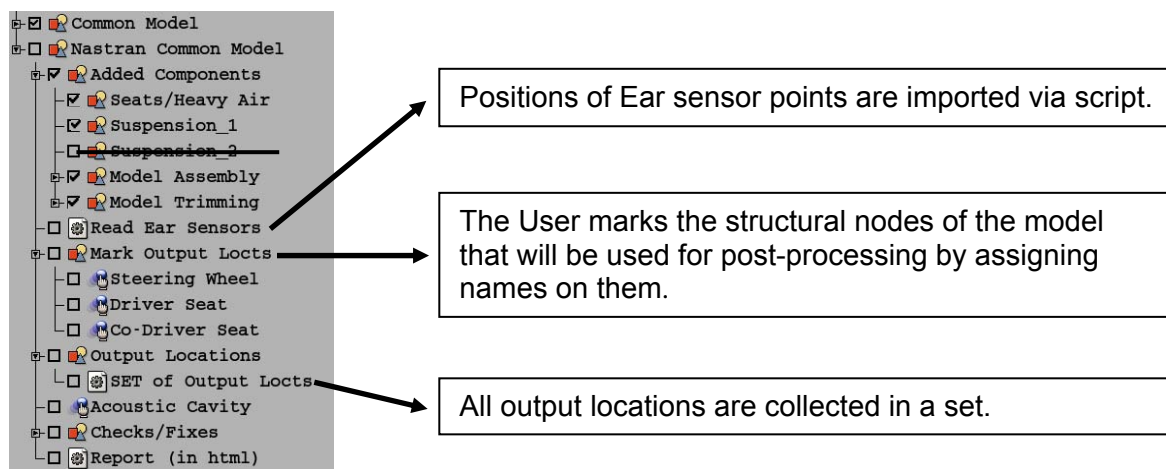
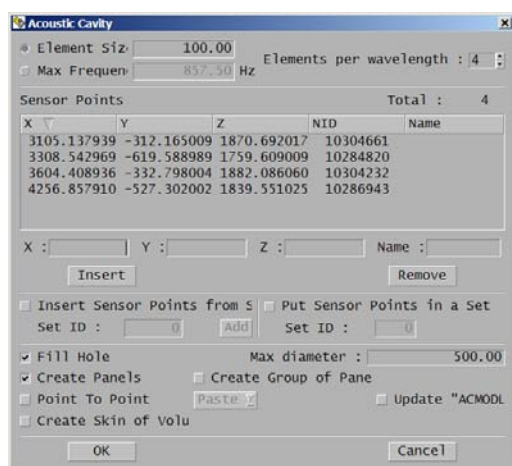


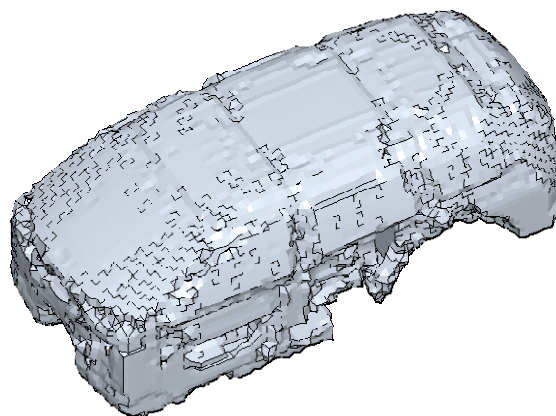
Figure 14

4.9. Creation of the Acoustic Cavity

When the Task Manager reaches the Acoustic Cavity task item, the respective ANSA tool (4) is automatically invoked and the user is prompt to specify all necessary parameters for the creation of the Acoustic Cavity mesh (5, 6) (Figure 15). It should be mentioned here, that it is assured that the Ear sensor points, which were previously imported, will consist nodes of the cavity mesh.



ANSA Acoustic Cavity tool



Acoustic Cavity mesh

Figure 15

4.10. Checks and Reporting

The last task items before the completion of the NVH Common Model are:

- The performance of checks and the consequent fixes of possible modelling problems. The following checks are included in this case study: Units System conformity, Model data and Dependency errors (4, 5).

- Final reporting on the NVH Common Model. A report with general information on the model is created automatically by ANSA in HTML format. The information that should be included in the report is fully controllable.

4.11. Storing the NVH Common Model in the ANSA DM

As soon as the NVH Common Model is completed, it can be stored in the ANSA DM. In this way, this model can be retrieved from the ANSA DM by other engineers and can be used as the starting point for the building-up of NVH models for specific loadcases.

It should be emphasised that if the NVH Common Model is correct, then all NVH loadcases can be easily built starting with loading this NVH Common Model in ANSA. During the building-up of any NVH loadcase, it is ensured that if any action affects the integrity and correctness of the NVH Common Model, the user is notified and the affected task items become unchecked (dependencies between task items).

5. BUILDING AN NVH LOADCASE: EXTRACTION OF NORMAL MODES

5.1. Preparation of the NASTRAN Model for Normal Modes extraction

The NASTRAN Load Case task related to the extraction of Normal Modes of the BiW between 0-150 Hz is loaded from the ANSA DM (Figure 16).

Since it is requested to calculate the Normal Modes only for the BiW parts, several sub-models should be disabled for this analysis from the Task Manager (Figure 17).

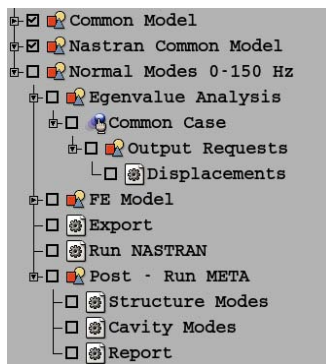


Figure 16

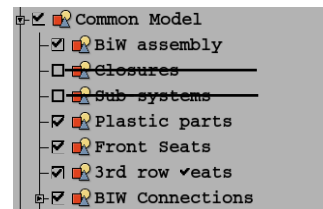


Figure 17

The Output requests, the exporting of the deck in NASTRAN format and the initiation of the solver via script are all actions performed through respective tasks in the Task Manager.

5.2. Post-Processing of the Normal Modes results

After the solver has run successfully, the post-processing is initiated through respective task items. These task items actually execute a script that launches μETA to run a μETA session file (7), which could be previously stored in the ANSA DM.

Alternatively, μETA can be launched in a listening mode, thus running as a server. In this way, μETA can execute directly μETA commands dictated by the Task Manager without a session file.

For this case study, μ ETA was run with three different session files (corresponding to three task items). The first animates the structural modes one by one and could also record these animations in a video file (Figure 18). The second animates the cavity modes and could also record them in a video file (Figure 19). Finally, the third session creates automatically an HTML report for a first assessment of the results (Figure 20). In this report, the zero modes have been identified from the rest normal modes and plotted in a bar chart. Therefore, this report provides directly a fundamental indicator of the correctness and integrity of the model (6, 8). For example, if the zero structural modes are more than 6, then this would possibly imply a modelling problem or the existence of misconnected parts. Consequently, the user can decide fast and effortlessly whether to proceed with further post-processing of Normal Modes results and then to build other NVH loadcases, or to discard the Normal Modes results and return to ANSA to correct the NVH model.

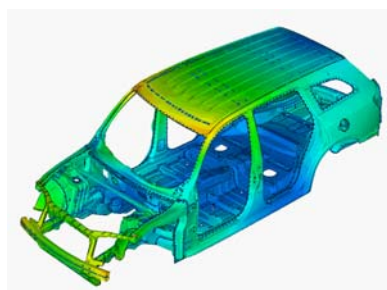


Figure 18

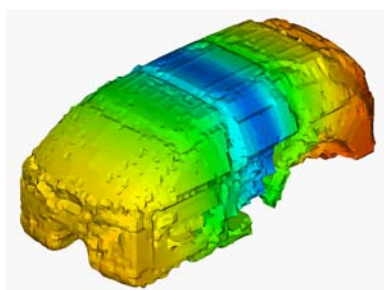


Figure 19

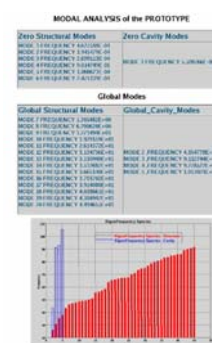


Figure 20

It should be mentioned, at this point, that μ ETA could also run these session files in batch mode without the Graphical User Interface being present.

6. BUILDING AN NVH LOADCASE: FREQUENCY RESPONSE ANALYSIS FOR ROAD NOISE

6.1. Preparation of the NASTRAN Model

After the completion of the post-processing of the Normal Modes and the evaluation of the results as being acceptable, the workflow continues with the building-up of a second NASTRAN Load Case related to the Frequency Response Analysis for the Road Noise.

The corresponding task is loaded from the ANSA DM (Figure 21).

For the needs of this analysis, the representation of each tyre is changed to that of a Modal model of a tyre (Figure 22). This Modal model is also stored in the ANSA DM and it is applied through the corresponding task of the Task Manager.

Following the inclusion of the Modal Model for the tyres in the model, four different subcases are defined. These subcases correspond to in-phase and out-of-phase loading of the front and the rear wheels respectively.

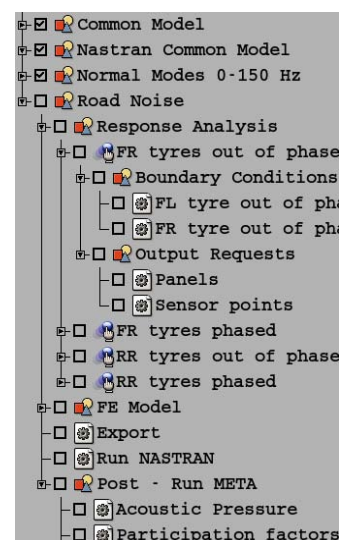


Figure 21

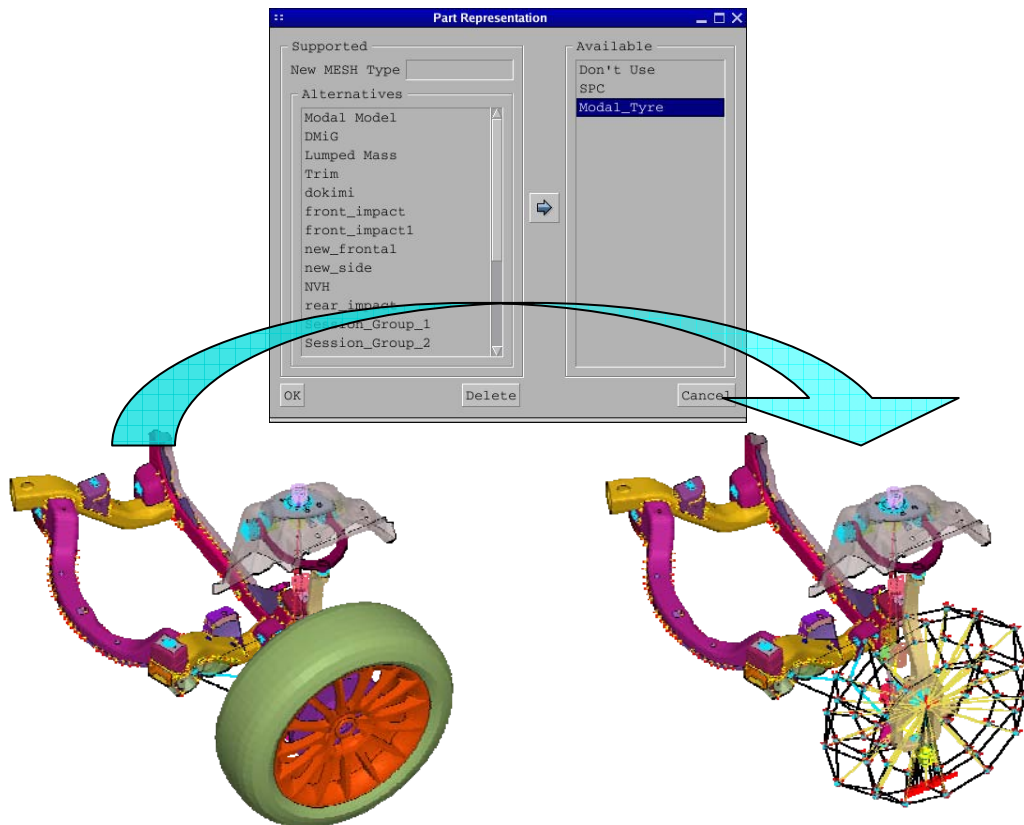


Figure 22

Each group of task items that correspond to a subcase includes the necessary items for the definition of the boundary conditions as well as the output requests for that subcase.

The boundary conditions are frequency dependant loads that apply on the tyres so as to represent the road noise entering the structure from the contact surface between the tyre and the road (Figure 23).

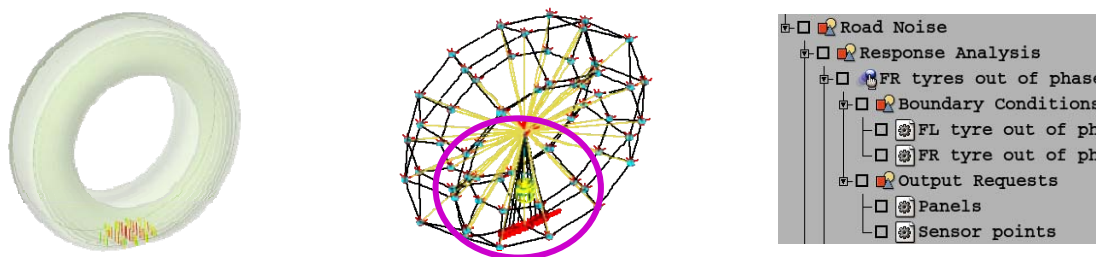


Figure 23

The output requests are related to the definition of panels and the sensor points.

Finally, the deck is exported in NASTRAN format and the solver is initiated via script.

6.2. Post-Processing of Frequency Response results

After NASTRAN has run successfully, the last items that correspond to the post-processing of the results with μETA, are executed. The first task item is related to the creation of a 2Dplot for the Acoustic Pressure results (Magnitude and phase) at the “ear” sensor points. The Acoustic Pressure magnitude accounting for a combination of loadcases is also calculated and displayed in μETA (7) (Figure 24).

The second task runs a μETA session that displays in contour plot the grid participation factor results of the structural panels that define the cavity (7). Through this session file, the areas that exhibit high grid participation are identified and exported as a set of elements (Figure 25). This set is then retrofitted back to ANSA so as to take measures in order to improve the dynamic behaviour of the model, thus, a closed loop for the improvement of the model can be established.

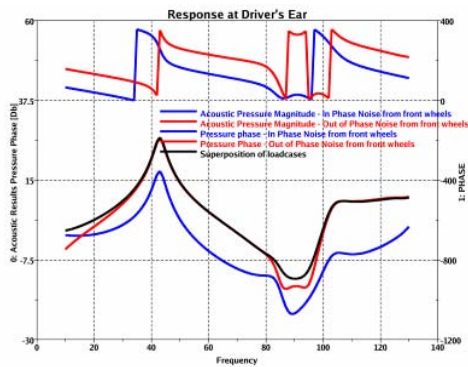


Figure 24

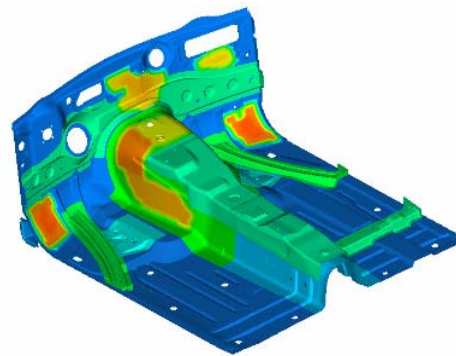


Figure 25

In order to improve the damping characteristics of a panel the user may either add some new features (beads, embosses, etc) using the ANSA Morph tool (Figure 26), or apply a damping patch through the Damping patch tool of ANSA (8) (Figure 27). In the first case, a new study version of the part(s) is created and is stored in the ANSA DM. In the second case, the creation of the damping patch could also be a part of the Task.

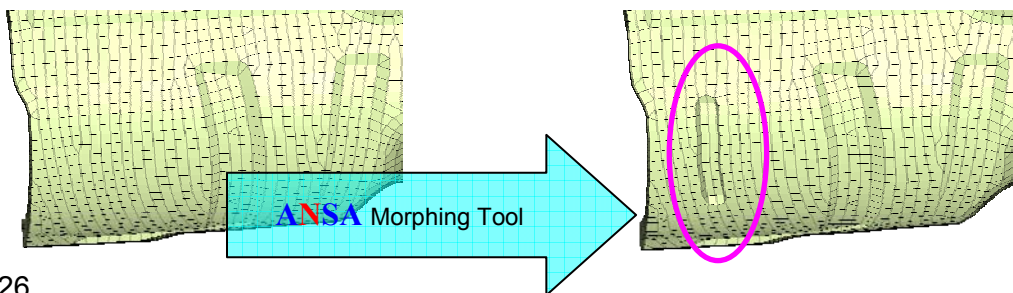
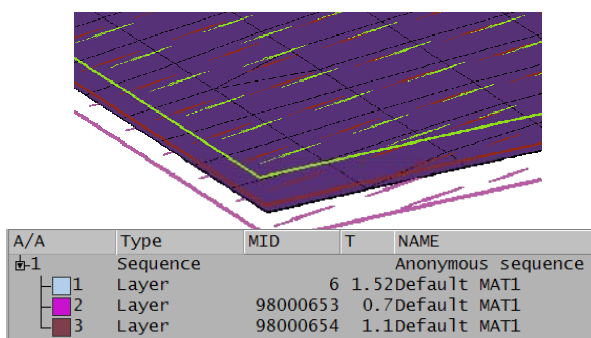
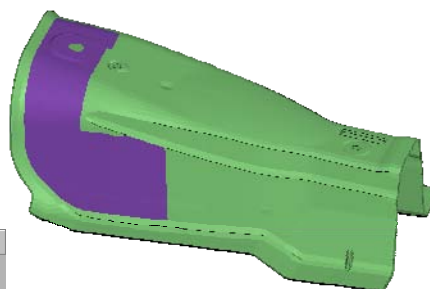


Figure 26



Damping Patch Tool – Damping Patches are represented and created as Composite materials



The Damping Patch is applied

Figure 27

7. CONCLUSIONS

The use of the Task Manager in association to the ANSA DM environment is certainly beneficial in many aspects for the realisation of the CAE cycle. The main merits that a CAE team can gain from the deployment of these tools within the workflow, are:

- The process of building up a model becomes repeatable.
- The quality of the model is assured and the errors, which are naturally involved with a complicated process, can now be avoided.
- The use of the ANSA DM and the Task Manager assists the user in avoiding certain repeatable actions since it minimises the user interaction.
- The engineer becomes more familiar with the model and in the same time dives deeper but easier in the whole CAE process.
- The CAE turnaround time is significantly reduced.
- The whole process is taking place inside ANSA and there is no hopping between different tools thus, saving time, simplifying the building up of a model and avoiding bottlenecks in the cooperation of different software products. When deploying several types of software for such complicated process, the bottlenecks arise mainly from compatibility issues as well as from the fact that it is not possible to establish dependencies between different actions throughout the whole CAE process.

REFERENCES

- (1) Georgios Nikolaidis, Dimitrios Zafeiropoulos, Konstantinos Ntamagkas, "Building Discipline Specific FE-Models with the Common Model Concept", BETA CAE Systems, 2nd ANSA & μETA International Congress, June 14-15, 2007
- (2) BETA CAE Systems, "ANSA Data Management Users Guide", ANSA v12.1.2 Documentation, 2007
- (3) BETA CAE Systems, "ANSA Task Manager Users Guide", ANSA v12.1.2 Documentation, 2007
- (4) BETA CAE Systems, "ANSA Users Guide", ANSA v12.1.2 Documentation, 2007
- (5) MSC Software, "MSC.Nastran 2004 Reference Manual", MSC.Nastran Documentation, 2004
- (6) MSC Software, "Advanced Dynamic Analysis User's Guide", MSC.Nastran Version 70, Documentation of MSC.Nastran 2004
- (7) BETA CAE Systems, "μETA PostProcessor v.5.4.0 User's Guide", μETA v.5.4.0 Documentation, 2006
- (8) Juan Jesus Garcia, Ismael Fernandez, Javier Iturbe, Ines Lama, "Fundamentals of Automotive NVH", Applus IDIADA, Course on NVH, May 2007

δYNAMIS: A NEW SOLVER FOR LINEAR AND NONLINEAR FINITE ELEMENT MODELS

¹Dimitrios Giagopoulos, ²Sotirios Natsiavas*

¹DYNAMical Systems Technology, Thessaloniki, Greece

²Department of Mechanical Engineering, Aristotle University, Thessaloniki, Greece

KEYWORDS - automated finite element modeling, substructuring, static and transient analysis, linear and non-linear frequency response, deterministic and random analysis.

ABSTRACT - δYNAMIS (**DYNA**mics of **Mechanical Systems**) is a numerical code leading to an automated determination of the response of mechanical systems, in an efficient way. These systems are geometrically discretized by finite elements. Frequently, this leads to models with a quite large number of degrees of freedom and strongly nonlinear characteristics. Therefore, one of the basic ideas employed in designing the code was to provide the option of reducing the order of the systems examined by applying appropriate methodologies, when necessary. Apart from increasing the computational efficiency and speed, this reduction makes amenable the application of numerical techniques, which are efficient for low order systems.

In particular, δYNAMIS starts by reading all the necessary data in standard NASTRAN format from pre-processor ANSA, in order to set up the corresponding equations of motion. Then, a number of static and dynamic analyses can be performed. Currently, the code can be used to carry successfully out the following types of analysis:

- Static Analysis (for linear and nonlinear systems),
- Eigenvalue Analysis (real and complex natural frequencies and mode shapes),
- Substructuring (static condensation, component mode synthesis, multi-level dynamic substructuring),
- Linear Transient Response Analysis (direct integration and modal analysis),
- Linear Frequency Response Analysis (direct determination of frequency response functions and modal analysis),
- Nonlinear Transient Response Analysis (direct integration),
- Nonlinear Frequency Response Analysis (direct determination of periodic steady-state response diagrams and stability properties under periodic excitation) and
- Random Analyses.

Once the analysis chosen is completed, the results are directed to post-processor μETA. In fact, in order to achieve compatibility with most state of the art CAE post-processors, these results are written in NASTRAN (op2 or punch file) format.

The validity and effectiveness of δYNAMIS was first illustrated by passing standard tests on the finite element level. Moreover, direct comparison was performed (in terms of accuracy, memory required, data transferred and numerical speed) with MSC.Nastran for several quite complex structures. Besides the computational advantages, the code developed brings a lot of new features and improvements, which can be enhanced further by a proper coupling with the pre- and post-processor. For instance, the structure of the code facilitates greatly the application of parallel processing procedures. In addition, a distinct capability of the code is related to the special contact elements developed for both static and dynamic analyses. Another remarkable and unique strength is the ability to perform frequency response of periodically excited nonlinear dynamical systems in a direct way. Finally, δYNAMIS provides valuable tools towards employing a single original model for all the possible analyses (e.g., vibration, acoustics, fatigue) that need to be run for systems of any geometric complexity.

δYNAMIS: A NEW SOLVER FOR LINEAR AND NONLINEAR FINITE ELEMENT MODELS

Dr. Dimitrios Giagopoulos
Dynamical Systems Technology
Thessaloniki, Greece

Prof. Sotirios Natsiavas
Department of Mechanical Engineering
Aristotle University
Thessaloniki, Greece

OUTLINE OF PRESENTATION

- ✿ **Design Process**
- ✿ **Class of Mechanical Systems**
- ✿ **Solver Capabilities**
- ✿ **Code Verification (Exact Solution, NAFEMS, NASTRAN)**
- ✿ **Types of Analyses Performed**
- ✿ **Additional Features**
- ✿ **Synopsis-Extensions**

Solver Capabilities

Types of Analyses Performed

- Static Equilibrium Analysis [Linear (101) / Nonlinear (106)]
- Eigenvalue Analysis [Real (103) / Complex (107)]
- Substructuring [Guyan, CMS, MLDS]
- Transient Response Analysis [Linear (109, 112) / Nonlinear (129)]
- Frequency Response Analysis [Linear (108, 111) / Nonlinear (128)]
- Random Analysis [Linear (108, 111)]

Solver Capabilities

- **Element Types**

Surface Elements : CQUAD4, CQUADR, CTRIA3, CTRIAR

Solid Elements : CHEXA, CPENTA, CTETRA

Other Elements : CBEAM, CBAR, CROD, CMASSi, CONMi, CELASi, CDAMPi, RBE2, RBE3, CBUSH1D, CBUSH, CWELD, CGAP

- **Material Types**

MAT1, MAT2, MAT8, MAT9, MATT1, MATT2, MATT8, MATT9

- **Boundary Conditions Types**

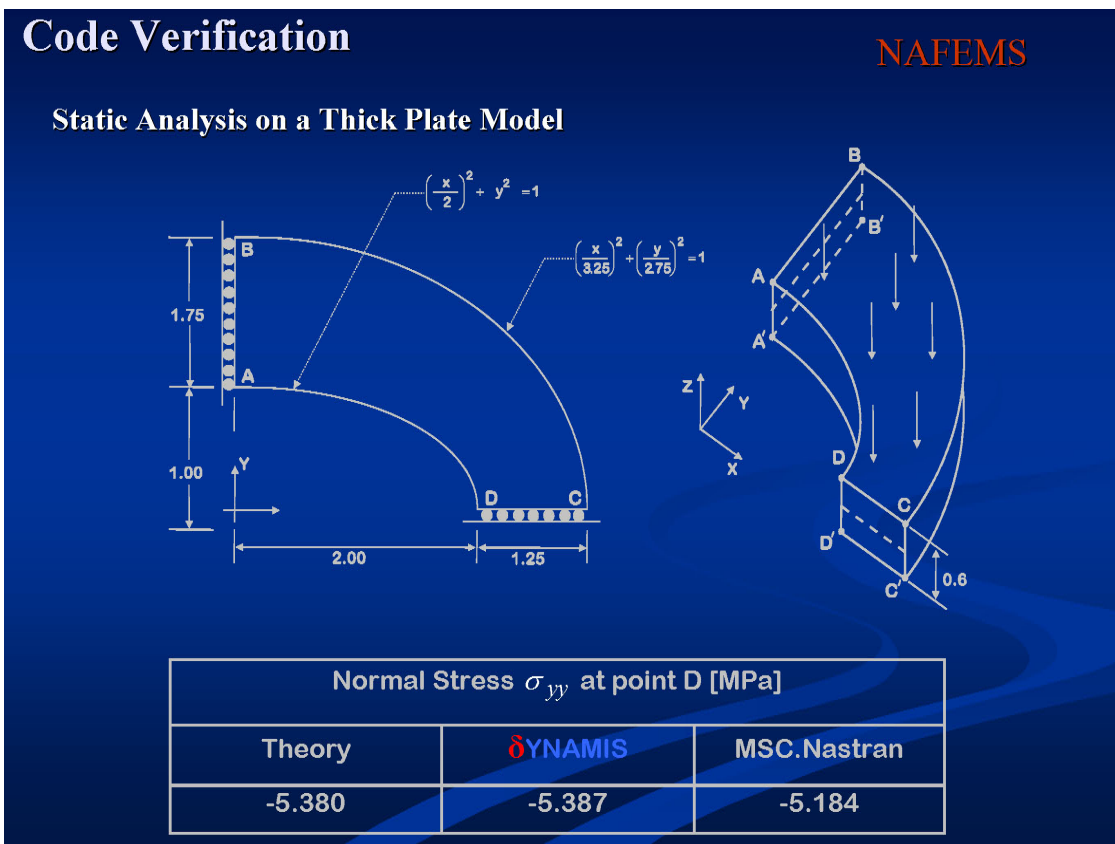
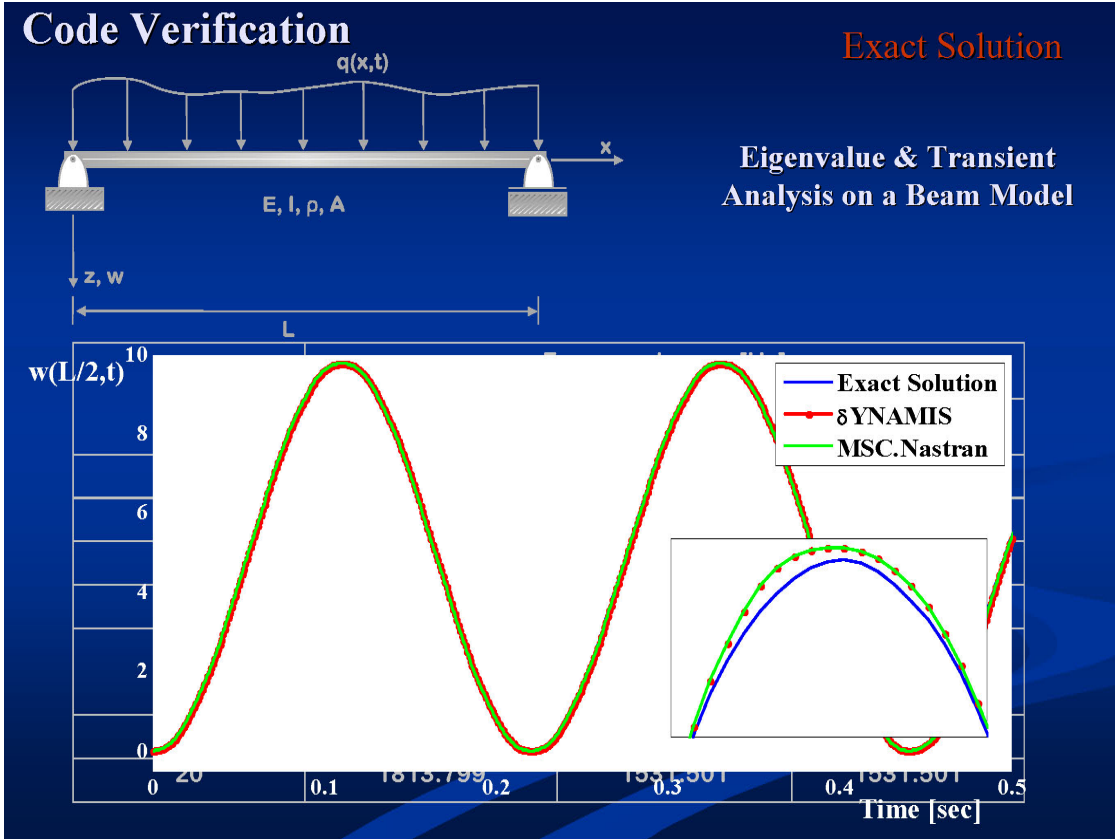
SPC, SPC1, SPCD, SPCADD, MPC, MPCADD

- **Loads**

FORCE, FORCEi, RFORCE, MOMENT, MOMENTi, SLOAD, PLOAD, PLOADi, GRAV, RLOADi, TLOADi, NONLINi, DAREA, DLOAD, DELAY, DPHASE, LSEQ

- **Solution Control**

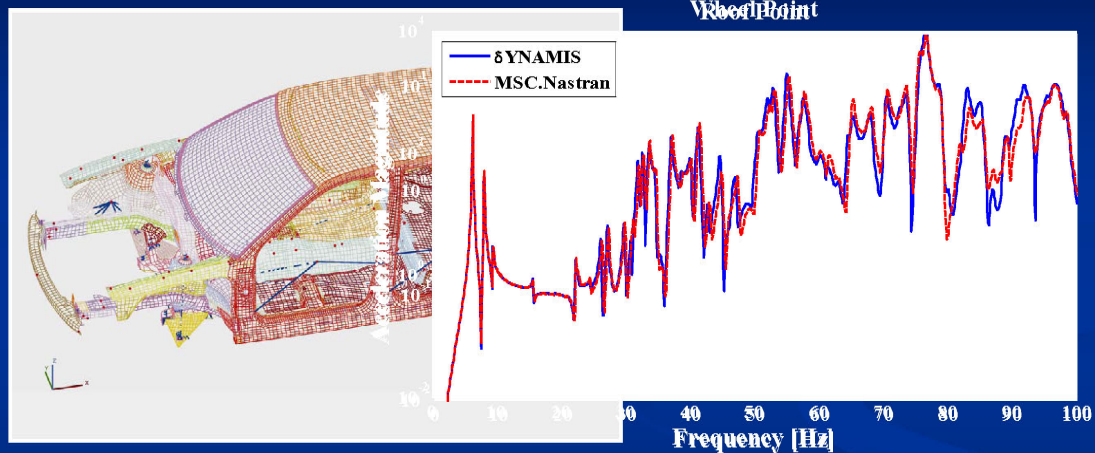
EIGR, EIGRL, EIGC, FREQ, FREQi, TIC, TSTEP, TSTEPNL, RANDPS, RANDT1, RCROSS, NLPARM



Code Verification

MSC.NASTRAN

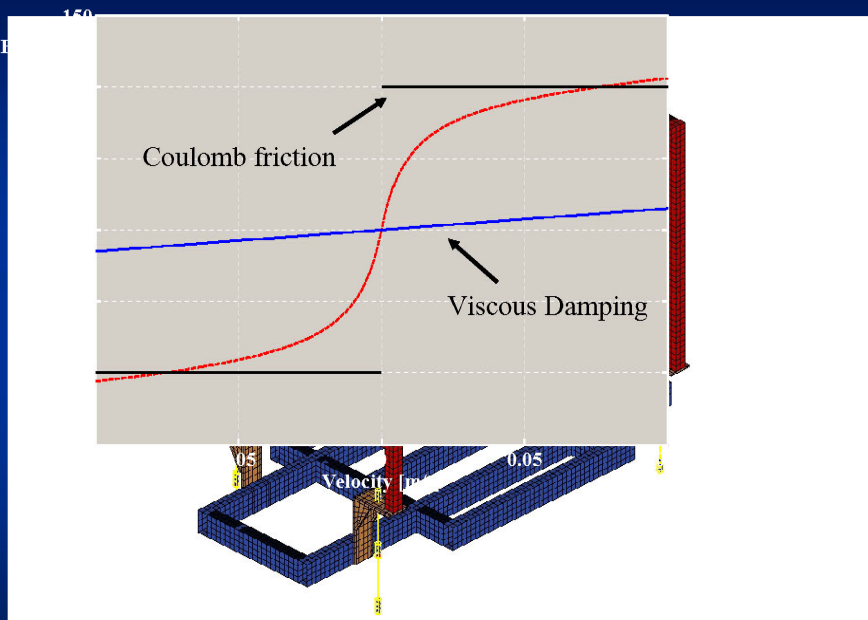
Vehicle Model



1,532,964 dof	[100Hz]	
	δ YNAMIS	MSC. Nastran
Memory Required [MB]	661	632
CPU Time [HH:MM:SS]	00:37:31	00:56:13
Elapsed Time [HH:MM:SS]	00:56:13	01:21:36

Structural Analyses Performed

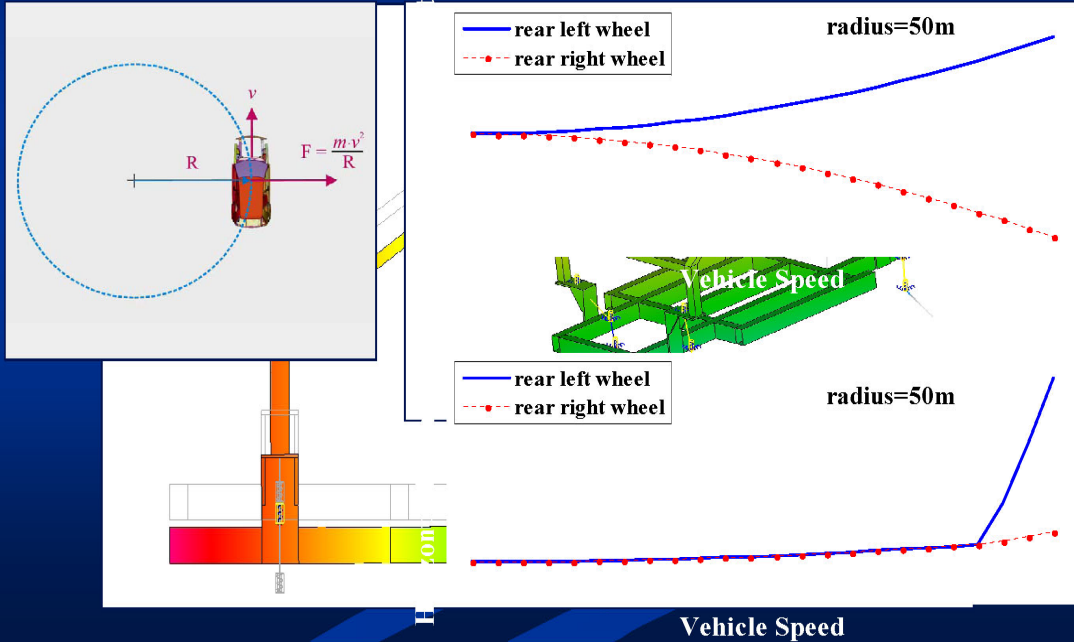
Mechanical Model



Structural Analyses Performed

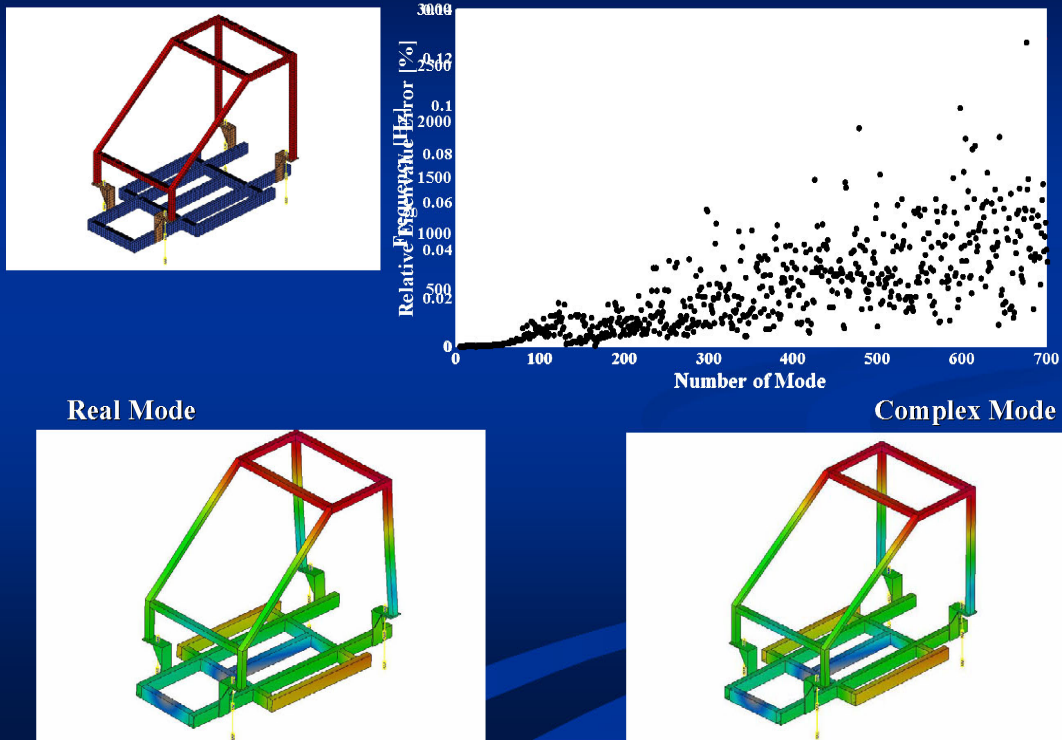
Static Equilibrium Analysis

Steady State Cornering (weight)



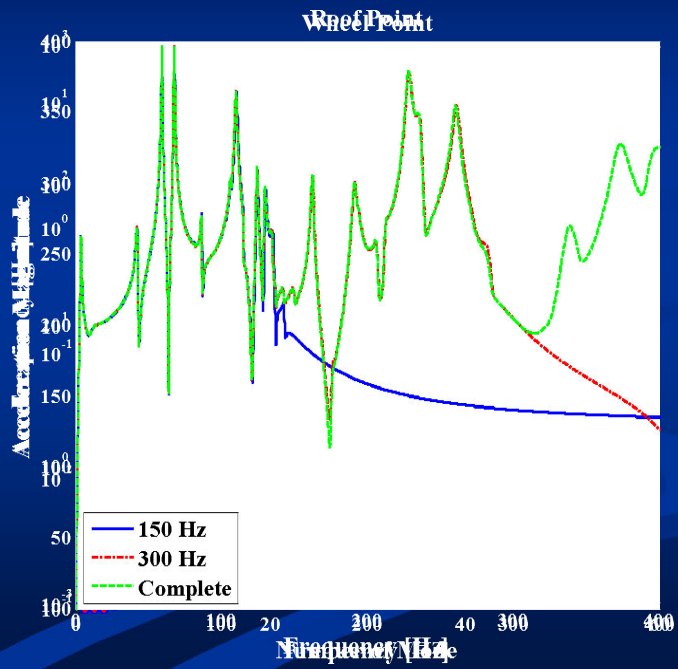
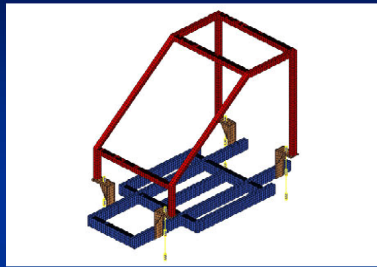
Structural Analyses Performed

Eigenvalue Analysis [Real / Complex]



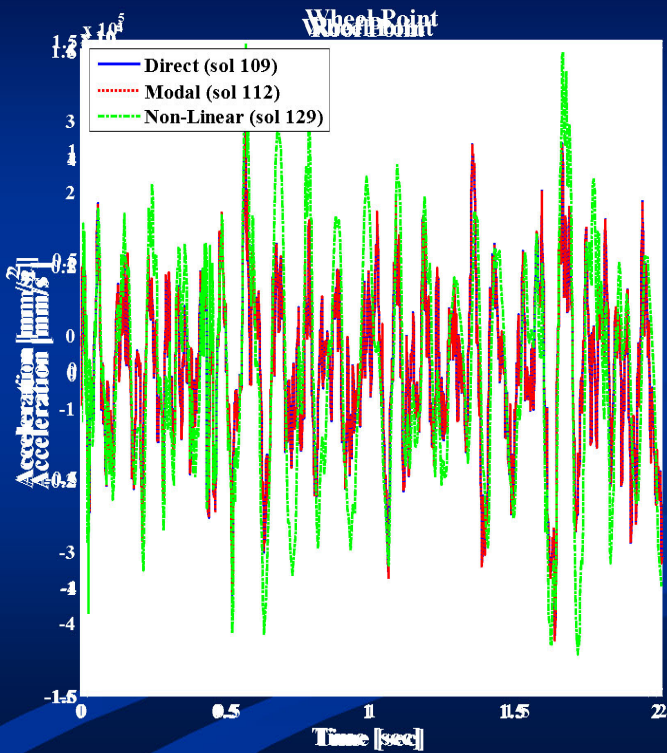
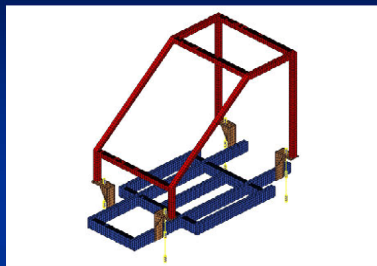
Structural Analyses Performed

Substructuring



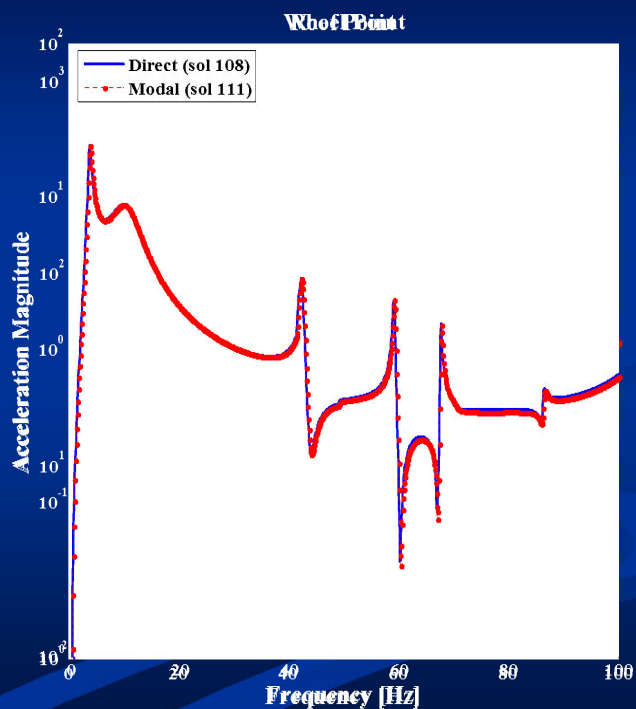
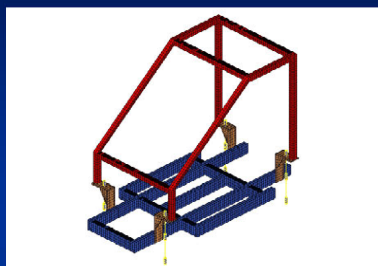
Structural Analyses Performed

Transient Response Analysis



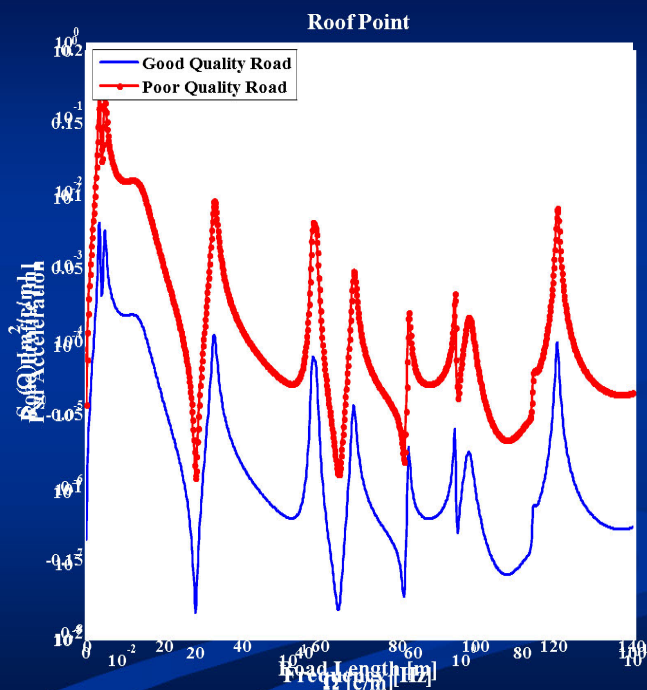
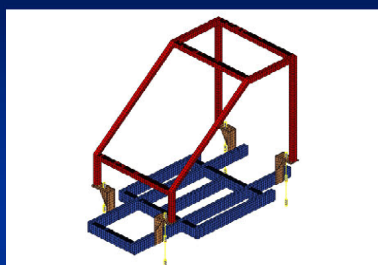
Structural Analyses Performed

Frequency Response Analysis



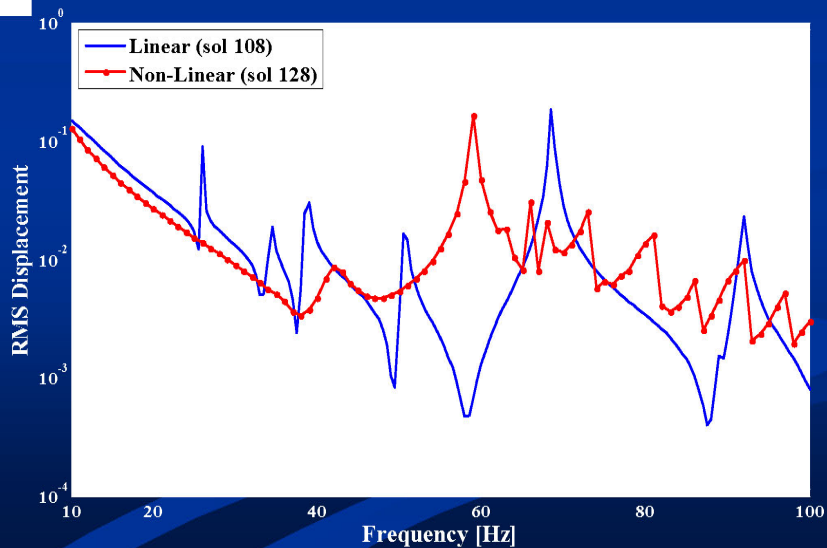
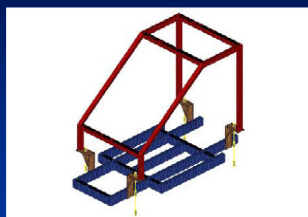
Structural Analyses Performed

Random Analysis



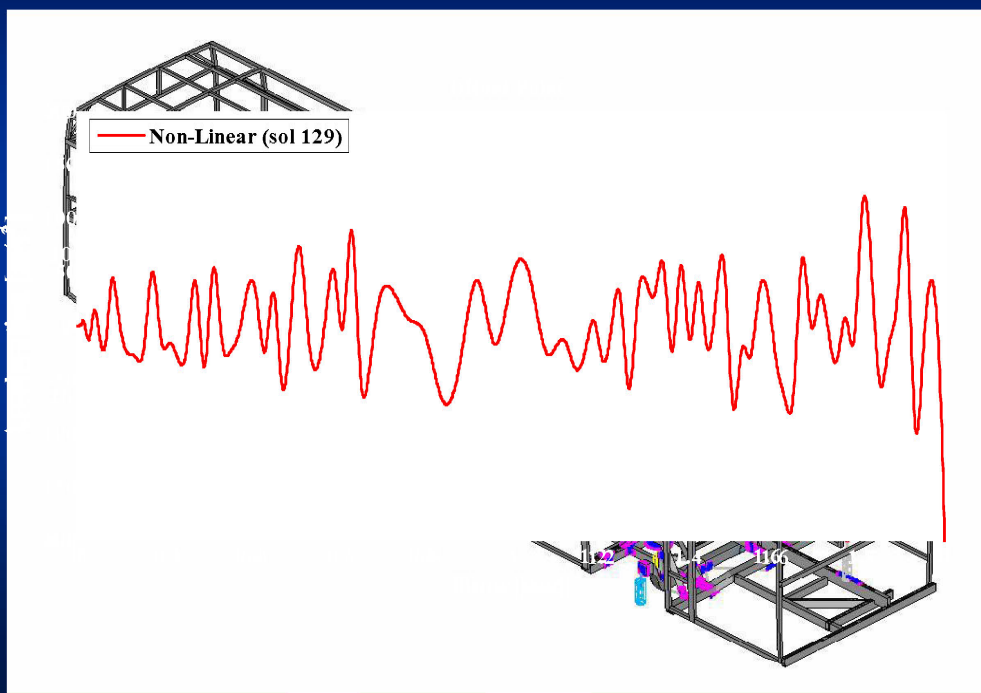
Additional Features

Non-Linear Frequency Response Analysis



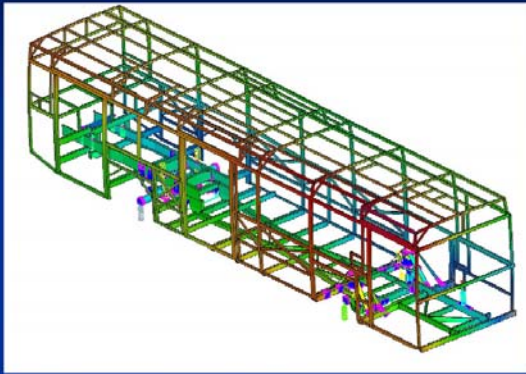
Additional Features

MLDS Substructuring on Non-Linear Transient Response Analysis



Additional Features

MLDS Restart Combination



δ YNAMIS	Elapsed Time [HH:MM:SS]	Time Save (%)
Analysis 1	00:37:06	
Analysis 2	00:45:58	0.0
Analysis 2 Restarted from Analysis 1	00:18:06	60.0

SYNOPSIS

- ✿ **Usability:** Full compatibility with Nastran data input files. Output in standard Output2 (op2) files
- ✿ **Completeness:** Full suite of analysis capabilities. Complete library of geometric cards, elements, constrains, loads, properties and materials for all kinds of structural analysis
- ✿ **Accuracy:** Extremely accurate line, shell and solid finite elements
- ✿ **Performance:** Highly sophisticated solvers exploit the very unique characteristics of the equations delivering solution in a fraction of time
- ✿ **Innovation:** New Non-Linear steady state analysis takes the classical linear frequency response into the non-linear domain, including continuation methods and stability analysis

EXTENSIONS

- **Parallel Processing**
- **Finite Elements (Gap, Composites, Superelements)**
- **Flexible Multi-Body Dynamics**
- **Extensions to Acoustics and Fatigue Problems**
- **Inverse Problems (Optimization, Identification, Control)**

δ YNAMIS

AUTOMATED PROCESS DEPLOYMENT FOR NASTRAN SOL 200 OPTIMIZATION ANALYSIS, USING ANSA/ μETA PACKAGE

Georgios Korbetis*, **Konstantinos Marmaras**

BETA CAE Systems S.A., Greece

KEYWORDS - optimization, NASTRAN, morphing, task management

ABSTRACT - The use of optimization techniques becomes increasingly popular both in the early design stages of the product and during the final testing using the Finite Element Analysis. Furthermore, the computational power now available is sufficient for using optimization on realistic product simulation models. As a result, the increasing complexity of the optimization problem and the subsequent complexity of the optimization software, render essential the use of a tool that organizes the definition of such processes and evaluates the results.

Pre-processing for the NASTRAN optimizer is possible through the Task Management functionality of ANSA which provides flexibility, reusability and knowledge transfer.

At the same time ANSA's Morphing Tool provides all the necessary functionality for shape optimization definition and easy coupling with the NASTRAN optimizer, while μETA PostProcessor offers an efficient way to evaluate the results.

TECHNICAL PAPER -

1. INTRODUCTION

The latest versions of ANSA and μETA support the pre- and post-processing of the optimization problem according to NASTRAN SOL 200. Property and Shape Optimization set up is possible.

NASTRAN offers four different methods to define a Shape Optimization problem. These are the *Manual Grid Variation Method*, the *Direct Input of Shapes*, the *Geometric Boundary Shapes* and the *Analytic Boundary Shapes*. Currently, ANSA supports the *Manual Grid Variation* method. Following this method, for every grid of the design space, the displacement vectors must be defined. These vectors prescribe the movement of every grid through the optimization loops for a given change in the relative design variable. So for each grid of the design space a DVGRID keyword must be defined which contains the information of the displacement vector and the design variable which drives the grid movement.

Even if this is a manual method, the use of ANSA Morphing Tool can automate the definition of DVGRID keywords in a way that all needed data are produced in a single step process. Furthermore, the Morphing Tool ensures that the deformed model's shape, at any stage of the optimization process, will be smooth. Finally the user can investigate, before running the solver, if an error is possible to come up in the optimization process due to elements quality failure, penetration, etc..

Property optimization is also supported. Currently, ANSA covers all the needed functionality for optimization according to element, material and connectivity properties.

Although all keywords concerning NASTRAN SOL 200 are supported in ANSA by functions and cards, the use of the ANSA Task Manager offers a flexible and user-friendly way to define the optimization problem. A case study of finding the optimal shape of a piston rod demonstrates the process set up.

ANSA Morphing Tool is able to provide morphing with various algorithms. These algorithms refer to the way that the FE-Model is modified for a given morphing process. The use of different algorithms can produce complicated shapes beginning from a simple geometry. In this way is possible to search for the optimal solution among many different shapes without having to declare a big number of design variables.

Finally, new enhancements of Morphing Tool like the new types of morphing parameters facilitate the definition of the shape optimization problem.

2. THE SHAPE OPTIMIZATION PROBLEM

ANSA Morphing Tool provides powerful functionality for the shaping of FE-Model. This capability can be efficiently used for the set up of a shape optimization problem. The definition of such problem is demonstrated by a case study. An FE-Model of a piston rod is subjected in static load. The objective of the optimization problem is to minimize the model's weight by modifying its shape. The maximum stress that appears in the model will be used as a constraint.

The design variables that are used to control model's shape (see Figure 1) are:

- *Radius:* The radius at the connection between housing and body
- *Taper:* The dimension that controls the taper of the rod
- *Curvature:* The dimension that applies a curvature at the body shape

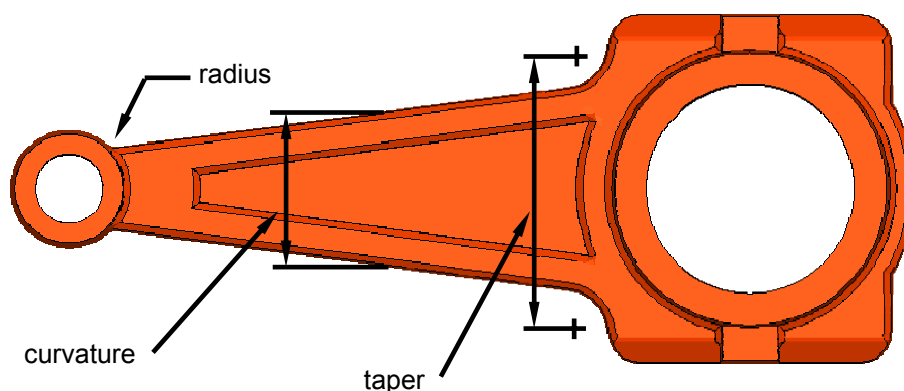


Figure 1. Design variables of the FE-Model

Morphing Boxes are special entities of the Morphing Tool which are fitted around the model to control its shape. The shape of the Morphing Boxes can be modified in several ways and handled by Control Points which facilitate any movement. The elements of the FE-Model surrounded from the Boxes follow the modification and in this way the shaping takes place.

For the definition of the above design variables, several independent groups of Morphing Boxes can be used. The group of Boxes shown in Figure 2 will be used for the definition of the *Taper* and *Curvature* design variables while the group shown in Figure 3 for the *Radius*.

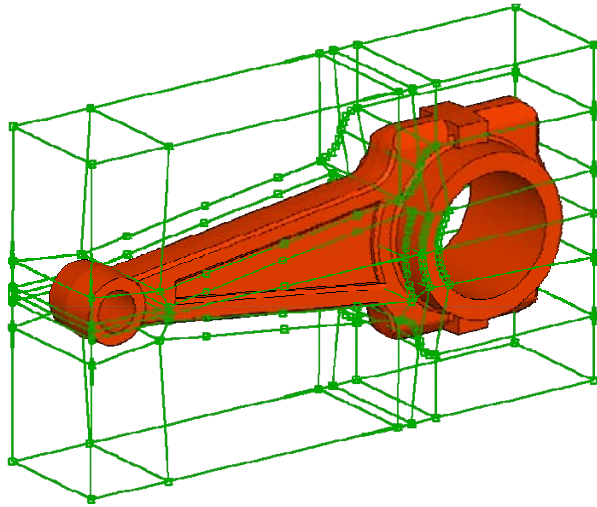


Figure 2. Group of Morphing Boxes for the Taper and Curvature

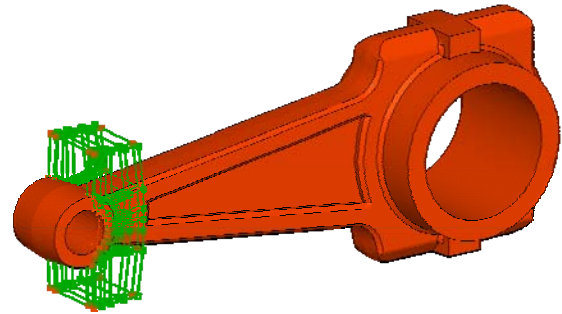


Figure 3. Group of Morphing Boxes for the Radius

The morphing process that will be applied by the Boxes shouldn't be a manual job since this process will be connected to an automatic sequence which will be executed to define all displacement vectors for all grids and design variables in one step. Therefore the modification of the Boxes shape is controlled parametrically by special entities, the Morphing Parameters. In Figure 4 the selected Control Points of the Boxes are moved along specified directions driven by one Morphing Parameter. Changing the parameters' value leads to the shaping of the model (see Figure 5).

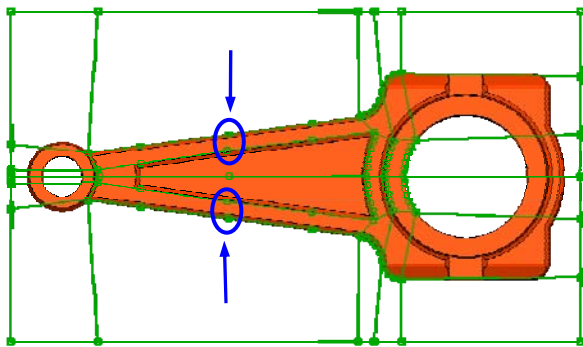


Figure 4. Morphing Parameter handles Control Points

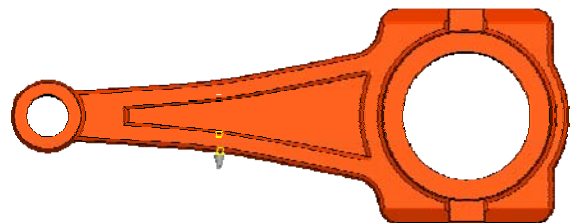


Figure 5. Shaping of the model by Morphing Parameters

Several types of Morphing Parameters cover a variety of movements which control efficiently the model shape. Using a Parameter of type *EdgeFit*, the modification that represents the *Radius* design variable is achieved. Using this Parameter, feature lines of the model can be fitted on special target curves (see Figure 6). The modified shape is shown in Figure 7.

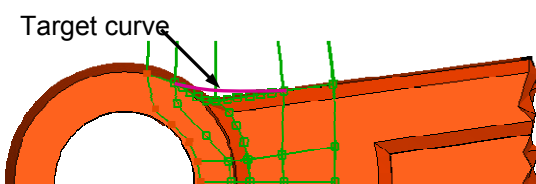


Figure 6. Fitting model's feature lines to curves

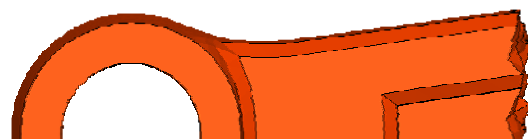


Figure 7. Modified shape

optimization loops, the grids will be moved by the displacement vector multiplied by the *Design Variable* value.

The DVGRID cards are defined in an automatic way with the use of the Morphing Tool. The Morphing Parameters that control the model shape are connected to the *Task Items* that represent the DVGRID cards (see Figure 10).

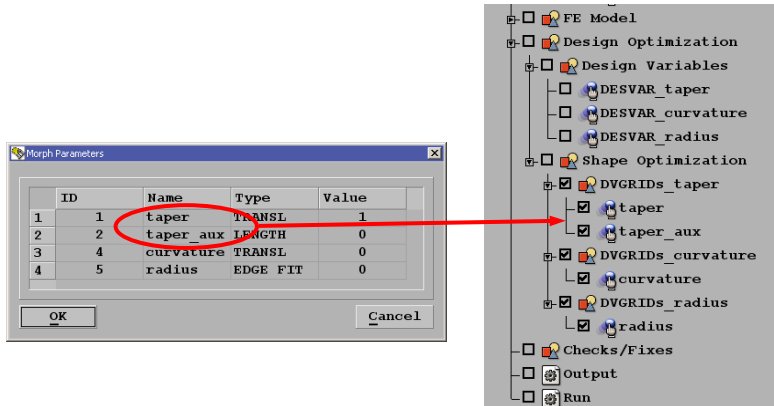


Figure 10. Connecting Morphing Parameters to DVGRID Task Items

By running the Task Manager sequence the following actions take place automatically (see Figure 11):

- The Morphing is applied to the model according to the connected Morphing Parameters.
- The DVGRID displacement vectors are calculated for all the grids that are affected from the Morphing.
- The model returns to its original position, as the initial shape is needed for the problem set up.
- The DVGRID keywords are stored in a list and they are assigned to the proper *Design Variables*.

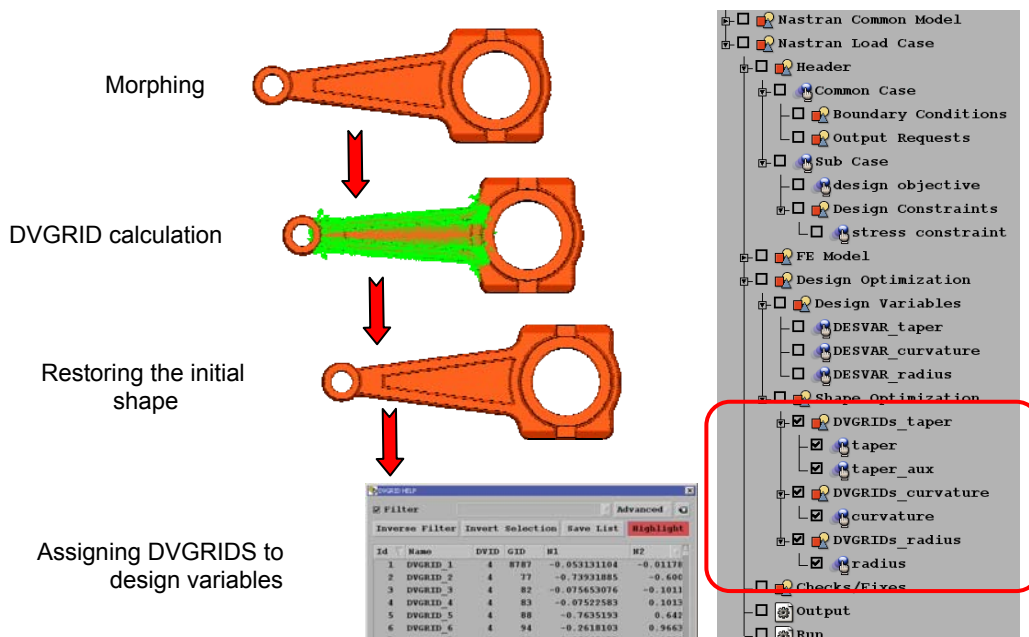


Figure 11. Defining DVGRIDS by the Morphing Tool

The Task Manager makes all the necessary checks and stops the process if a Task Item is not properly defined. Finally, it outputs the model in a ready to run NASTRAN file.

4. POST PROCESSING FOR NASTRAN SOL 200

The result files can be read into μETA Post since the NASTRAN Solution 200 is supported. The figures 12, 13 show the initial and optimal shape of the model.

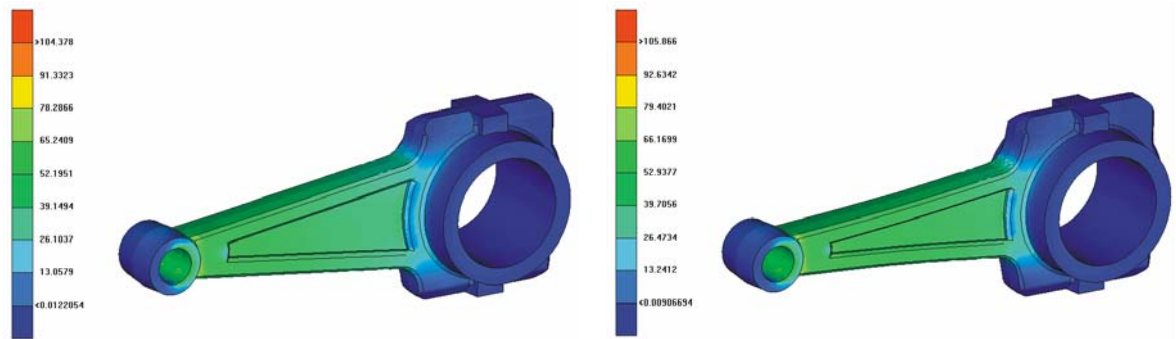


Figure 12. Initial shape

Figure 13. Optimal shape

Also in the 2D Plot of μETA Post is possible to draw the *Objective Function* and the *Design Variables* in relation to the optimization cycles (see Figure 14).

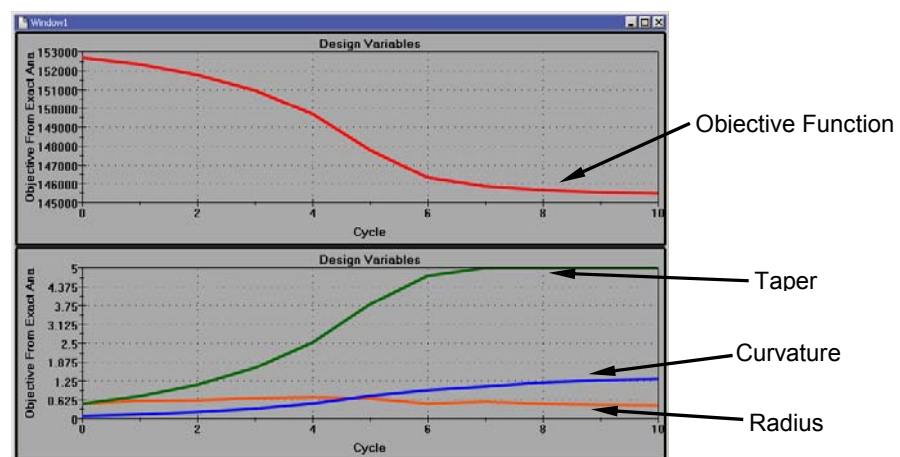


Figure 14. Objective Function and Design Variables in μETA Post 2D plot

5. DIRECT MORPHING FOR OPTIMIZATION

The Direct Morphing functionality of the Morphing Tool is a way to morph the model without the need of Boxes. Using this functionality the user can select the entities that will be moved, the constrained entities and the elements that will be affected by this movement. Direct Morphing is possible to be driven by Morphing Parameters so it can be connected to the Task Manager sequence. In Direct Morphing it is also possible to affect the model shape using different algorithms. These algorithms refer to the different way that the selected elements are modified by a specific Direct Morphing movement.

In the following example (Figure 15) of a planar FE-Surface, the middle node is moved upwards by the Direct Morphing function, while the edges of the surface are constrained. The intermediate elements will be affected by this movement. For these elements a *Linear* or *Cubic* algorithm can be applied. The results from the *Cubic* algorithm can be controlled by a variable.

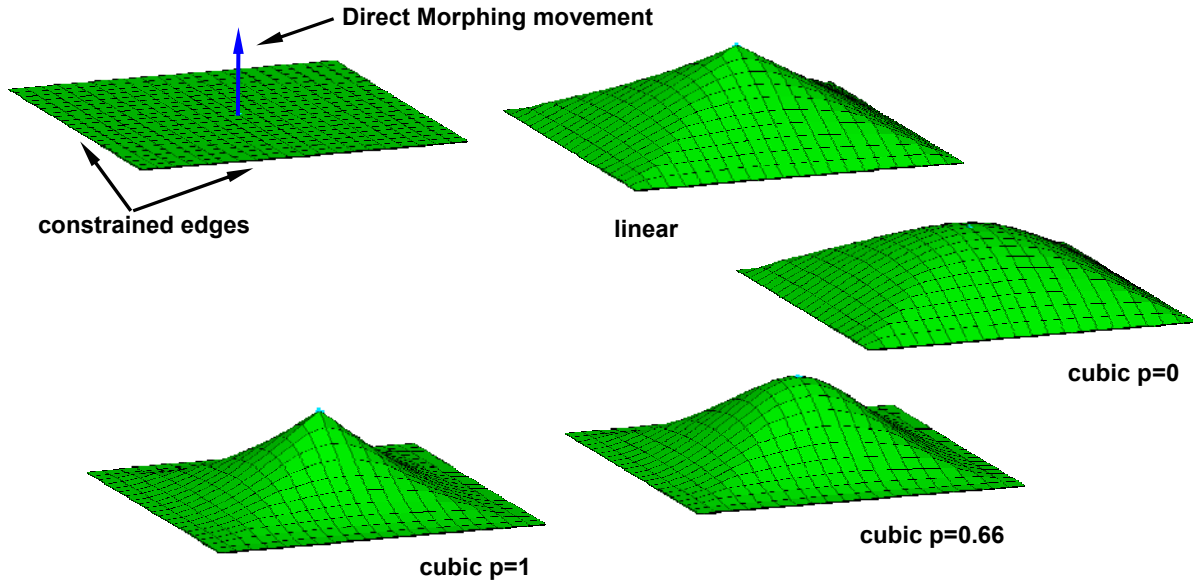


Figure 15. Applied different algorithms on FE-Surface

By adding morphing with different algorithms on the same FE-Surface (Figure 16), it is possible to get complicated shapes beginning from only a basic geometry. This can be proved to be very useful for the definition of shape optimization, since many design variables can be applied to a basic geometry searching for a complex optimal shape.

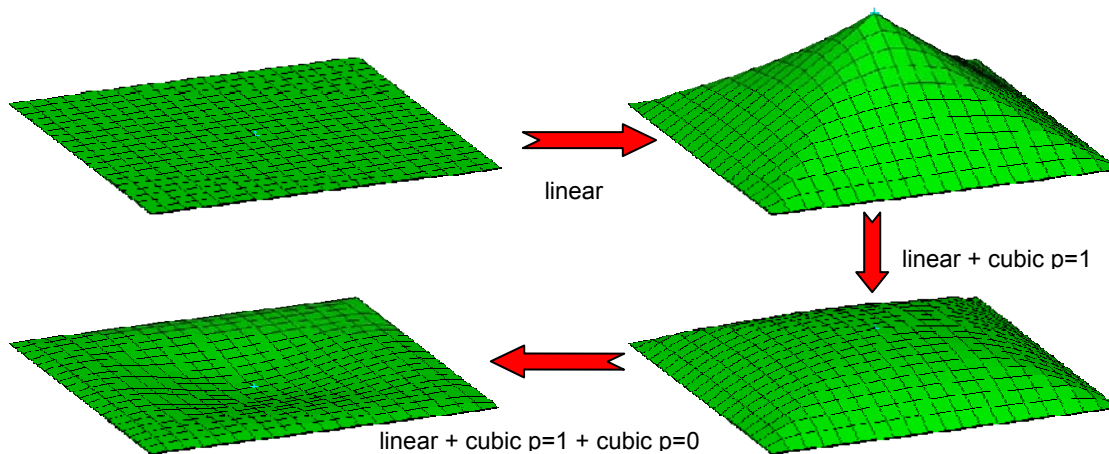


Figure 16. Combined morphing algorithms on FE-Surface

The following example demonstrates the application of combined morphing algorithms to a shape optimization problem. A simple vessel is subjected to inner pressure. The target is to minimize the volume by flattening the spherical surface. The maximum stress is used as a constraint which must be kept within a specific range.

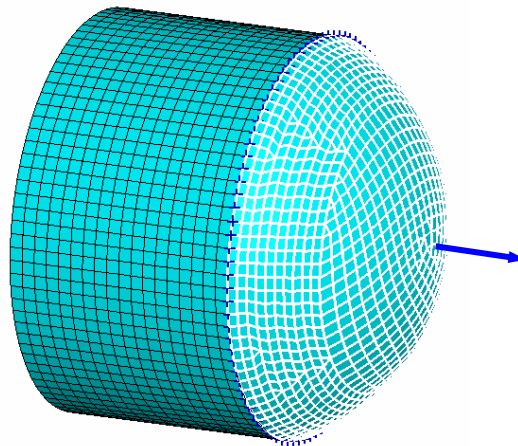


Figure 17. Pressure vessel optimization

Direct Morphing is applied on the spherical surface. The middle node of the surface is moved as shown in Figure 17 while the edges of the surface are constrained. The intermediate elements are morphed using different morphing algorithms.

The design variables are:

- *Linear*: Linear algorithm
- *Cubic $p=0$* : Cubic algorithm with parameter 0
- *Cubic $p=1$* : Cubic algorithm with parameter 1

The optimization process starts from the initial model with a surface of constant curvature and ends up with an optimum variable curvature shape (see Figures 18, 19).

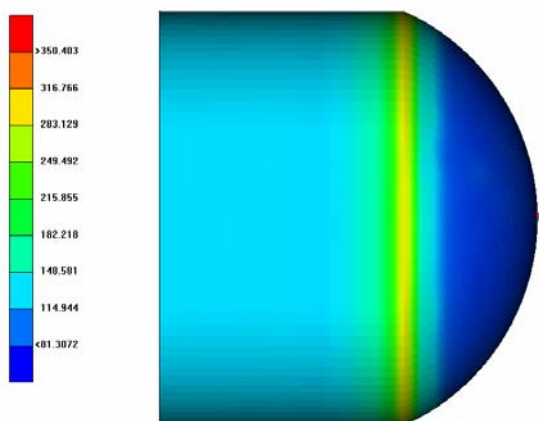


Figure 18. Initial shape with constant curvature

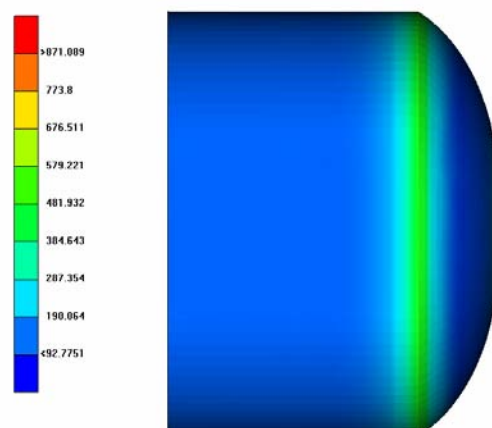


Figure 19. Optimal shape with variable curvature

The design variables and objective function are drawn in the 2D Plot of μ ETA Post in relation to the optimization cycles. The values of the design variables at the last stage represent the usage of each design variable to the composition of the optimal shape.

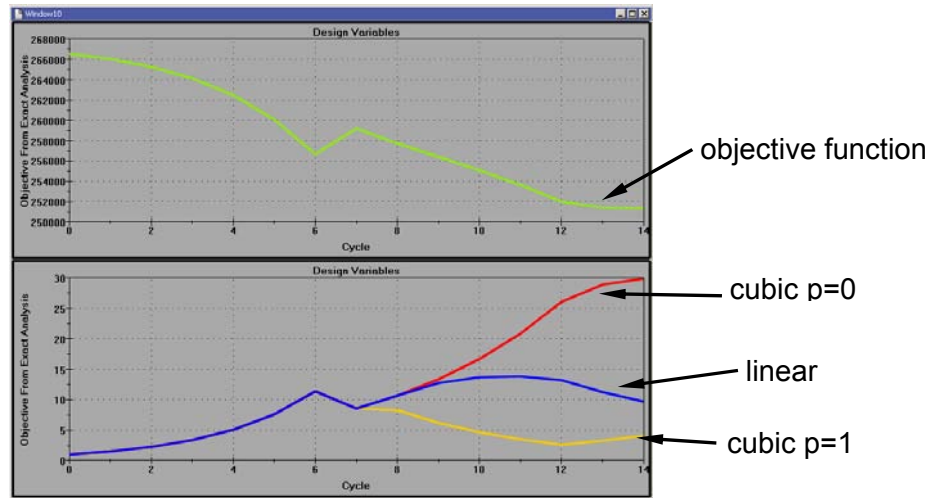


Figure 20. Objective Function and Design Variables in μ ETA Post 2D plot

6. THE DEFORMATION PARAMETER

The Morphing Tool can be used for the definition of the displacement vectors (DVGRIDS). For this purpose the Morphing Tool must reach the deformed shape of the model beginning from the initial shape. The difference in position between the initial and deformed shape of each grid gives the displacement vector. In many cases, many morphing functions must be applied in order to reach the deformed shape. Even though most of them can be controlled by Morphing Parameters, this is not possible for any manual adjustments that may be needed. As a result the manual adjustments cannot be connected to the Task Manager. Also the connection of the Morphing Parameters to the Task Manager sequence becomes a complex task when a big number of Parameters have to be connected in a specific order (Figure 21).

A new type of Morphing Parameter can facilitate this process. The Parameter of type *Deformation* can record all the morphing actions that take place from the initial to the deformed shape even if there is morphing through Parameters or manual adjustments.

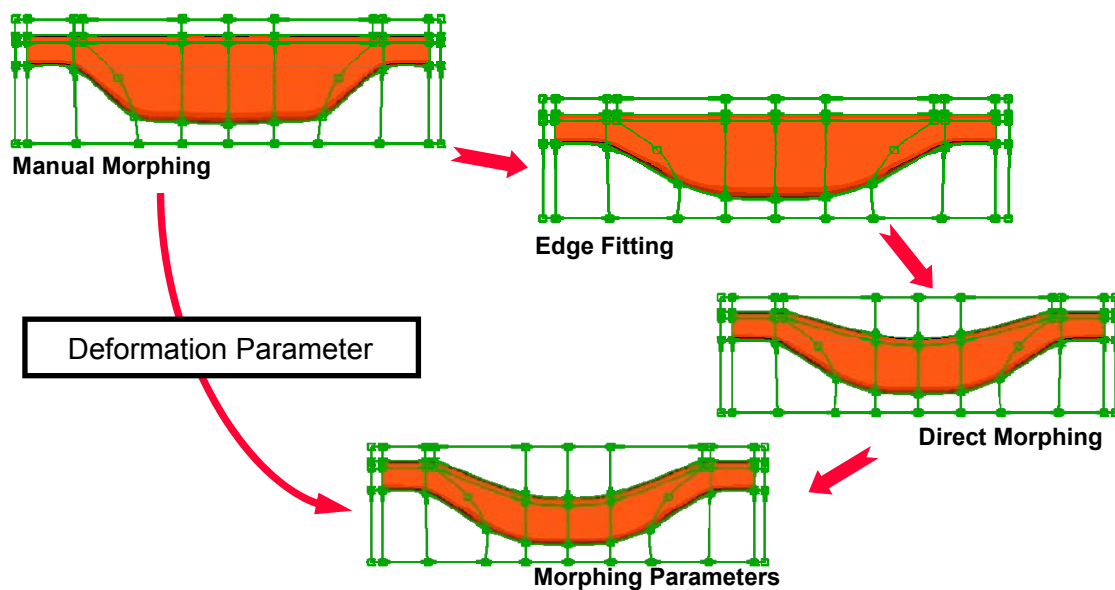


Figure 21 Deformation Parameter

Using this Parameter the initial or the deformed shape can be reached at any time by giving the value 0 or 1 respectively (Figure 22, 23). Furthermore, it is possible to reach any linear interpolation or extrapolation of the two shapes.



Figure 22. Initial shape.
Parameter value =0



Figure 23. Deformed shape.
Parameter value =1

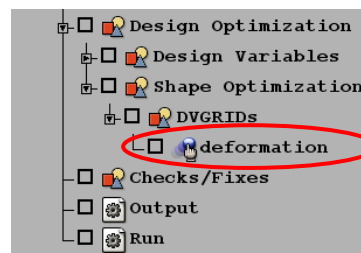


Figure 24. The Deformation parameter in the Task Manager

Using this functionality even a complicated morphing application with many manual adjustments can be driven by a single Morphing Parameter and connected easily to the Task Manager sequence.

In this way the definition of the displacement vectors (DVGRIDs) becomes even more flexible (Figure 24).

7. CONCLUSIONS

The set up of shape and property optimization for NASTRAN is possible in the ANSA pre-processor. META Post also supports the NASTRAN Solution 200 results and provides an easy and user-friendly way to evaluate the results.

The Morphing Tool is able to define the displacement vectors (DVGRIDs), for the shape optimization according to the *Manual Grid Variation Method*. The Morphing Tool provides a powerful functionality for the shaping of the model which is the key for the shape optimization for NASTRAN but also for all optimizers. The use of various morphing algorithms enables the definition of complicated shapes using a small number of design variables.

The pre-processing of the optimization problem can be automated by the Task Manager. The connection of the Morphing Tool with the Task Manager offers a powerful interface for the parametric shaping of the model and shape optimization set up.

REFERENCES

- (1) MSC.NASTRAN 2004, "Design Sensitivity and Optimization User's Guide", MSC.SOFTWARE, 2004
- (2) MSC.NASTRAN 2005, "Quick Reference Guide", MSC.SOFTWARE, Volume I, 2004
- (3) MSC.NASTRAN 2005, "Quick Reference Guide", MSC.SOFTWARE, Volume II, 2004
- (4) BETA CAE Systems S.A., "ANSA v12.1.2 User's Guide", BETA CAE Systems S.A., 2007

AN EFFICIENT RE-ANALYSIS METHODOLOGY FOR OPTIMIZATION OF LARGE-SCALE VIBRATION SYSTEMS

¹Zissimos Mourelatos*, ²Efstratios Nikolaidis,

¹Oakland University, Rochester MI, USA, ²The University of Toledo, Toledo OH, USA

KEYWORDS - Optimization, vibration, re-analysis, reduced-order modelling

ABSTRACT - Finite-element (FE) analysis is a well-established methodology in structural dynamics. However, optimization and/or probabilistic studies can be prohibitively expensive because they require repeated FE analyses of large models. Various re-analysis methods have been proposed with the premise to effectively calculate the dynamic response of a structure after a baseline design has been modified, without recalculating the new response.

The parametric reduced-order modelling (PROM) and the combined approximations (CA) are two re-analysis methods, which can handle large model parameter changes in a relatively efficient manner. Although both methods are promising by themselves, they can not handle large FE models with a large number of degrees of freedom (DOF) (e.g. greater than 100,000) and a large number of design parameters (e.g. greater than 50), which are common in practice. In this paper, the advantages and disadvantages of the PROM and CA methods are first discussed in detail.

Subsequently, a new re-analysis method is proposed where the original CA method is modified to further improve its efficiency, especially for problems where a large number of modes must be retained. The modified CA (MCA) method and Kriging interpolation are then integrated with the PROM approach, to formulate an efficient re-analysis method which can be used for optimization studies of complex structures. The method can efficiently handle large FE models with many design parameters that vary in a wide range.

A vibro-acoustic analysis of a realistic vehicle finite-element model is presented to demonstrate the efficiency and accuracy of the new re-analysis method and a design optimization study highlights its capabilities.



An Efficient Re-Analysis Methodology for Optimization of Large-Scale Vibration Systems



Zissimos P. Mourelatos
Mechanical Engineering Department, Oakland University, Rochester, MI 48309-4478, USA

Efstratios Nikolaidis
Mechanical, Industrial and Manufacturing Engineering Department, University of Toledo, Toledo, OH 43606, USA

Zissimos P. Mourelatos

2007 ANSA & mETA Int'l Congress

1





Overview

- **Introductory Remarks**
 - Reduced-Order Modeling in Structural Dynamics
- **Review of Existing Re-analysis Methods**
 - Parametric Reduced-Order Modeling (PROM) Method
 - Combined Approximation (CA) Method
- **New Re-Analysis Method**
 - Modified Combined Approximation (MCA) Method
 - Integration of MCA with Optimization
- **Summary and Conclusions**

Zissimos P. Mourelatos

2007 ANSA & mETA Int'l Congress

2



 **Reduced-Order Modeling (ROM)
(Modal Model)** 

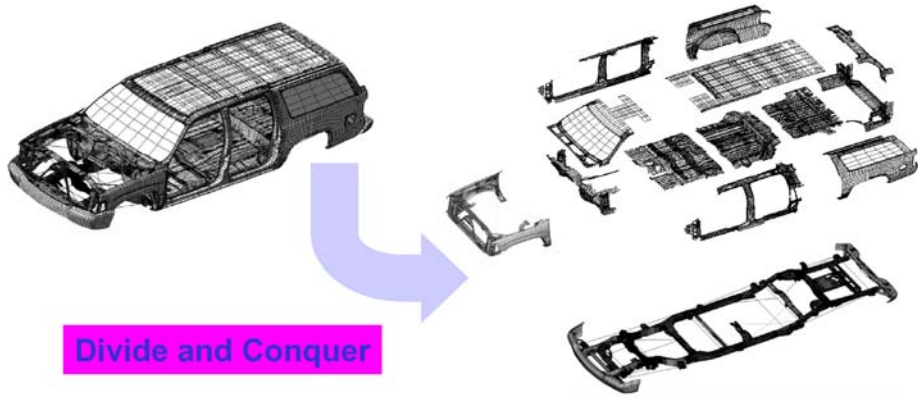
- **Eigenvalue Analysis**
 - Lanczos Algorithm
- **“Math” Substructuring**
 - Automated Multi-Level Substructuring (AMLS)
- **“Physical” Substructuring**
 - Component Mode Synthesis (CMS)
 - Craig-Bampton (Fixed Interface)
 - CMS with Interface Modes

Zissimos P. Mourelatos

2007 ANSA & μ ETA Int'l Congress

3

 **Reduced-Order Modeling** 





Divide and Conquer

Zissimos P. Mourelatos

2007 ANSA & μ ETA Int'l Congress

4

Reduced-Order Modeling

$$[\mathbf{K} - \omega^2 \mathbf{M}] \mathbf{d} = \mathbf{F}$$

Modal Representation: $\mathbf{d} = \Phi \mathbf{U}$

Modal Basis: $\Phi = [\phi_1 \quad \phi_2 \quad \cdots \quad \phi_n]$

Modal Model: $[\Phi^T \mathbf{K} \Phi - \omega^2 \Phi^T \mathbf{M} \Phi] \mathbf{U} = \Phi^T \mathbf{F}$



Practical Issues:

- Basis Φ must be recalculated for each new design
- Many modes must be retained
- Calculation of “triple” product $\Phi^T \mathbf{K} \Phi$ can be expensive

Zissimos P. Mourelatos

2007 ANSA & mETA Int'l Congress

5

Our Solution

Re-analysis methods: PROM and CA / MCA

Practical Issues:


- Basis Φ must be recalculated for each new design
- Many modes must be retained
- Calculation of “triple” product $\Phi^T \mathbf{K} \Phi$ can be expensive

Kriging interpolation


Zissimos P. Mourelatos

2007 ANSA & mETA Int'l Congress

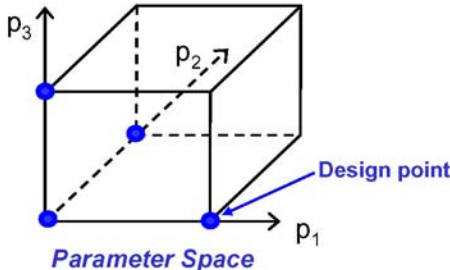
6



Parametric Reduced-Order Modeling (PROM)

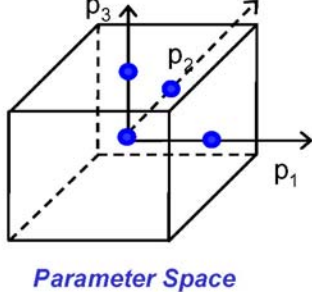


*Zhang et. al.'s Approach
(Corner Points)*



Parameter Space


*Balme's Approach
(Center Points)*




Parameter Space

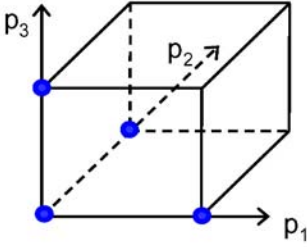
$$P = [\Phi_0 \quad \Phi_1 \quad \Phi_2 \quad \Phi_3] \leftarrow \text{Reduced Basis}$$

- PROM method is an extension of Rayleigh-Ritz method
- Quality of approximation is decided by number and location of design points
- Both approaches require (p+1) design points
- **Mode shapes from the first approach are less likely to be linear dependent**



PROM: Procedure Steps





p_1, p_2, p_3 : design parameters

Eigen-analysis of full matrices

$$eig(\mathbf{K}_p, \mathbf{M}_p) \Rightarrow \lambda^p, \Phi_p$$

1. Form reduced basis:

$$P = [\Phi_0 \quad \Phi_1 \quad \Phi_2 \quad \Phi_3]$$
2. Project system matrices to reduced basis:

$$\mathbf{K}_R = P^T \mathbf{K}_p P \quad \mathbf{M}_R = P^T \mathbf{M}_p P$$
3. Eigen-analysis of reduced matrices:

$$eig(\mathbf{K}_R, \mathbf{M}_R) \Rightarrow \tilde{\lambda}^p, \Theta$$
4. Obtain approximate eigenvectors:

$$\tilde{\Phi}_p = P \Theta$$

- **Advantage:** Re-analysis is done using the reduced basis
- **Disadvantage:** Condensation of matrices can be expensive due to large size and high density of mode matrix P



Combined Approximation (CA) Method



Original Eigenvalue Problem

$$\mathbf{K}_0 \Phi_0 = \lambda_0 \mathbf{M}_0 \Phi_0$$

Modified Model

$$\mathbf{K}_p = \mathbf{K}_0 + \Delta \mathbf{K}$$

$$\mathbf{M}_p = \mathbf{M}_0 + \Delta \mathbf{M}$$

Direct Solution for Modified Eigenvectors

$$(\mathbf{K}_0 + \Delta \mathbf{K}) \Phi_p = \lambda_p \mathbf{M}_p \Phi_p$$

$$\text{or } \Phi_p = \lambda_p \mathbf{K}_0^{-1} \mathbf{M}_p \Phi_p - \mathbf{K}_0^{-1} \Delta \mathbf{K} \Phi_p$$

Iterative Solution for Modified Eigenvectors

$$\Phi_{p,j} = \lambda_p \mathbf{K}_0^{-1} \mathbf{M}_p \Phi_{p,j-1} - \mathbf{K}_0^{-1} \Delta \mathbf{K} \Phi_{p,j-1}$$

Definition and formation of base vectors

$$\mathbf{R}_j = \Phi_{p,j} - \Phi_{p,j-1}$$

$$\mathbf{R}_1 = \mathbf{K}_0^{-1} \mathbf{M}_p \Phi_0$$

$$\mathbf{R}_j = -\mathbf{K}_0^{-1} \Delta \mathbf{K} \mathbf{R}_{j-1} \quad j = 2, \dots, s$$

$$\mathbf{R} = [\mathbf{R}_1 \quad \mathbf{R}_2 \quad \dots \quad \mathbf{R}_s]$$

Zissimos P. Mourelatos

2007 ANSA & mETA Int'l Congress

9



Combined Approximation (CA) Method



Project system matrices to reduced basis:

$$\mathbf{K}_R = \mathbf{R}^T \mathbf{K}_p \mathbf{R} \quad \mathbf{M}_R = \mathbf{R}^T \mathbf{M}_p \mathbf{R}$$

Eigen-analysis of reduced matrices:

$$\text{eig}(\mathbf{K}_R, \mathbf{M}_R) \Rightarrow \tilde{\lambda}^p, \Theta$$

Obtain approximate eigenvectors:

$$\tilde{\Phi}_p = \mathbf{R} \Theta$$

- **Advantages:**
 1. Very accurate because base vectors are updated at every new design point
 2. Decomposition is performed once on \mathbf{K}_0
- **Disadvantages:**
 1. For a large number of simulations, the cost to obtain base vectors \mathbf{R} may be prohibitive
 2. Savings from decomposing only \mathbf{K}_0 may be negligible for a large number of modes

Zissimos P. Mourelatos

2007 ANSA & mETA Int'l Congress

10



CA Method: Cost vs. Number of Modes



Major cost of CA method

$$\mathbf{R}_1 = \mathbf{K}_0^{-1} \mathbf{M}_p \Phi_0 \longleftrightarrow \text{SOLVE} = \text{DCMP} + \text{FBS}$$

■ Example Problem:

- Model: Vehicle with 65,000 DOF
- Machine: SUN ULTRA workstation
- Software: Nastran V2001

	1 Mode	500 Modes
DCMP Cost	4 seconds	4 seconds
FBS Cost	0.1 second	50 seconds
Total Cost of SOLVE	4.1 seconds	54 seconds
Conclusion	Cost dominated by DCMP	Cost dominated by FBS

- When cost of SOLVE is dominated by FBS, the computational advantage from inverting \mathbf{K}_0 only once is insignificant



Modified Combined Approximation (MCA) Method



Direct Solution of Modified Eigenproblem

$$\mathbf{K}_p \Phi_p = \lambda_p \mathbf{M}_p \Phi_p$$

$$\text{or } \Phi_p = \lambda_p \mathbf{K}_p^{-1} \mathbf{M}_p \Phi_p$$

Iterative Solution of Modified Eigenproblem



$$\Phi_{p,j} = \lambda_p \mathbf{K}_p^{-1} \mathbf{M}_p \Phi_{p,j-1}$$

Definition and formation of basis vectors

$$\mathbf{T}_1 = \mathbf{K}_p^{-1} (\mathbf{M}_p \Phi_0)$$

$$\mathbf{T}_i = \mathbf{K}_p^{-1} (\mathbf{M}_p \mathbf{T}_{i-1}) \quad i = 2, 3, \dots, s$$

$$\mathbf{T} = [\Phi_0 \quad \mathbf{T}_1 \quad \mathbf{T}_2 \quad \dots \quad \mathbf{T}_s]$$

CA vs. MCA

CA Method

$$\mathbf{R}_1 = \mathbf{K}_0^{-1} \mathbf{M}_p \Phi_0$$

$$\mathbf{R}_j = -\mathbf{K}_0^{-1} \Delta \mathbf{K} \mathbf{R}_{j-1} \quad j = 2, \dots, s$$

$$\mathbf{R} = [\mathbf{R}_1 \quad \mathbf{R}_2 \quad \dots \quad \mathbf{R}_s]$$

\longleftrightarrow

MCA Method

$$\mathbf{T}_1 = \mathbf{K}_p^{-1} (\mathbf{M}_p \Phi_0)$$

$$\mathbf{T}_i = \mathbf{K}_p^{-1} (\mathbf{M}_p \mathbf{T}_{i-1}) \quad i = 2, 3, \dots, s$$



$$\mathbf{T} = [\Phi_0 \quad \mathbf{T}_1 \quad \mathbf{T}_2 \quad \dots \quad \mathbf{T}_s]$$

- **Comparison between CA and MCA**
 - Both have high accuracy, due to updated basis vectors at each new design
 - MCA spends more effort on DCMP of \mathbf{K}_p
 - MCA needs fewer iterations (smaller s)
 - MCA uses a smaller basis (\mathbf{T} vs. \mathbf{R})
 - Overall cost of MCA is less than CA if a large number of modes is retained

Zissimos P. Mourelatos

2007 ANSA & mETA Int'l Congress

13

Integration of MCA and PROM Methods

Parameter Space

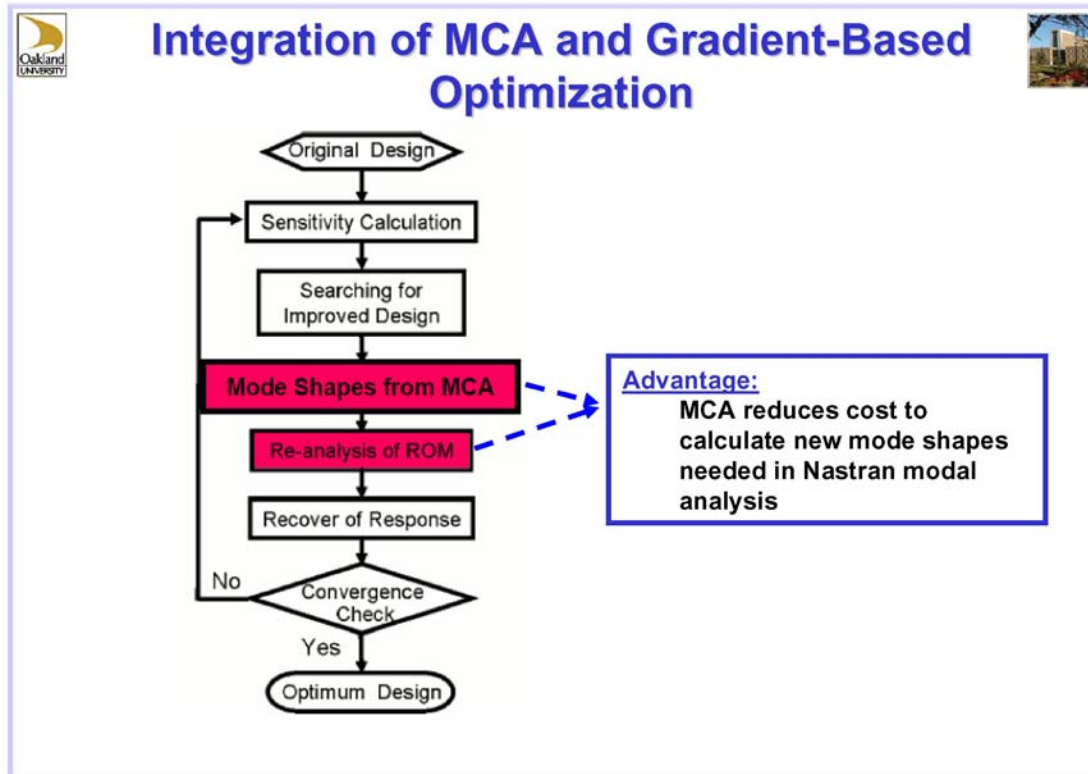
$$\mathbf{P} = [\Phi_0 \quad \Phi_1 \quad \Phi_2 \quad \Phi_3]$$

- Beneficial for very large number of re-analysis (Probabilistic studies, Genetic Algorithms)

Zissimos P. Mourelatos

2007 ANSA & mETA Int'l Congress

14



Zissimos P. Mourelatos

2007 ANSA & mETA Int'l Congress

15

Model:
Pickup truck with 65,000 DOF

Excitation:
Unit harmonic force applied at engine mount points in X, Y and Z directions

Response:
Sound pressure level (SPL) at driver's ear location


■ **Hardware and Software:**

- Machine: SUN ULTRA workstation
- Software: Nastran V2001


Zissimos P. Mourelatos

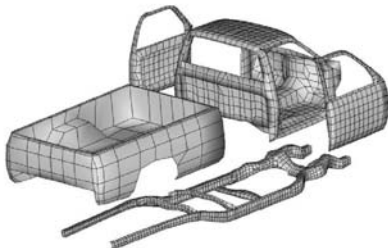
2007 ANSA & mETA Int'l Congress

16



Vehicle Model: Design Change






Param. #	Description (thickness of)	Initial Design	Modified Design
1	Chassis	3.137 mm	6.274 mm
2	Chassis cross link	3.611 mm	7.222 mm
3	Cabin	2.370 mm	4.740 mm
4	Bed	2.500 mm	5.000 mm
5	Left and right doors	1.240 mm	2.480 mm

➤ **Large parameter changes (100%)**


Zissimos P. Mourelatos

2007 ANSA & mETA Int'l Congress

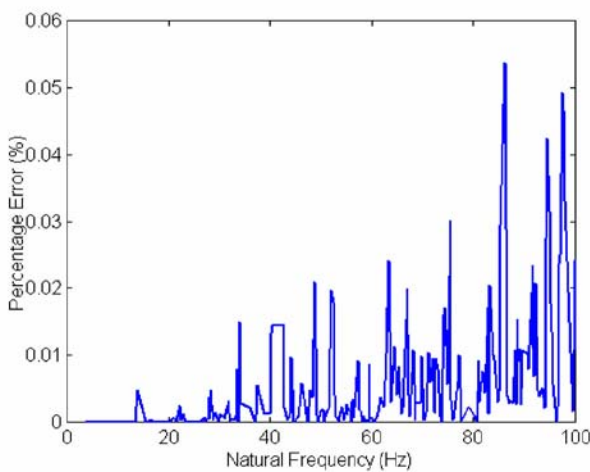
17



Accuracy of Modes



Eigen-Frequencies: MCA+PROM vs. Nastran

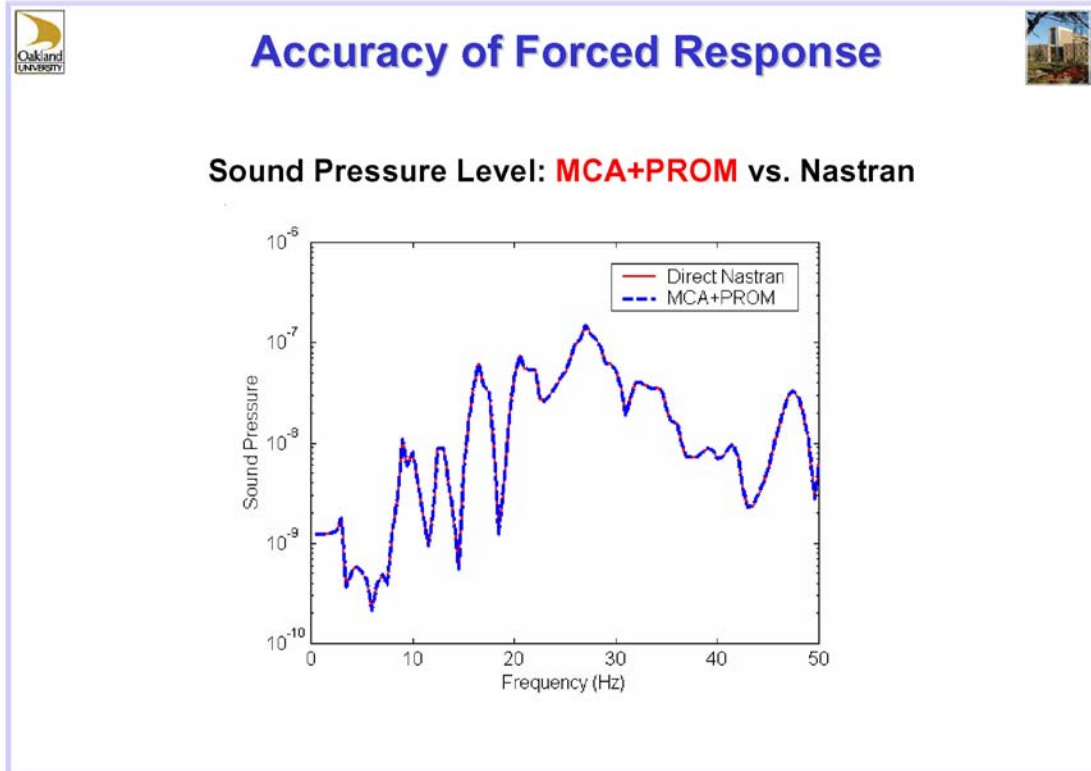


➤ **Maximum error is 0.06% in the frequency range of 0-100 Hz.**

Zissimos P. Mourelatos

2007 ANSA & mETA Int'l Congress



18



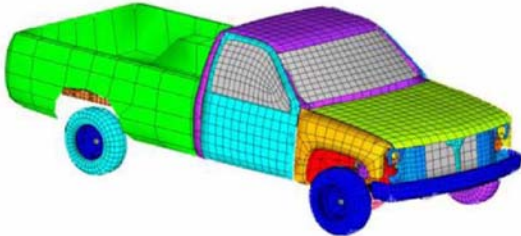
Zissimos P. Mourelatos

2007 ANSA & mETA Int'l Congress

19



Vehicle Model: **Design Optimization**



- **Objective:** Minimize sound pressure level at driver's ear
- **5 Design Variables**

Zissimos P. Mourelatos

2007 ANSA & mETA Int'l Congress

20



Observations

- Two acoustic modes at **95.9 Hz** and **128.3 Hz**
- Approximately **1050** modes in the **0 – 300 Hz** range
- **500** significant modes were identified and used in modal model

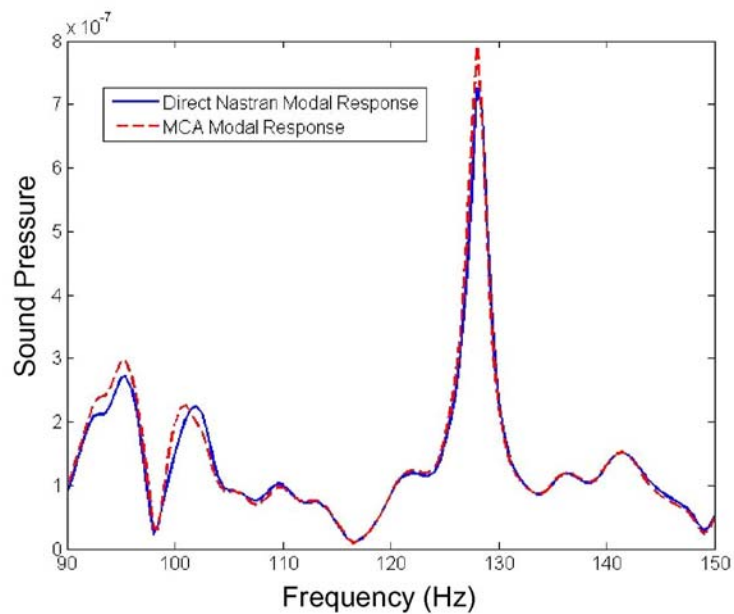
Zissimos P. Mourelatos

2007 ANSA & mETA Int'l Congress

21




Accuracy of MCA Method




Zissimos P. Mourelatos

2007 ANSA & mETA Int'l Congress

22



Optimization Results

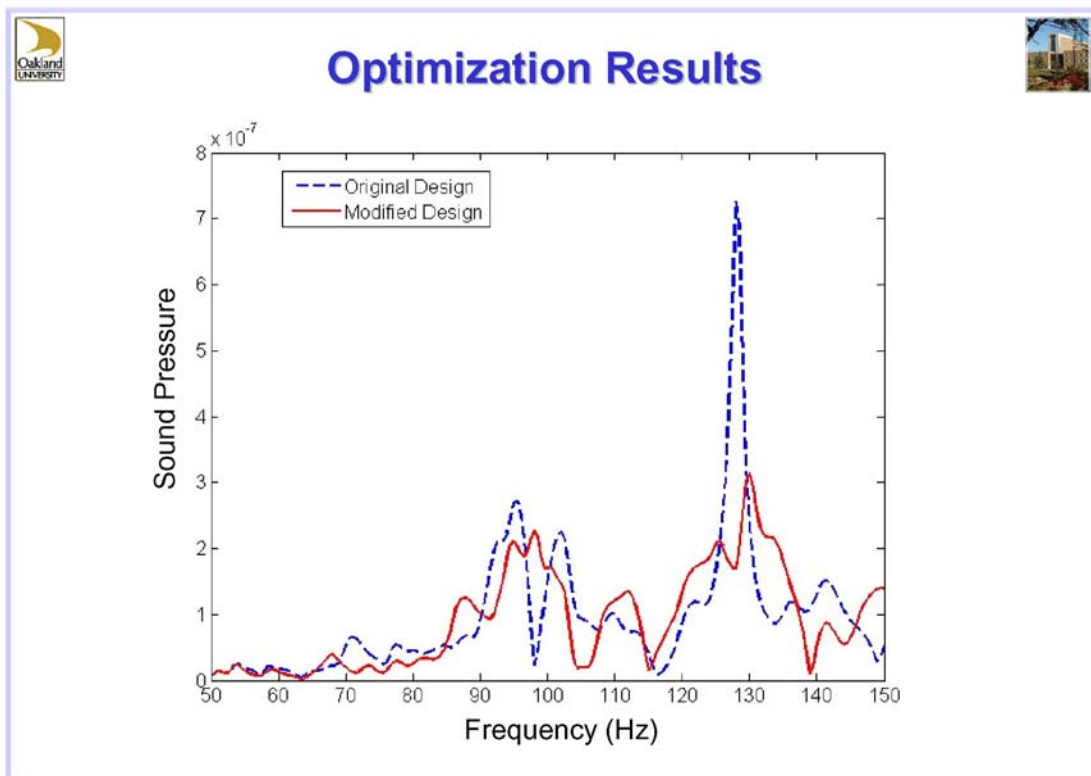


Design Variable	Description (thickness of)	Baseline Design (mm)	Optimal Design (mm)	% Change
1	Chassis	3.137	3.218	+2.6
2	Chassis cross link	3.611	5.225	+44.7
3	Cabin	2.370	3.555	+50.0
4	Bed	2.500	2.170	-13.2
5	Left and right doors	1.240	1.730	+39.5

Zissimos P. Mourelatos

2007 ANSA & mETA Int'l Congress

23



Zissimos P. Mourelatos

2007 ANSA & mETA Int'l Congress

24

Session H2.3

CASE STUDY ON THE FE-MODEL AND GEOMETRY MORPHING IN STRUCTURAL ANALYSIS

George Panagos, Nikolas Drivakos*

BETA CAE Systems S.A., Greece

KEYWORDS - geometry morphing, FE- model morphing, morphing, design process, optimization

ABSTRACT - In order to minimize time and resources needed to develop new prototypes, designers use already built models and based on these they continue with the creation of the new one. Again, in order to minimise development cost, old parts, doors, bonnets etc., are modified in order to be used in new prototypes. There are also cases that for completed models some modification are needed in order to meet new requirements, (creation of embosses to control deformation) but minimal or no manual intervention is wanted either for the mesh or the boundary conditions.

This procedure, modifying an existing design in order to develop a new one or to meet specific requirements for some parts, can be achieved using ANSA Morphing Tool. With the morphing tool the engineer is capable of shaping his design according to his needs. Till now, ANSA Morphing Tool worked only on FE-models and in conjunction with the mesh reconstruction/regeneration capabilities of ANSA, it was possible to modify complete models with minimal or no user intervention. The only drawback of this procedure is that since geometry is not included in the morphing, the final shape can not be outputted and reused by the CAD software.

This present paper, ANSA Morphing Tool for geometry is introduced for the first time. The procedure of Geometry Morphing is presented for a number of cases, alongside with FE-model morphing for the same cases, starting from the initial geometry and concludes after morphing to the final model that also includes the new geometric definition which can be used by CAD software.

TECHNICAL PAPER -

1. INTRODUCTION

The creation of a new prototype is a procedure that requires both time and resources. In order to minimize time and the resources spend on it, before a prototype is actually built, a virtual prototype is first created. Using this virtual prototype, the CAE engineer is capable of running a number of tests on it, study its behaviour, and then according to his analysis propose any modifications if needed. Fig. 1 illustrates the complete circle made for a “virtual” prototype in order the initial CAD concept to be finally constructed. After the initial concept the product is designed in CAD. Using a pre-processor like ANSA, the prototype is meshed, analysis dependant forces and boundary conditions are applied and the solver input file is created. Following, the solution is obtained, and the results are analyzed using a post-processor (μETA). In the case that the results of the analysis are satisfactory, the production of the prototype is authorized and the part is built for the first time. On the other hand, if the results are not satisfactory then modifications are made to the part. The part is designed again, and the same process is repeated till the appropriate results are obtained. This whole process needs the cooperation of more than one departments (CAD – CAE), increasing in this way the complexity of the task, cooperation is in most cases time consuming and as a result this “circle” has proven to be slow and expensive.

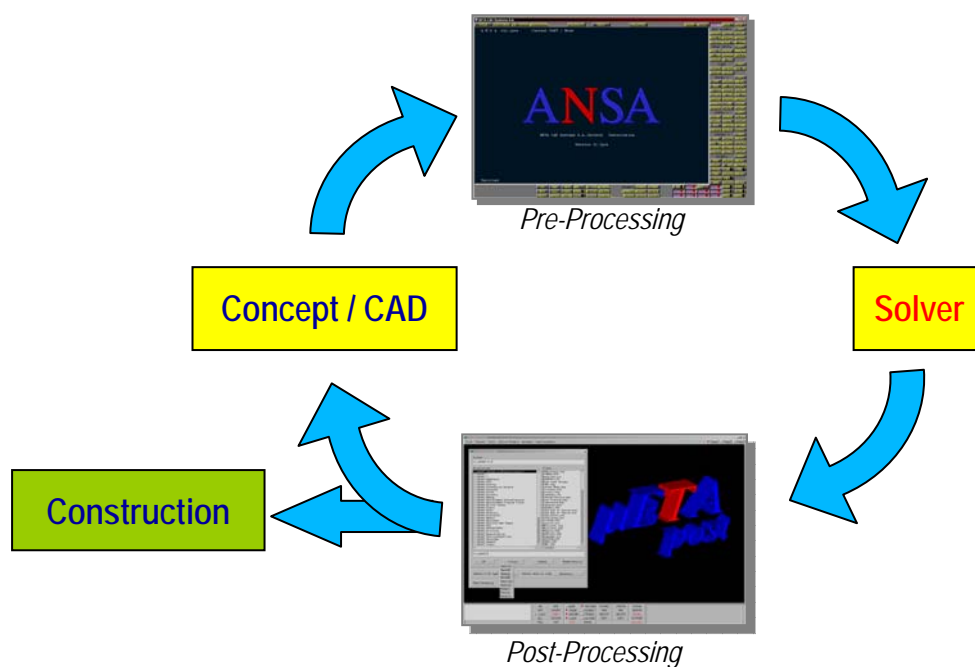


Fig. 1: The creation of a prototype.

In order to minimize both time and cost, most companies start developing a new prototype not from scratch but try to further develop / modify, a part that already exists. In other cases, again to minimize cost, companies try to make use of existing old parts in new assemblies with as few modifications as possible. This is the case of old rails fitted in new platforms or old doors to new frames.

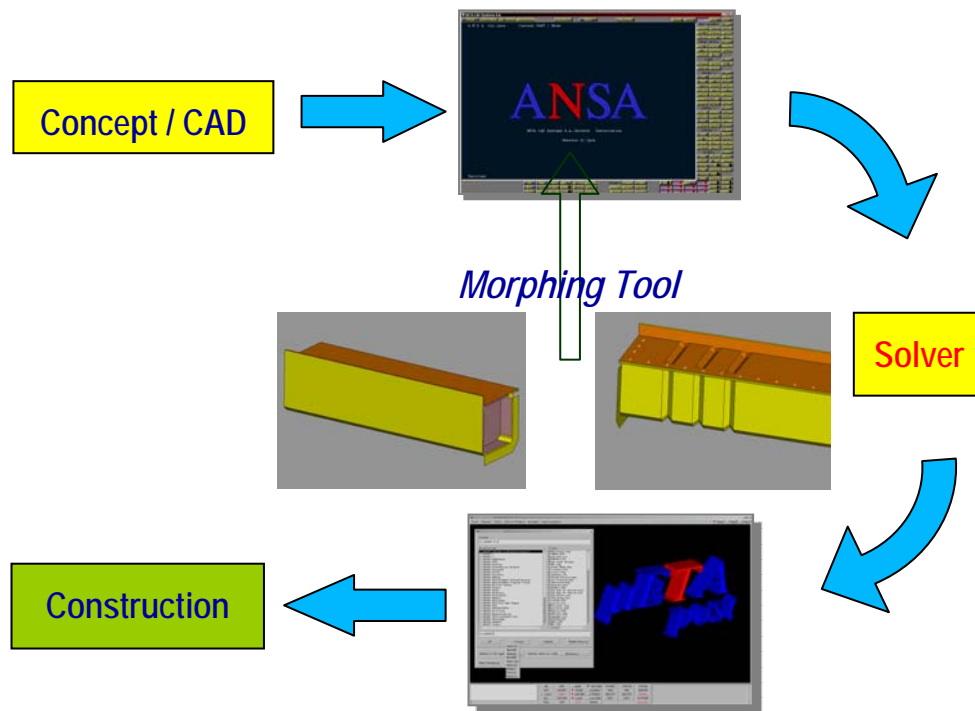


Fig. 2: The use of ANSA Morphing tool in part creation.

For the above reasons, some years ago, the Morphing Tool was introduced in ANSA. Using the Morphing Tool the CAE engineer was able to make any modifications he wished directly to the FE model without having to return to the CAD department, saving in this way significant time. With the Morphing Tool, the engineer was able to make any needed modification, either to a specific area of his model or on the whole model and without losing the initial mesh of the part. In the case that the mesh after morphing did not meet the quality specifications set, the reconstruction function is used, and the mesh is automatically regenerated and corrected in order to meet the quality specifications. Since, forces and boundary conditions are not lost during morphing, the model is ready to be solved again, Fig. 2. This process can be fully automated if an optimizer is used in conjunction with the solver. The optimizer communicates with ANSA via the ANSA scripting language, control the morphing parameters and so the optimum solution is reached automatically.

Using ANSA's Morphing Tool inside an optimizing circle, the CAE engineer is capable of reaching an optimum solution for his model, fast, with low cost and with no or minimum interaction between different departments (CAD/CAE). Currently, the only drawback of this procedure is that morphing is only applicable on FE-models, meaning that the desired information derived from the optimization circle cannot be directly passed to the CAD department. So, the only way to get the information to the CAD department, is first to convert the FE-model to geometry and then output the geometry using a neutral format (*.igs, *.stp). Unfortunately, this conversion doesn't always produce good results, since in most cases information of fillets and other curvatures of the part is not retained in FE. For this reason, ANSA from version v12.2.x incorporates for the first time the possibility to use the Morphing Tool directly on geometry (Geometry Morphing).

2. ANSA MORPHING TOOL

FE-model Morphing

FE-model Morphing is conducted in ANSA using Morphing Boxes. Morphing Boxes can be reshaped by moving the Control Points that are located along their Edges. All entities shell / solid elements, 3D points, must be loaded in a morphing box in order to be morphed. The user can move the Control Points in order to reshape the boxes in two modes. The first one is the non-morphing mode, where the boxes are simply reshaped in order to better fit the model geometry. The second is the morphing mode, where the boxes are reshaped and their loaded elements are morphed accordingly.

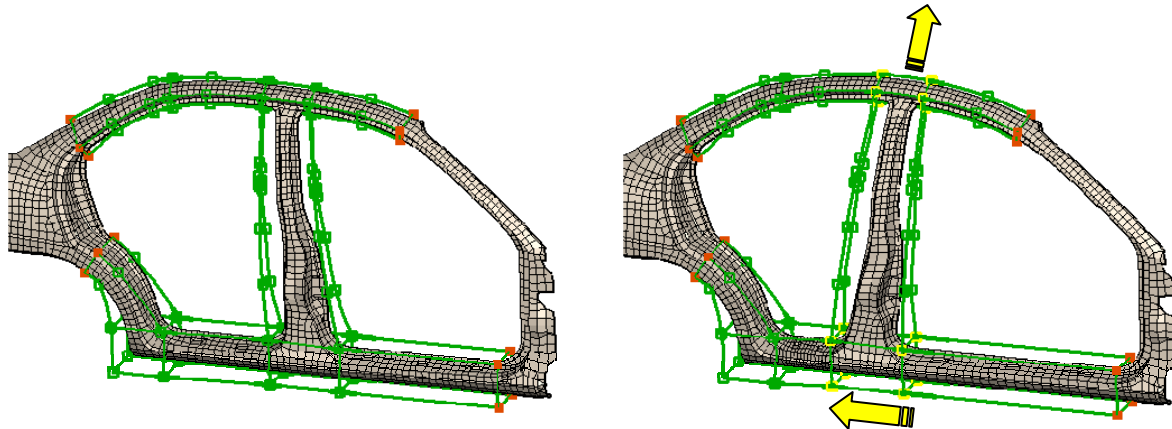


Fig. 3: Morphing Boxes follow the shape of the structure

One way to use the morphing boxes is to follow the shape of the structure. As shown in Fig. 3 moving or sliding of Control Points results in the morphing of the model in the desired direction. The second way is to create a single morphing box and then to split it into many with their edges fitted on the feature lines of the model, Fig. 4. By doing so, the surrounding boxes can act as buffer zones of the morphing action, thus ensuring continuity of the deformed neighbouring shell of solid elements. At the same time, the ability to move the fitted Morphing Box edge by exact translations, rotations or even snapping onto pre-defined target 3D curves, allows for highly controllable and precise modifications of the actual mesh.

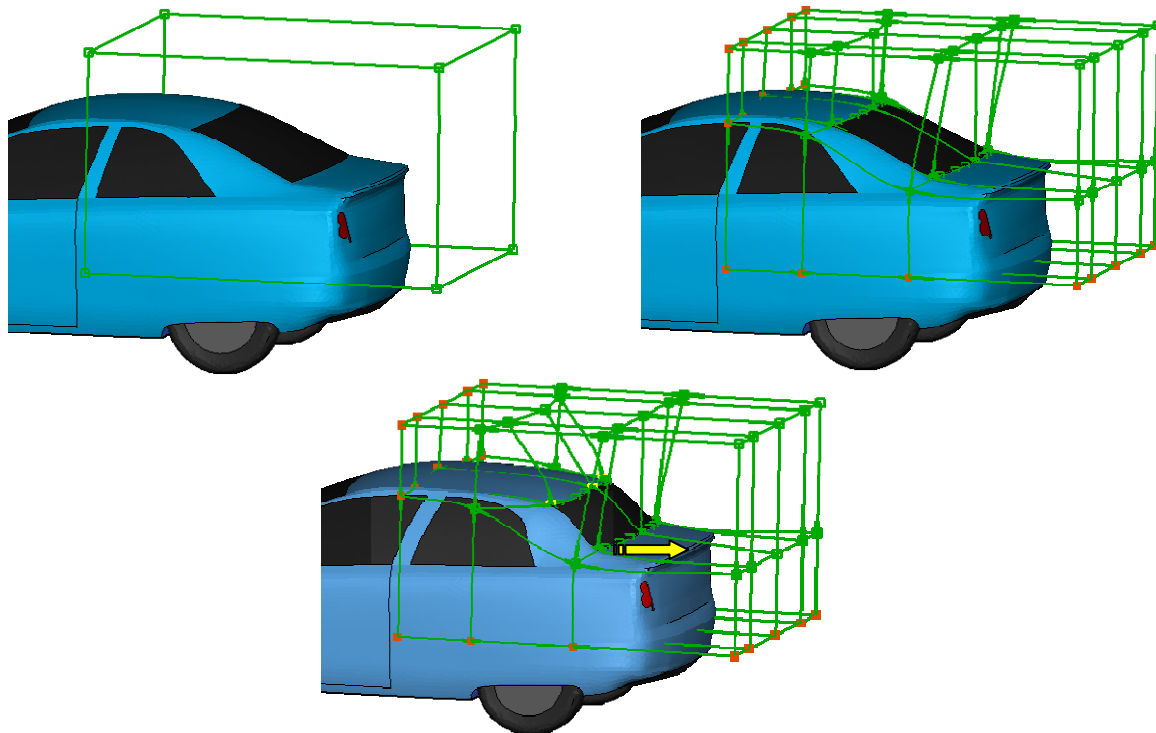


Fig. 4: A single Morphing box split into many.

Geometry Morphing

Starting with version v12.2 ANSA Morphing Tool will also support Morphing on Geometry. Geometry Morphing incorporates a number of advantages:

- Can be applied on geometry. No mesh is required.
- Geometry Morphing is conducted in the same way as FE-model, by using Morphing Boxes.
- The user can use functions that work only on geometry like Reshape (automatically join macros to produce mesh of better quality), or have options applicable only on geometry Reconstruct (fillets treatment).
- Use of ANSA's Batchmeshing Tool after Geometry Morphing.
- Morphed Geometry can be output using neutral format to be used by CAD software (CATIA, NX, Pro/E).

As mentioned before, Geometry Morphing works under the same principles with FE-model morphing. The user creates boxes in the same way as before and instead of elements, geometric entities (faces) are loaded in the Morphing Boxes, Fig. 5. At the same time, it is also possible for a Morphing box to be loaded with more than one type of entities. This means that a box can be loaded with FE, faces as well as 3D points or other entities. By moving the Control Points of the box all the entities that have been previously loaded into it are morphed.

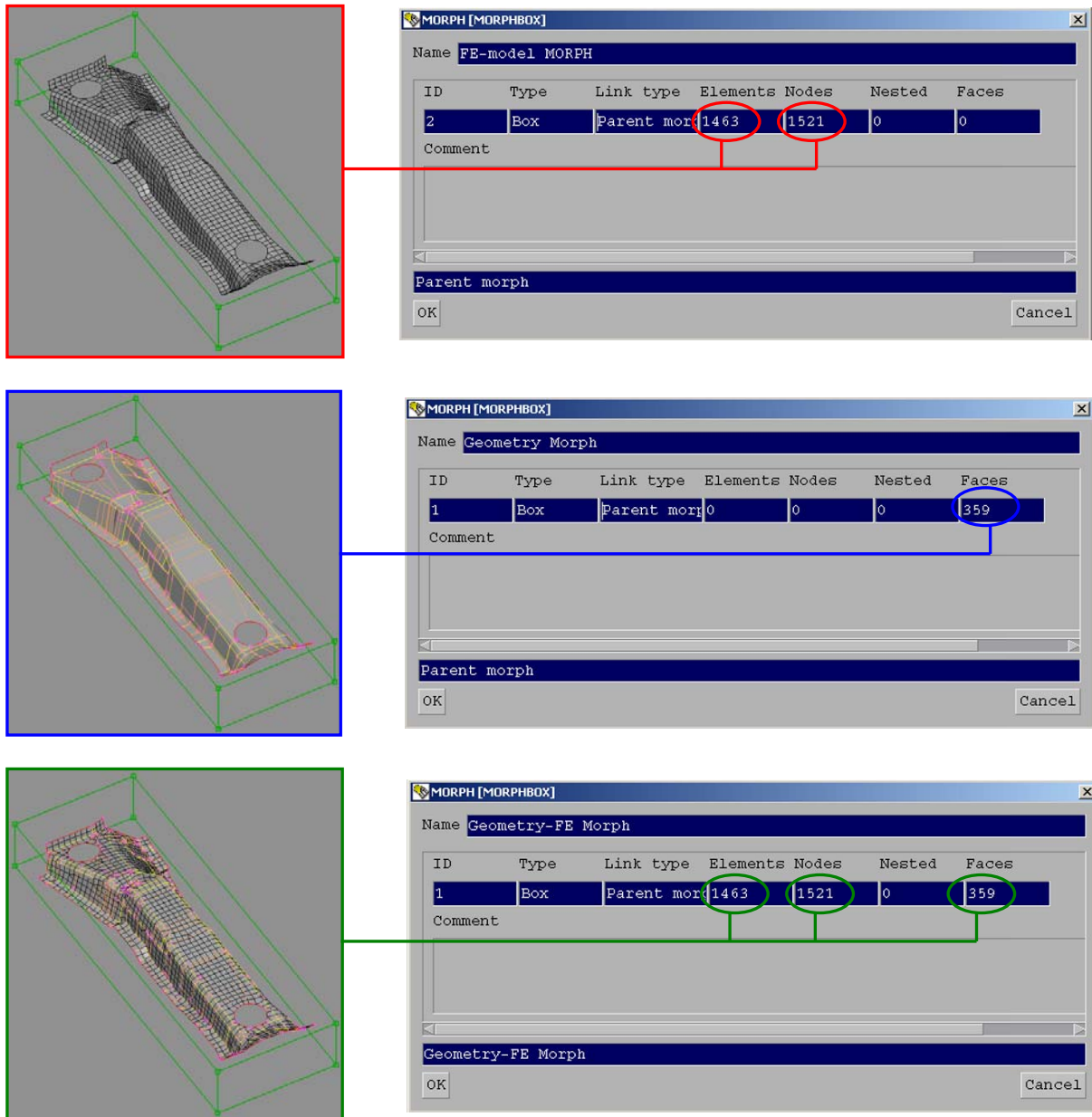


Fig. 5: Geometry morphing. Box Definition.

In ANSA the mesh created on a part, always resides on the CAD definition. In the case that a face being morphed has been meshed the mesh on the face is not lost, Fig. 6, but the mesh is being morphed as well. As stated above, in many cases in order to ensure that the changes made will only affect a specific area, the technique of using one box that has been split into many is used. With geometry morphing, where faces are loaded in the boxes, sometimes a face could be intersecting the common side of two boxes. In these cases, when the Control Points are moved and the box is morphed a cut is automatically created on the intersecting face. In this way the part of the face that belongs to the box being morphed follow the movement while the rest remain either at the initial position or follows according to any constrains between the boxes (of tangential constrain between the boxes). These cuts are made automatically and only in the cases that they are needed.

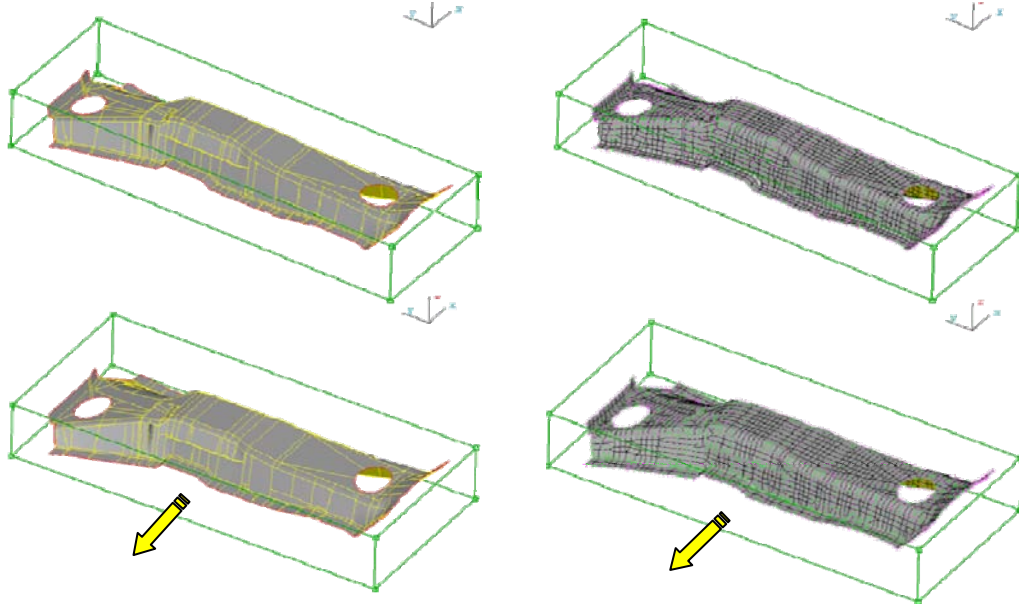
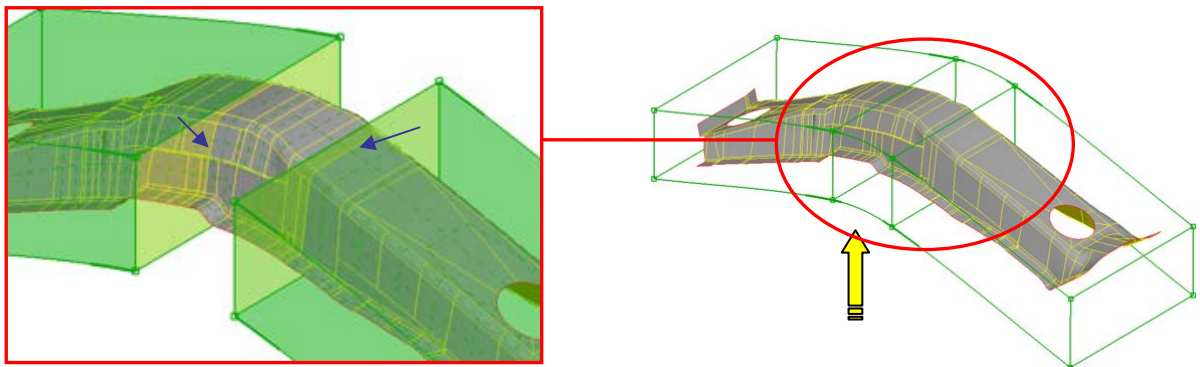
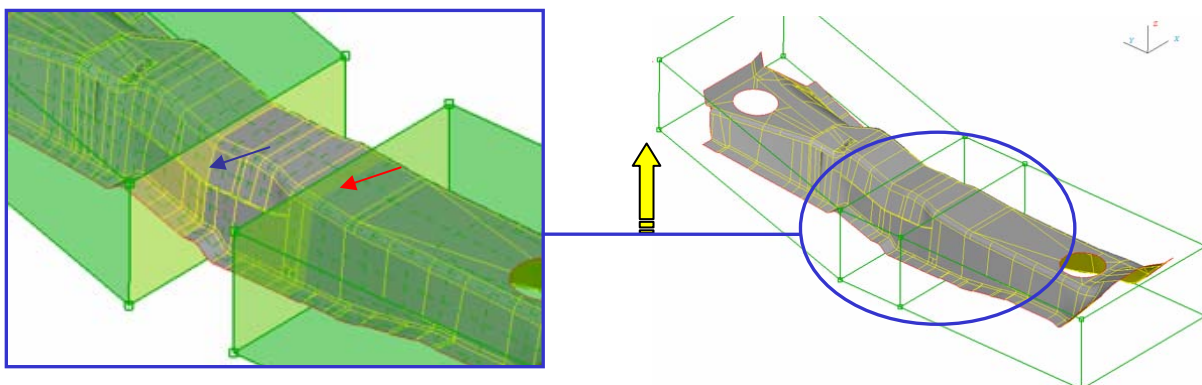


Fig. 6: During Geometry morphing the mesh on the faces is not lost, but it is morphed at the same time.

Fig. 7a, b, show Geometry Morphing applied on a rail. In Fig. 7a, all three boxes share a tangential constrain. Moving the central Control Points upwards results in the automatic cutting of the faces, indicated by the blue arrows. On the other hand, in Fig. 7b there are no constrain between the boxes. In this case the Control Points on the left side are moved upwards, and since there are no constrains between the boxes, only the contents of the left box are affected. So, a cut on the faces is automatically created at that point (blue arrow), while on the intersection of the right and middle boxes with the faces no cut is made.



a) Middle Box has tangency constraints with both boxes.



b) Middle Box does not have any tangency constraints with the other boxes.

Fig. 7: Boxes that intersect with the geometry, depending on continuity requirements can automatically perform cuts on the faces.

3. STUDY CASES

To better evaluate Geometry Morphing a number of different test cases have been analysed and are presented. The part under investigation was a complete door assembly, which consists of 12 different parts, Fig. 8. For this assembly three different cases have been addressed.

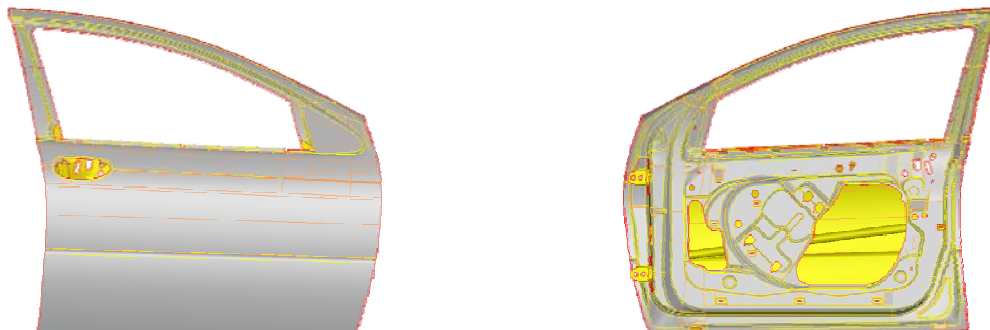


Fig. 8: Door assembly used for Geometry Morphing

The cases simulate the actual problem of trying to fit an existing door assembly either to a new outer design, or to a new frame. These are:

- Case A: Fit the door's outer frame to a predefined surface
 - A1: The inner frame should keep its initial position
 - A2: The inner frame alongside the rest of the parts should follow the outer frame.
- Case B: Fit the door's outer frame to specific cross sections

Setting Up – Morphing the assembly

In order to morph either an FE-model or geometry the procedure the user should follow is exactly the same and can be summarised in few simple steps, Fig. 9:

- Create a morphing box that includes the whole assembly (door).
- Split the initial box to smaller boxes, in order to have better control of different areas / features and isolate specific areas.
- Optionally the user can add control points to the edges of the boxes or have it done automatically. Since the control points are those that actually will coincide with the target curves more points will lead to better results.
- Create initial curves for the source geometry.
- Fit morphing boxes edges to the source curves.
- Create target curves from target surface.

After this stage the model is ready to be morphed. Morphing is conducted by selecting the appropriate morphing function and then fitting the boxes edges which reside on the initial curves to the target curves, or simply by moving Control Points.

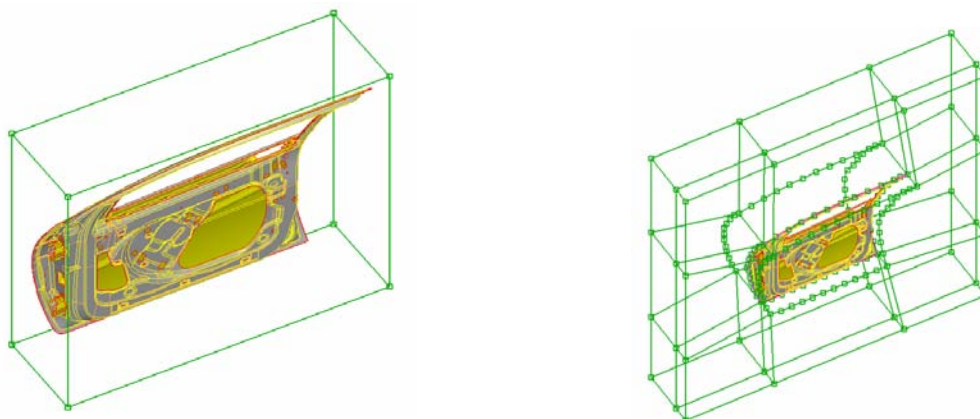
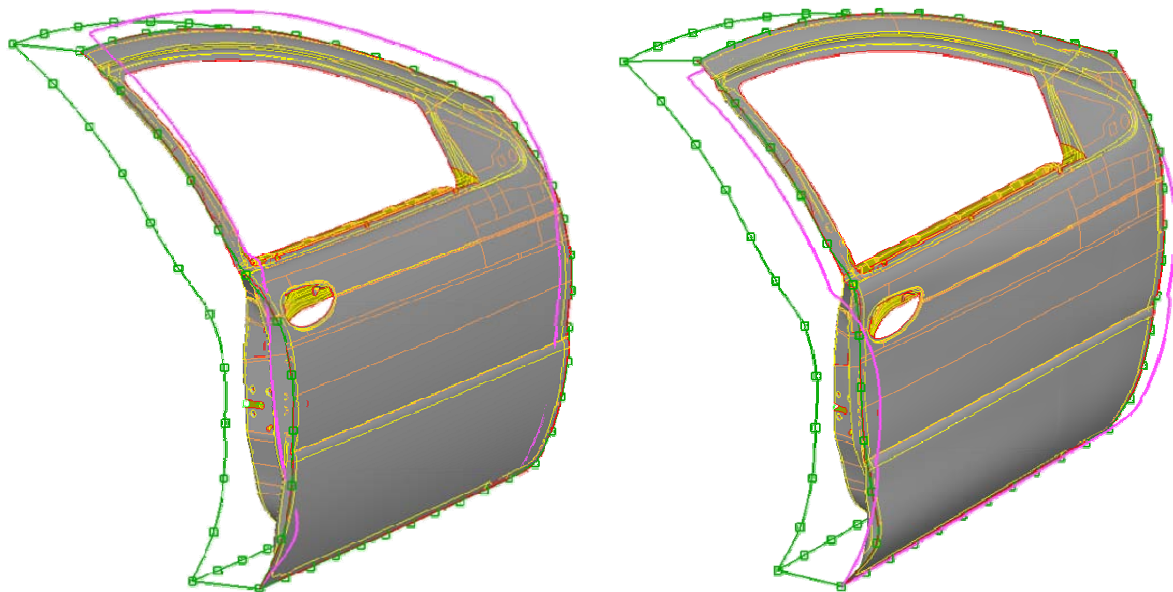


Fig. 9: Door assembly used for Geometry Morphing

Results

For case A1 the morphing function Edge.Fit has been used. This function modifies the shape and position of elements that are loaded on a Morphing Box by fitting a box's edge on a target 3D-curve. The assembly before and after morphing is shown in Fig. 10. In Fig. 10a the target curve are coloured in magenta, while in Fig. 10b the morphed assembly is shown with the initial unmorphed position coloured this time, in magenta.

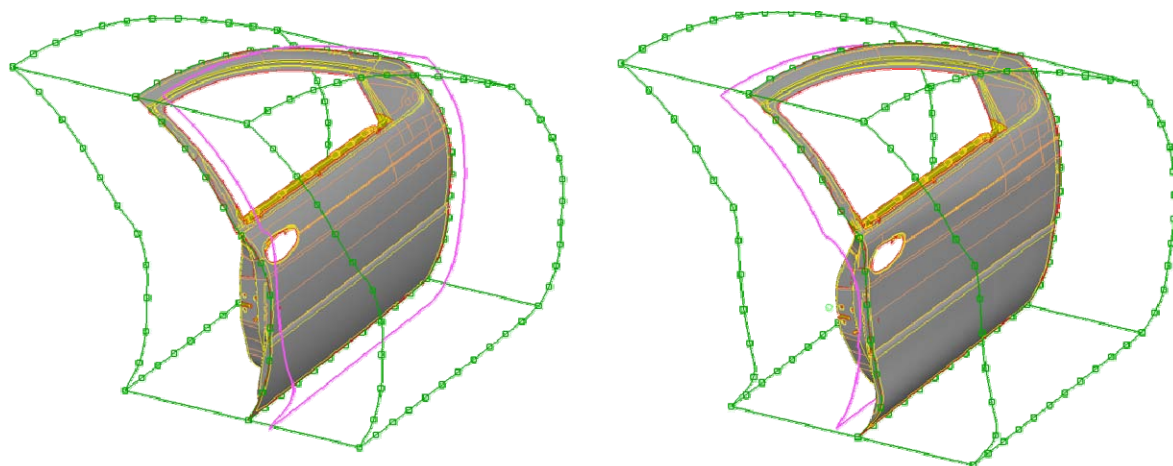
For the A2 case the Master-Slave Fit function has been used. With this function the edge of the morphing box is selected to be fitted on the target 3D-curve. At the same time a one or more edges of the morphing box can be selected to follow as slave the movement of the first selected edge. In this way all entities inside the morphing box are morphed in a uniform way. The results of Geometry Morphing on the door assembly are shown in Fig. 11 for the Master / Slave Fit function.



a) Before Morphing

b) After Morphing

Fig. 10: Case A1. Edge Fit function in geometry morphing



a) Before Morphing

b) After Morphing

Fig. 11: Case A2. Master-Slave function used in geometry morphing

Fig. 12 and Fig. 13, show the difference between the results obtained using the two functions used for Geometry Morphing. Using the Edge-Fit function, the inside panel of the door assembly is almost not affected at all from the morphing process, while with the Master-Slave fit, where the second edge of the box follows the movement, it follows the trends of the target curves. Continuing in Fig. 13, at the front part of the door in case A1 (Edge-Fit) the hinges were left at the original position while in A2 (Master-Slave) the hinges were morphed.

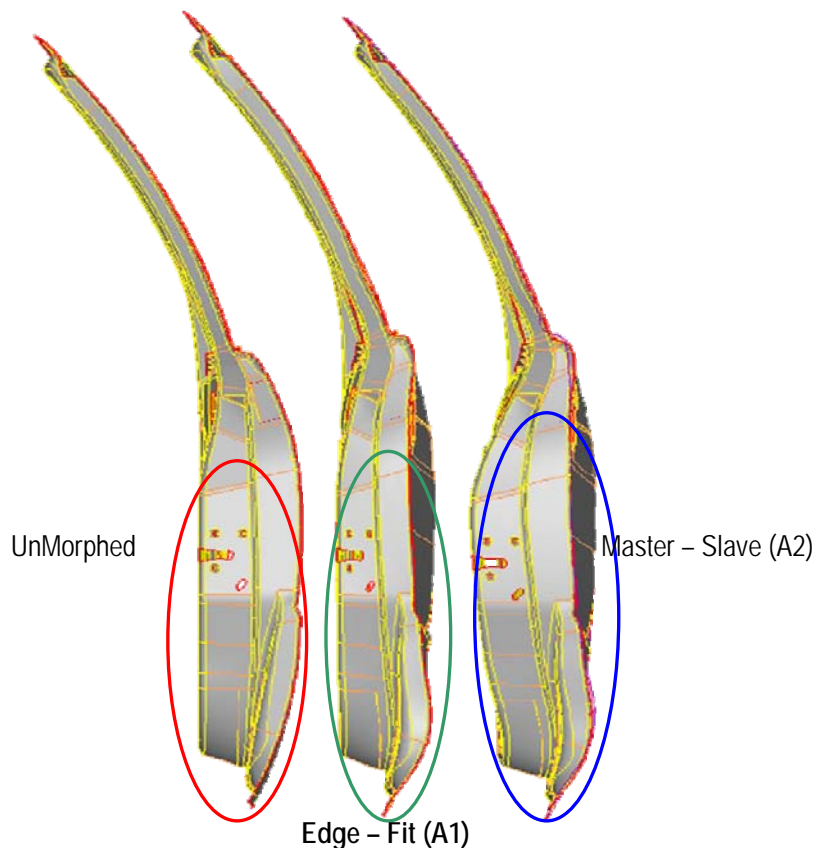


Fig. 12: Geometry Morphing, Case A1, A2 Rear View

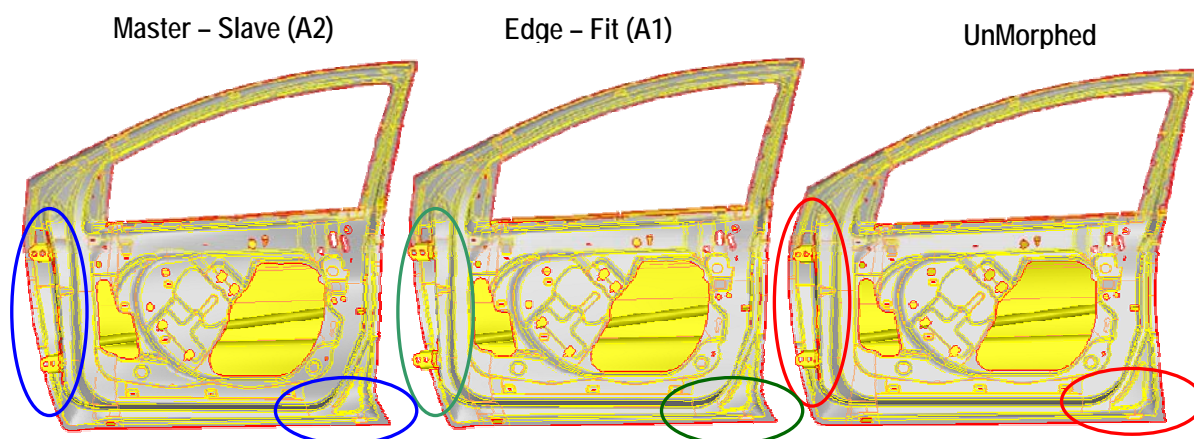


Fig. 13: Geometry Morphing, Case A1, A2 Side View

According to case B scenario, the door assembly should be fitted to specific cross sections. This case is addressed in the same way as the A2 case. Only here since there are more than four target curves more morphing boxes have been created so that more edges would be fitted. In this way the user specifying more target curves has a better control on specific areas. The unmorphed assembly with the target curves can be seen in Fig. 14a while the final morphed door with the initial curves in Fig. 14b. In this example at the position of the cross sections, cuts have been made automatically during Geometry Morphing on the faces, in order to better be fitted to the target curve, Fig. 15.

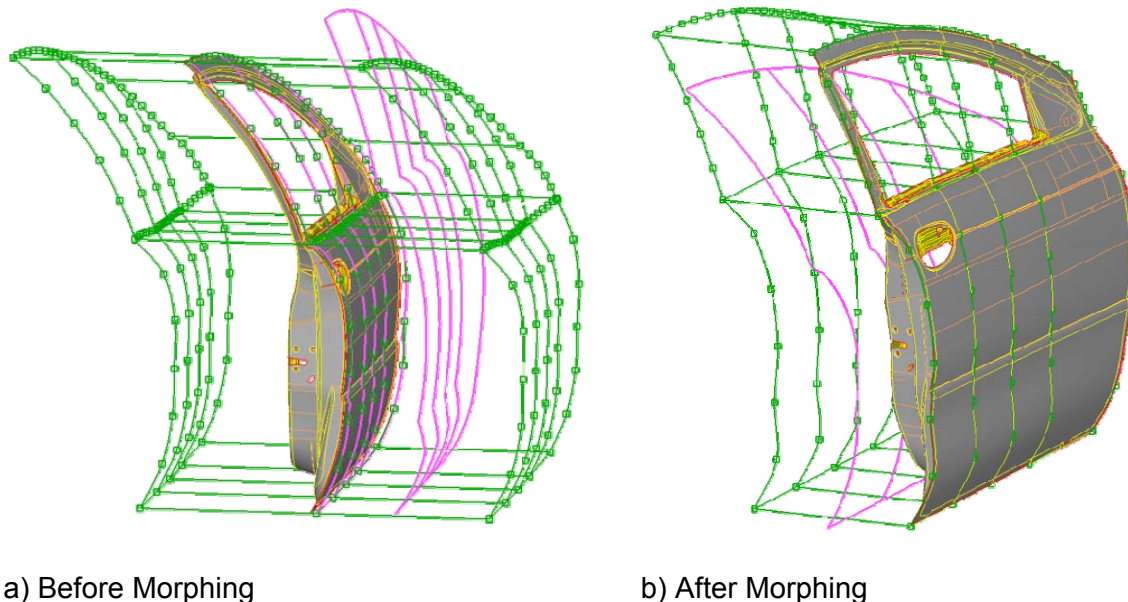


Fig. 14: Case B. Master-Slave function used in geometry morphing, in conjunction with a number of cross-sections.

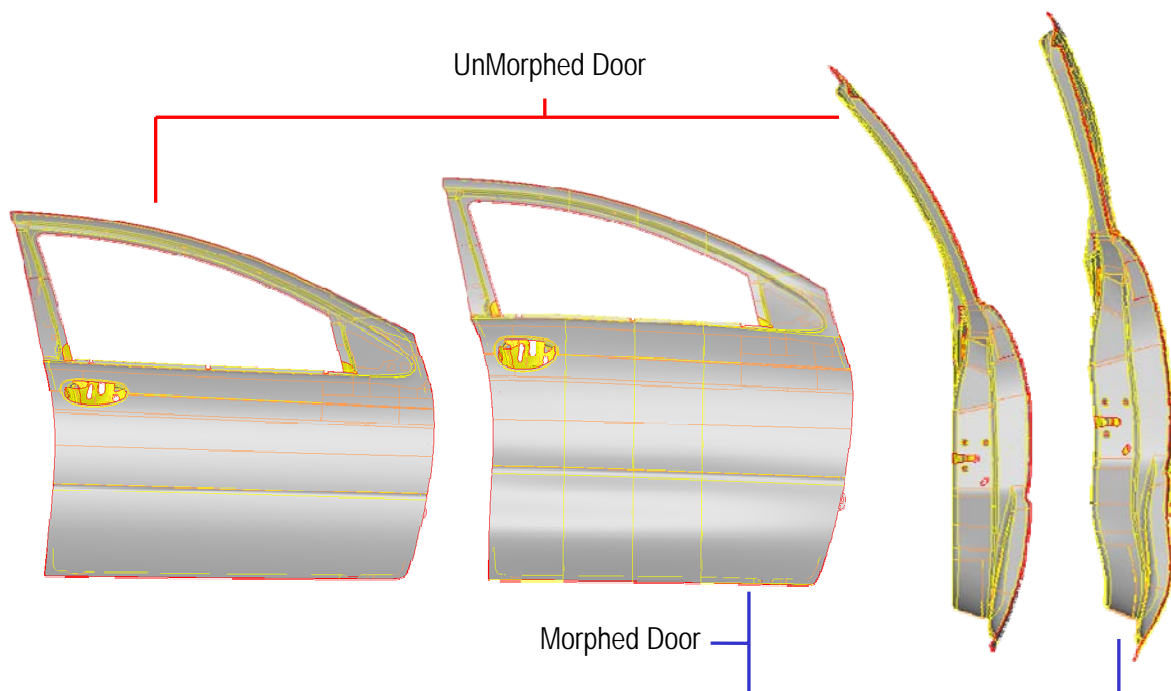


Fig. 15: Geometry Morphing, Side and rear view of case B.

4. COMPARISON TO FE-MORPH

For reference, the assembly under investigation has been meshed with a coarse (mean element length 12 mm), and a fine (mean length 5 mm) mesh. Following, the mesh was released from the geometry and two FE-models of the assembly were created, the first with 14 846 elements (12 mm) and the other with 91 931 elements (5 mm), Fig. 16. These models were morphed in the same way as with the geometry cases. Morphing (FE-model / Geometry) were conducted using an AMD Athlon 64 Dual Core Processor 5600+, with 4 GB of RAM. The times needed in each time to complete the operation are summarized in Table 1.

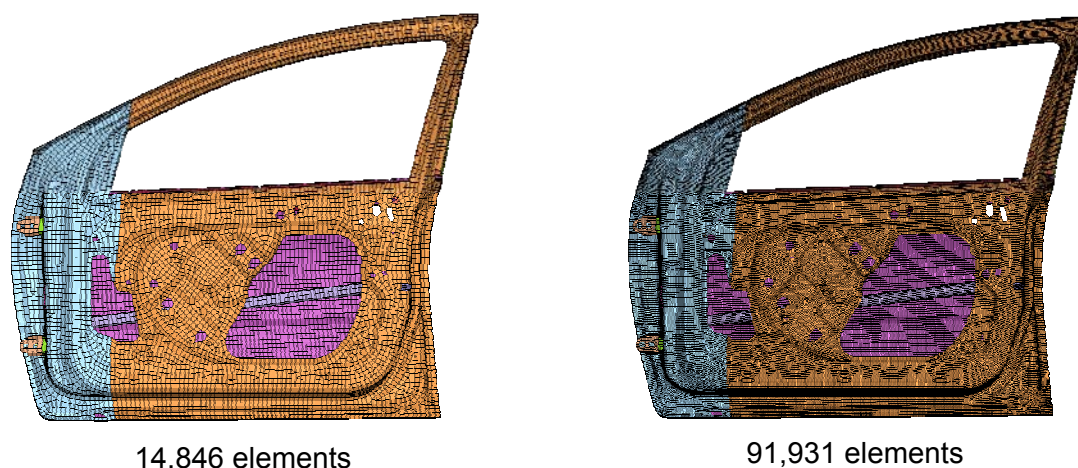


Fig. 16: FE model of door assembly

Table 1: Statistics of FE-model and Geometry Morphing

		Case A1, A2 M/S-Fit /Edge-Fit (min:sec)	Case B M/S-Fit (min:sec)
FE-model, 12mm	14 846 elements	0:03	0:03
FE-model, 5 mm	91 931 elements	0:10	0:10
Geometry	2 410 faces	1:05	4:30

The time needed for the FE-model morphing is merely seconds, depending on the number of elements of the model. On the other hand, for cases A1 and A2, the time needed to morph the geometry rises to one minute. Continuing for case B while the FE-model morphing needs the same time as in cases A1 and A2, for the Geometry Morphing the time needed rises to 4:30 minutes. This excess time needed compared to geometry morph of cases A1 and A2 is due to cuts that are being automatically created on the whole assembly.

5. CONCLUSIONS

In this case study it has been shown that from ANSA's version v12.2.x morphing will be available also for geometry with very satisfactory results. At the same time any mesh that resides on the geometry is not only kept but it can also be automatically reconstructed after the Geometry Morphing finishes. As expected, Geometry Morphing needs more time compared to an FE-model, but all the information about the morphed geometry can be returned to the CAD software, (Fig. 17) without having to transform the FE-model to geometry. At the same time, since geometry is not lost, important information of the parts, like fillets, holes, curvatures, are retained. Continuing, the batch meshing tool of ANSA can be used, taking advantage of its filters, special defeaturing and treatment capabilities in order to create a mesh of high quality.

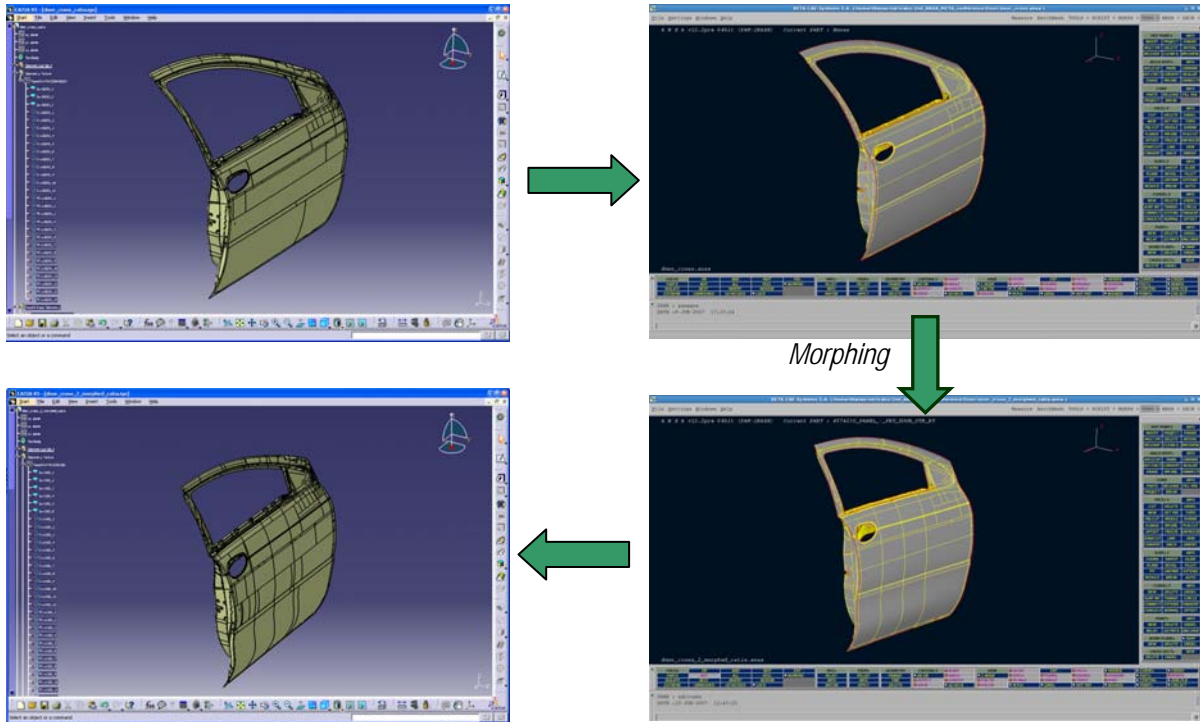


Fig. 17: Completing the CAD-CAE-CAD circle.

The time difference observed between Geometry and FE-model is currently too big to be ignored, in order to substitute FE-model morphing with Geometry Morphing inside an optimization circle. What is proposed though, is the following. First a good quality mesh should be created, and following the mesh should be released from the geometry thus creating a FE-model. Then, create an optimization circle between a solver/optimizer and ANSA Morphing tool on this FE-model. From this procedure the optimum modifications of the parts can be obtained alongside the final movement of the control points of the boxes. The next step is to use the information of these morphing boxes and apply the same morphing using this time morphing on geometry to the initial part. By this way, the obtained optimized modifications are passed to the geometry. Then, output the geometry using a neutral format so that it could be used by CAD software. In this way the optimised solution is finally returned from the CAE to the CAD department saving both time and resources.

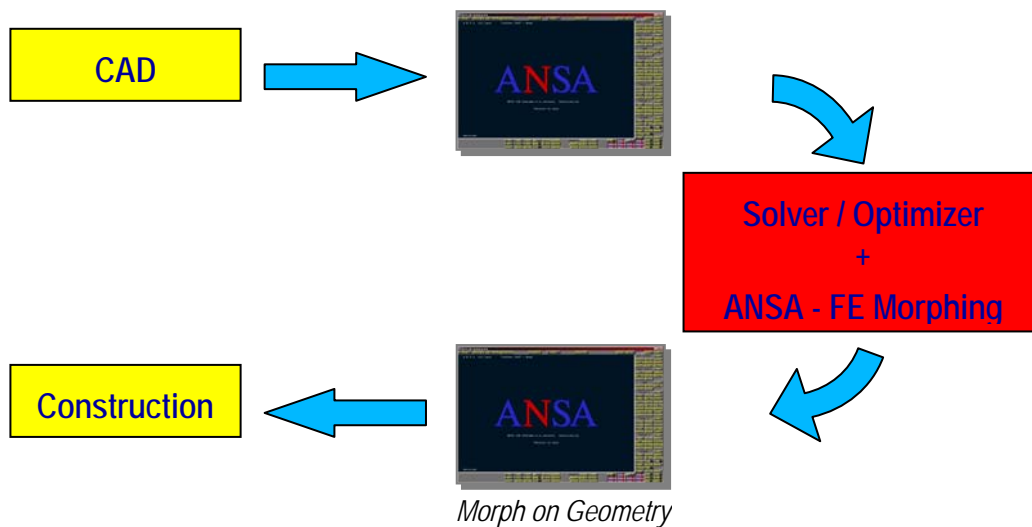


Fig. 18: Proposed solution combining both FE-model and geometry morphing.

APPLICATIONS OF SHAPE OPTIMIZATION WITH LS-OPT AND ANSA

¹Heiner Müllerschön*, ¹Marko Thiele, ²Wolfram Mühlhuber, ²Uwe Gerlinger

¹DYNAmore GmbH, Germany, ²AUDI AG, Germany

KEYWORDS - Optimization, Morphing, META-Models, Crashworthiness, Process Flow

ABSTRACT - The purpose of this paper is to explore aspects of shape and geometry optimization for nonlinear applications and to propose optimization strategies for such problems.

Different optimization strategies are discussed and pros and cons are compared. The application of the Successive Response Surface Method (SRSM) for optimization of nonlinear applications is demonstrated. This is performed using LS-OPT as optimization software and ANSA as pre-processor for geometry variation. For this ANSA is run in batch mode and is driven by parameterized control files, which interface with the optimization software LS-OPT. By the variation of morphing control parameters or just geometrical translational or rotational operations the design is optimized with respect to shape properties and geometrical configuration. After morphing operations usually automated batch meshing of the considered parts is applied.

The set-up of the process flow and how the several programs interface with each other is also described in the paper.

In addition, a methodology to get a reliable surrogate model using neural networks is introduced. The surrogate model (META-Model or Response Surface Model) approximates the relationship between design parameters and a simulation response and can be used to visualize and explore the design space.

One of the regarded examples treats the optimization of a crash box at AUDI. The procedure of generating an advanced μ ETA-model to get an approximation of the global design space using neural networks is demonstrated for this example. Furthermore, the visualization of multi-dimensional meta-models in two- and three-dimensional design space is illustrated by using the software D-SPEX. The program D-SPEX interfaces with LS-OPT as an advanced optimization and stochastic post-processor.



Applications of Shape Optimization with LS-OPT and ANSA



Heiner Müllerschön, Marko Thiele
DYNAmore GmbH, Germany
Wolfram Mühlhuber, Uwe Gerlinger
AUDI AG, Germany

DYNAmore GmbH
Industriestraße 2
70565 Stuttgart
<http://www.dynamore.de>

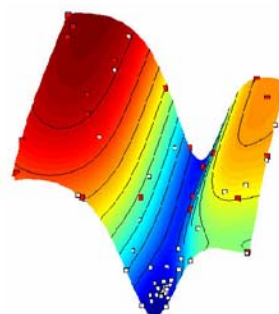
Applications of Shape Optimization with LS-OPT and ANSA – 14.06.07

1



→ Overview

- Introduction
- Methodologies for Optimization in LS-OPT
- Example I
 - Optimization of a Crash Box
 - Conclusions
- Example II
 - Sensitivity Study (DOE) for Radiation Analysis
 - Conclusions



Applications of Shape Optimization with LS-OPT and ANSA – 14.06.07

2

Introduction

- Introduction
- Methods – Optimization
- Example I – Crash
- Conclusions
- Example II - Radiation
- Conclusions

→ About DYNAmore

- Distributor of LS-DYNA and related software products in Germany, Austria, Switzerland and other european countries
- Further development and customization in collaboration with LSTC (long term relationship)
- DYNAmore in total 34 People (June 2007)
- LS-DYNA Software Models
 - Many Dummy Models
 - Barrier Models
 - Pedestrian Safety Models
 - Human Models (Thums)

Visit us at
www.dynamore.de

Applications of Shape Optimization with LS-OPT and ANSA – 14.06.07
3

Introduction

- Introduction
- Methods – Optimization
- Example I – Crash
- Conclusions
- Example II - Radiation
- Conclusions

→ Optimization Competence Center at DYNAmore

- Many experience particularly in crashworthiness optimization, reliability and robustness studies, MDO, Meta-Modelling...
- Main optimization customers

software

- LS-OPT (LSTC)
- Vanderplaats (VR&D) optimization products
- D-SPEX

seminars

- several training classes
 - optimization
 - robustness/reliability
 - parameter ident.
- informational events

engineering

- optimization engineering services
- consulting
- benchmarks

services

- support (phone, on-site)
- software development
- system integration and process flow

Applications of Shape Optimization with LS-OPT and ANSA – 14.06.07
4

137

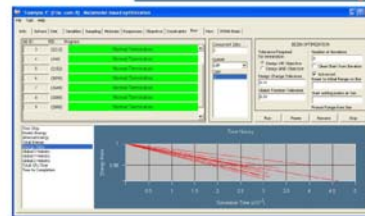
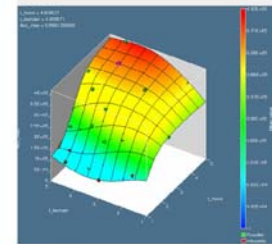


➔ About LS-OPT

- LS-OPT is a **product of LSTC** (Livermore Software Technology Corporation)
- LS-OPT can be linked to any **simulation code** – stand alone optimization software

■ Methodologies/Features:

- Successive Response Surface Method (SRSM)
- Reliability based design optimization (RBDO)
- Multidisciplinary optimization (MDO)
- Multi-Objective optimization (Pareto)
- Discrete Optimization
- numerical/analytical based sensitivities
- Analysis of Variance (ANOVA)
- Stochastic/Probabilistic Analysis
- Monte Carlo Analysis using Metamodels
- ...



➔ About LS-OPT

- Job Distribution - Interface to Queuing Systems
 - PBS, LSF, LoadLeveler, AQS, etc.

- LS-OPT might be used as a “Process Manager”

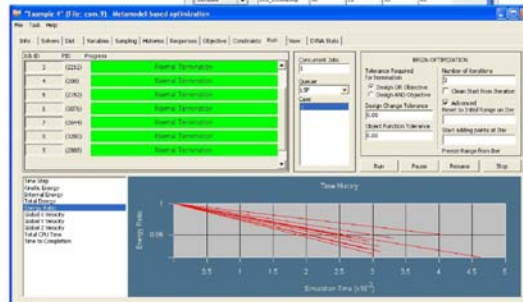
■ Shape Optimization

- Interface to SFE-Concept, Hypermesh ANSA, DEP-Morpher
- User-defined interface to any Pre-Processor

■ Parameter Identification Module

■ Visualization of Statistical Quantities on the FE-Model

Type	Name	Starting	Range	Minimum	Maximum
Variable	SHA_VENT	24	20	15.70	24
Variable	PAR_APT1_01a	40	18	15	330
Variable	CUR_POR1	9.5	1	1	1
Variable	CUR_POR2a	45	1	10	45
Variable	PAR_POR1	1.20	1	1	1.5
Variable	PAR_POR2a	36	18	10	100
Variable	PAR_APT1_01b	40	18	15	100
Variable	PAR_POR2a	36	18	10	100
Variable	PAR_APT1_01c	45	24	10	100
Variable	CUR_POR2a	45	1	10	45
Variable	PAR_POR2a	36	18	10	100
Variable	PAR_APT1_01d	45	18	10	100
Variable	PAR_POR2a	36	18	10	100

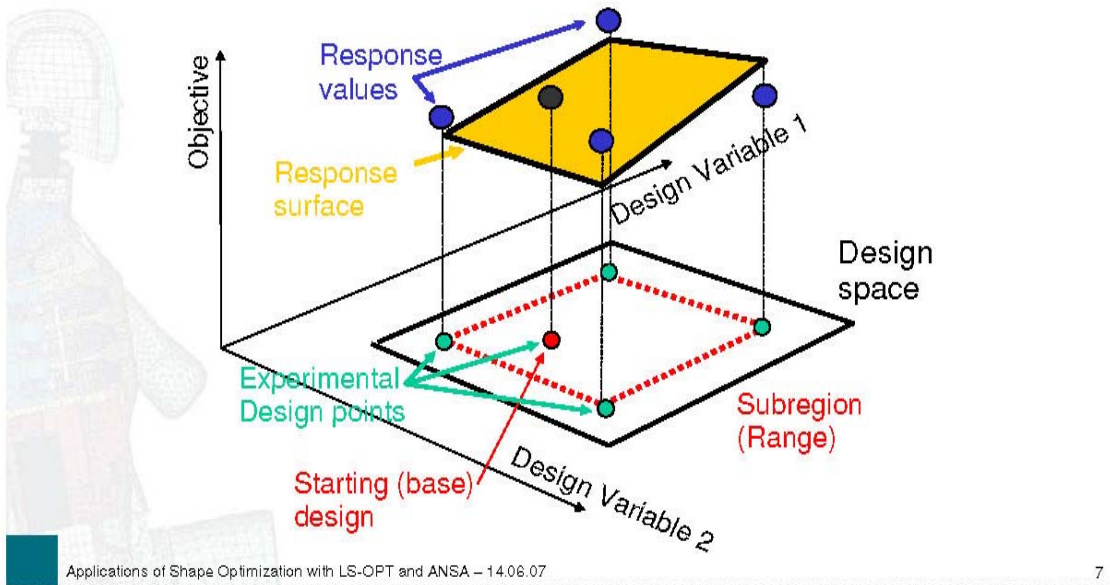


Methods - Optimization

- Introduction
- **Methods - Optimization**
- Example I - Crash
- Conclusions
- Example II - Radiation
- Conclusions

DYNA MORE

→ **Response Surface Methodology - Optimization Process**

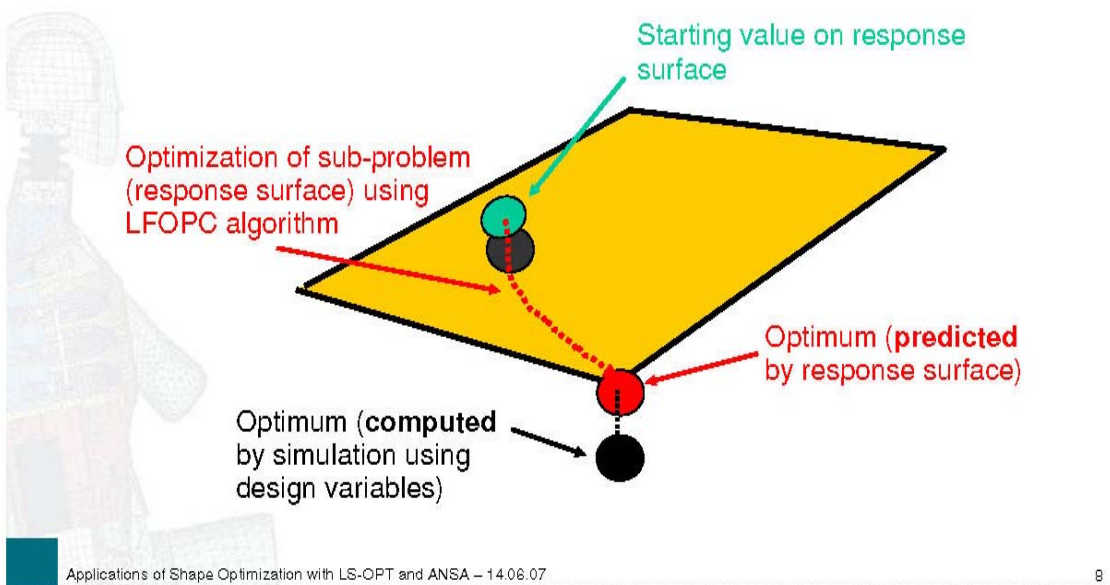


Methods - Optimization

- Introduction
- **Methods - Optimization**
- Example I - Crash
- Conclusions
- Example II - Radiation
- Conclusions

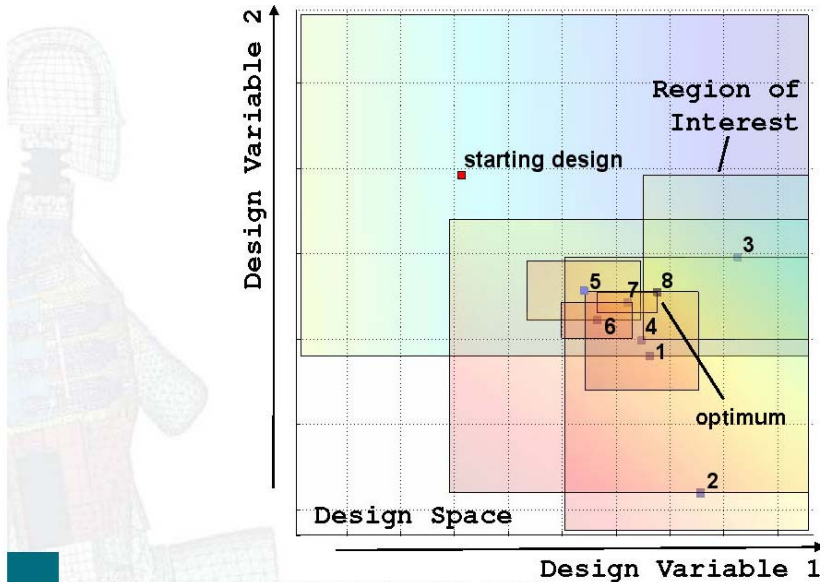
DYNA MORE

→ **Find an Optimum on the Response Surface (one iteration)**





→ **Successive Response Surface Methodology**



Applications of Shape Optimization with LS-OPT and ANSA – 14.06.07

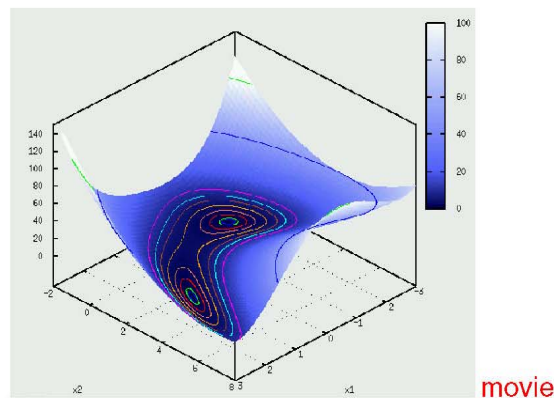
9



→ **Successive Response Surface Methodology**

■ Example - 4th order polynomial

$$g(\mathbf{x}) = 4 + \frac{9}{2}x_1 - 4x_2 + x_1^2 + 2x_2^2 - 2x_1x_2 + x_1^4 - 2x_1^2x_2$$




Applications of Shape Optimization with LS-OPT and ANSA – 14.06.07

10

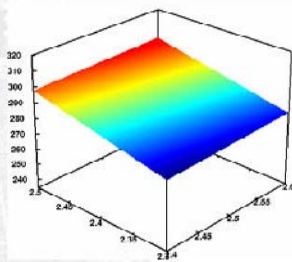
Methods - Optimization

- Introduction
- **Methods - Optimization**
- Example I - Crash
- Conclusions
- Example II - Radiation
- Conclusions

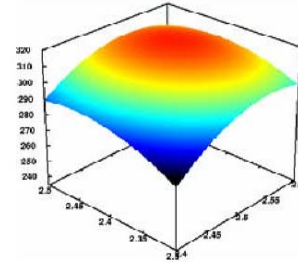


→ **Response Surfaces (Meta Models)**

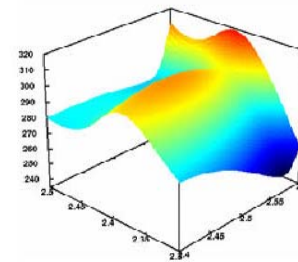
- Linear, Quadratic and Mixed polynomial based
- Neural Network and Kriging for Nonlinear Regression



linear polynomial



quadratic polynomial



neural network

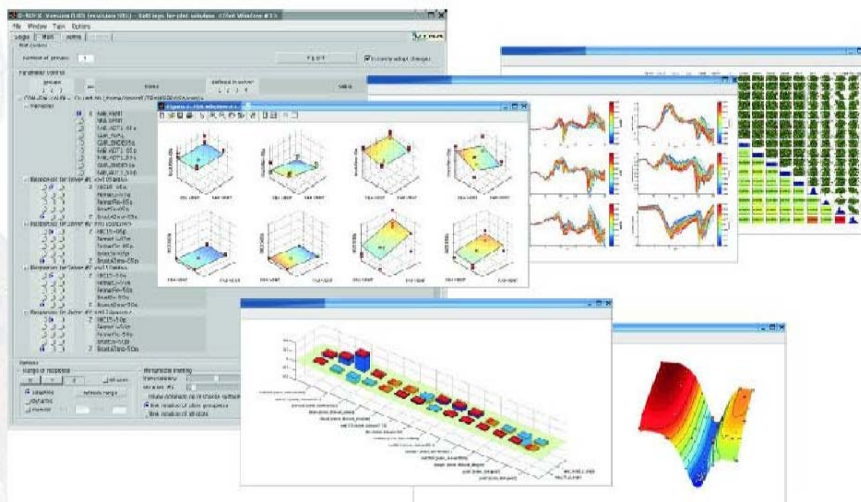
Exploring Design Space using D-SPEX

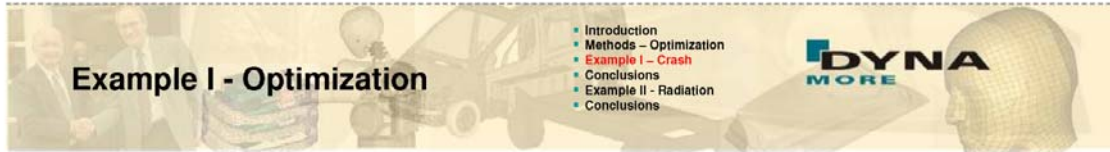
- Introduction
- **Methods - Optimization**
- Example I - Crash
- Conclusions
- Example II - Radiation
- Conclusions



→ **D-SPEX Meta-Model Viewer - Exploration of Design Space**

- Compare response surfaces, curve plots, ant-hill plots, ...

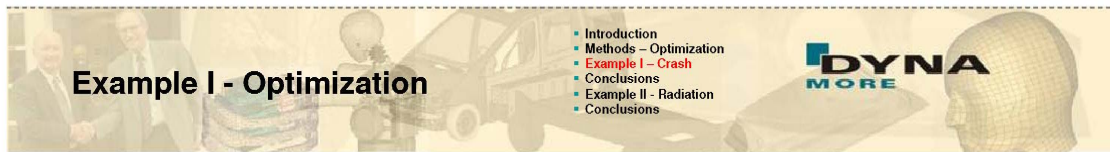
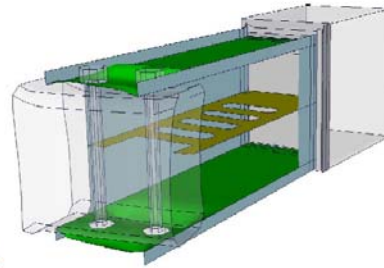




Example I - Optimization

→ Optimization of a Crash Box

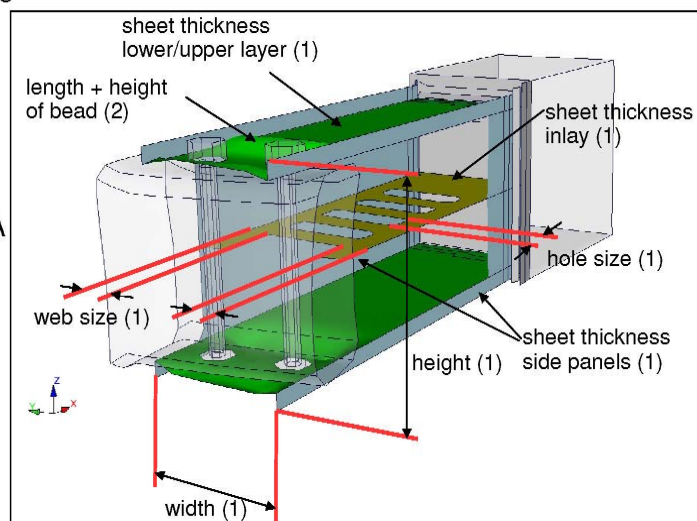
- The objective is to improve the energy absorption of a crash box and to reduce the maximum force level
- **Sheet thickness variables** as well as **geometric variables** are considered
- **Test load is 1 m/s** boundary prescribed motion applied by a rigid wall
- Optimization formulation: a maximum load level (contact force) has not to be exceeded (**constraint**) while a maximum of energy has to be absorbed (**objective**)



Example I - Optimization



→ Optimization of a Crash Box

- Total 9 design variables
- Use of Successive Response Surface Method with LS-OPT
- Parameterization by Morphing through ANSA
- In total 240 simulations within 15 iterations



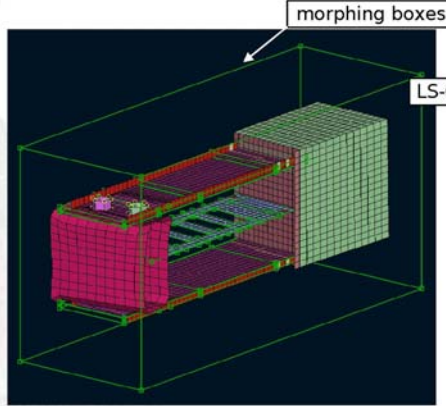
Example I - Optimization

- Introduction
- Methods - Optimization
- Example I - Crash**
- Conclusions
- Example II - Radiation
- Conclusions

➔ **Morphing with ANSA and LS-OPT**

- ANSA is specified as Pre-Processor in LS-OPT
- Multiple crash simulation input files are generated automatically through ANSA in batch mode





Type	ID	Value	Name
morph_param	1	<<BREITE>>	Breite_rechts
morph_param	1	<<BREITE>>	Breite_links
morph_param	1	<<RUERE>>	Hohe_oben
morph_param	1	<<RUERE>>	Moede_unten
morph_param	1	<<LAEHGE_STICKE>>	Interfuehle_Laenge
morph_param	1	<<RUERE_STICKE>>	Schraefenloch_Hohe_oben
morph_param	1	<<MOEHL_STICKE>>	Anlaufuehle_Moede_unten
morph_param	1	<<LOCH_BREITE>>	Loch_Breite_rechts
morph_param	1	<<LOCH_BREITE>>	Loch_Breite_links
morph_param	1	<<LOCH_LAEHGE>>	Loch_Laenge_rechts
morph_param	1	<<LOCH_LAEHGE>>	Loch_Laenge_links

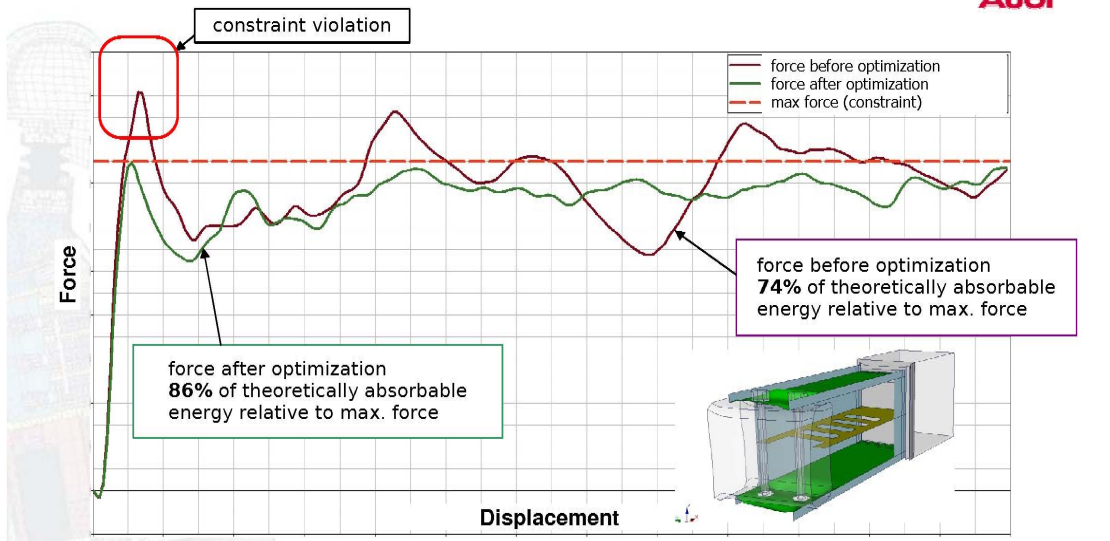
Applications of Shape Optimization with LS-OPT and ANSA – 14.06.07

Example I - Optimization

- Introduction
- Methods - Optimization
- Example I - Crash**
- Conclusions
- Example II - Radiation
- Conclusions





➔ **Optimization Result**



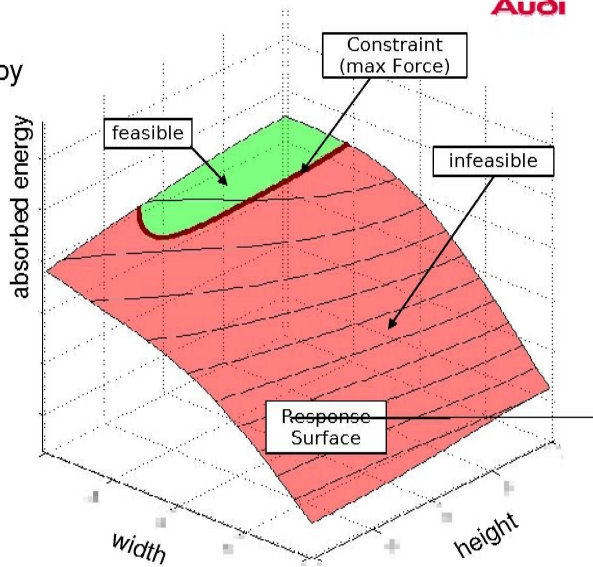
Example I - Optimization

- Introduction
- Methods – Optimization
- Example I – Crash**
- Conclusions
- Example II - Radiation
- Conclusions



➔ **Design Study using D-SPEX**


- Visualization of the relationship between variables and responses by means of a response surface
- Can give a deeper understanding of the influences of parameters upon the results



Applications of Shape Optimization with LS-OPT and ANSA – 14.06.07

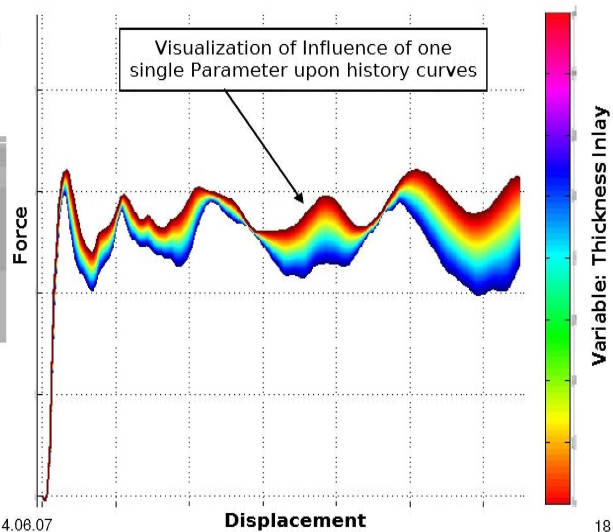
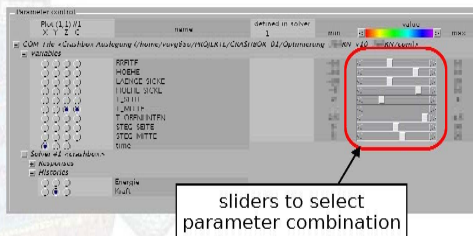
Example I - Optimization

- Introduction
- Methods – Optimization
- Example I – Crash**
- Conclusions
- Example II - Radiation
- Conclusions



➔ **Enhanced Visualization of Simulation results using D-SPEX**

- Utilizing response surfaces to approximate curves for specific parameter combination

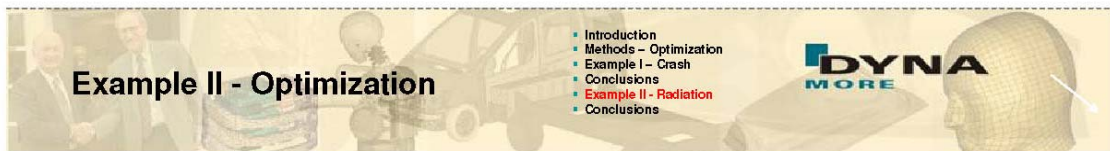


Applications of Shape Optimization with LS-OPT and ANSA – 14.06.07



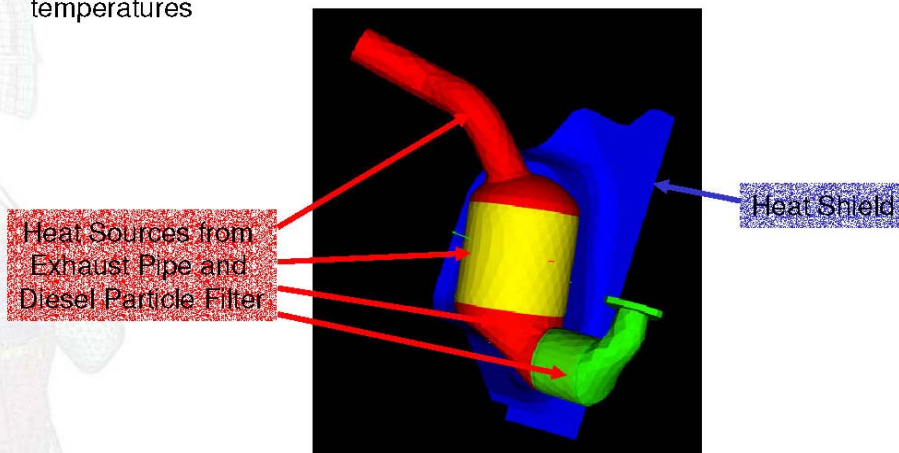
→ Conclusions

- LS-OPT is a suitable tool for crash box optimization
- Numerical optimization achieved better design and can save manpower in the design process of a crash box
- Morphing capabilities of ANSA are essential in order to realize geometric parameterization
- Visualization of results with D-SPEX can give you a deeper understanding of the influences of parameters upon the results



→ DOE Sensitivity Analysis for Radiation Analysis

- Problem Description: Heat shield to protect environment from high temperatures

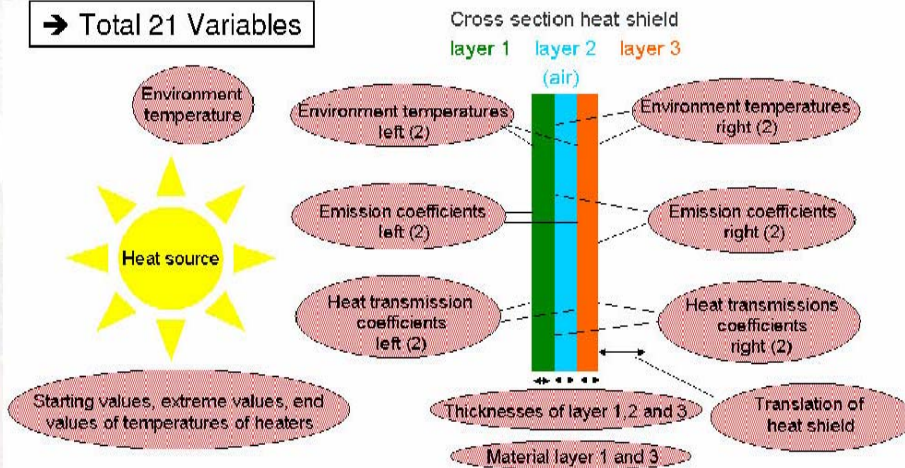




→ DOE Sensitivity Analysis for Radiation Analysis

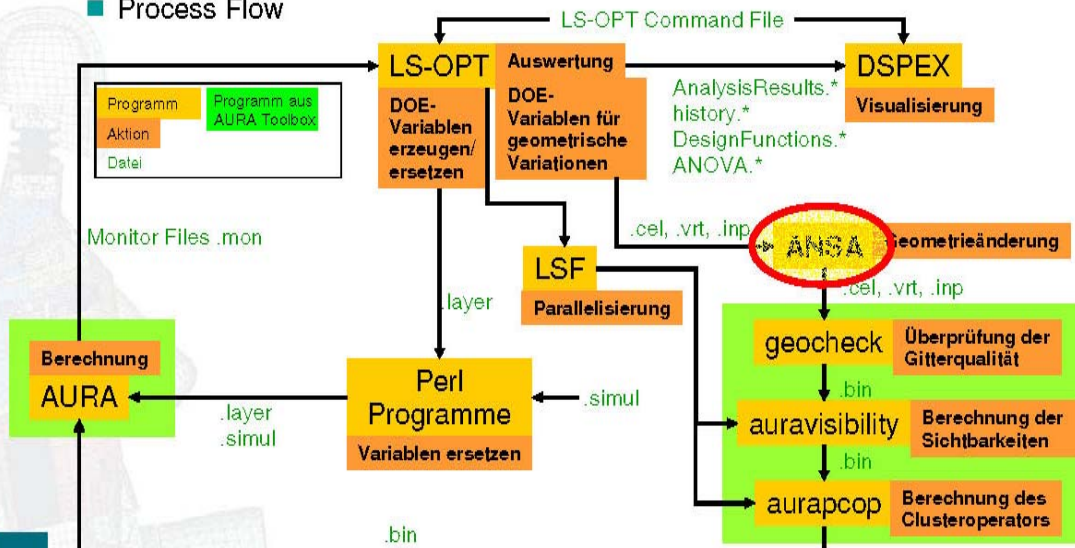
■ Variables considered for DOE

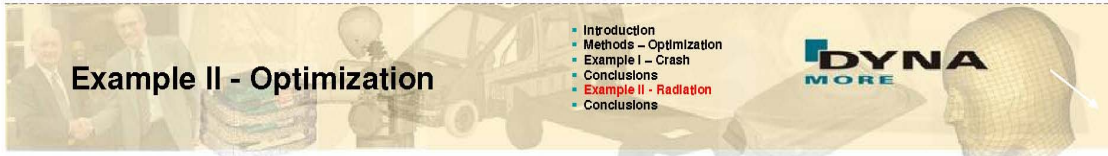
→ Total 21 Variables



→ DOE Sensitivity Analysis for Radiation Analysis

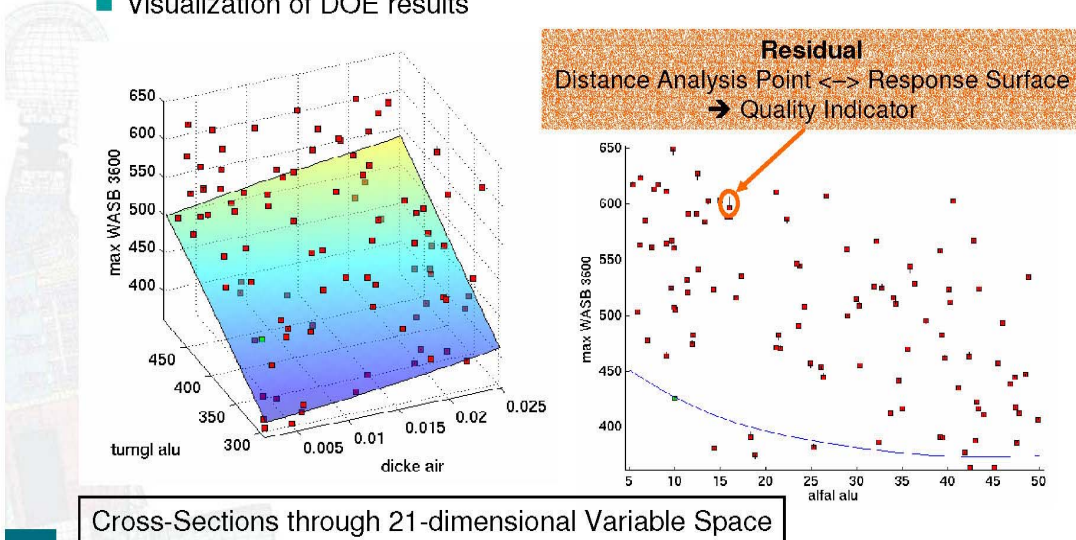
■ Process Flow



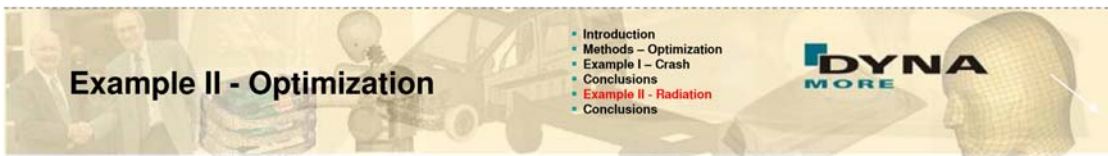


→ DOE Sensitivity Analysis for Radiation Analysis

■ Visualization of DOE results

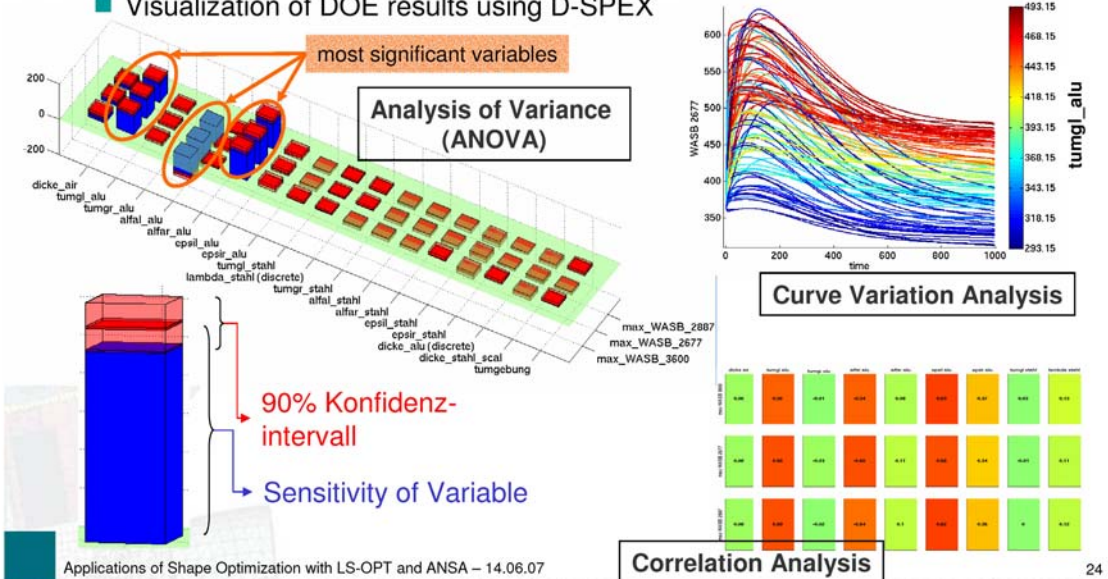


Cross-Sections through 21-dimensional Variable Space



→ DOE Sensitivity Analysis for Radiation Analysis

■ Visualization of DOE results using D-SPEX



Correlation Analysis



Conclusions

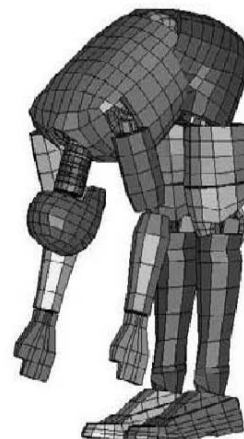
- Introduction
- Methods – Optimization
- Example I – Crash
- Conclusions
- Example II - Radiation
- **Conclusions**

→ Conclusions

- Meta-Modelling capabilities of LS-OPT are utilized successfully for a sensitivity analysis of a heat radiation problem
- Screening of significant and insignificant variables is performed
- Problem: High dimensional design variable space (21-dim.)
- D-SPEX is a helpful tool to explore the multi-dimensional variable space



Thanks for your attention!



ANALYSIS OF COMPONENT JOINTS IN FINITE-ELEMENT MODELS OF CAR BODIES

Hans Wüstenberg*

Volkswagen AG, Germany

KEYWORDS - Finite-Element, Model, Check, Connectivity, Optimisation

ABSTRACT - A body-in-white of a car in sheet-metal integral design is composed of components connected by suitable joints. Challenge for the body development is to generate a stiff and lightweight body-in-white structure according to the performance specifications. The finite element analysis is the appropriate method to investigate the performance of a given design.

The stiffness of a body-in-white can be rated using results of a modal analysis or a static loading obtained from a finite element model. Crucial for the usability of the produced results and for subsequent computations is the appropriate definition of the joints in number and location. The checking of models for missing or misplaced joints and the redistribution of joints is a time consuming manual process. To simplify this task a method is suggested which reduces the manual effort.

The key of the suggested method is a reduction of the body-in-white to surface elements which are located in contact distance to each other. During the process of reduction, a projection algorithm is used to identify possible contact surfaces in irregular finite element meshes. Results of a finite element analysis with the full structure are needed to find suitable criteria for the quality of the joining technique. Scalar quantities or vector data on nodes or elements produce usable criteria. Typically, from the results of a modal analysis, the relative displacement between the component surfaces or the strain energy in the metal sheets is used.

A rating of the chosen criteria at the connection faces identifies regions with a potential for improvements of the joining technique. The magnitude of the improvement can be estimated by an automated redesign of the joining technique in sensitive regions. The application of the method is presented on recent car configurations of Volkswagen Nutzfahrzeuge.

Analysis of Component Joints in Finite-Element Models of Car Bodies

Hans Wüstenberg

Volkswagen Nutzfahrzeuge

2nd ANSA & META International Congress
June 14-15, 2007



In presentation mode:

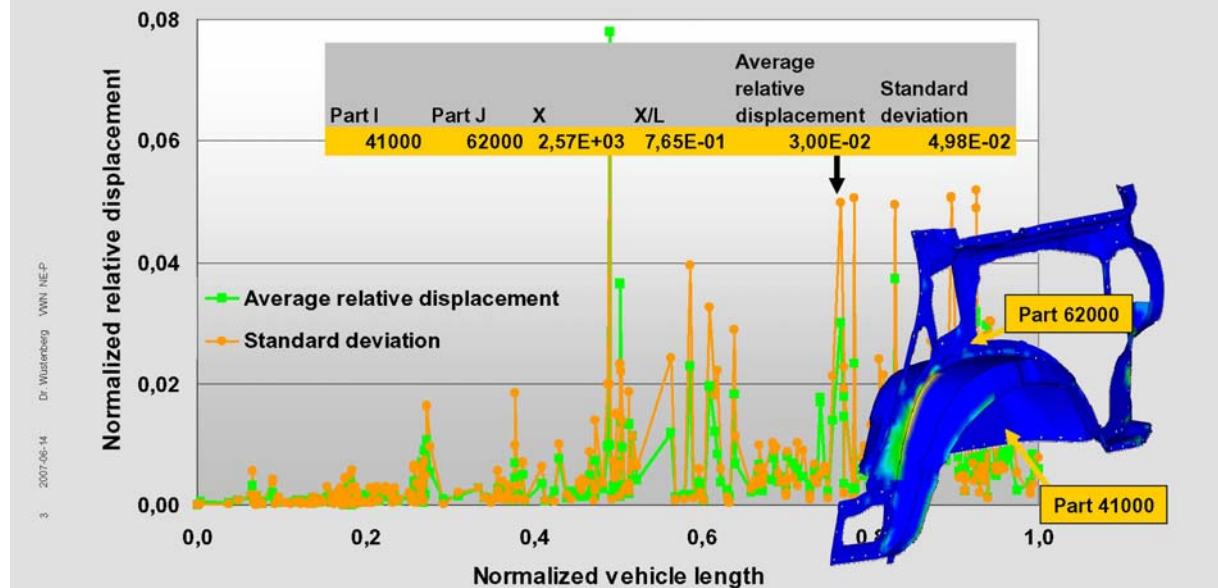
- Picture 3 should show animated pictures flying in
- Picture 4 starts an avi-animation with a click on the picture
- Picture 5 should start the animation without interaction



Connectivity rating in modal analysis

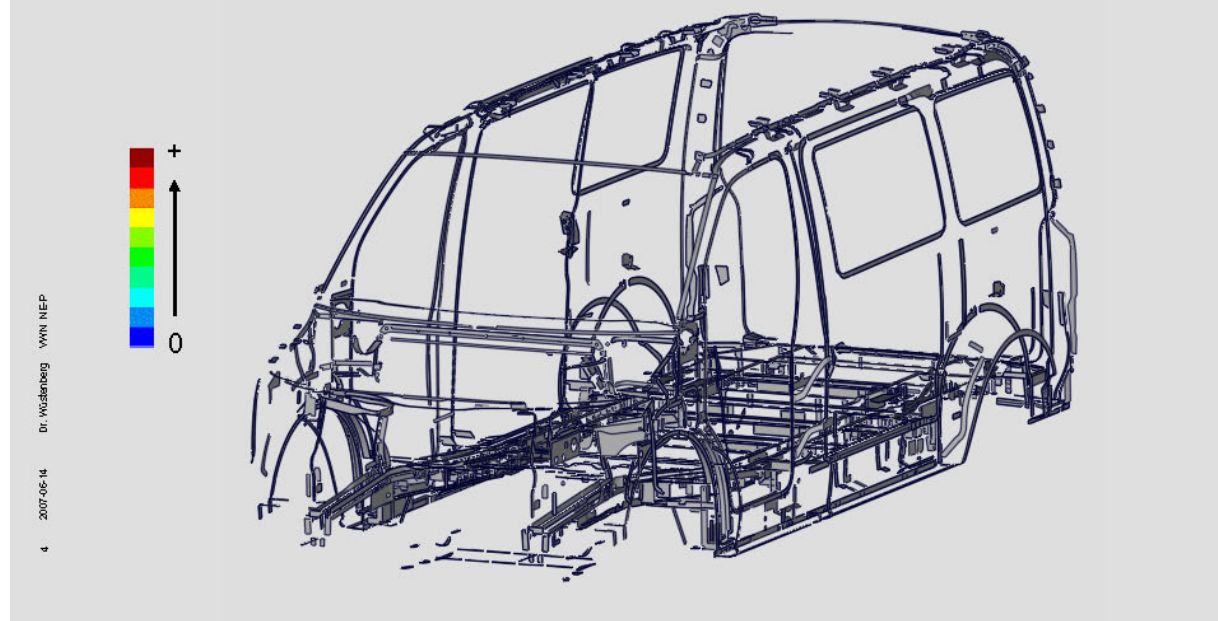
Rating of part connectivity

Statistical analysis of relative displacements



Connectivity rating in modal analysis

Relative displacements in torsion eigenmode



Session H2.5

OVERVIEW ON OPTIMIZATION METHODS

Ioannis Nitsopoulos*, **Boris Lauber**
FE-DESIGN GmbH, Germany

KEYWORDS – Non-parametric optimization, Parametric Optimization, Design of Experiments, Response Surface Modelling, Multidisciplinary Optimization

ABSTRACT - Structural optimization plays an important role in industrial application. A variety of optimization methods for the improvement of structural components exist. Each of these methods has its advantages and drawbacks. The choice of the right optimization method depends on different conditions: The problem size, type of objectives and constraints, number of design variables and much more. Not only the suitable optimization strategy has to be selected but in many cases, the parameterization of the inputs is also an important issue.

The presentation will give an overview of a variety of types of parametric and non-parametric optimization methods and their use on different applications. It will be pointed out how ANSA is supporting the optimization workflow for preprocessing and parameterization of models used for optimization. Not only the preprocessing itself but also the automation of these steps is very important for an optimization procedure, where manual interaction has to be avoided.

TECHNICAL PAPER -

1. INTRODUCTION

Optimization is more and more used for different types of application. One can distinguish a variety of optimization methods:

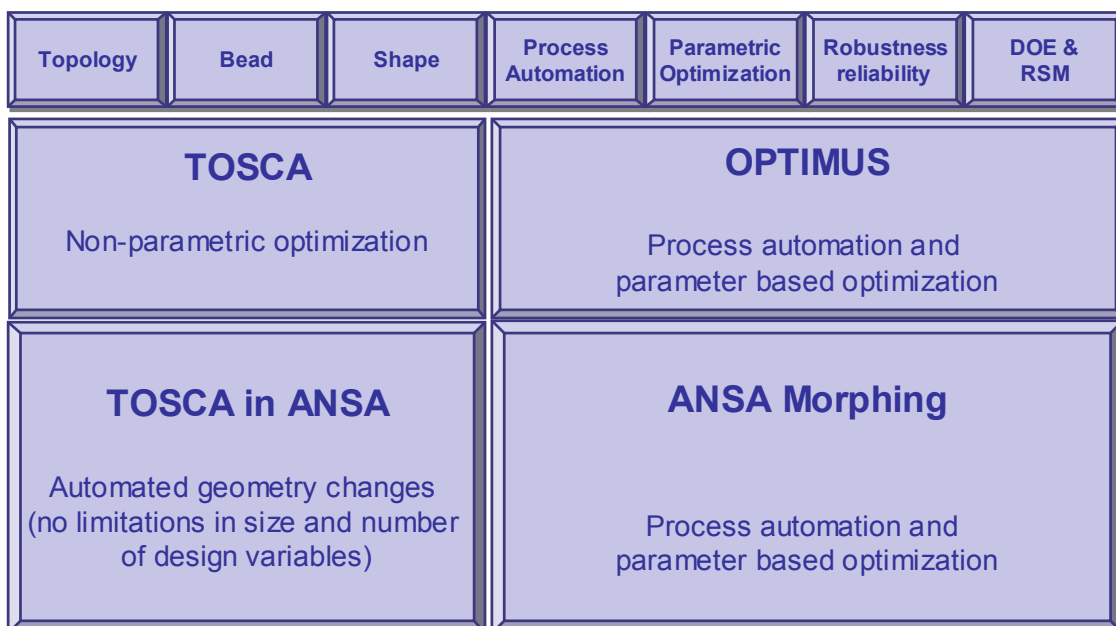


Fig. 1: Different types of structural optimization

The different optimization approaches are differing in the type and definition of design variables, the type and number of objectives and constraints, the type of responses that are considered for the optimization procedure and additional restrictions.

SELECTION OF THE RIGHT METHOD

The user has to select the right method for his optimization problem. He is faced with a number of questions:

- What are the design variables?
- What is the number of design variables?
- Are there modifications of geometry or FE-mesh?
- Is there a relevant distribution of the input quantities?
- What are the objective function(s) and the restrictions?
- Which analyses have to be considered for the optimization?
- Which accuracy is required for the optimization?

Dependent on the requirements, the corresponding optimization strategy has to be selected.

2. OVERVIEW OF OPTIMIZATION METHODS

NON-PARAMETRIC TOPOLOGY OPTIMIZATION

Topology optimization is used for completely new design proposals in a very early phase of the product development process. Starting from the available design space and all existing loads and boundary conditions, a new design concept is found. Different objectives and constraints may be considered for the formulation of the optimization task. The new structure gives an indication of the optimal energy flow considering all loadcases that are applied to the structure.



Images courtesy
of AUDI AG

Fig. 2: Topology optimization example

During the optimization process void areas are generated in the finite element structure. The result of topology optimization typically is a very rough surface representation that has to be smoothed and a new geometric model has to be generated for the transfer to a CAD environment. The TOSCA.smooth module in TOSCA is used to realize this step.

Topology optimization often generates designs that are optimal considering the mechanical point of view but are not manufacturable. TOSCA allows considering various manufacturing restrictions during the optimization procedure. Undercuts may be avoided for castings, various mesh independent symmetry conditions may be defined and the maximum or minimum thickness of trusses may be influenced.

NON-PARAMETRIC SHAPE OPTIMIZATION

In shape optimization, the coordinates of the surface nodes are regarded as design variables. TOSCA.shape is based on a non-parametric approach – a parametrization of the mesh or the underlying CAD geometry is not necessary. The design variables are defined via node groups in the finite element preprocessor. During the modification of the surface, powerful mesh smooth algorithms ensure a good mesh quality.

During shape optimization, local changes of the components surface lead to a homogeneous stress distribution on the components surface. The stress distribution is not the only design response for the optimization algorithm in TOSCA. If durability aspects have to be considered during multiaxial stress conditions, the design response may also be a damage distribution that is determined by a fatigue simulation. TOSCA has interfaces to commercial fatigue software tools like FALANCS, FEMFAT and MSC.Fatigue.

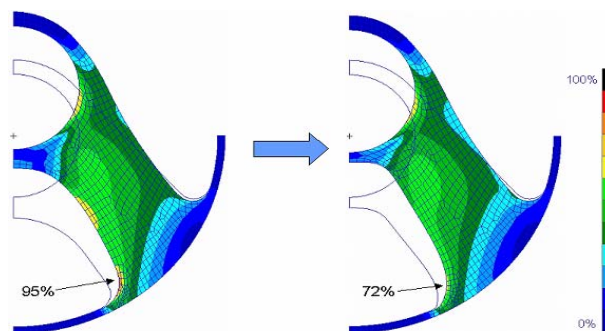


Fig. 2: Shape optimization example

NON-PARAMETRIC BEAD OPTIMIZATION

Beads are a widespread technology for reinforcing sheet metal structures. They can be applied without any noteworthy manufacturing efforts and without significant weight increase. The two main bead applications are to increase the stiffness for static loading conditions and to reduce the noise and vibrations for dynamic loadings.

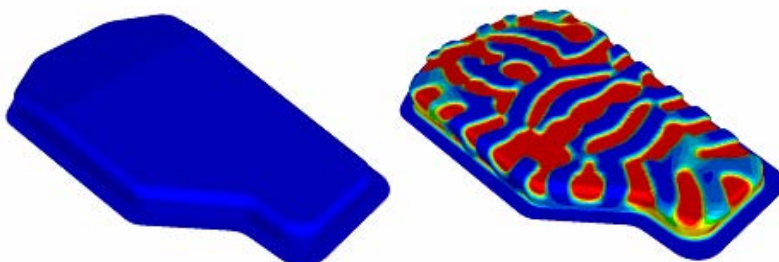


Fig. 3: Bead optimization example

Based upon the results of the finite element analysis, TOSCA determines the optimal bead location and bead orientation. The maximization of the moment of inertia leads to designs that have a maximum bending stiffness for the existent loading conditions.

PROCESS AUTOMATION

This methodology guides the user in setting up the Sequence of Analysis functions that describe the complete simulation - much like setting up the test laboratory apparatus. For example, if the functional performance of the design depends on stresses, vibrations and acoustics the engineer will use stress, vibration and acoustic analysis programs to simulate the corresponding performance. This methodology enables the engineer to set up the Sequence of Analysis steps graphically through point and click operations. The analysis sequence specifies the flow of information from the design factors to the decision responses.

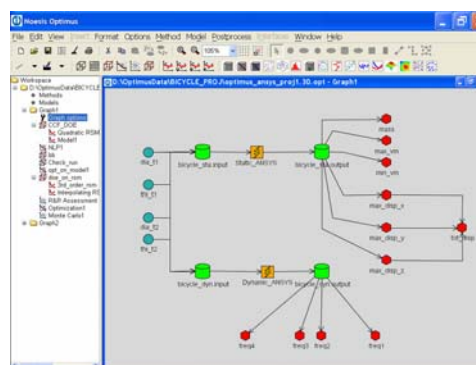


Fig. 4: Process Automation

For example, in simulating the static and acoustic behavior of a motorcycle gearbox the engineer has to run a static simulation to calculate the behavior of the design under static loading. Then, calculating the eigenfrequencies and finally through coupling of the dynamic structural behavior to an acoustic simulation calculating the sound pressure level at a specified location over a specified frequency range.

Connections for each analysis to the required input files and the corresponding output files are drawn. The design variables are identified and connected to the input files. The performance variables that have to be extracted are identified and connected to the output files. Format independent mechanisms for executing the variable modification and extraction are available. The complete workflow results in a dependency graph which is a powerful formulation for conducting the simulations that will be needed during the design synthesis.

The graph formulation enables a few innovative mechanisms inside the software:

- Selective computation and investigation. If some simulation runs do not depend on a subset of the design variables, or some performance variables are temporarily not needed, the software automatically determines where simulation runs can be eliminated. If some performance variables do not depend on some design variables, this knowledge can be exploited in model construction and visualization.
- Distributed and parallel computation. The data distribution over the computation nodes and the interdependencies between the simulation runs is determined on the graph.

PARAMETRIC OPTIMIZATION

Parameter based optimization is always based on a parameterized input for the optimization system. The parameters may be of different types:

- Shell thicknesses and material properties
- Geometric entities like radii, lengths or spline supporting points
- Forces, Boundary conditions
- Any other parameter that may be accessed in the model.

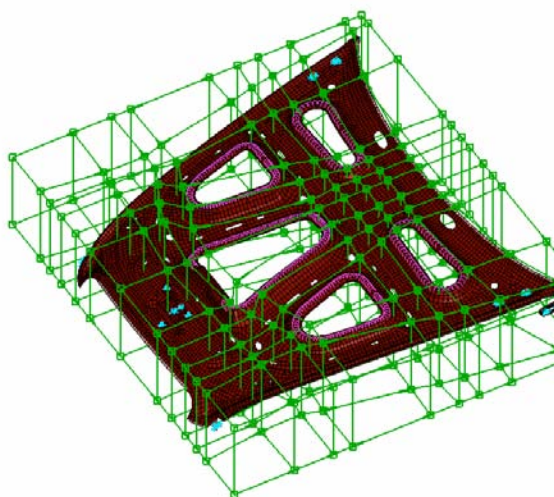


Fig. 5: Parametrization of a bonnet with ANSA Morphing

The variation of the design parameters is introduced into the simulation model by changing the parameterized model.

A very effective way to parameterize geometric entities in existing models is the use of ANSA morphing. The finite element mesh is parameterized by external morphing boxes. The parameters are applied on the control points of the morphing boxes. The movement of the control points is then applied to the underlying finite element mesh. For large geometric changes, one has to ensure the mesh quality during modification. As the mesh topology remains unchanged during the morphing procedure, elements may get distorted. If areas of high distortion are recognized during the morphing procedure, a mesh reconstruct may be applied on selected areas or the complete design in order to keep the needed mesh quality for simulation.

DESIGN OF EXPERIMENTS (DOE) and RESPONSE SURFACE MODELING (RSM)

DOE is a methodology that aims to maximize the amount of information obtained from experimentation while minimizing the amount of experiments [4]. DOE plans include two and three level full and partial factorials, adjustable factor level factorial, Plackett-Burman, Taguchi, Box-Behnken, and Composite designs. Each of the DOE plans listed above differs in the number of function evaluations required. Depending on the DOE plan selected, the degree of non-linearity of the subsequent RSM will vary. For instance, a three level full factorial DOE is sufficient in order to fit a second order Taylor polynomial model, while a Taguchi DOE will only produce sufficient data for a linear model. Figure 3 demonstrates the points of the design to be evaluated in a three level full factorial design for three design parameters. The corners of the (hyper-) cube represent the low and high values each factor is allowed to take.

There are a number of Response Surface Models that can be selected to fit the data generated from the DOE [5, 6]. The model shown is an RSM in five design variables. The representative types of RSMs available are polynomial type RSMs the order depending on the DOE type, with and without stochastic correction terms. The general form of the RSM is:

$$RSM(\mathbf{x}) = \sum_{i=1}^n a_i * F_i(\mathbf{x}) + Z(\mathbf{x})$$

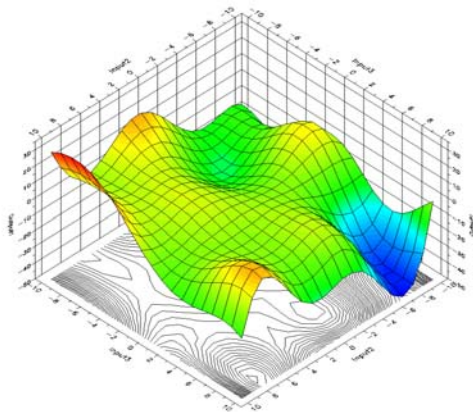


Fig. 6: Stochastic interpolation RSM

where i represents the number of approximating functions, a_i are the coefficients to be determined through Least Squares, $F_i(\mathbf{x})$ are the polynomial -or any user defined- mathematical functions. In the case of pure Taylor Polynomials the $Z(\mathbf{x})$ is set to zero.

A second type of RSMs are based on Stochastic Interpolation. In that case $F_i(\mathbf{x})$ is considered to be a constant. In computer experiments, observations are made on a response function by running the analysis sequence.

Some of the immediate benefits from a DOE/RSM approach are:

- All the models can be used as surrogates to the actual analysis sequence, replacing the computational costly simulation models
- The RSMs allow the engineer to interactively explore the design space prior to applying numerical optimization
- The most dominant design variables are detected, and their influence on the design outputs is quantified
- Correlation among the design outputs is revealed, such that conflicting optimization targets are detected in an early stage

ROBUSTNESS AND RELIABILITY

The optimal designs that are found by the use of optimization technologies are often found on the boundary of the design space meaning that one of the constraints is active. As soon as variability of the input parameters has to be taken into consideration, the scattering output data may lead to infeasible design in the failure domain. So the optimum point should be displaced in order to fulfill all constraints under consideration of scattering input data. The use of probabilistic design approaches helps to take these effects into account during optimization.

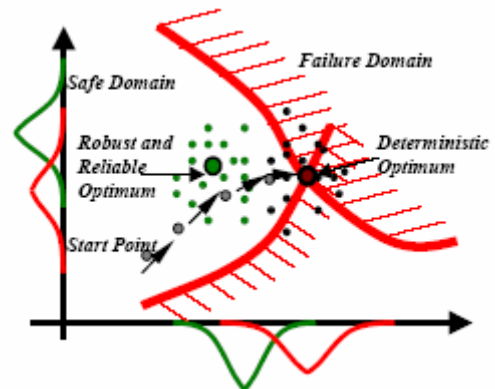


Fig. 6: Stochastic interpolation RSM

MULTIDISCIPLINARY OPTIMIZATION (MDO)

For every discipline to be considered in the MDO, the simulation workflow has to be automated in order to be executed multiple times. The automation must include the entire workflow from preprocessing over setup of the analysis to post-processing. The user has to assure that all relevant results for a design evaluation are extracted. Sometimes, objectives that seem very simple in the interactive evaluation of a design are very complicated to automate. For example the necessary space for the side-airbag between seat and door during a side-crash is more than just one value and this visual criterion has also to be defined to allow the optimization to rate the results.

REFERENCES

- (1) Bakhtiary, N., Allinger, A., Friedrich, M., Mulfinger, F., Sauter, J., Müller, O., Puchinger, M.: "A new Approach for Sizing, Shape and Topology Optimization", SAE International Congress and Exposition, 26.-29. Februar 1996, Detroit/Michigan (USA).
- (2) N. Tzannetakis, P. van Vooren, B. Lauber "The Use of OPTIMUS for Advanced Multi-Disciplinary Structural Optimization in Automotive Applications", NAFEMS Seminar: Optimization in Structural Mechanics, April 2005, Wiesbaden Germany
- (3) Noesis Solutions / OPTIMUS Users Manual Revision 5.2 / 2007

OPTIMIZATION OF A VEHICLE FRONT PART STRUCTURE AT AUDI USING ANSA MORPHING AND OPTIMUS

¹Michael Kaufmann, ²Boris Lauber*, ²Dr. Christoph Katzenschwanz

¹AUDI AG, Germany, ²FE-DESIGN GmbH, Germany

KEYWORDS - Mesh Morphing, Reconstruction, Structural Optimization, ANSA, OPTIMUS

ABSTRACT - Simulation techniques are used in an early design phase to generate design variants for the evaluation of the components behaviour. The generation of these design variants may be very time consuming. Many aspects have to be considered during the setup of the different simulation inputs. The geometry must be correct, the mesh quality must be adequate and all boundary and loading conditions for the simulation must be applied correctly. The use of mesh morphing techniques brings an enormous benefit as existing simulation models, which are already validated, may directly be used for the parametrization. The availability of mesh reconstruction algorithms ensures the quality of the finite element mesh during the modification procedure.

In this paper, mesh morphing techniques in ANSA are used on the optimization of a vehicle front part structure. Different targets like the weight, packaging, and other functional requirements had to be considered during the optimization. The introduction of shell thickness modifications as design variables did not lead to satisfactory results. So larger geometry changes were introduced by mesh morphing. An existing simulation input is parameterized and the new defined control points may be used as design parameters. The underlying mesh is modified corresponding to the control point movement. This parametrization is now to be used in the optimization system OPTIMUS to build up an automated workflow, which may be used for optimization.

TECHNICAL PAPER -

1. INTRODUCTION

During the concept phase, one is faced with the problem to quickly evaluate different design variants. The influences of changes of different design parameters have to be evaluated to be able to find a design that fulfils all requirements. If the parameters to change are geometric parameters, it is a challenging task to do a parameterisation that may be used in an automatic procedure for variant calculations, Design of Experiments (DOE) or optimization. For these methodologies, the modification of the design variables has to deliver an updated simulation input deck without manual interaction in order to be used in the automated processes. Geometric changes may be implemented in different ways. One possibility is to change the underlying geometric information directly. This always implies that a finite element mesh has to be automatically applied on the modified geometry. For complex geometries having specific loading conditions and joints this is not automatically to achieve. Powerful methods to do a mesh based parameterization are mesh morphing technologies. Any existing finite element mesh may be used for this kind of parameterization. The introduction of control points parameterizes the mesh. These external control points may be displaced and the mesh is following the external modifications. The mesh topology remains unchanged during this modification and nodes having active boundary or loading conditions are treated as hard nodes and will not be moved during this modification procedure. Different morphing approaches exist in order to define a large variety of parameterizations.

In combination with the optimization software OPTIMUS, the batch morphing technology in ANSA is a powerful toolbox to implement automatic changes on simulation files in order to do variant assessment or design optimization.

Different morphing technologies and the integration of the morphing setup into the optimization workflow will be presented on an optimization of a car front part structure.

2. PARAMETERIZATION USING MESH MORPHING TECHNOLOGIES

In the concept phase of new cars one is faced with the problem that many new design variants have to be evaluated. At the same time, the simulation models for the design variants do not exist and have to be quickly generated. For the use of parameterization techniques in an automatic optimization procedure one has to ensure, that the new design variants can be generated in a complete automatic procedure with no user interaction. The generated designs have to be of good mesh quality in order to be solved by the corresponding simulation tool. Additionally, all existing evaluation capabilities (e.g. scripts for post processing, ...) have to be easily adapted to the new simulation input decks.

3. CAD BASED GENERATION OF DESIGN VARIANTS

One possibility for the generation of design variants is the generation of a new CAD design of the component. If parametric CAD models exist, the generation of new design variants can be achieved very quickly. The advantage of this approach is that all changes are directly applied on the geometry what implies that no new geometry has to be generated manually for the transfer back into the design process. On the other side, a simulation mesh has to be generated on the modified geometry and all boundary and loading conditions have to be applied. As the node and element ID's are changing during the automatic mesh generation, this additional information may not be defined mesh independently and often requires manual interaction.

4. MESH BASED PARAMETRIZATION BY MESH MORPHING

A very effective way to generate design variants of complex simulation models is the use of mesh morphing technologies. Mesh morphing allows generating design variants based on an existing finite element mesh containing all detailed load case definitions. The mesh is parameterized externally and may now be modified even in an automated procedure. The mesh topology remains unchanged and all loaded/fixed elements and nodes are automatically frozen during the modification. Additionally, one may specify frozen and nested nodes what allows a large field of application for mesh morphing. For the parameterization by morphing, different approaches exist. In ANSA, two main approaches are implemented:

Direct Morphing

In direct morphing, the displacement values are directly applied on the mesh. The movement may be specified on nodes in the model. A transition zone is defined which is used for mesh adaptation. The nodes in the transition zone are moved smoothly between the moving nodes and the fixed nodes. This approach may be used to implement in plane or out of plane movement.

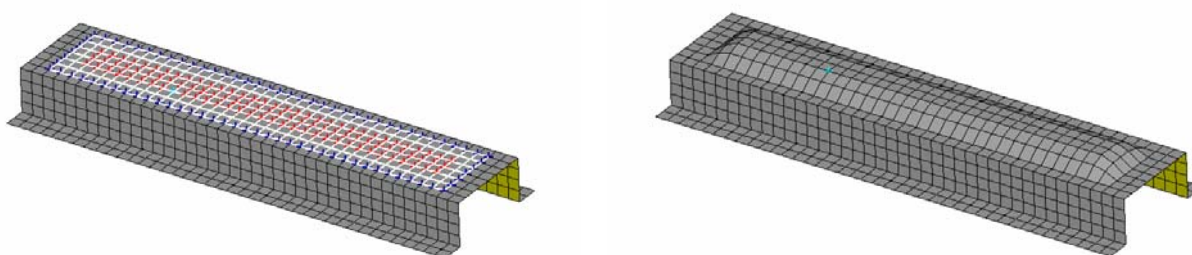


Fig. 1: Example for direct morphing

Box Morphing

A possibility to define more complex morphing parameters is the use of the box morphing technology. Morphing Boxes are defined additionally to the finite element mesh. The mesh is loaded into the boxes, and so all nodes and elements may be assigned to a certain morphing box. The corners of the morphing boxes are the control points for the modification procedure. If a control point is moved, the shape of the box is changed. Each node, which is loaded into the morphing box, now is displaced according to its geometric position in the morphing box.

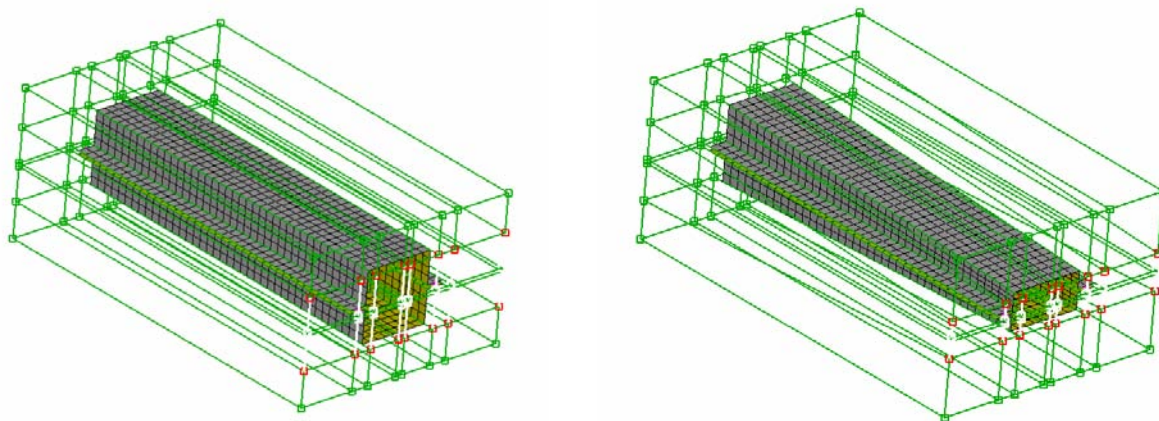


Fig. 2: Box morphing example

Mesh Reconstruct

During the mesh morphing procedure, the nodes of the existing mesh are moved but the connectivity of the mesh remains unchanged. For large geometry changes this may lead to large modifications of the element edge lengths. These modifications of the mesh may lead to poor quality meshes that may not be used in the simulation, as the results will not be meaningful or even the convergence of the solver may not be ensured. In ANSA this problem may be solved by applying a so-called reconstruct on the critical components. The reconstruct generates a new mesh based on the existing one but applying new values for the demanded element edge length.

All parts that are critical concerning the element edge length modification during the morphing procedure are reconstructed at the end of the morphing step in order to keep the quality of the finite element mesh for the crash analysis.

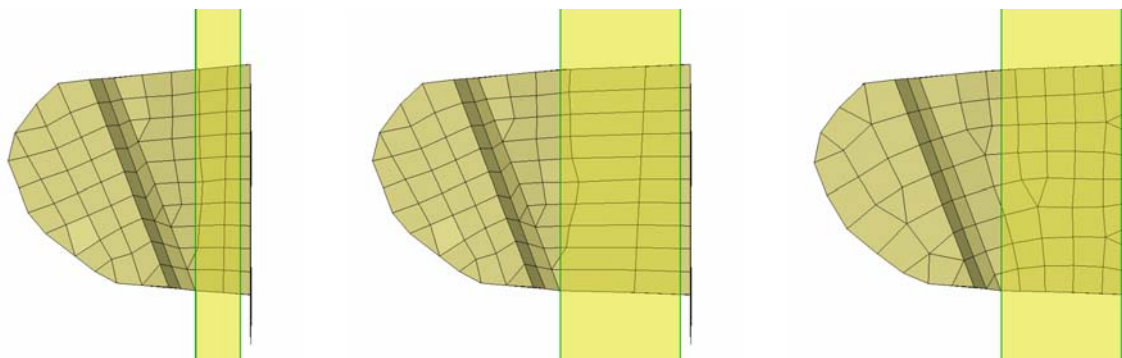


Fig. 3: Example for Mesh Reconstruct after Morphing

Automation of a Mesh Morphing Setup in ANSA

The morphing setup may be automated in ANSA by the use of ANSA scripting. Once, the different morphing parameters are defined, one can access these parameters via scripting and run ANSA in batch mode. So the new mesh configurations may be generated based upon the changing parameters and the morphing procedure may be implemented in automated simulation workflows. This is the prerequisite to be able to use morphing in an optimization.

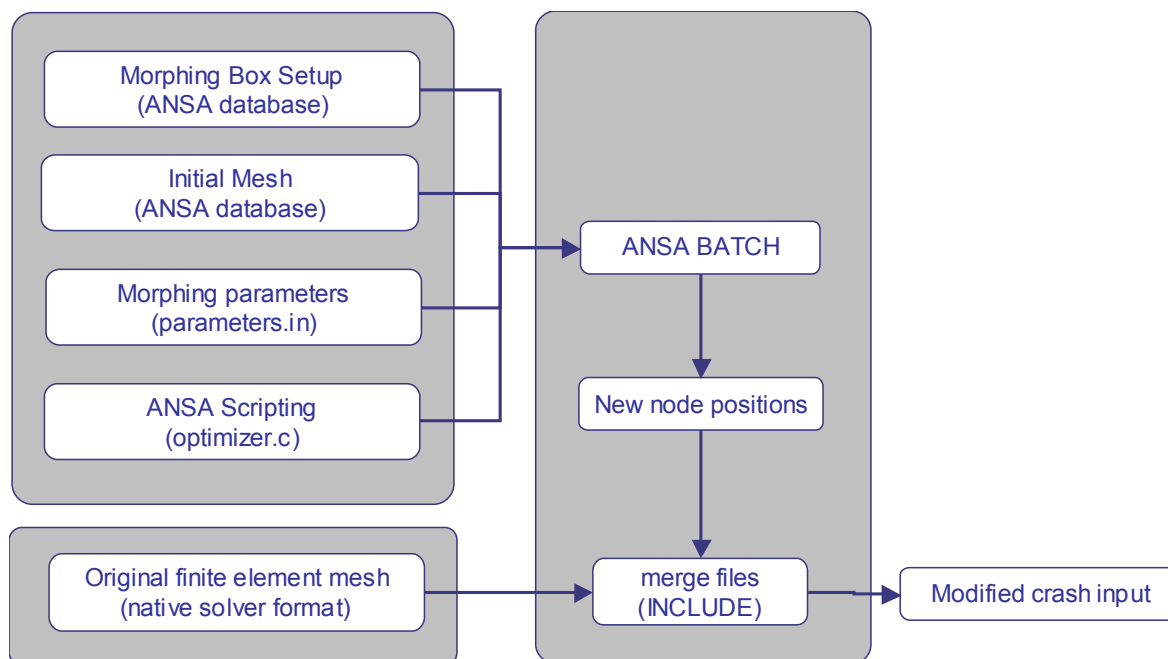


Fig. 4: Batch morphing setup for automated procedure

5. OPTIMIZATION OF A CAR FRONT PART STRUCTURE

PROBLEM DESCRIPTION

The aim of this optimization project is to improve the crash behaviour of a vehicle in a concept stage. The relevant response is the Occupant Load Criterion (OLC). The OLC is a criterion for occupant safety, which is determined during deceleration of the vehicle. These OLC values are calculated based upon the results of a front crash analysis.

6. SHELL THICKNESSES OPTIMIZATION

The optimization target is to find a design with OLC values in a feasible domain. In a first step, this target is to be reached by a modification of the shell thicknesses of the front part. As design variables, 20 sheets are selected, for which the thickness is modified. The simulation process is automated in the optimization system OPTIMUS. The thicknesses may easily be parameterized for the optimization. The thickness may directly be modified in the property definition in the finite element input deck. In OPTIMUS, so-called template files are generated, where the values for the thicknesses are replaced by OPTIMUS variables. For each design variant, which has to be evaluated for an optimization method, the OPTIMUS variables are substituted by the actual variable values. This allows to quickly automate the modification of the shell thicknesses.

The optimization target is to minimize the maximum OLC value of the design. A self adaptive evolution strategy was used in order to approach the optimum solution in the design space.

The optimization could improve the design and a design could be found with a smaller OLC value than the initial design. The target range of the OLC values could not be reached by changing the shell thicknesses only – a feasible design could not be found.

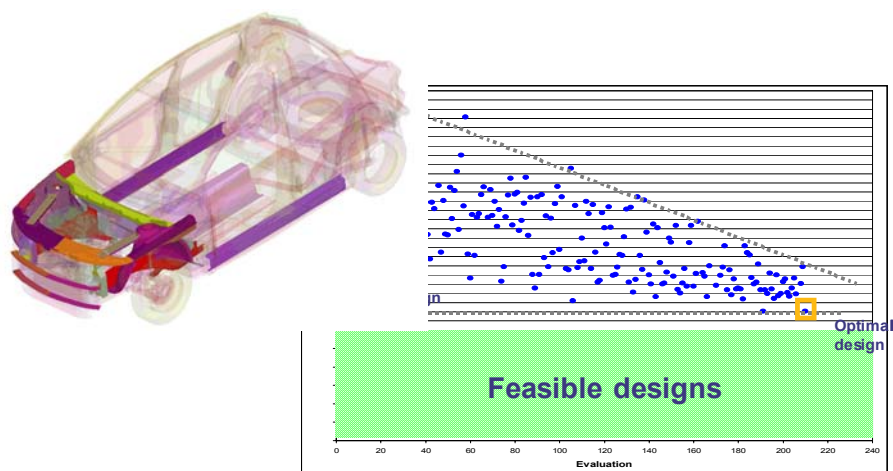


Fig. 5: results of shell thickness optimization

7. MESH MORPHING OF THE FRONT PART STRUCTURE

As the optimization of shell thicknesses did not end up in a feasible design, a new approach was chosen. An increasing deformation zone is necessary to fulfil the OLC requirements. In pre-examinations, 3 areas of possible modifications were detected. The distance between front wall and the engine should be changed. Additionally at the front of the car the distance between engine and cooler as well as the distance between the cooler and the bumper where possible design variables.

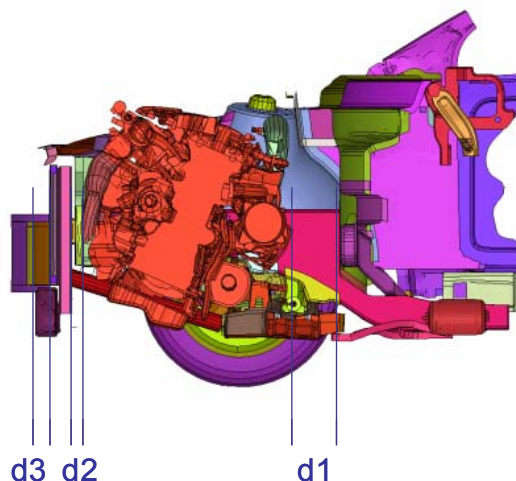


Fig. 6: Description of morphing parameters in car front part structure

3 Design variables are introduced:

- D1: Distance between front wall and engine
- D2: Distance between engine and cooler
- D3: Distance between cooler and bumper

The geometric changes are realized by mesh morphing. The use of morphing technology allows using the already existing simulation model with all existing boundary and loading conditions. Additionally, the post-processing routines could be easily reused as the mesh topology may be kept in the areas of interest. Only the components, which have to be

changed by the corresponding design parameter, may be loaded into the morphing boxes. This enables the definition of quite complex design parameters for the geometry changes.

Parameter D1

The modification of Parameter D1 basically includes the length change of the front side member, the y-connections and the back part of the wheel housing. All parts in the front of the car (engine block, bumper, ...) get a translatic movement in x-direction of the car.

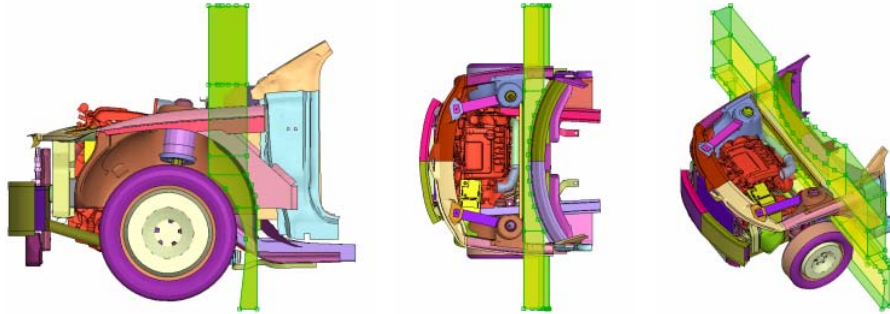


Fig. 7: Morphing parameter D1

Parameter D2

The second morphing parameter includes the front part of the wheel housing and the bottom and top front members. The engine, which geometric position is also located inside the morphing boxes, is not loaded for the modification of the parameters. The engine position will not be modified in this morphing step.

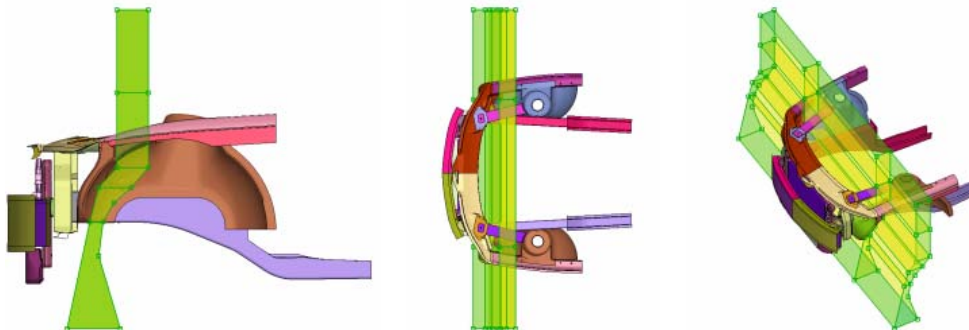


Fig. 8: Morphing Parameter D2

Parameter D3

The third morphing parameter is only affecting the front of the car. The bumper is moved in x-direction. This is realized by a change of the length of the crash box.

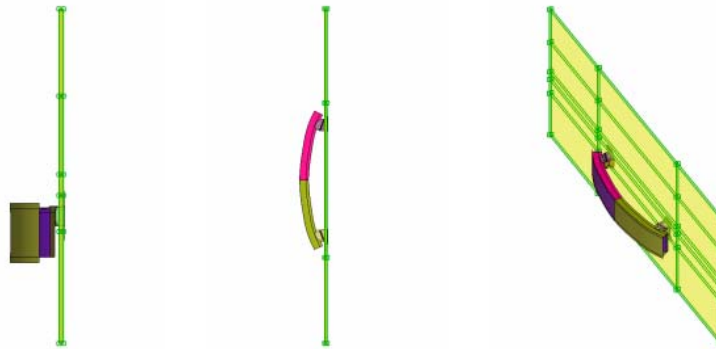


Fig. 9: Morphing Parameter D3

Assembly of the morphing boxes

The complete morphing setup includes a connected set of morphing boxes. A translational displacement in x-direction is defined for the control points of the single morphing parameters. Stepwise, the single parts of the front part structure are loaded into the morphing boxes and displaced. First, the parameter D1 is applied and D2 and D3 get the same displacement amount – these areas of the front part structure remain unchanged. In the next step, D2 is morphed and D3 gets the same displacement – the last morphing step is their modification of parameter D3.

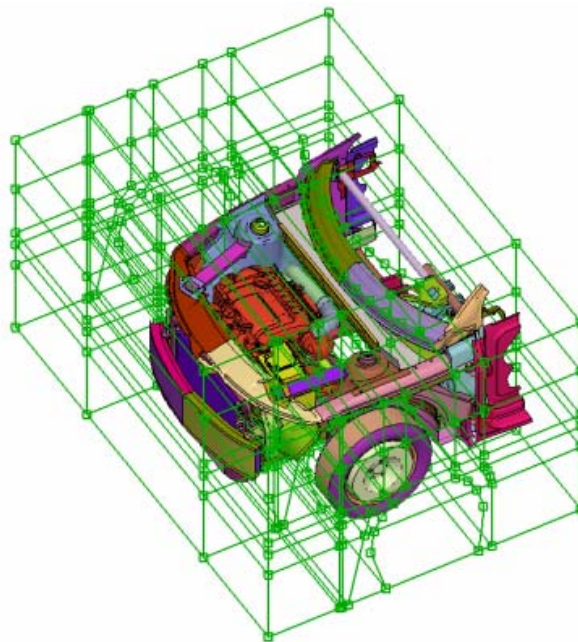


Fig. 10: Car front part structure with Morphing Boxes

This procedure allows to apply the different design parameters and to generate a new input file for the crash analysis. The single morphing areas are not overlapping and therefore not influencing each other.

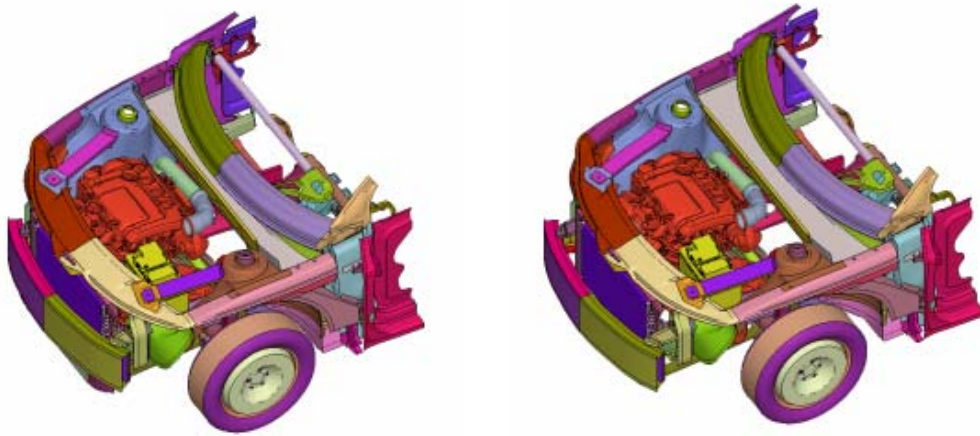


Fig. 11: Morphing of the complete car front part structure

Optimization

The morphing setup is now to be integrated into the optimization loop. Therefore, the complete morphing has to be executed in batch mode in order to generate the different design variants automatically. For this purpose, ANSA scripting is used to implement the morphing procedure in the optimization software OPTIMUS. An input template file for the ANSA batch run is generated where the design variables are parameterized via OPTIMUS variables. The batch morphing procedure is always based upon an ANSA database containing the initial input deck and the morphing boxes. After the batch morphing in ANSA is executed, the new node positions are exported. In case of reconstruction, also the new generated nodes and elements have to be exported.

These files are included into the main deck of the crash analysis. The crash analysis is executed on a compute cluster. On the cluster, the extraction of the accelerations and the calculation of the OLC value are executed by a post processing script. Only the interesting responses for the optimization are transferred back to the optimization host and the corresponding response value is extracted from the result file.

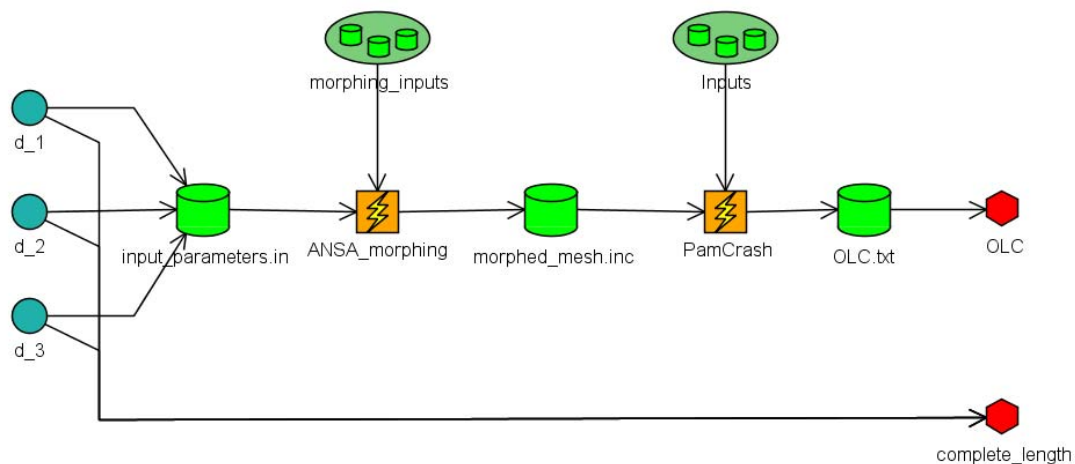


Fig. 12: Simulation workflow including mesh morphing

For the front part structure, the shell thickness distribution from step 1 was used for the initial design. The formulation of the objective was modified compared to the shell thickness optimization. The longitudinal changes in the front part of the car can reduce the OLC values but due to design restrictions, changes in the front structures length should be avoided. So the objective was to minimize the complete length of the front part with a constraint on the OLC value. The necessary changes in the length should be applied in the area where geometric changes have the largest influence on the considered response. A global optimization approach was used for optimization.

Results

Using the optimum shell thickness distribution from the previous optimization, a feasible design could be found. The advantage of the global optimization is the generation of a large number of design variants that also allow the identification of the influence of the design changes on the design criterion. For 2 design areas, a weak influence of the modification of the inputs could be recognized. But for one of the design areas, a correlation between the geometric changes and the corresponding OLC value was found. This area is the most important one to implement the geometric changes, as the influence on the OLC performance is very strong.

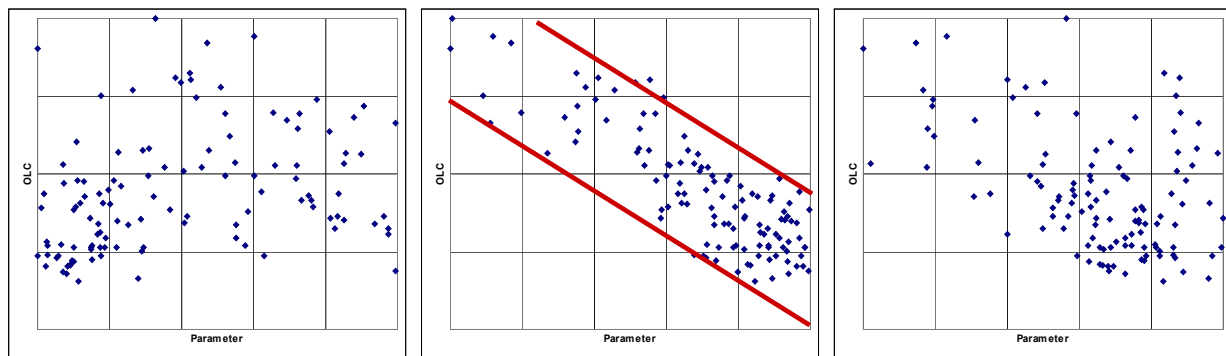


Fig. 13: Important area for design changes

8. CONCLUSION

The use of optimization technologies allows to quickly evaluate different design variants and to optimize components concerning a large variety of objectives considering a large number of constraints. However, the parametrization plays an important role. The design space strongly depends on the selected design variables. The easiest way to parameterize an input for a simulation procedure is to access and modify values in the simulation input deck. The number of parameters here is very limited so one is faced with the challenge to introduce more advanced parameterizations. The modification of a component's geometry is often necessary in order to widen the design space. At the same time the introduction of geometry parameters for an automated use in an optimization procedure is not easily to achieve as mesh quality plays an important role for simulation.

The example of the vehicle front part structure shows, that the modification of the shell thicknesses only did not lead to a satisfactory design performance. Larger geometric changes were needed in order to have a larger design space for modification. The use of mesh morphing technologies was the selected parametrization technology as existing and validated input decks can easily be used and the mesh quality can be checked and modified if necessary.

Morphing is used to quickly adapt existing simulation inputs to new design variants. The automation via scripting allows integrating these changes into automatic Design studies like Design of Experiments or complete optimization projects.

REFERENCES

- (1) Beta CAE-Systems S.A. / ANSA Version 12.1.0 Users Guide / 2007
- (2) Noesis Solutions / OPTIMUS Users Manual Revision 5.2 / 2007

A NEW APPROACH FOR THE PREPROCESSING OF TOSCA OPTIMIZATION TASKS IN ANSA

¹Lauber, Boris*, ²Korbetis, George, ²Marmaras, Dinos,
¹FE-DESIGN GmbH, Germany, ²BETA CAE Systems S.A., Greece

KEYWORDS – Non-parametric structural optimization, shape optimization, bead optimization, topology optimization, TOSCA, ANSA

ABSTRACT - Non-parametric optimization methods are an efficient way to find an optimal design on a very early phase of the design process. Topology optimization may be used to find new design proposals based upon a maximum design space. Shape optimization is reducing local stress peaks or increasing components lifetimes by modifying the components surfaces only. Bead optimization increases the stiffness of sheet metal structures by introducing stiffeners. These different types of structural optimization are available in the non-parametric optimization software TOSCA. A completely new approach of executing preprocessing for non-parametric optimization tasks will be presented in the ANSA environment. The intuitive optimization environment provides an easy-to use optimization preprocessor that supports the complete design process. The use of the application will be demonstrated on existing examples of structural optimization.

TECHNICAL PAPER -

1. INTRODUCTION

The development of lightweight designs is a quite challenging task. Not only the target has to be fulfilled but also all relevant constraints and restrictions have to be considered. The engineer is faced with a large number of requirements during the design phase of a new component. Different optimization methodologies exist, which are helping the designer and analyst to design right the first time. Design proposals may be found that are already optimal considering different requirements. But not only the optimization algorithms must be powerful and able to solve the optimization problem. The complete Optimization procedure must be available in an easy to use Optimization environment.

2. THE OPTIMIZATION SYSTEM TOSCA

A non-parametric optimization approach as used in the program TOSCA allows one to use standard industrial CAE-solvers (e.g. ABAQUS, ANSYS, MSC.Nastran, MSC.Marc, NX Nastran, or Permas) for solving large-scale optimization problems in the fields of topology, shape and bead optimization. Using existing CAE solvers for solving optimization problems is essential in the industry. Additionally to the finite element input deck, an additional file containing the optimization task definition has to be defined. All objectives, constraints and existing manufacturing restrictions have to be defined here.

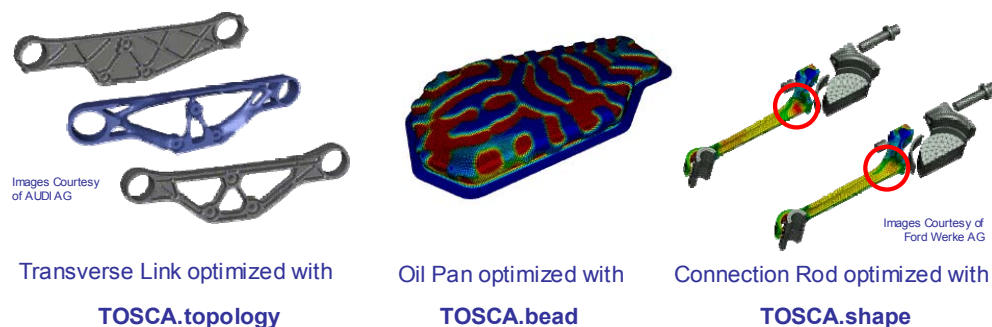


Fig. 1: Optimization methods available in TOSCA

TOPOLOGY OPTIMIZATION

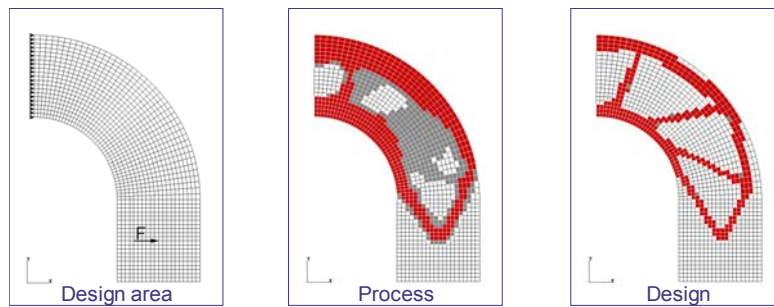


Fig. 2: Topology optimization

Topology optimization is used to find a design proposal in a very early design phase. The maximum allowed design space has to be available as finite element input deck. All relevant loadcases have to be applied on the design space model. A typical objective for topology optimization is the minimization of compliance

corresponding to maximize the stiffness using a mass constraint for a given amount of material. Also the dynamic behaviour of components may be a target of the optimization by specifying objectives or constraints on the eigenfrequencies. The optimization of the mechanical behaviour of the components is very often combined with restrictions from the manufacturing. For casting parts, undercuts must be avoided in draw direction in order to be able to manufacture the part by casting. For some manufacturing types, restrictions on the minimum or maximum wall thickness have to be applied.

SHAPE OPTIMIZATION

Shape optimization is used in a later phase of the design process. The components topology remains unchanged in shape optimization. Only the components surface is modified in order to reduce local stresses or to increase the components lifetime. In TOSCA, a non-parametric optimization approach is implemented. No parameterization of the part is necessary. Each node on the surface of the component is a possible design node. A powerful mesh-smoothing algorithm is adapting the mesh after the design node movement in order to keep a good quality mesh for the analysis.

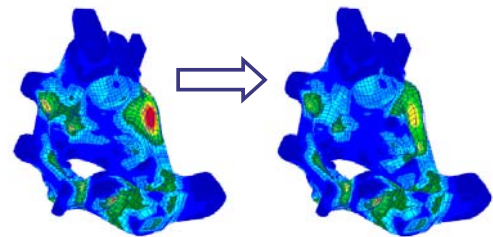


Fig. 3: Shape Optimization

BEAD OPTIMIZATION

Bead optimization is used to find the optimal bead layout for sheet metal parts. For complex loading conditions, a good bead design is hard to find. The bead optimization module helps to find a good location and orientation of bead stiffeners in a sheet metal structure. In bead optimization, the dynamic behaviour of the components is the most important target.

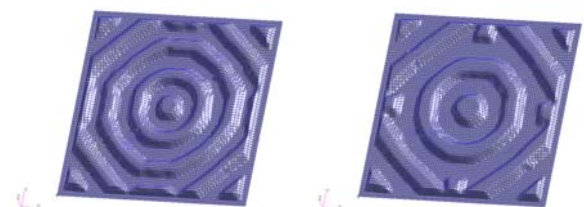


Fig. 4: Bead optimization

3. INTERACTIVE PREPROCESSING OF TOSCA TASKS IN ANSA

The definition of an optimization task contains the definition of the optimization target by defining the objective function and constraints, and the definition of existing restrictions concerning the allowed modification of the design variables. These definitions have to be made additionally to the setup of the finite element model for the analysis.

The new environment for the setup of Optimization Tasks in ANSA is designed that the user is guided by a task manager that defines the step-by-step procedure.

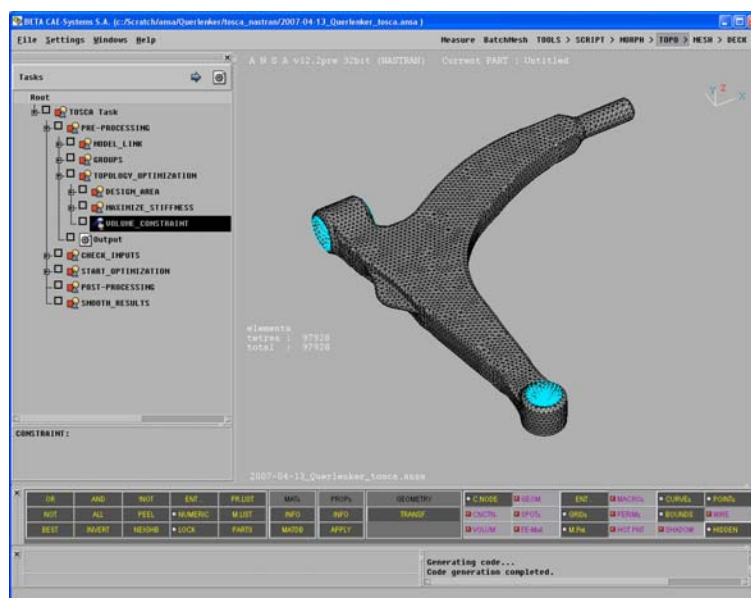


Fig. 5 : TOSCA Environment in ANSA

PRE PROCESSING

The complete preprocessing of the optimization task for topology, shape or bead optimization is executed. First, the link to the finite element model, which is used for optimization, is generated. The corresponding finite element model is loaded and visualized in the working area.

The user may now specify groups, which should be used for the optimization definition. Typical groups are design nodes, design elements, or groups for which restrictions have to be defined. If the groups are already defined in the finite element deck, they are imported into the database and may directly be used for the setup of the optimization task.

Dependent on the selected type of optimization, the design variables are defined and all necessary manufacturing constraints may be added as design variable constraints.

The definition of the objective function and constraints is added to finish the setup of the optimization task.

CHECK INPUTS

All dependencies are automatically checked while output the model. The user can additionally add additional checks e.g. to check complex restriction definitions for shape optimization. The checks are executed after the update of the preprocessing task.

START OPTIMIZATION

The next step is to execute the complete optimization. This may be done interactively but the more convenient way is to output the necessary input files and to start the optimization on a computation server. The optimization is an iterative procedure, where the finite element solver and the TOSCA optimization module is launched in each design cycle. The modification of the input file is made by the TOSCA application dependent on the selected type of optimization.

POST-PROCESSING

After the optimization is executed, the results are prepared for post-processing. Additionally to the finite element results, specific optimization results are provided. For topology optimization, the material distribution is output on the mesh of the design space. For shape and bead optimization, the optimization movement is output for post-processing.

SMOOTH RESULTS

The topology optimization results in very rough design proposals, where elements from the initial design space model have a very low density and are hidden for post-processing. A result based smoothing of these results allows generating a smooth surface distribution of the topology optimization results. These smoothed surfaces may be used for further processing of the results in the design process.

Additionally to the smoothed surfaces, cutting splines may be requested in order to be able to transfer the optimization results to CAD systems. The user selects a coordinate system axis and the cutting splines are calculated normal to the selected axis. An arbitrary number of cuts may be requested, that is output as Iges Splines to be imported into different CAD System for generation of new CAD data.

4. OPTIMIZATION EXAMPLE: WISHBONE

The example to be optimized is a wishbone. The optimization target is to reduce the weight of the component, and not to exceed the maximum stresses in the design space. The proposed workflow is to start with a topology optimization in order to find a minimum compliance design for a certain target volume. The next step is the redesign and validation of the optimized component considering the von Mises stress distribution. To reduce the Maximum stresses in the design, a shape optimization is executed at the end to minimize local stress peaks in the design.

GENERATION OF DESIGN SPACE MODEL

The first step in topology optimization is to determine the maximum available design space. A finite element model of the design space is generated and all loads and boundary conditions have to be applied to the design space model. In our example, a predecessor design existed. The cavities where filled with material in order to have a larger design space for the optimizer.

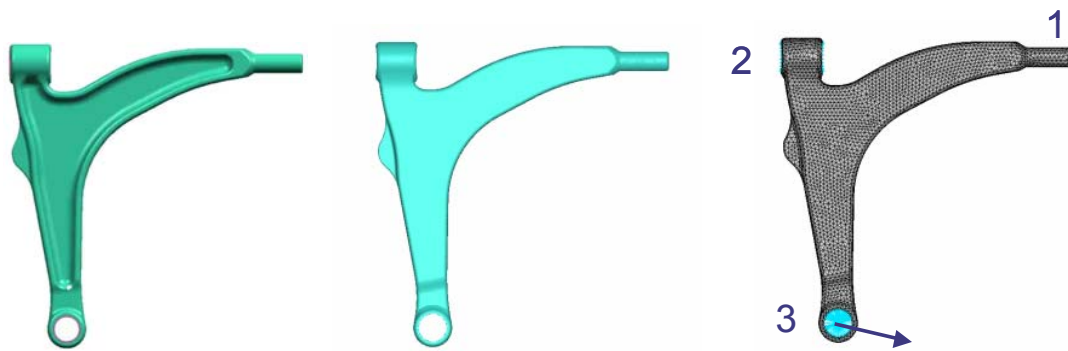


Fig. 6: Initial Design, Design Space Geometry and Finite Element Mesh for Topology Optimization

The design space model has to be prepared for the finite element analysis. All relevant loadcases for the layout of the component have to be applied. For this example, the following loading conditions are applied for the 3 loading points:

Point 1: Fixed in direction 2,3,5,6

Point 2: Fixed in direction 1,2,3,5,6

Point 3: Braking load

TOPOLOGY OPTIMIZATION

Additionally to the finite element deck, the definitions for the optimization have to be made. This information may be setup in the TOSCA.environment.

The first step is the definition the design area. The density of each element in the design area is a design variable that changes during the iterative modification procedure. For the wishbone example, additional design variable constraints have to be defined, that restrict the modification of the design variables. The areas of the 3 loading points and the area of the bracket are frozen for the optimization procedure. Additionally, a demolding constraint is activated with a parting plane lying in the symmetry plane of the structure. The wishbone is produced by a forging procedure so no undercuts are allowed for the design proposal.

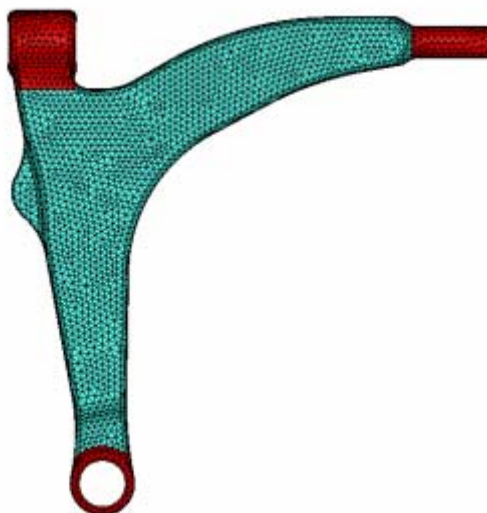


Fig. 7: Frozen Elements (red) for Topology Optimization

The objective is to find a minimum compliance design with a constraint on the volume. Topology optimization is started and the iterative optimization procedure is launched.

POST-PROCESSING OF TOPOLOGY OPTIMIZATION RESULTS IN μ ETA

Topology optimization results of TOSCA may be post-processed in different ways. During the optimization loop, the finite element solver is executed in each design cycle with a modified input deck having the actual property values for the elements. So for each design cycle, a native finite element results file exists if the user selected to keep all result files. These files may be used for a standard post-processing. Additionally, TOSCA exports the additional topology results. The material properties are exported to a VTF file that may be visualized with the TOSCA.view module that is used for a quick post-processing of the results. These specific results for topology optimization may also be exported to result files that can directly be imported by μ ETA. In μ ETA, the material distribution may be visualized as contour plot, iso-surfaces and also animations may be generated.

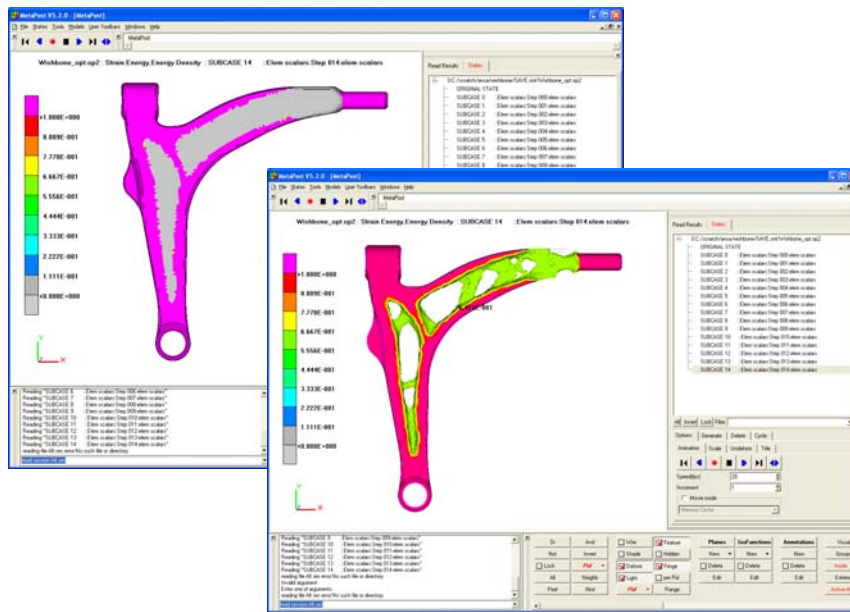


Fig. 8: Contour Plot of Material distribution and Iso-surface in μ ETA

SMOOTHING TOPOLOGY RESULTS

The smoothing procedure generates a new surface mesh from the material distribution of the results from topology optimization. All void elements are now removed from the structure and a new component for transfer to CAD or for the generation of a new finite element deck is generated.

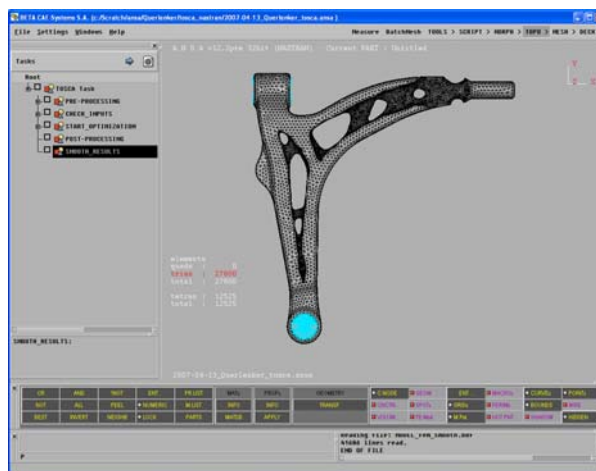


Fig. 9: Smoothed design of the wishbone imported in ANSA

VALIDATION OF TOPOLOGY OPTIMIZATION RESULTS

After the smoothed design is imported into ANSA, the surface mesh quality is checked and if necessary a reconstruct is performed. The so-generated shell mesh is used for the generation of a new solid tetra mesh that may now be used for a validation run. All boundary conditions from the initial design space model are applied and a new analysis is executed.

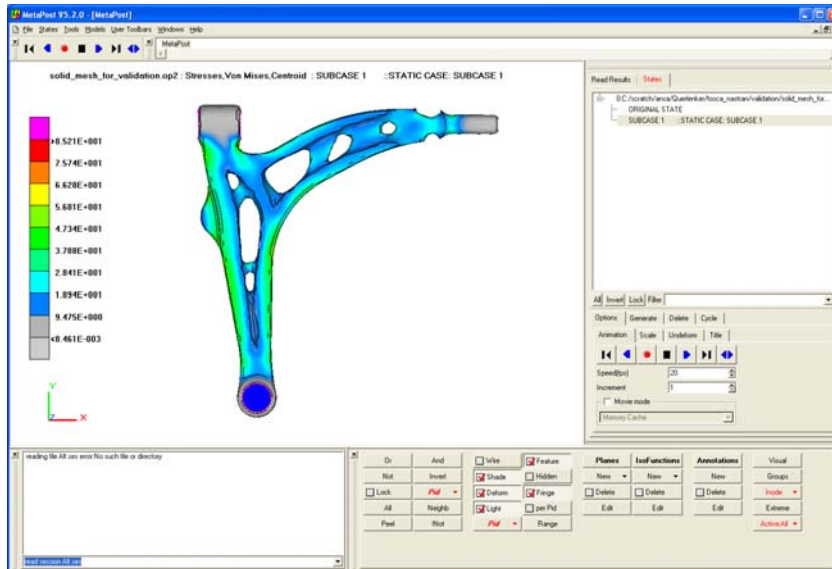


Fig. 10: Post-processing of validation run in μETA

GENERATION OF GEOMETRY

Additionally to the generation of a surface mesh, geometry information may be generated by using TOSCA.smooth. For the wishbone, 80 cuts in x and y direction as well as 10 cuts in z-direction are calculated. For each cut through the model, a cutting spline on the surface of the smoothed component is output as parametric or interpolated cubic spline in IGES format.

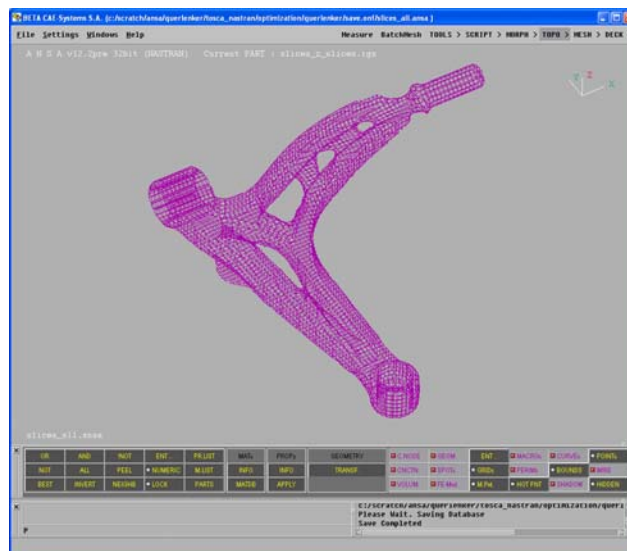


Fig. 10: Cutting splines for CAD transfer

New geometry information is generated from the results of topology optimization. During the generation of the new geometry, all detailed requirements for manufacturing are taken into account and the design proposal from topology optimization is used as design draft.

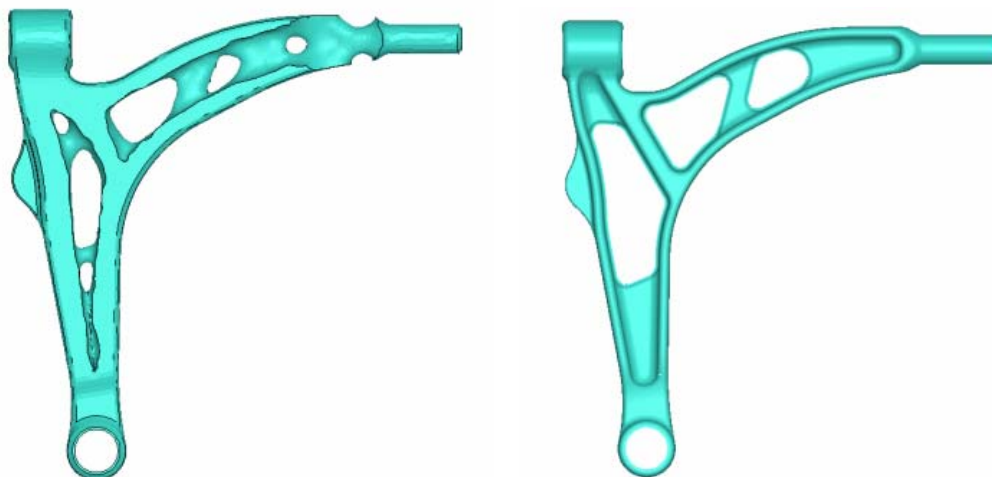


Fig. 11: Generation of new geometry from design proposal

5. CONCLUSION

Non-parametric structural optimization is an efficient tool for the improvement of components. Additionally to the optimization algorithms, the handling for the setup of the optimization task plays an important role. The setup of the optimization task should be made in an intuitive way. The new TOSCA environment is a tool for the guided setup of the topology, shape or bead optimization task in TOSCA. But not only the preprocessing is supported – the complete optimization process starting with the setup, including the start and post-processing of the optimization and the smoothing and CAD transfer is included. This environment helps the user to setup and control the optimization tasks in an efficient way.

The TOSCA optimization environment in ANSA supports the definition of topology, shape and bead optimization tasks. The complete optimization workflow may be setup including the smoothing and generation of a new solid finite element mesh from topology optimization to perform a validation analysis. In case of areas of critical stresses after topology optimization, a shape optimization task may directly be defined in order to optimize the components shape.

REFERENCES

- (1) M.P.Bendsoe, O.Sigmund (2003), Topology optimization Theory, Methods and Applications, Springer
- (2) Maute, K. (1998) 'Topologie- und Formoptimierung von dünnwandigen Tragwerken', University of Stuttgart., Institute of Structural Mechanics, Ph. D. Theses.
- (3) Bendsoe M. P., Kikuchi N: Generating Optimal Topologies in Structural Design Using a Homogenization Method, Computer Methods in Applied Mechanics and Engineering, 71_197:224, 1988
- (4) Meske, R., Sauter, J., Güngör, Z. (2001) 'Recent improvements in topology and shape optimization and the integration into the virtual product developments process', NAFEMS World Congress, Como (Italy).

Session H3.5

ANSA FOR CFD - OVERVIEW AND OUTLOOK

Marco Lanfrit*, Thomas Lehnhäuser

ANSYS Central & Eastern Europe - Fluent Deutschland GmbH, Germany

KEYWORDS - CFD, Preprocessing, FLUENT, Morphing, Meshing


ABSTRACT - Preprocessing is the primary and underlying Step in every CFD process. It is mandatory for a good and reliable result of the subsequent simulation. As computer resources grow and get cheaper, Engineers of all industries want to simulate in more detail and thus deal with complex geometries and a variety of CAD and mesh formats.

Based on an existing mesh, mesh deformation in combination with design optimisation methods yield significant gains in term of CFD productivity and turnaround time.

ANSA offers advanced tools to deal with complex geometries and mesh deformation. It is known as one of the most reliable Preprocessing tools in the world.

The application of ANSA in the CFD process is shown for a specific industrial case.

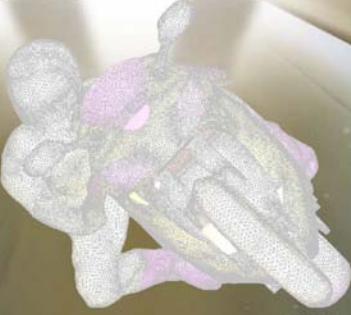
At the end of the presentation, the future demands of CFD users with respect to a Preprocessing tool will be highlighted.



ANSA for CFD

Overview and Outlook

Dipl.-Ing. Marco Lanfrit
Teamleader Consulting & Applications
Fluent Deutschland GmbH
ANSYS Central & Eastern Europe




© 2006 ANSYS, Inc. All rights reserved.


1

ANSYS, Inc. Proprietary

Agenda



- Why ANSA?
- ANSA's CFD specific tools
- Optimization using Morphing Methods
- Future demands and trends in Preprocessing for CFD




© 2006 ANSYS, Inc. All rights reserved.

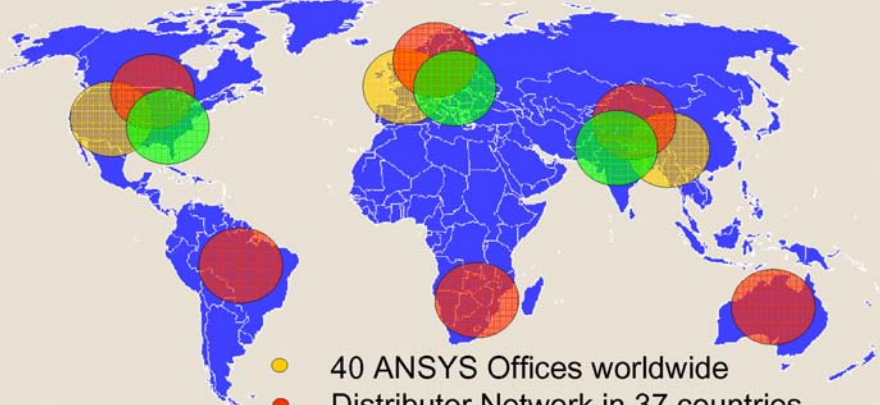
2

ANSYS, Inc. Proprietary

ANSYS worldwide



Headquarter: Canonsburg (Pittsburgh), Penn.



- 40 ANSYS Offices worldwide
- Distributor Network in 37 countries
- 17 Software Development Centres

> 1.400 employees
> 280 Mio. \$ revenue in 2005

© 2006 ANSYS, Inc. All rights reserved. 3 ANSYS, Inc. Proprietary

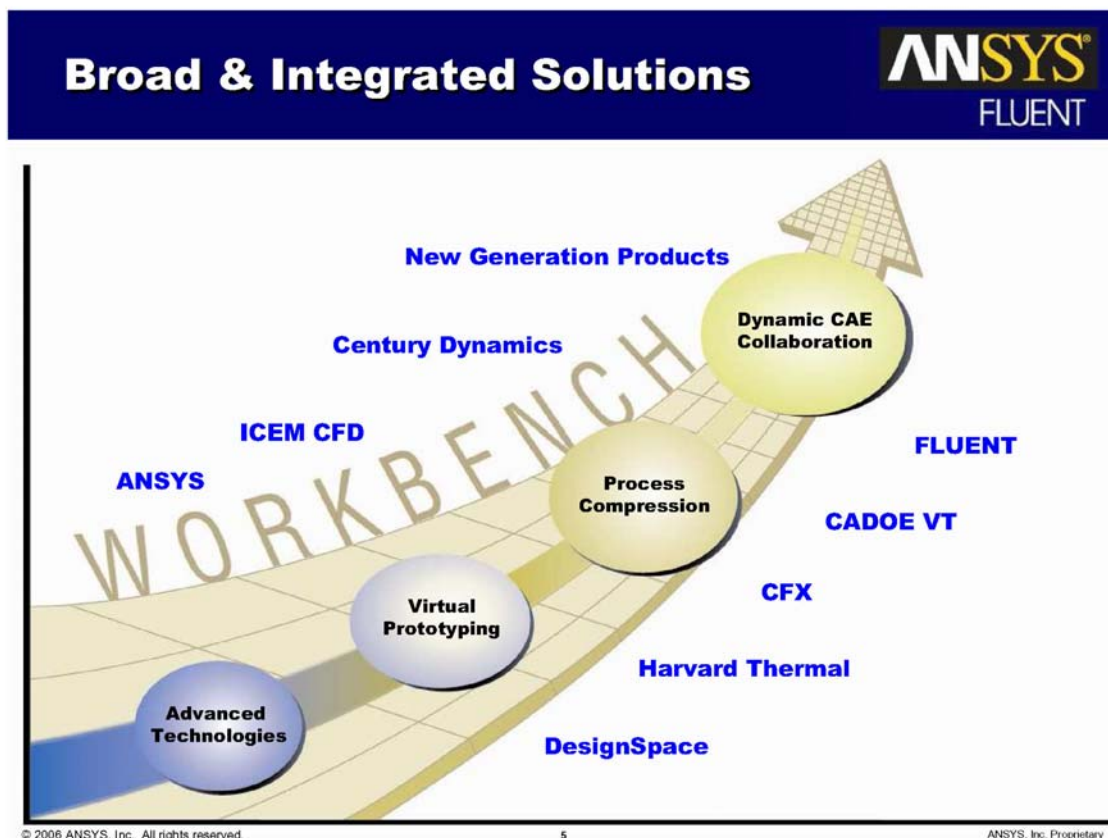
ANSYS - Vision



- Simulation Driven Product Development**
 - BETTER** – Innovative & higher-quality products
 - FASTER** – Dramatic time-to-market improvement
 - CHEAPER** – Minimize development, warranty & liability costs



© 2006 ANSYS, Inc. All rights reserved. 4 ANSYS, Inc. Proprietary



Agenda

- Why ANSA?
- ANSA's CFD specific tools
- Optimization using Morphing Methods
- Future demands and trends in Preprocessing for CFD

© 2006 ANSYS, Inc. All rights reserved. 6 ANSYS, Inc. Proprietary

Why ANSA ?



There are two main reasons, why ANSYS engineers are coming in contact with ANSA:

1. A lot of our customers are using ANSA, either in combination with our or other CFD Codes, or for structural analysis
2. ANSA is a very flexible and effective tool for preprocessing, especially for complex geometries

© 2006 ANSYS, Inc. All rights reserved.

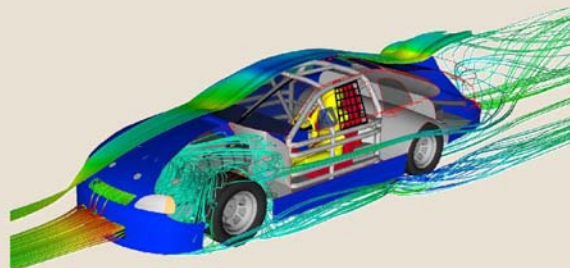
7

ANSYS, Inc. Proprietary

Beta Cae and Fluent a winning team since many years



- First combined application of ANSA / TGrid in 1995 at Renault, France (via NASTRAN)
- 1996: FLUENT Interface (surface mesh)
- Highly flexible and efficient approach to create high quality CFD-meshes for complex configurations
- Has become a very successful and efficient combination of tools amongst automotive users



© 2006 ANSYS, Inc. All rights reserved.

8

ANSYS, Inc. Proprietary

Collaboration



Beta Cae and ANSYS/Fluent have a loosely collaboration:

- Software Exchange
- Fluent delivers input for CFD/Fluent specific functionalities
- Fluent provides access to code know-how (e.g. skewness definition, output formats, ...)
- Beta CAE offers tools, which are custom made for FLUENT users (e.g. CFD Mesh)



© 2006 ANSYS, Inc. All rights reserved.

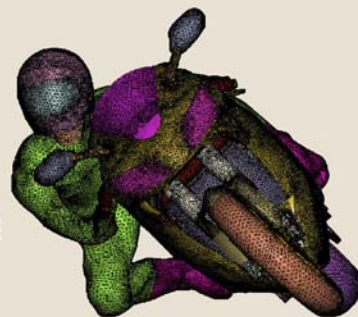
9

ANSYS, Inc. Proprietary

Agenda



- Why ANSA?
- ANSA's CFD specific tools
- Optimization using Morphing Methods
- Future demands and trends in Preprocessing for CFD




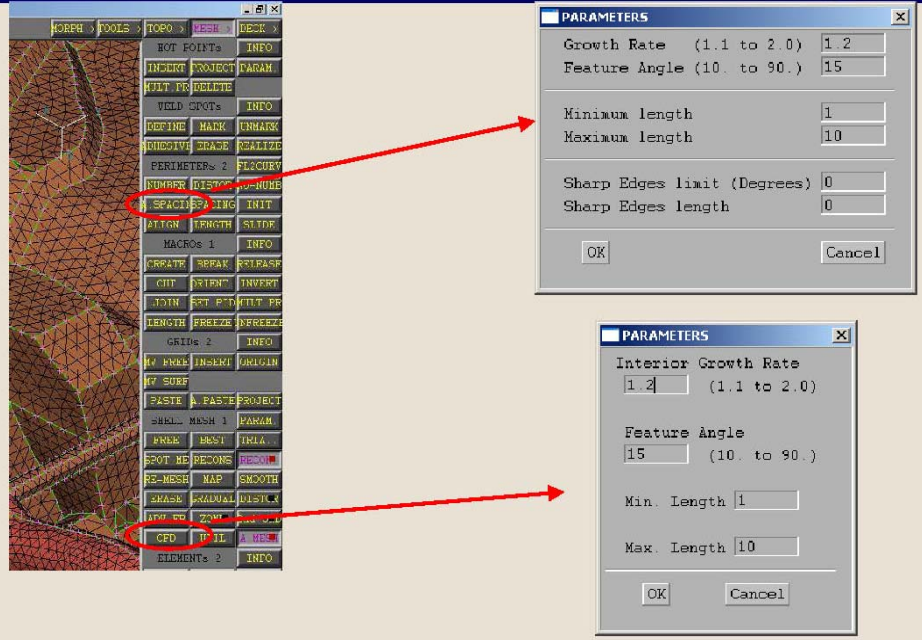
© 2006 ANSYS, Inc. All rights reserved.

10

ANSYS, Inc. Proprietary

CFD Mesh





PARAMETERS


Growth Rate (1.1 to 2.0)	1.2
Feature Angle (10. to 90.)	15
Minimum length	1
Maximum length	10
Sharp Edges limit (Degrees)	0
Sharp Edges length	0

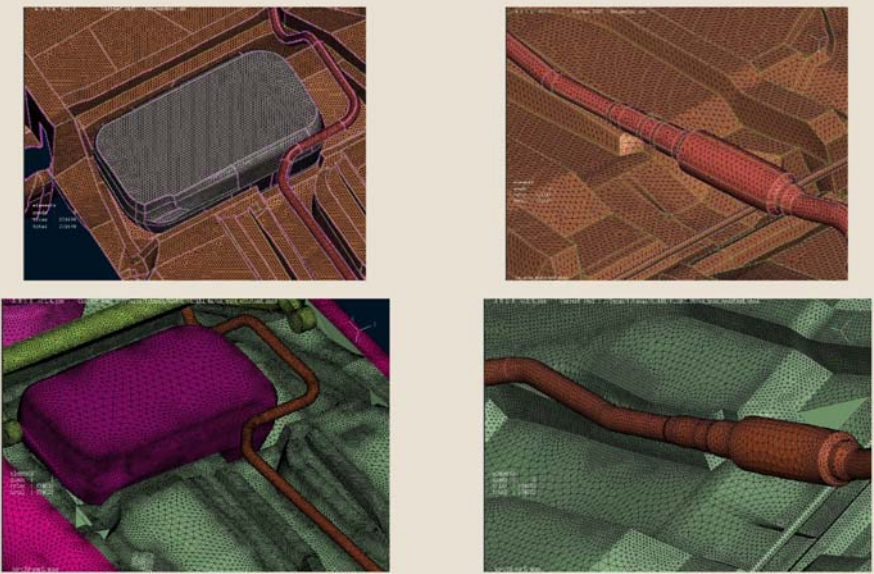
PARAMETERS

Interior Growth Rate	1.2 (1.1 to 2.0)
Feature Angle	15 (10. to 90.)
Min. Length	1
Max. Length	10

© 2006 ANSYS, Inc. All rights reserved. 11 ANSYS, Inc. Proprietary

CFD Mesh





© 2006 ANSYS, Inc. All rights reserved. 12 ANSYS, Inc. Proprietary

Ford Ka – Meshing Benchmark



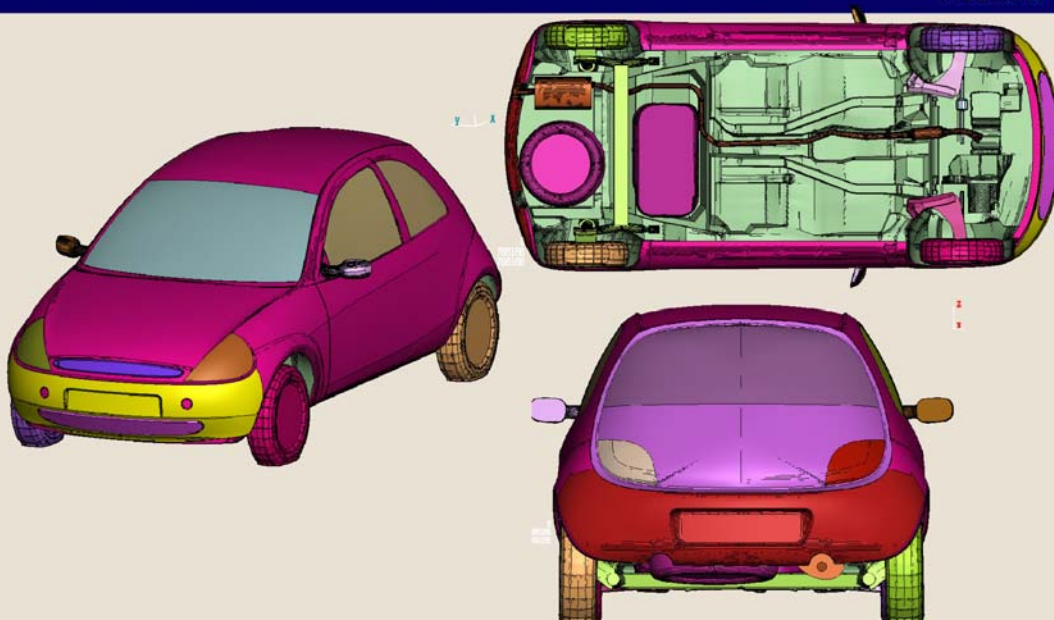
- Geometry was used for EADE Benchmark and following studies
- Detailed Underbody, Side Mirrors, Wheelhouses
- „Conventional Way“ took around 2 – 3 weeks for Surface Meshing, because a high resolution mesh with highly non-uniform element sizes was aimed
- Mesh shown in the following took around 1 hour for Meshing in ANSA v.12.0
- Quality is similar

© 2006 ANSYS, Inc. All rights reserved.

13

ANSYS, Inc. Proprietary

Ford Ka – Meshing Benchmark




© 2006 ANSYS, Inc. All rights reserved.

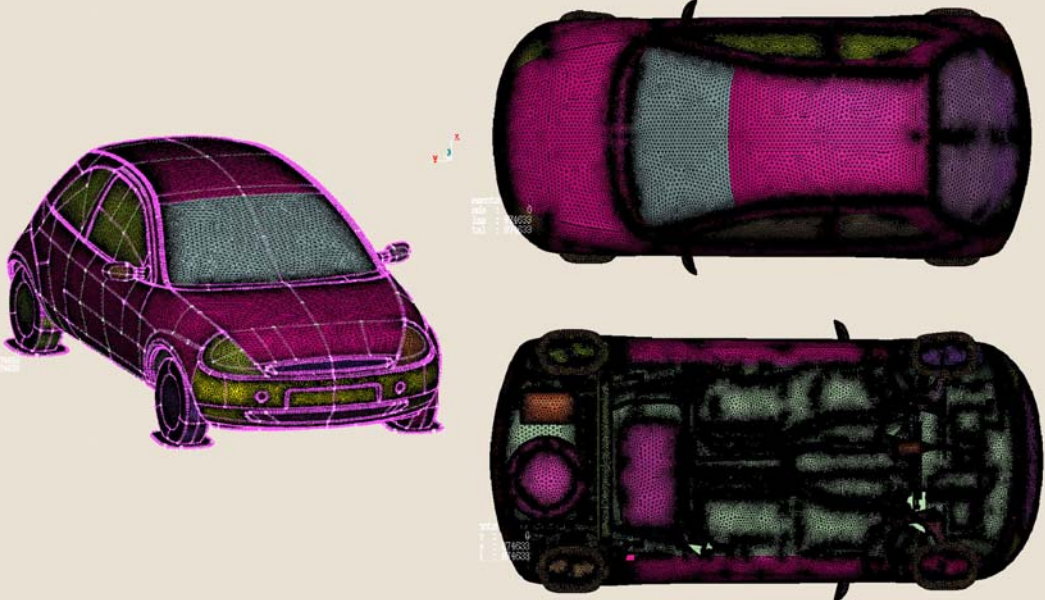
14

Courtesy of FORD Werke Köln

ANSYS, Inc. Proprietary

Ford Ka – Meshing Benchmark




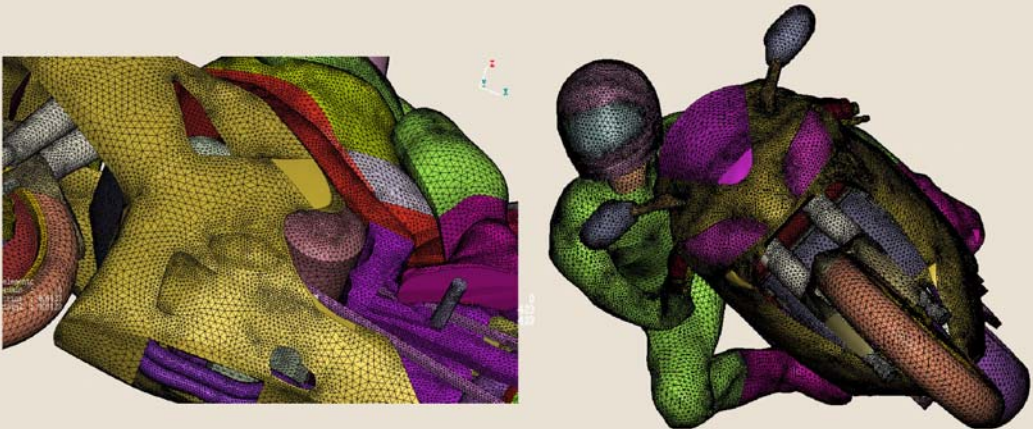


Courtesy of FORD Werke Köln

© 2006 ANSYS, Inc. All rights reserved. 15 ANSYS, Inc. Proprietary

Motorbike - Example

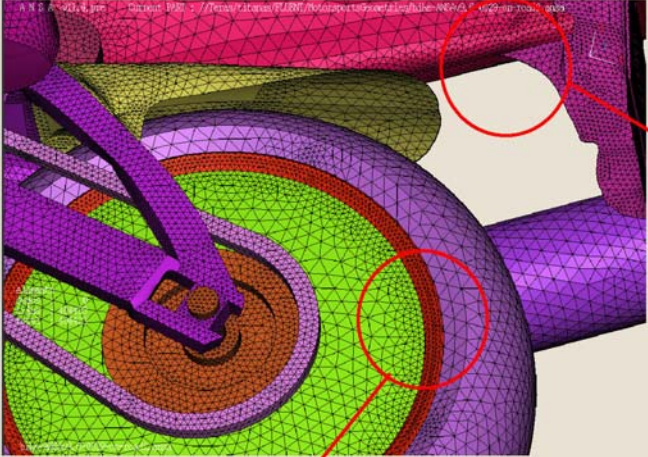





Courtesy of Advantage CFD

© 2006 ANSYS, Inc. All rights reserved. 16 ANSYS, Inc. Proprietary

Motorbike - Example




Curvature Refinement

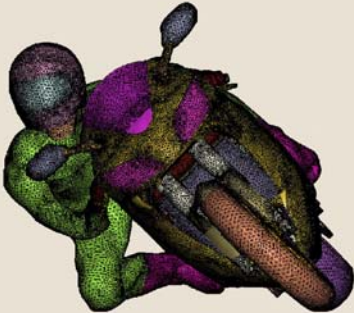
Sharp Edge Refinement

© 2006 ANSYS, Inc. All rights reserved. 17 Courtesy of Advantage CFD ANSYS, Inc. Proprietary

Agenda



- Why ANSA?
- ANSA's CFD specific tools
- Optimization using Morphing Methods
- Future demands and trends in Preprocessing for CFD

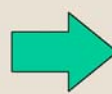
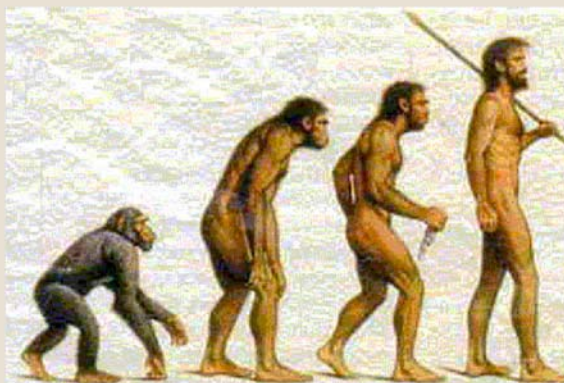


© 2006 ANSYS, Inc. All rights reserved. 18 ANSYS, Inc. Proprietary

Optimization



Improvement of specific attributes/qualities through parameter adaption and variation



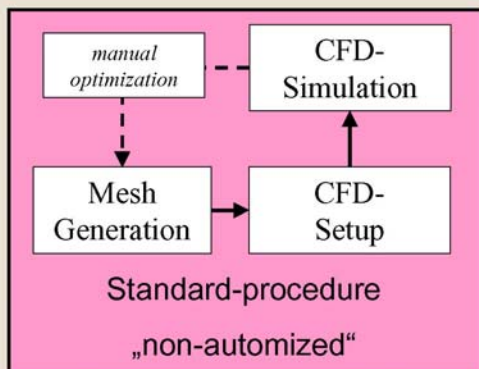
Global Optimum?

© 2006 ANSYS, Inc. All rights reserved.

19

ANSYS, Inc. Proprietary

Optimization - process

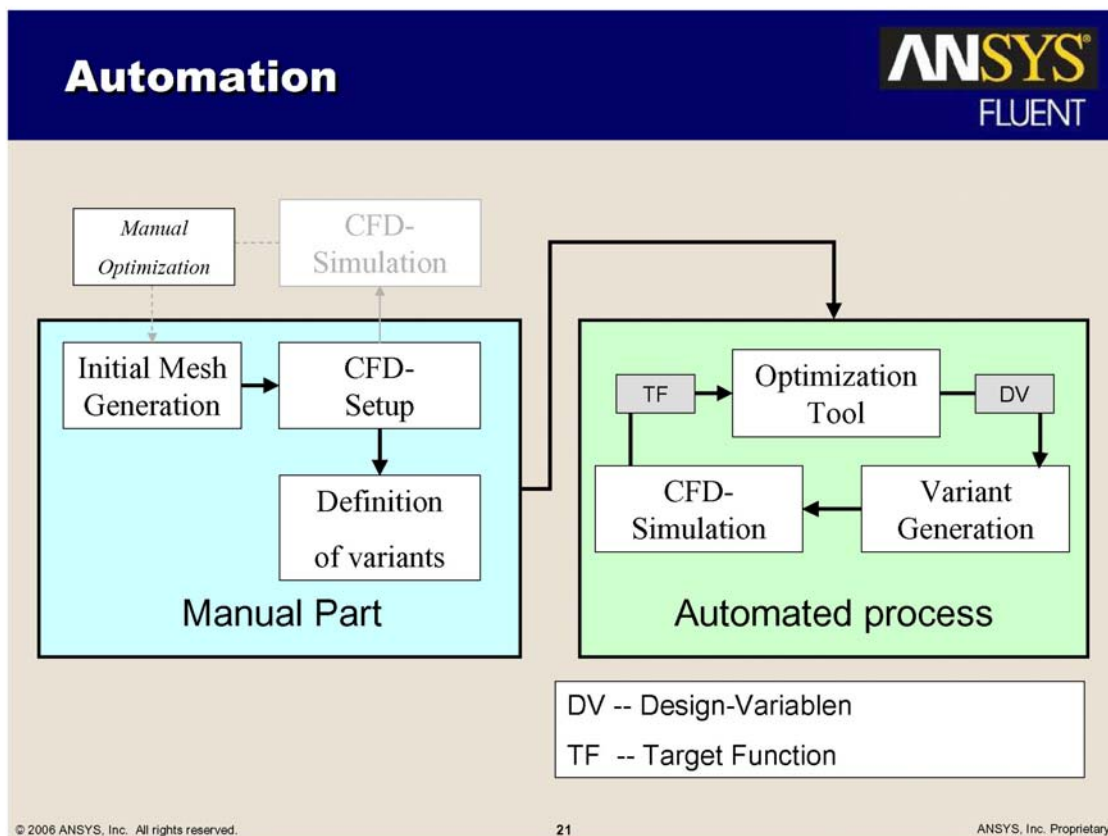


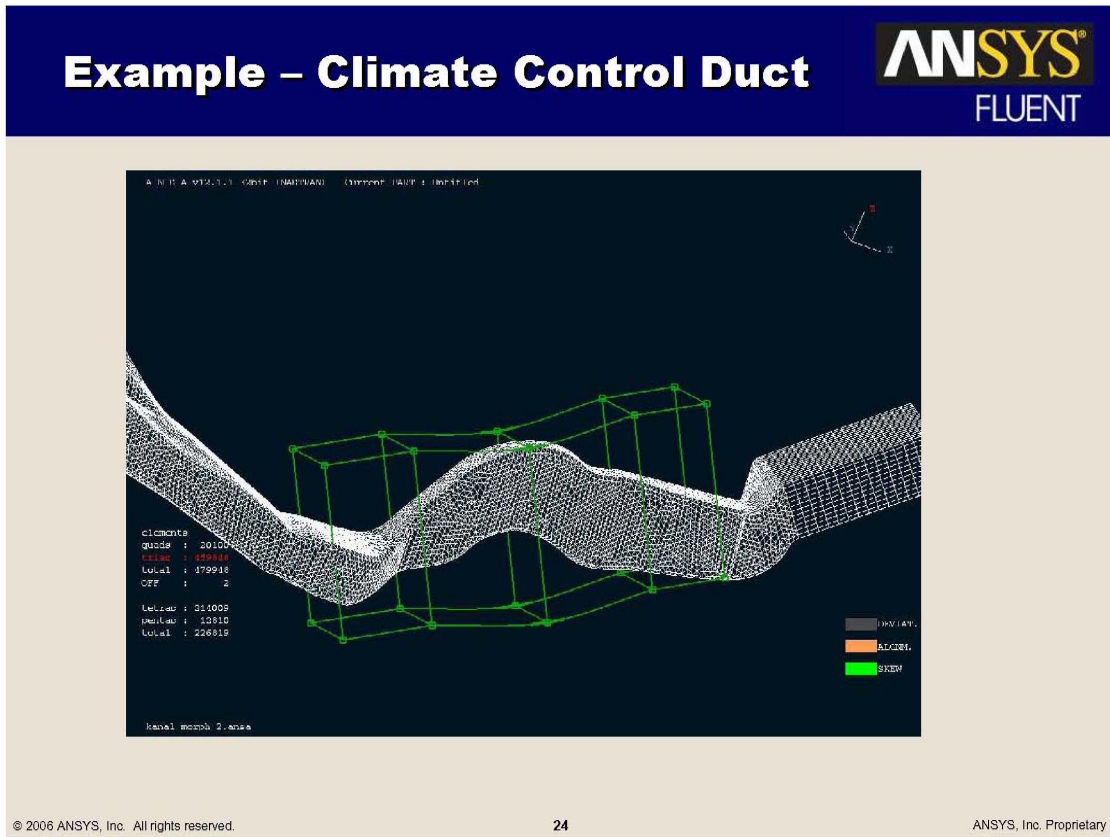
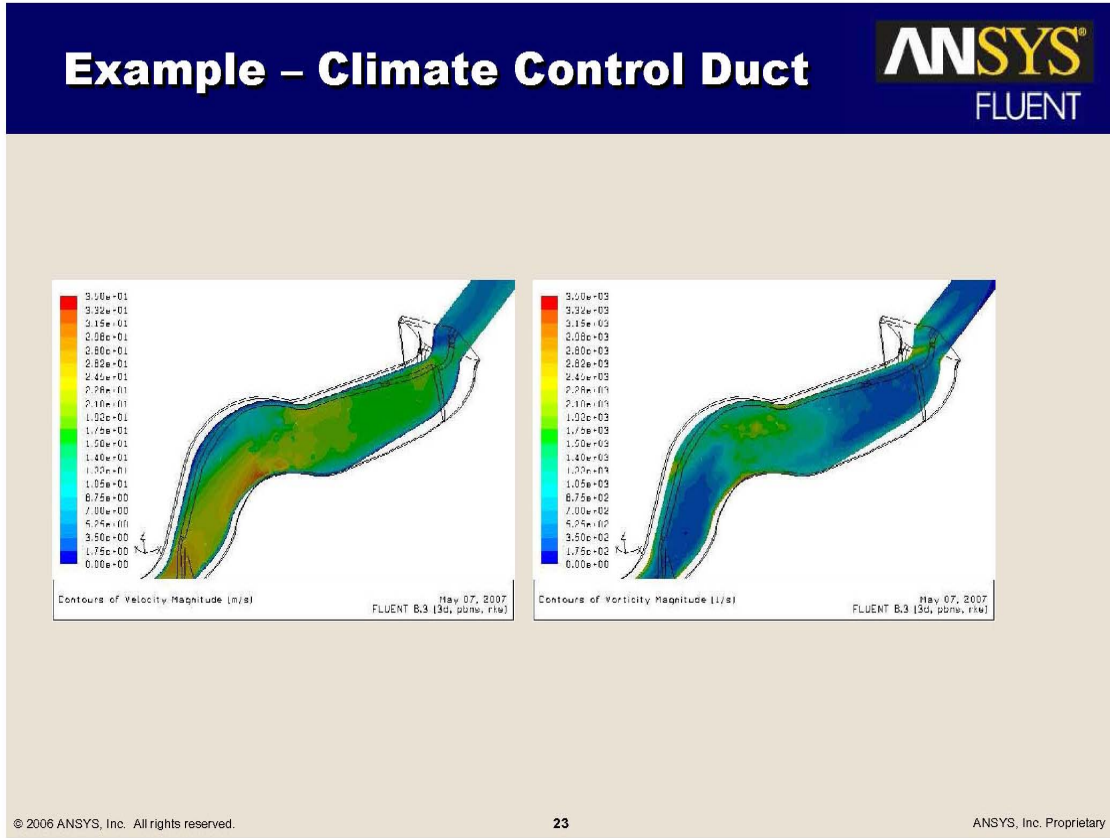
- „easy“ automizable
 - Mesh generation
 - CFD-Setup
 - CFD-Simulation
- „difficult“ automizable
 - manual optimization

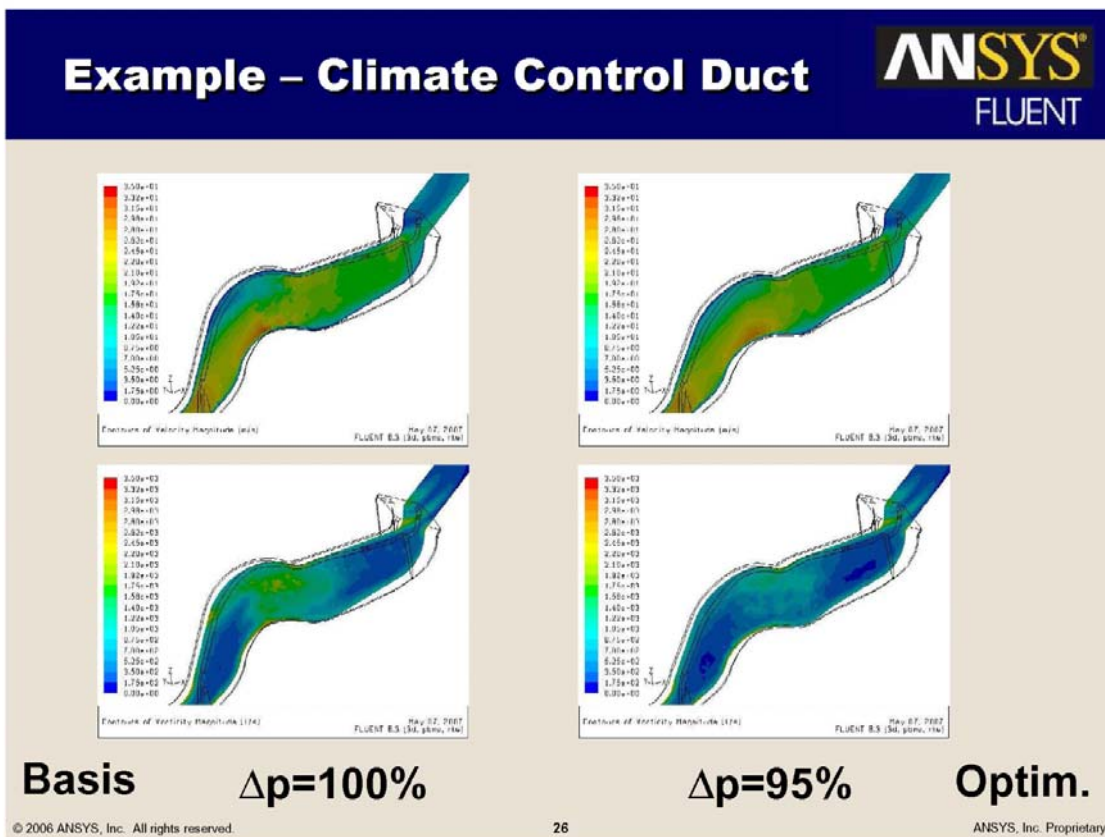
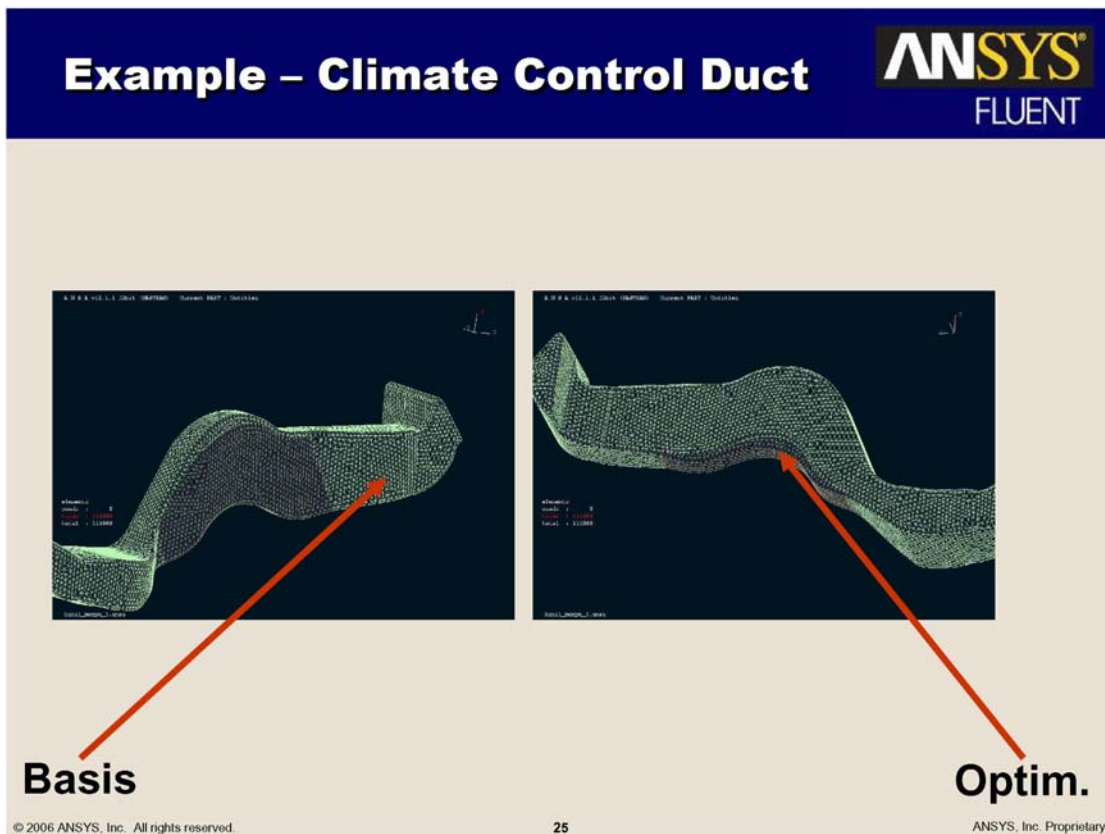
© 2006 ANSYS, Inc. All rights reserved.

20

ANSYS, Inc. Proprietary



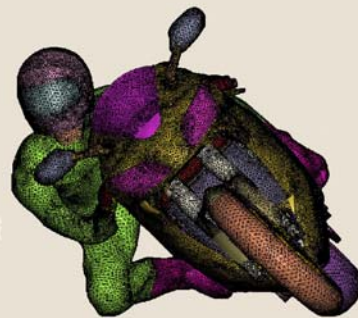




Agenda



- Why ANSA?
- ANSA's CFD specific tools
- Optimization using Morphing Methods
- Future demands and trends in Preprocessing for CFD



© 2006 ANSYS, Inc. All rights reserved.

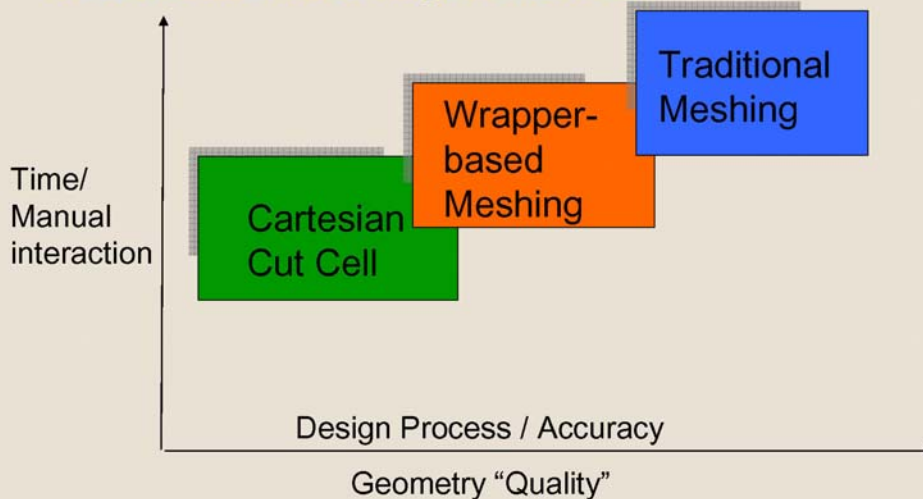
27

ANSYS, Inc. Proprietary

Trends in CFD



- Provide the right mesh for the right problem
- Reduce the meshing bottleneck



© 2006 ANSYS, Inc. All rights reserved.

28

ANSYS, Inc. Proprietary

Trends in CFD Preprocessing



- Cavity Remeshing (TGrid Prototype)
- Cut Cell Meshing (TGrid Prototype)
- Surface Wrapping (TGrid Release)
- Immersed Boundaries (Roll out during EACC 2007 in Frankfurt)

© 2006 ANSYS, Inc. All rights reserved.

29

ANSYS, Inc. Proprietary

Cavity Remesh



- Exchange (surface) parts in an existing volume mesh
- no need to re-mesh the complete domain
- Saves huge amount of time
 - 100 Mio cell mesh (Formula 1) 1h vs. 18h for volume mesh creation



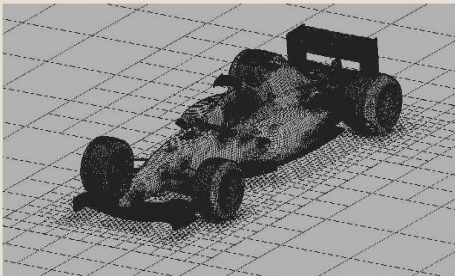
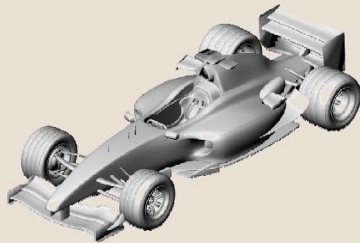
Cavity-remesh2.exe

© 2006 ANSYS, Inc. All rights reserved.

30

ANSYS, Inc. Proprietary

Cut Cell Approach



- Push button approach
- Very low turnaround time
- Sufficient accuracy
- Early design evaluation

© 2006 ANSYS, Inc. All rights reserved.

31

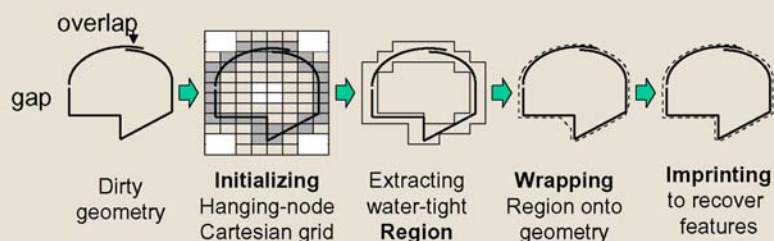
ANSYS, Inc. Proprietary

What does wrapping mean ?



- Main Entry: **1wrap**
Pronunciation: 'rap
Function: *verb*
Inflected Form(s): **wrapped; wrap·ping**
Etymology: Middle English *wrappen*
transitive senses
1 a : to cover especially by winding or folding **b** : to envelop and secure for transportation or storage : **BUNDLE** **c** : **ENFOLD**, **EMBRACE** **d** : to coil, fold, draw, or twine (as string or cloth) around something

- In TGrid 4




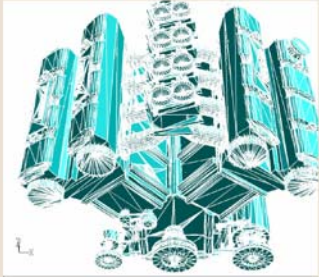
© 2006 ANSYS, Inc. All rights reserved.

32


ANSYS, Inc. Proprietary

Surface Wrapping

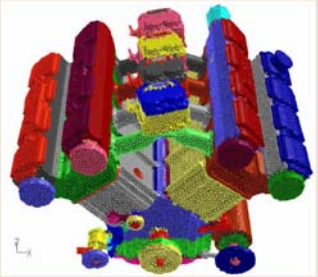




Unconnected STL

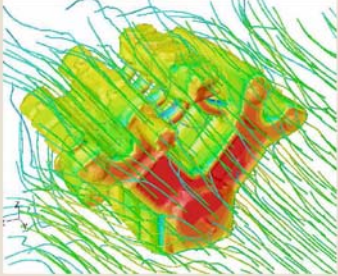


Connected STL




CFD triangular mesh

CFD solution

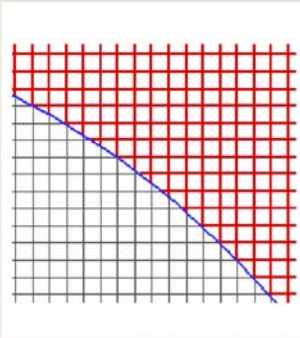


© 2006 ANSYS, Inc. All rights reserved. 33 ANSYS, Inc. Proprietary

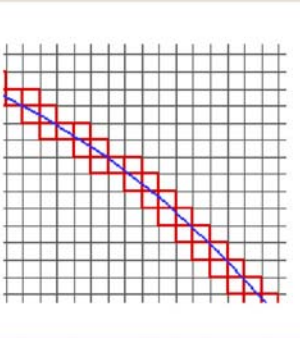
Immersed Boundary Technique



Grids **DO NOT conform** with the boundaries of the CFD domain




Cell-Cut Approach
Computational stencils are modified to use information on the boundaries.
(Direct BC)



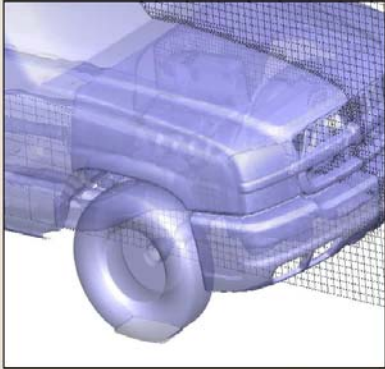
Immersed Boundary
The governing equations are modified in the cells cut by the interface by adding a source term **(Indirect BC or Forcing)**

© 2006 ANSYS, Inc. All rights reserved. 34 ANSYS, Inc. Proprietary

Start from STL Geometry




- Avoids time-consuming and error-prone CAD to CFD geometry conversion/clean-up issues
- Locally refined, high quality, Cartesian mesh is generated automatically
- Sufficient accuracy for preliminary studies

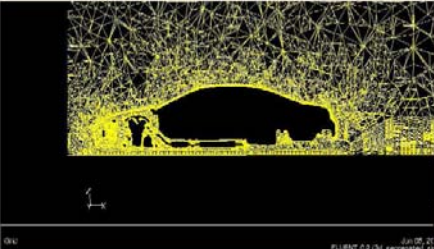

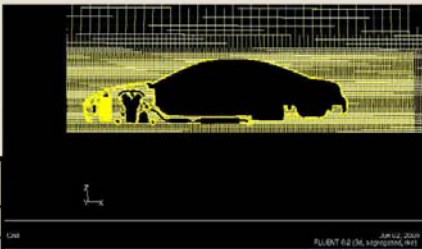


*Courtesy of
General Motors Corporation*

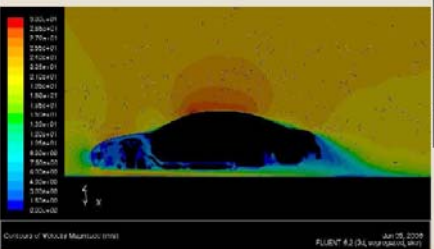
© 2006 ANSYS, Inc. All rights reserved. 35 ANSYS, Inc. Proprietary

IB Validation for a Car

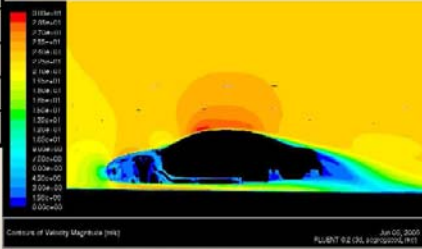


Grand-prix	Drag coefficient
Experiments	100
BF1, 7M cells	95.6
BF2, 10M cells	94.4
IB1, 12M cells	101.1
IB2, 16M cells	99.4
IB3, 17M cells	100.8

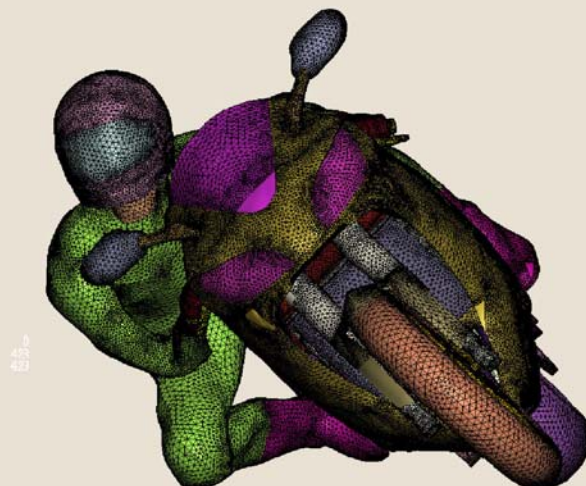


**Results Courtesy
GM**



© 2006 ANSYS, Inc. All rights reserved. 36 ANSYS, Inc. Proprietary

Thank you very much, and ... m1

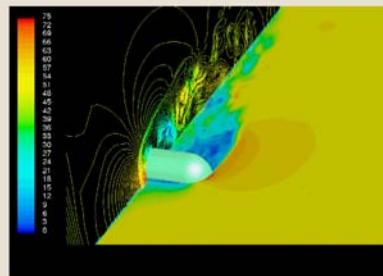
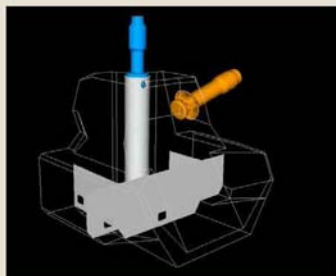
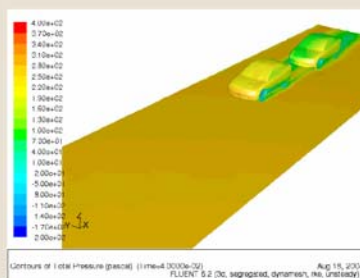


© 2006 ANSYS, Inc. All rights reserved.

37

ANSYS, Inc. Proprietary

Questions ?



© 2006 ANSYS, Inc. All rights reserved.

39

ANSYS, Inc. Proprietary

COMBINING QUALITY, PERFORMANCE & EFFICIENCY IN CFD PRE-PROCESSING

Evangelos Skaperdas*, Christos Kolovos

BETA CAE Systems S.A., Greece

KEYWORDS - CFD pre-processing, CFD best-practices, meshing, model organization, morphing

ABSTRACT - The creation of mesh models for complicated automotive applications is an increasing challenge as demands for high simulation accuracy and short time cycles are mandated by current market needs. Several steps are included in the preparation of a CFD model and some of them are quite laborious. Many advances have taken place in fully automatic pre-processing for structural applications, but the additional complexity of CFD pre-processing does not allow this yet. The best possible solution for CFD pre-processing must balance well between mesh quality, which will allow and ensure reliable simulation results, and process efficiency with respect to time of manual and automatic operations and the handling of very large amounts of data.

Accepting the fact that user intervention and actions are currently required to ensure a high quality mesh, a case study of a CFD model creation for a racing motorbike is here presented. Following all common CFD recommended practices, a complete mesh model is prepared in ANSA. An investigation of the feasibility of the generation of various mesh configurations and densities with respect to user effort is made. In particular, the geometrical complexity of the model with its multiple interconnected zero-thickness walls provides a challenge for the generation of boundary layer volume elements. In addition, the treatment of the exposed sides of the boundary layer elements with and without conformal interfaces is considered. Representative simulation results are presented and compared to available literature findings. Finally, mesh morphing is performed to examine the possibilities of reshaping and reusing the same mesh model to modify the motorbike's flow characteristics.

TECHNICAL PAPER -

1. CURRENT STATUS AND OBSTACLES IN CFD PRE-PROCESSING

The preparation of a mesh for CFD analysis of an automotive application is a complex and laborious process that used to require large amounts of man hours from experienced users and usually involved the combination of different software that are designed for specific tasks. All this, in combination with the huge model sizes that are currently necessary for realistic and accurate CFD simulations and are nowadays feasible by the available hardware resources, make the process stiff and error prone. Many advances have taken place in fully automatic pre-processing for structural applications, but the additional complexity of CFD pre-processing (mainly watertight preparation and dependency of volume mesh on surface mesh) does not allow this yet. The process usually consists of the steps shown in Table 1. Several of these steps are currently straight forward within the ANSA pre-processing environment, like for example the input of CAD data. The available CAD translators (for Catia v4 and v5, Unigraphics, ProEngineer and JT Open) offer automated and error free geometry input and diminish the need for cleanup operations. Even with traditional neutral CAD data exchange formats (IGES, STEP etc.) the powerful geometry handling capabilities of ANSA make cleanup a simple task.

Geometry Handling	<ul style="list-style-type: none"> - CAD data input - Cleanup - Outer surface extraction - Watertight creation - De-featuring - Treatment of proximities - Computational domain and sub-volume definitions
Meshing	<ul style="list-style-type: none"> - Surface meshing - Boundary layer elements generation - Volume meshing
Model Organization	<ul style="list-style-type: none"> - PDM and CFD solver specific Part Name Conventions - Boundary condition specification - Model integrity checks

Table 1: Typical steps involved in the pre-processing of a CFD model

The more complicated task of outer surface extraction is a step that can vary in difficulty depending on the data and communication with the CAD department. Standard conventions, like for example the management of Parts in different CAD layers for different use, that can be established in cooperation between the CAD and CAE people, can ensure that the CAE side gets only the information that is necessary. Still, ANSA possesses the tools that are needed for the extraction of outer flow-wetted surfaces, from thin sheet parts, as well as thick assemblies, as shown in Figure 1.

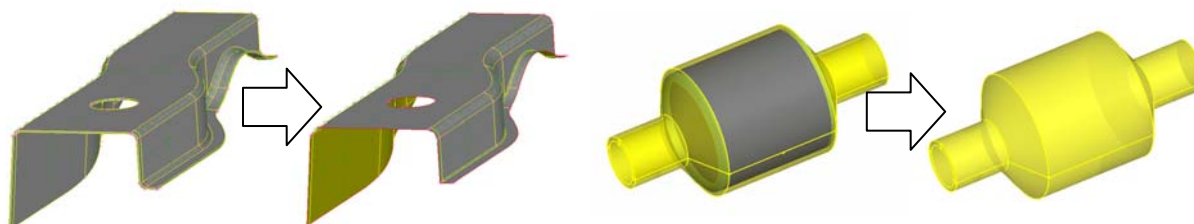


Figure 1: Extraction of outer surface examples in thin parts and thick assemblies

The creation of a watertight-model, that is a model that is fully closed for valid volume definitions, is currently the most difficult obstacle. There are many areas where sheet metal parts overlap and these need to be merged together into a single outer surface. Also there are several gaps that need to be sealed (Figure 2). Although development in the automation of these tasks is underway, for the moment this is a manual operation.

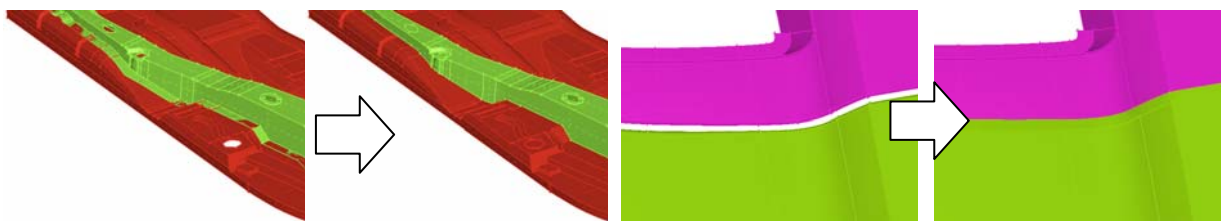


Figure 2: Generation of a watertight model: examples of overlapping flanges and gap closures

The de-featuring step (removal of small, unimportant for the flow simulation, features) is also something that can be handled easily in ANSA both in geometry and in mesh level. In the first case, the user can modify the geometry locally using the available CAD tools, while in the second the user can join macros together so that the mesh will flow over them uninterrupted. The benefit of the latter approach is that the original geometry remains unaffected and all the de-featuring can be easily undone, if so required.

In the meshing step, a mesh of variable size is usually required, fine enough in certain areas while coarser in others, so as to capture all important flow features while remain within a reasonable range of element count, which can be handled by the available hardware and time resources.

Finally, all the model preparation must be implemented with the following issue in mind. The user must be able to manage the Part information extracted from the PDM system of the company, so as to trace it back if a modification is required, but they must also account for different name conventions which are required for the CFD solver needs. A double parallel Part reference system which can combine both can be very useful.

2. QUALITY, EFFICIENCY AND PERFORMANCE IN CFD PRE-PROCESSING

Model Quality is very important as it ensures that our CFD simulation will converge easily and that our results can be trustworthy. In addition quality, not only restricted in simple terms of element quality criteria, but also as the fidelity by which we discretize the model, ensures that we are, in fact, simulating the real problem and not one that has unintentionally lost its geometrical characteristics. Quality requires user control for the geometry handling and mesh resolution for different areas and specific case. Quality also requires consistency and this is something that may not be available among different users.

Efficiency, on the other hand, is demanded by the industry which is forced to compress the time cycles of CAE studies. Therefore quality cannot come at any cost.

To achieve Efficiency the process must rely as less as possible to user interaction and leave all the tedious and heavy workload to computers. Efficiency also implies the ability that once a model is completed, a modification can be implemented without having to restart the whole process loop from the beginning. Finally, an efficient process is one that is straight forward and achieved with few resources. Exchanging data between different software to perform specific steps for which each may be specialized adds in investment costs and in extra time and storage required for the data exchange between them. Ideally one software should be able to perform all the pre-processing tasks.

Finally, Performance is also an important issue as it refers to the ability of the hardware and software to handle the huge model sizes that CFD has always required in the most demanding end of the CAE world. Although hardware performance is mounting rapidly, the burden is also spread to the software's ability to manage the data based on smart algorithms and efficient programming techniques.

Although some automated solutions are commercially available in the market, their disadvantages include lack of absolute user control when needed, mesh quality issues that may have adverse effects in solver accuracy [1], and difficulty for the user to pin point the cause when the process fails for some reason. Finally, a lack of flexibility in the reusability of the model when certain modifications are required is also an issue with these approaches.

The best possible solution for CFD pre-processing must therefore balance between mesh quality that will allow and ensure reliable simulation results, and process efficiency with respect to time of manual and automatic operations and the handling of very large amounts of data. Accepting the fact that user intervention and actions are currently required to ensure a good quality mesh we will examine how we can facilitate and streamline the mesh model build up process by providing all the necessary tools for it.

In this study we will follow the ANSA approach, which combines Quality, Efficiency and Performance, and demonstrate that a high quality mesh, satisfying CFD best practices that will ensure an accurate and valid CFD simulation, can be created without great effort and user expertise.

3. TEST CASE STUDY: MODEL OF THE YAMAHA R1 MOTORCYCLE

The model of the YAMAHA R1 motorcycle was kindly provided by Advantage CFD for this study (Figure 4). The model was selected for the following reasons: it is characterized by several geometrical complexities, proximities and multiple inter-connected zero-thickness walls, which pose problems in the definitions of the volumes and also make the generation of boundary layers quite a difficult task. In addition, the model has relatively small dimensions, which means that for the same mesh resolutions used in typical current external aerodynamics simulations for cars, we end up with moderate mesh sizes with which we can run simulations and derive conclusions very fast. Some basic dimensions of this model include a wheelbase of 1.42 m, and a frontal area of 0.645 m² and 0.493 m² with and without the rider respectively.

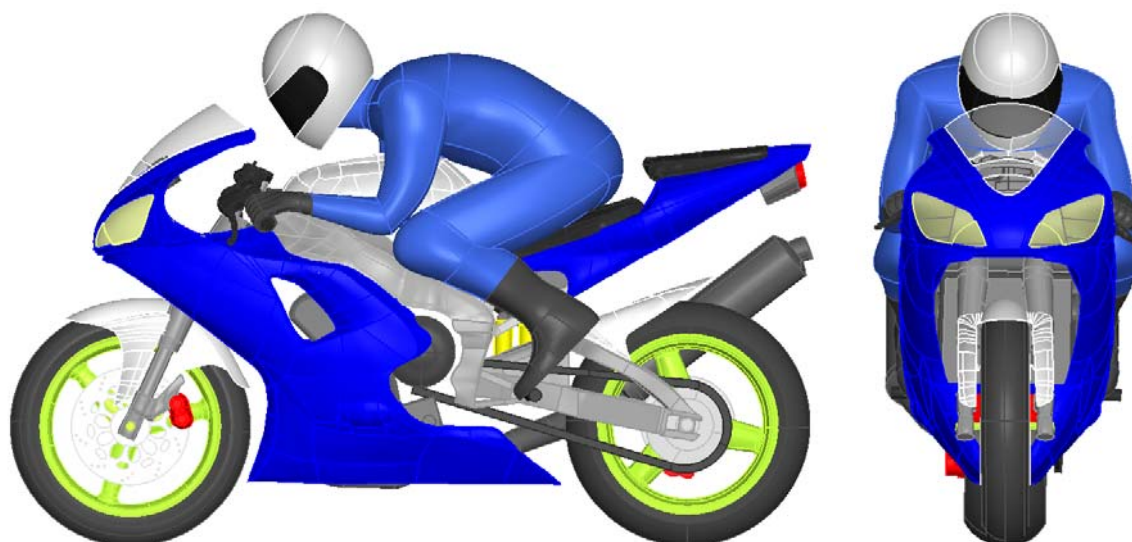


Figure 3: Geometry model of YAMAHA R1 (model courtesy of Advantage CFD)

Past work related to this was retrieved from the literature and includes the work of Piazza et al. [2] on a motorcycle without a rider, and Lewis et al. [3] on the same model. This current work focuses more on the mesh model preparation process and its impact on the simulation results, and goes a step beyond with respect to the generation of layers from all the complicated areas and the zero-thickness walls.

The commercial ANSA version 12.1.2 was used, with the exception of the generation of the layers from the zero-thickness walls, where the currently under development ANSA v12.2pre was used. All CFD simulations were performed with Fluent v6.3.26. The platforms involved were Windows XP Professional 64bit with P4 3.6GHz and XEON 2.66GHz processors and Linux Fedora Core 6 with AMD Athlon Dual Core 2.8GHz.

3.1 MODEL PREPARATION

The steps that were followed for the preparation of the CFD model are described below. The model was provided in ANSA database format so there were no translation or cleanup issues.

Computational Domain

A computational domain was constructed spanning 20 body lengths downstream, and 10 upstream as well as in the two lateral directions, as shown in Figure 4. This results in a very small blockage area ratio of 0.16 %, so the simulation refers to an open road test case.

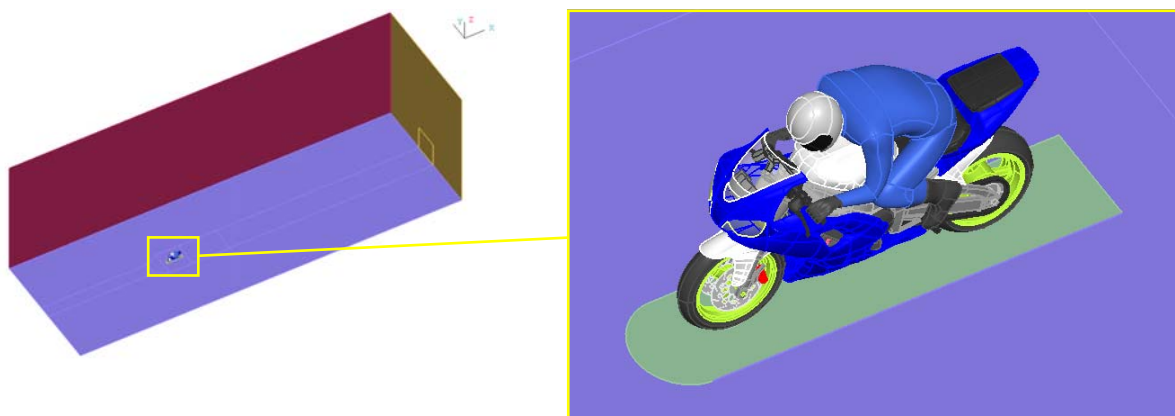


Figure 4: Computational domain and close up of motorcycle and rider model

Treatment Of Proximities In Geometry Level

Complicated automotive CFD models have several areas that suffer from narrow proximity problems. These usually result in bad tetra elements, or make the growth of layers impossible. The treatment of proximities in geometry level is something that can be treated efficiently in ANSA using the proximity detection algorithms and the “fuse” functionality. ANSA can isolate the Faces that are close together within a specified range and then, depending on the case, the user can employ the “fuse” function and either completely remove the enclosed space (Fig.5 left) or place it in a separate volume (Fig. 5 right) like for example the area around the wheel contact patch, which regardless if layers are grown or not, it is best to be volume-meshed separately. This allows the user to better prepare the surface mesh in that area.

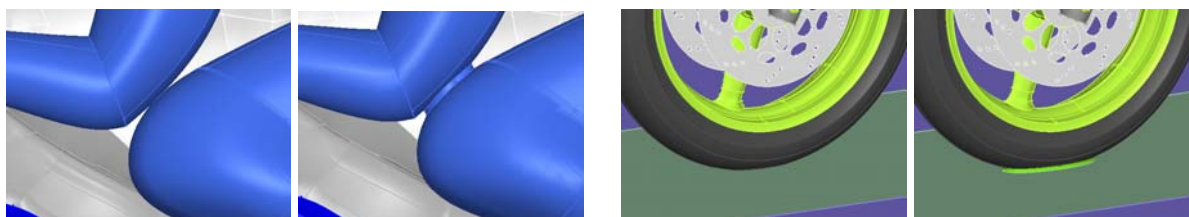


Figure 5: Treatment of proximities in geometry level using the “fuse” functionality

Definition Of Sub-Volumes And Management Of Parts And Properties

For the proper specification of the boundary conditions for the rotating wheels and the pressure drop of the radiator, separate sub volumes were constructed.

The creation of the Interior faces that enclose the sub-volumes inside the wheel and around the spokes area were carefully constructed to enclose only the proper volume, but also to avoid proximity with the disc brakes and to accommodate for the generation of the layers from both sides by being placed at a suitable normal angle from the wheel surfaces, as shown in Figure 6.

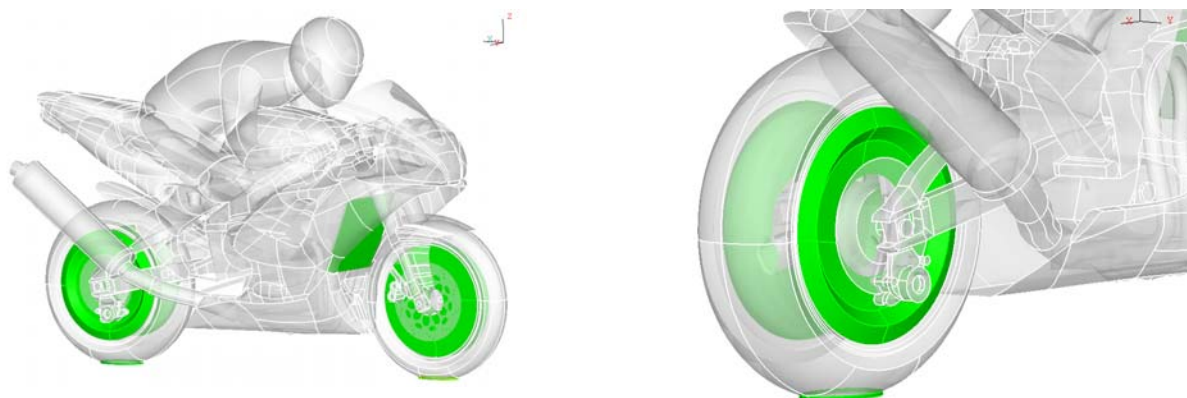


Figure 6: Definition of sub-volumes (shown in light green) for proper specification of boundary conditions in the solver.

To be able to handle this model, and other more complicated CFD models, the user must come up with a suitable part name convention, which will allow the simple management of the model for boundary condition specification in the solver as well as for post processing. Usually some parts are merged together so as to have fewer in the solver. However this leads to loss of Part reference information in the simulation,

The double and parallel Property (PID) and Part management system available in ANSA (Fig. 7) allows the user to keep the original Part Name, ID and hierarchy as extracted from the company's PDM system, while use a Part grouping and name convention suitable for the CFD solver, where for example they can give Properties name special prefixes so that they can quickly identify them within the solver environment. The ANSA Part Manager can also be used to manage the additional geometry that is created for the simulation, like the interior and computational domain boundary surfaces, as well as some points and curves that have information of the axes of rotation of the wheels for example.

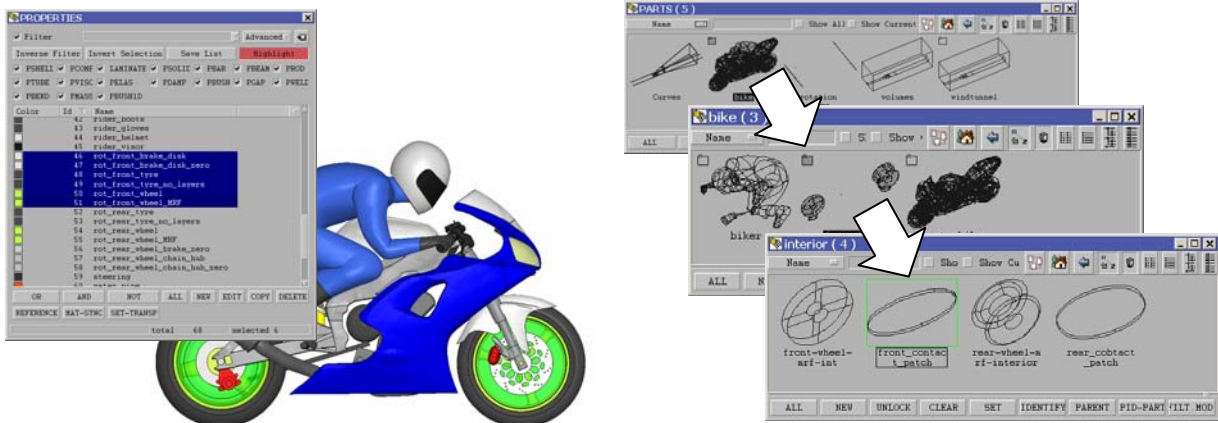


Figure 7: Model management through double name convention system: Property Names for CFD solver needs (left) and Part Manager (right).

Detection Of Zero Thickness Walls

The presence of zero-thickness walls in a model reduces the mesh size but adds complexity in the definition of boundary layers and volumes. The user cannot identify these parts by name, as there is no such information from CAD. In addition, the zero-thickness simplification may be done during the pre-processing step of geometry de-featuring, and some Parts may be half zero-thickness wall and half solid description. The identification of these areas and separation in different Property must be made.

The functionality of Volume Detection in ANSA is of great assistance in this case. The user can let ANSA detect all closed volumes in the model and then by removing these volumes from visible, only the zero thickness surfaces remain (see Fig. 8). These can be easily placed to separate PIDs with the same name plus a suffix like `_zero_thickness`. This will be very useful later when layers will be grown from these areas with the extra option to grow from both sides.

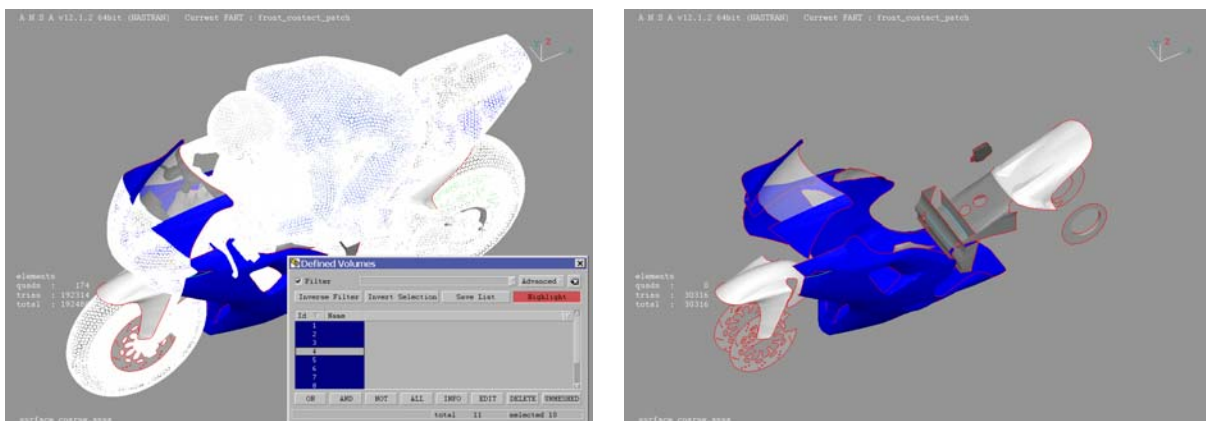


Figure 8: Detection and separation of zero-thickness wall surfaces for placement in separate PIDs

Assignment Of Boundary Condition Types

Having distributed and assigned the correct property names to all the parts, the user can also specify the boundary condition types for the Fluent solver (Fig. 9), so that the mesh can be read directly into the solver, with all the required information.

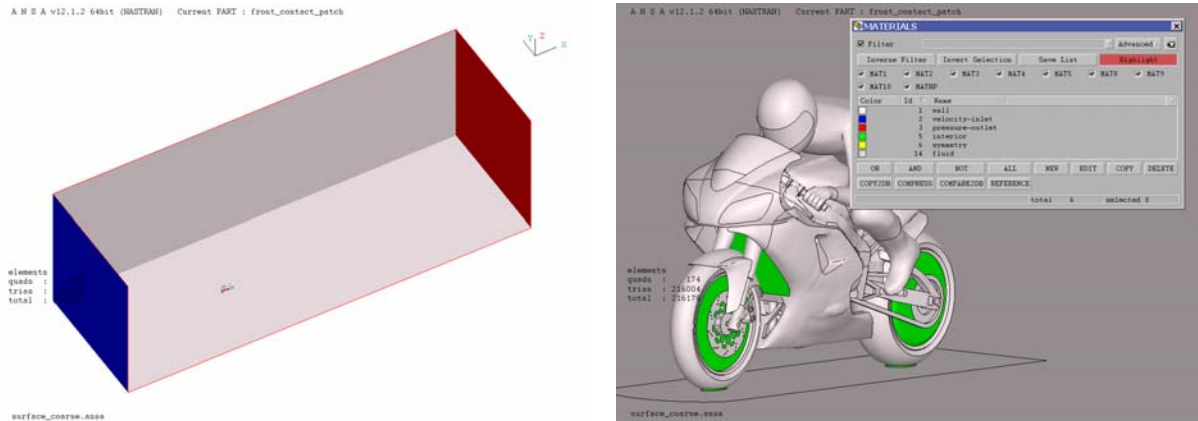


Figure 9: Definition of boundary condition types

Surface Meshing

The surface meshing step is very straight forward. Two surface meshes were generated. A coarse one, with more or less uniform element length, and a fine one, with size variation and refinement of all important areas.

The coarse mesh consists of 182 thousand surface elements (Fig. 10). It was prepared in around 15 min. This time also includes the fixing of some bad surfaces in the model and the quality improvement. Quality according to Fluent EquiArea skewness was kept below 0.5.

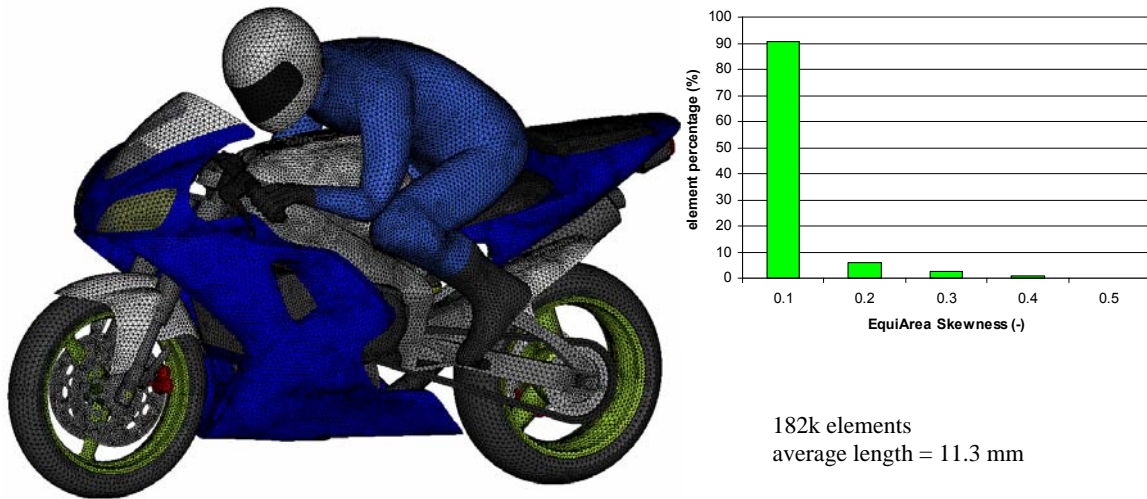


Figure 10: Coarse surface mesh

When a coarse mesh is used there may be some problems of proximity which were not considered initially at the geometry level, but arise now due to the large element length in these areas. ANSA functionality of proximity detection according to local element length and automatic refinement was employed to fix problems like the one shown in Figure 11.

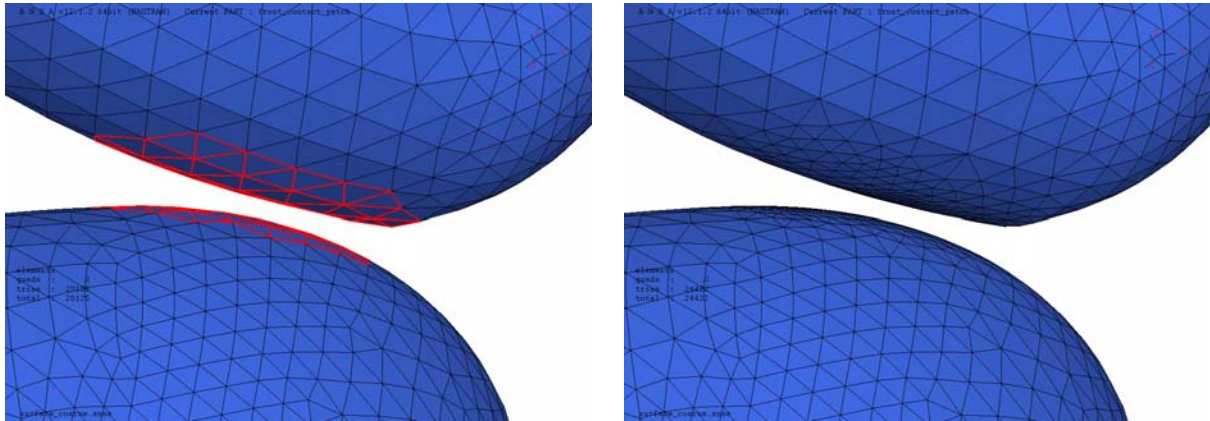


Figure 11: Treatment of proximities by automatic mesh refinement

The fine mesh consists of 544 thousand surface elements (Fig. 12). In this case the CFD spacing and meshing algorithm of ANSA was used. This allows the user to just specify a feature angle for the mesh, a growth rate, a minimum and a maximum length and ANSA meshes and refines automatically all the curvatures accordingly. In addition, the user can select to refine all sharp edges of the model where usually high gradients in the flow appear, down to a specific element length. Finally, using ANSA scripting all single and triple connectivity edges of the model, like the trailing edges of the zero-thickness walls were also automatically refined to a user specified value. This resulted in better mesh quality especially when the layers were grown, as the exposed quad facets at the free single boundaries were of good aspect ratio.

Mesh preparation and quality improvement was in this case even less than for the coarse mesh, as the smaller the minimum length, the fewer the elements and areas that needed improvement. With minimum manual work a high quality mesh was obtained. Fluent skewness was again below 0.5.

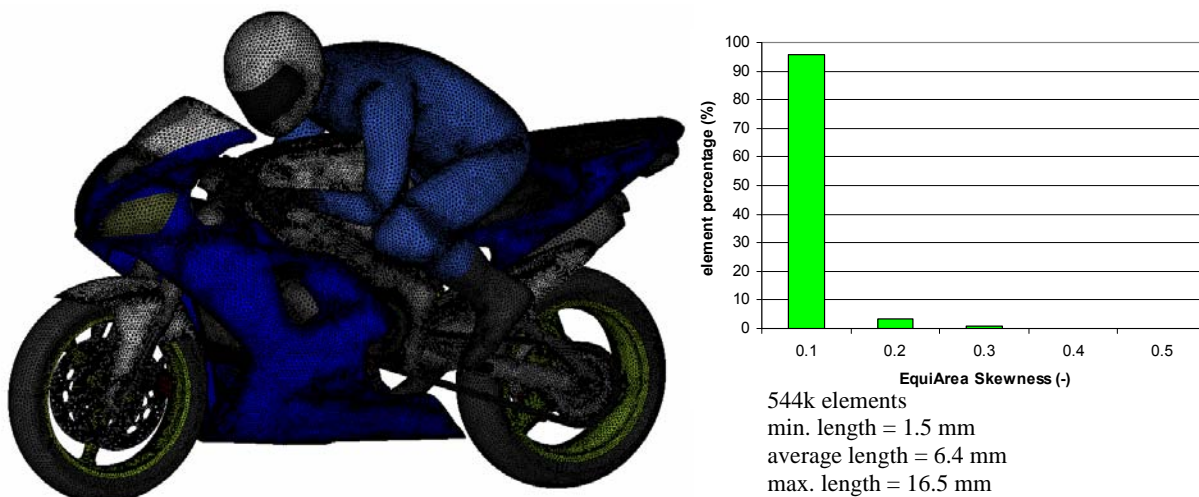


Figure 12: Fine surface mesh close ups

Meshing Of Small Sub Volumes

Having completed the surface mesh, the five sub-volumes that were constructed earlier (radiator, rotating volumes in wheels and volumes around contact patches) were meshed. The volumes around the contact patches were the ones with the worst elements, due to the very steep angle between the tyre and the road. Some manual fix was required there to ensure that Fluent EquiVolume skewness was kept below 0.95. The radiator was meshed with pentas.

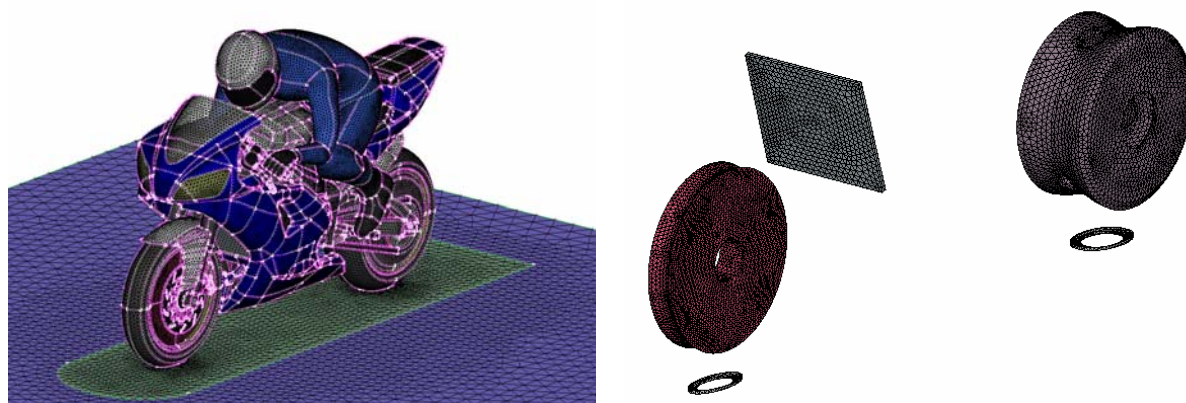
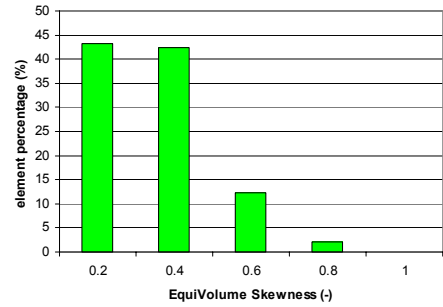
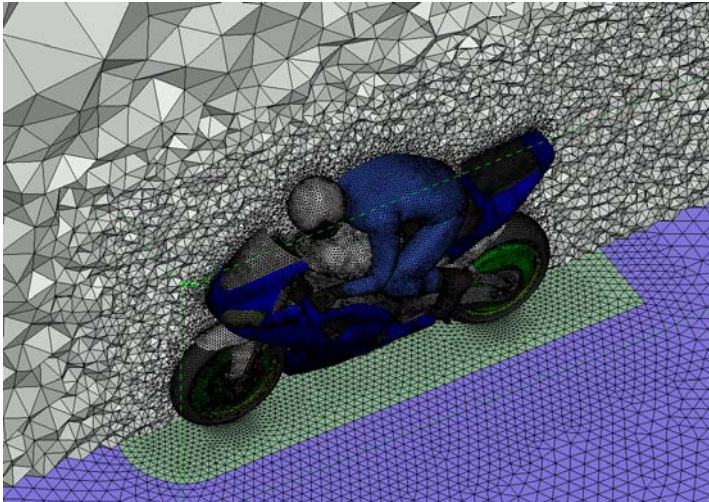


Figure 13: Volume meshing of small sub-volumes

Volume Meshing Of Main Domain

Based on the two surface meshes, three volume meshes (tetra coarse and fine and Hexa-Interior coarse) were created initially, without boundary layer elements, as shown in Figure 14. Time for volume meshing was between 5 to 15 minutes depending on the size of the mesh (from 3 to around 10 million elements). Refinement boxes were also placed to control the size of the elements around and downstream of the motorcycle.



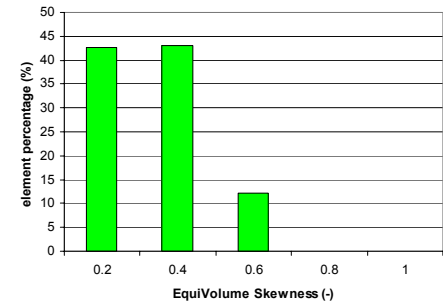
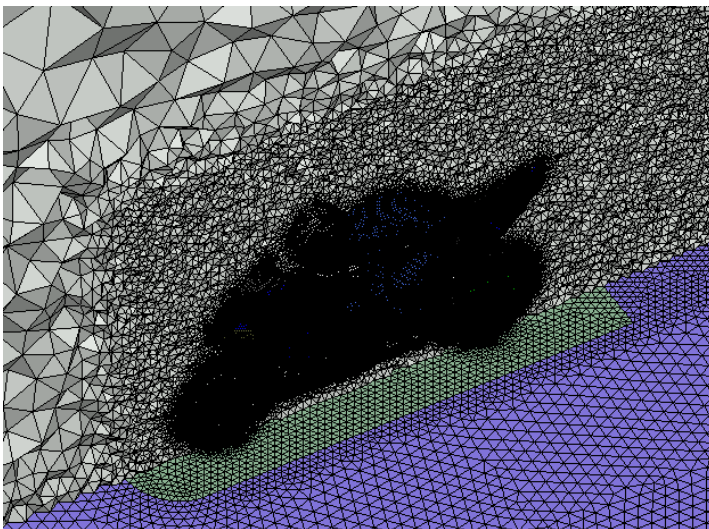
coarse tetra mesh 3.1 million

Refinement boxes:

Around bike max length = 50 mm

Along wake max length = 500 mm

Max tetra size = 1000 mm



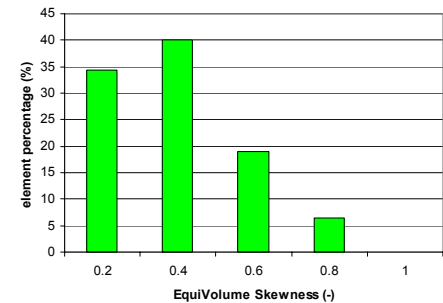
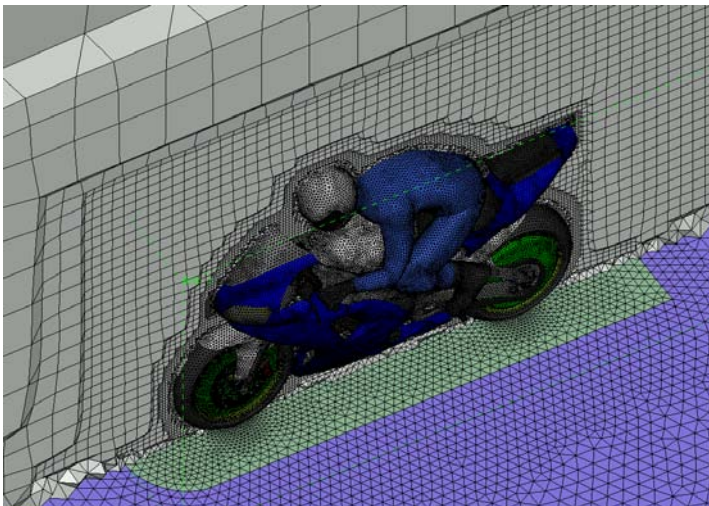
fine tetra mesh 9.8 million

Refinement boxes:

Around bike max length = 40 mm

Along wake max length = 250 mm

Max tetra size = 1000 mm



fine tetra mesh 3.2 million

Refinement boxes:

Around bike max length = 60 mm

Along wake max length = 500 mm

Max tetra size = 1000 mm

Figure 14: Volume meshes without layers

Volume Meshing With Boundary Layer Elements

To test the ability of ANSA v12.2pre under development version, boundary layer elements were generated from the coarse surface mesh. The advanced algorithm for the generation of layers lets the user to select the areas to grow layers from, with different parameters if required, and possesses clever algorithms that allow the automatic exclusion of certain areas that would result to the generation of bad quality elements or even intersections. Squeezing of layers is also available to avoid collisions and proximities. ANSA creates temporary shell elements in the excluded areas (shown in yellow in Fig 15) and thus does not modify the Properties of the original surface mesh. Five layers with growth rate 1.2 and first height 0.2 aspect were generated from all surfaces of the motorcycle and the rider. The layers were placed for demonstration purposes here in two different volume properties for the regular and the zero-thickness areas (red and purple respectively in Fig. 15).

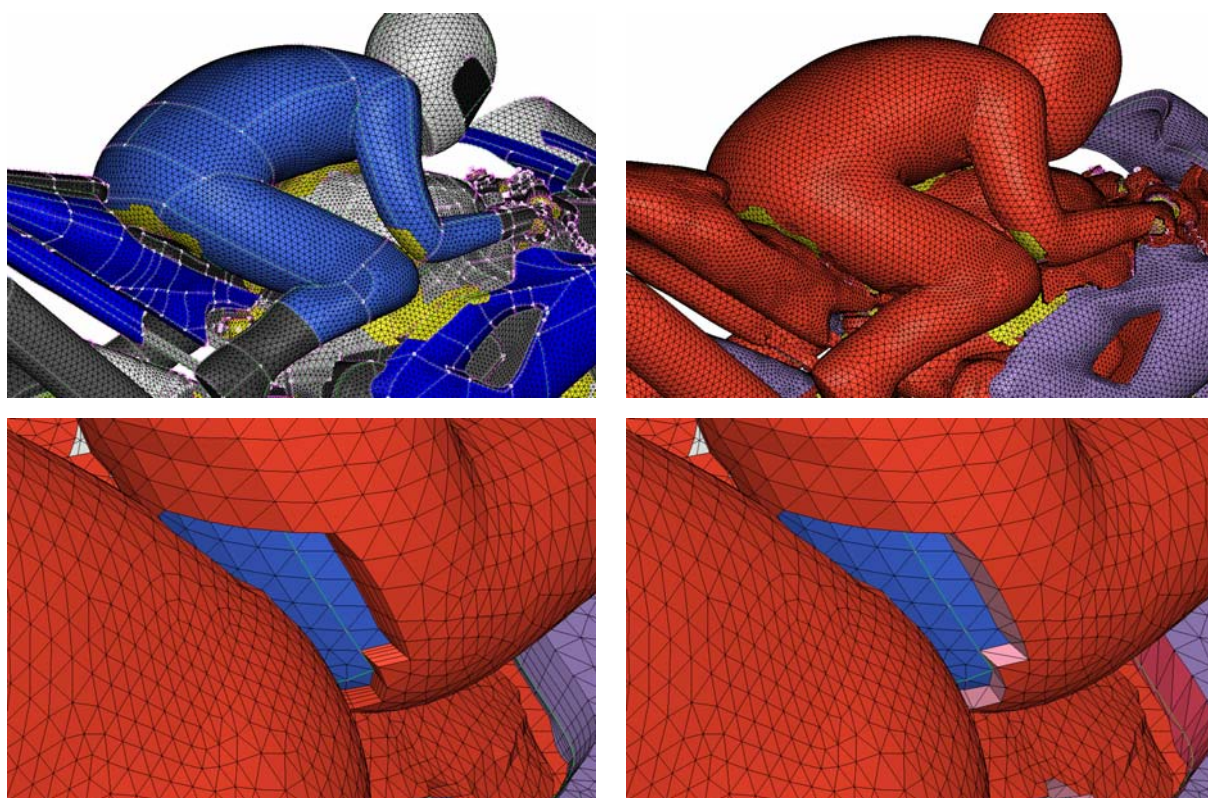


Figure 15: Generation of layers and excluded areas treatment

The exposed sides of the layers along the single boundaries or around the excluded areas are automatically treated in two ways: conformal quad facets or triangular non-conformal interfaces (Fig. 15). The definition of the outer remaining volume is a straight forward task as name conventions that are used to facilitate the isolation of the created shells that cover the layers. A volume mesh was then created consisting of 3.8 million elements (pentas and tetras). Note that for this model the layers were grown first from inside the rotating wheel sub-volumes and then from the outer main volume and were auto-connected to the interior boundary. Again for demonstration purposes the layers and the tetra mesh were placed in different properties, although for the actual simulation they were all merged in one.

Only the non-conformal approach was followed for the layer sides, as the generation of pyramids lead to bad elements. This subject is something that will be examined further to access the possibilities and the required development. Details of the model are shown in Figure 16.

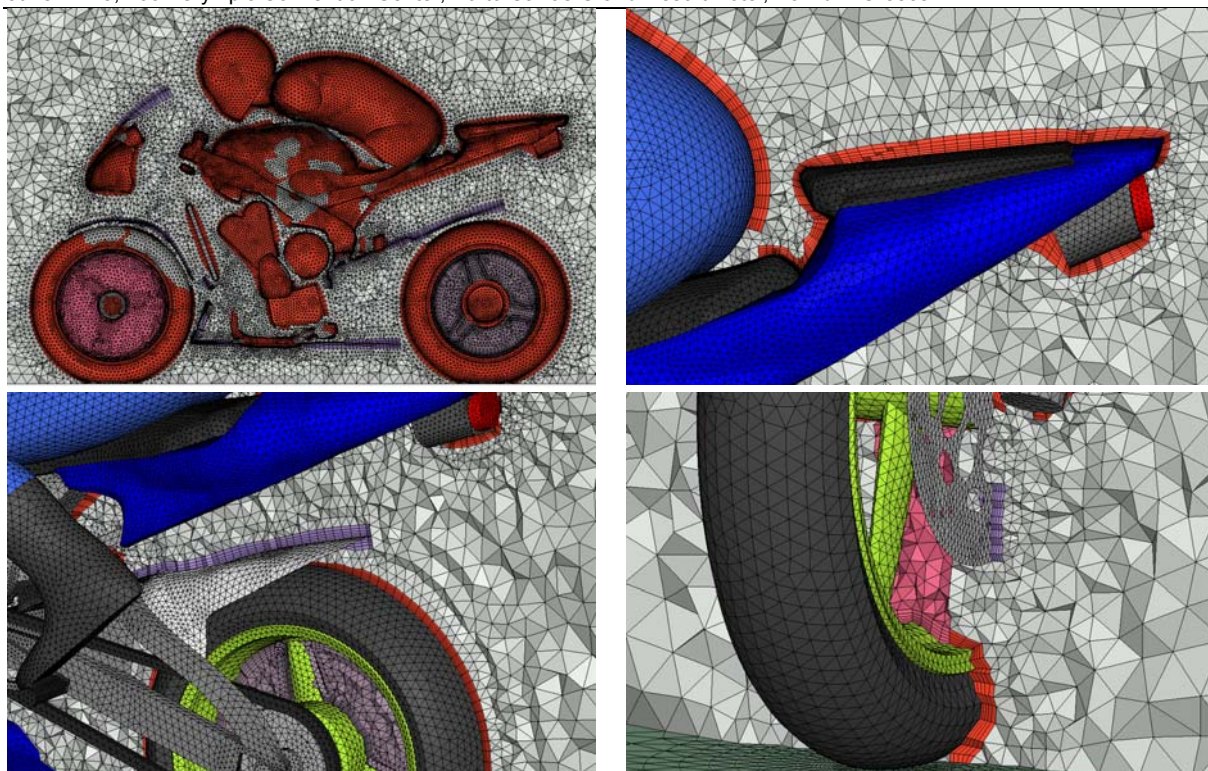


Figure 16: Details of the model with layers (3.8 million elements)

3.2 MORPHING THE COMPLETE MODEL

Having completed the models, the ANSA Morphing tool was used to make a modification of the front windscreen. The morphing boxes were constructed on the surface mesh model. The preparation time was less than 15 minutes. The boxes are snapped on the actual geometry of the model so that absolute control on all movements and deformations is available. The boxes extend outward by a considerable distance, thus allowing the mesh deformation to be distributed to more volume elements (Fig. 17). The morphing boxes were placed in a separate Part in the Part Manager so that they can be saved separately and later merged to the database with the complete volume mesh model, in this case the coarse tetra mesh model of 3.1 million elements. Then morphing is applied on both surface and volume.

The high quality of the volume mesh allowed the deformation of the front windscreen upwards by 70mm without deteriorating the mesh quality (skewness below 0.95). The morphing process is instantaneous and as many variants as required can be quickly output. The process can be also be parameterized and automated.

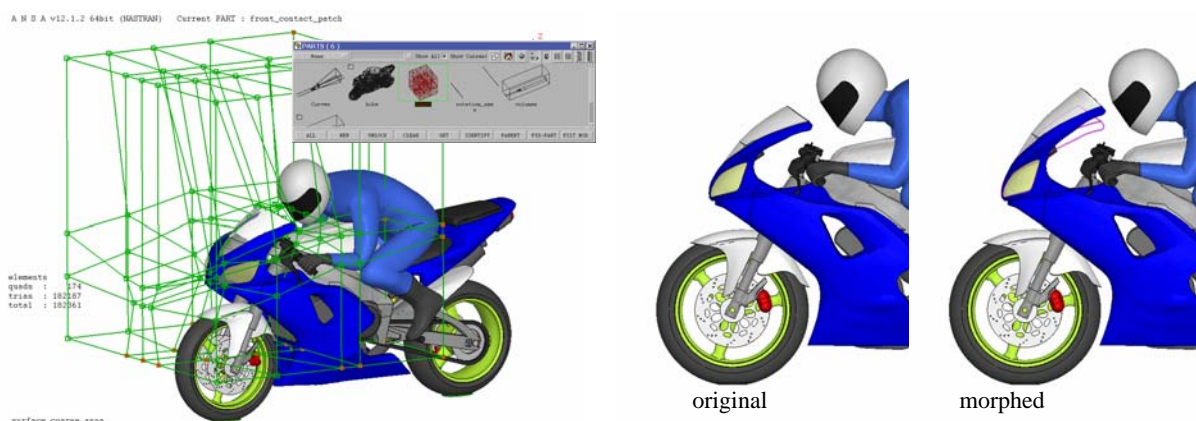


Figure 17: Morphing box setup and applied deformation of the front windscreen by 70 mm upwards.

3.3 SETUP OF THE CFD SIMULATION

The simulations were setup according to the best practices recommended by Fluent [4]. For simplification, steady state simulations were run. The $k-\epsilon$ realizable turbulence model was employed with non-equilibrium wall functions at the walls. A free stream velocity of 40 m/sec with 0.05% turbulence intensity and a turbulent viscosity ratio of 1 were applied. Translational velocity of 40 m/sec was also imposed on the road. The MRF model was used for the rotating wheel sub-volumes and rotational speeds for the wheels, tyres and disc brakes were applied. Symmetry conditions were used for the top and side boundaries. The porous model was used for the radiator with pressure drop calibration data from [5]. Fifty iterations were initially performed with first order discretization schemes for all variables and then 950 more with second order scheme.

Residuals and drag coefficient were monitored for all four cases. Figure 18 shows the smooth residual drop, indicating the quality of the model and the simulation setup.

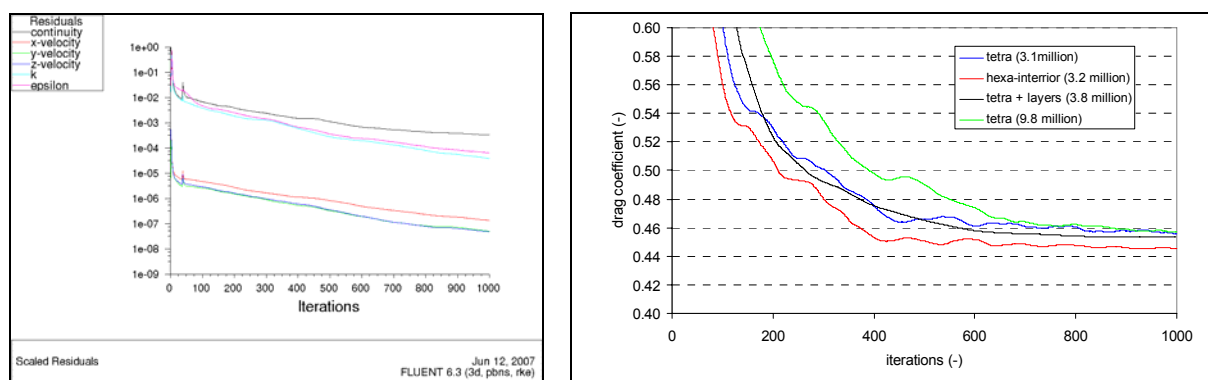


Figure 18: Representative residuals plots (for coarse tetra mesh case) and drag coefficient convergence history for the four different mesh configurations

3.4 COMPARISON OF RESULTS FROM DIFFERENT MESHES

Figure 18 shows that all four different mesh models converged to very similar drag coefficient predictions. Table 2 displays the drag coefficient and its two components, pressure and viscous drag, as well as the lift coefficient. The viscous contribution is around 5% of the total drag, which is expected as the rear wake of the model dominates. Lift is about 20% of the drag.

The two plain tetra meshes are in full agreement indicating mesh independent solution with respect to mesh refinement. The tetra plus layers and the hexa-interior meshes are also very close.

	C_D pressure	C_D viscous	C_D total	C_L total
tetra (3.1 million)	0.435	0.022	0.457	0.098
tetra (9.4 million)	0.434	0.024	0.458	0.105
tetra + layers (3.8 million)	0.430	0.023	0.453	0.093
hexa interior (3.2 million)	0.424	0.022	0.445	0.101

Table 2: Simulation results for four different meshes

Unfortunately, there are no experimental data for the exact motorcycle and the mesh models are not enough to draw exact conclusion as to which one is the most accurate, as some features that may gain in accuracy like the presence of layers and a fine mesh in the wake are not both present in one model.

Figure 19 shows velocity contours along the centre plane for the fine tetra and for the coarse tetra plus layers models. The fine tetra mesh has better refinement in the wake and shows better resolution of the flow in that area (especially close to the road), while the coarse tetra mesh with layers shows some low velocity areas downstream of the helmet and the rider's back which are not shown in the plain tetra mesh.

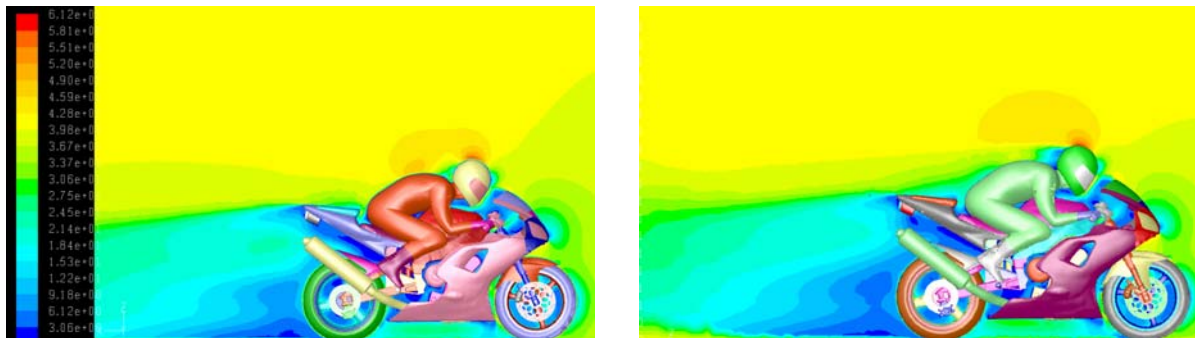


Figure 19: Velocity contours for fine tetra mesh (left) and coarse tetra mesh plus layers (left).

Figure 20 shows the y^+ contours on the surface for the tetra coarse and the tetra coarse plus layers. It is clear the the model with the layers is more suitable for the application of the non equilibrium wall functions and the boundary layer flow is better resolved.

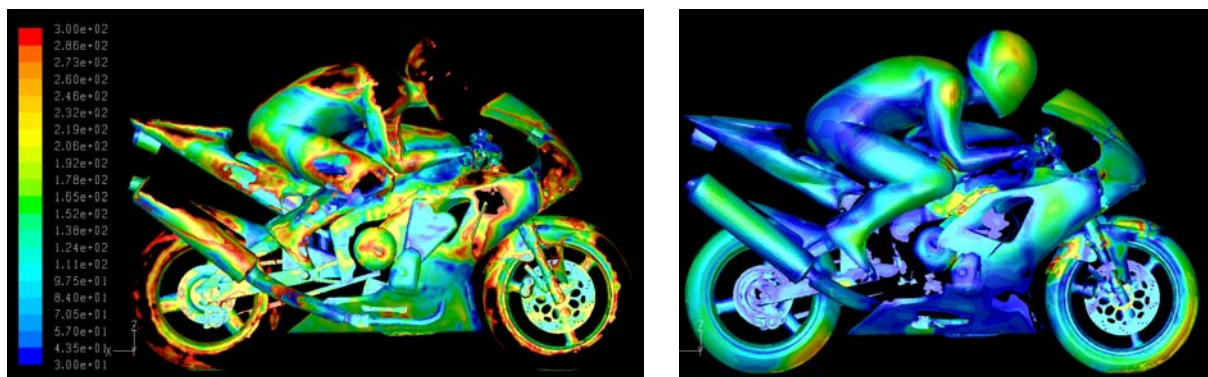


Figure 20: y^+ contours in the range of 30 to 300 for the coarse tetra mesh (left) and the coarse tetra mesh plus layers (right).

Figure 21 displays the velocity vectors at the centre plane and clearly shows that the plain tetra mesh cannot predict the separation that the tetra plus layers model can, near the top of the helmet. The fine tetra mesh did not either predict the separation, and gave exactly the same results as the coarse tetra.

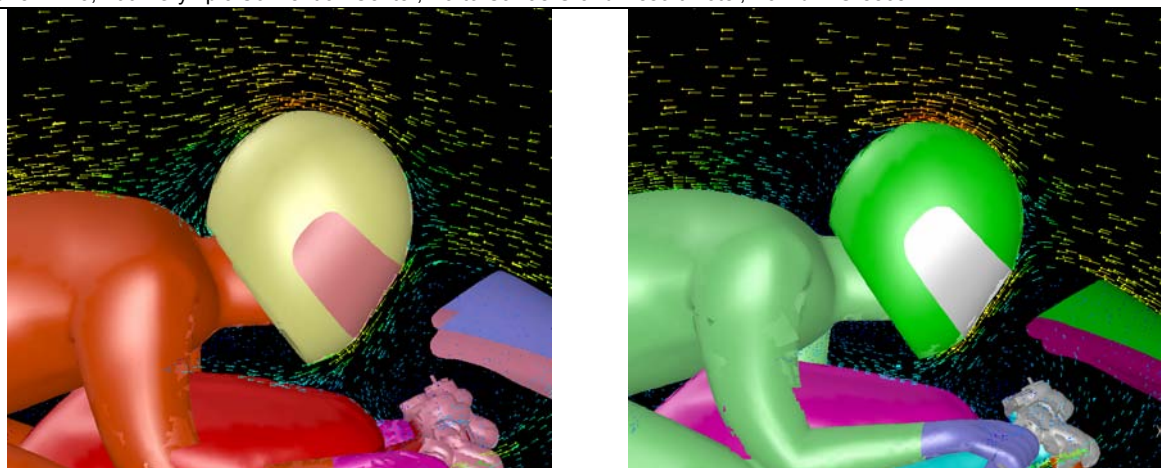


Figure 21: Velocity vectors for coarse tetra mesh (left) and coarse tetra mesh plus layers (right).

The model with layers predicts the separation near the top of the helmet

Figure 22 shows also how the tetra plus layers model accurately predicts the skin friction on the surface and the abrupt drop to zero at the separation area.

Finally, Figure 23 shows the different streamline pattern without and with the predicted separation.

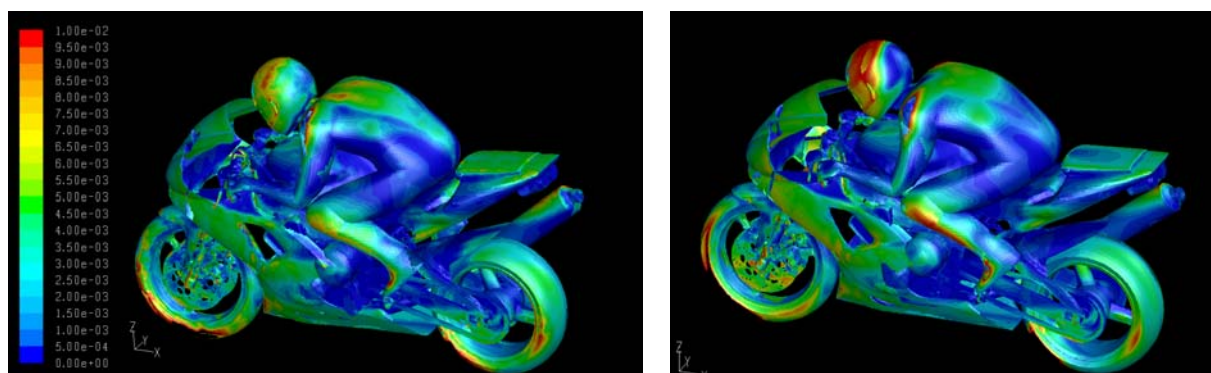


Figure 22: Skin friction coefficient contours for coarse tetra mesh (left) and coarse tetra plus layers mesh (right)

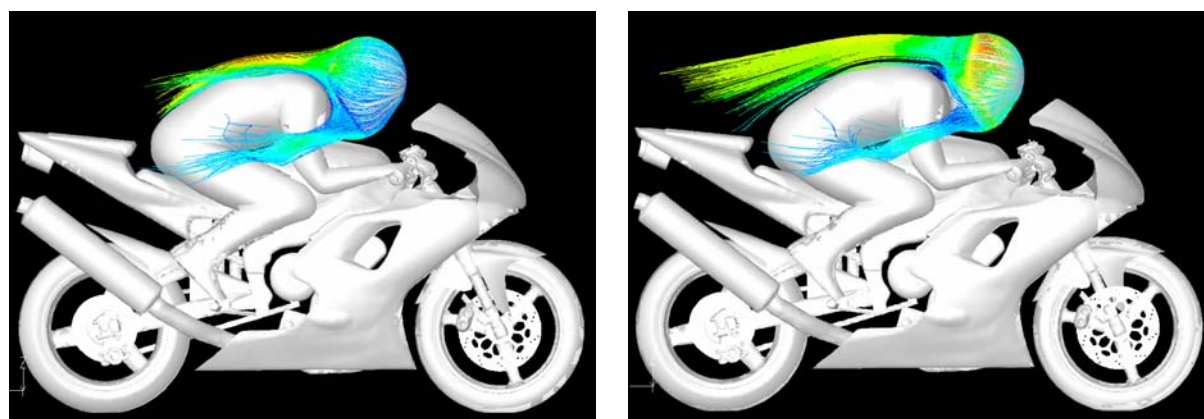


Figure 23: Streamlines released from helmet for coarse tetra mesh (left) and coarse tetra plus layers mesh (right)

Still even with this discrepancy in the flow resolution, the resulting drag coefficient is very similar for both cases, as most of the drag comes from the main wake.

3.5 COMPARISON OF RESULTS BETWEEN ORIGINAL AND MORPHED MODEL

The last simulations were performed on the tetra coarse mesh for the original and the morphed geometry. Table 3 shows the predicted drag and lift coefficients for the two models. The sensitivity of the simulation to this geometrical change is evident as the drag was increased by 7% and the lift coefficient was reduced by 46 %.

	C_D pressure	C_D viscous	C_D total	C_L total
tetra original (3.1 million)	0.435	0.022	0.457	0.098
tetra morphed (3.1 million)	0.467	0.024	0.491	0.053

Table 3: Simulation results for original and morphed models of tetra coarse mesh

Figure 24 shows the pressure coefficient distribution, where it is evident that in the morphed model a lot of the frontal high pressure area was moved from the rider's helmet to the front fairing of the motorcycle. Figure 25 shows the streamlines near the centre plane.

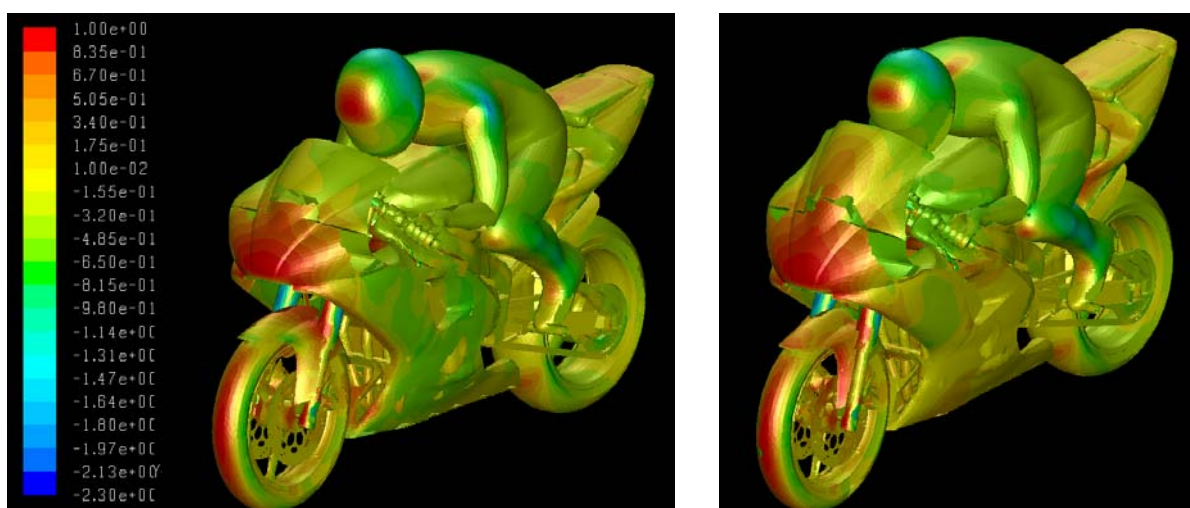


Figure 24: Pressure coefficient contours for original model (left) and morphed model (right) for the same coarse tetra mesh

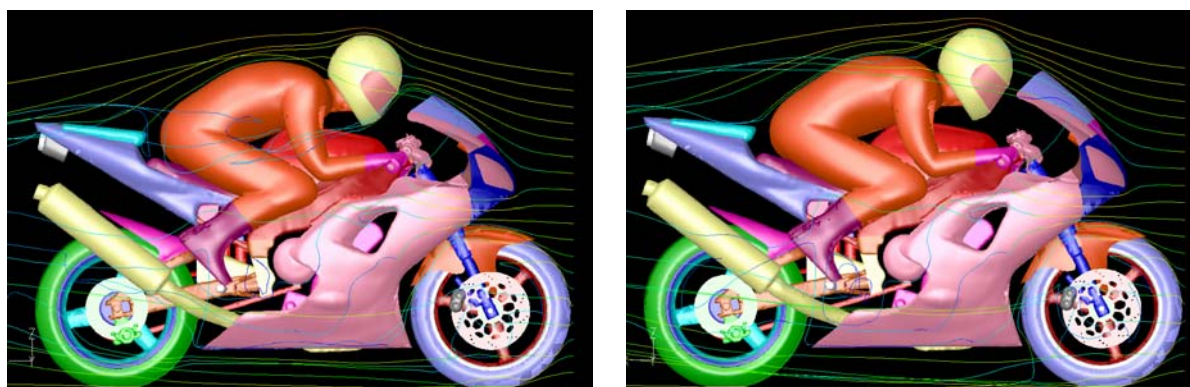


Figure 25: Streamlines for original model (left) and morphed model (right) for the same coarse tetra mesh

3.6 COMPARISON WITH LITERATURE RESULTS

A literature survey was made to collect some experimental results from similar motorcycles [6-8]. Table 4 gives a summary of these findings which are in good agreement with the CFD simulations in this work, bearing in mind all variations in motorcycle geometries and of course in rider characteristics. In particular, the findings of Meijaard [7] and Sharp [8], which are the most recent ones, are in very good agreement, taking into consideration the sensitivity of the results to the morphing of the front upper fairing.

4. CONCLUSIONS

ANSA performed successfully all the tasks involved in the complete and efficient preparation and modification of a high quality mesh with feature dependant surface mesh, boundary layer generation from complex geometries and user controlled volume mesh, with minimum effort. All meshes gave very similar results in drag and lift coefficient prediction, which correlate very well to relevant literature data, indicating the quality of all the models. Only the mesh with the layers was capable of predicting the separation around the rider helmet, showing the importance of the presence of the layers when accurate results are required. ANSA morphing was performed successfully and efficiently and demonstrated the sensitivity of the CFD simulation on model geometrical changes.

	A	C_D	$C_D \cdot A$	C_L	$C_L \cdot A$	Reference
Kawasaki ZX-10 	0.70	0.50	0.35	-	-	Hucho [6]
Kawasaki KR 250 	0.45	0.49	0.22	0.11	0.05	Hucho [6]
Suzuki GSXR-1100 	0.71	0.52	0.37	-	-	Hucho [6]
YAMAHA TZR-250 	-	-	0.30	-	0.01	Hucho [6]
YAMAHA FZR-1000 	0.65	0.52	0.34	-	-	Hucho [6]
Aprilia RSV 1000 	-	-	0.27	-	-	Meijaard [7]
TRIUMPH CFD model 	0.65	0.48	0.31	0.078	0.051	Sharp [8]
Morphed CFD model 	0.645	0.457	0.295	0.098	0.063	this work
Morphed CFD model 	0.645	0.491	0.317	0.053	0.034	this work

Table 4: Comparison of literature data (frontal area, drag and lift coefficients) and simulation results (although not depicted in the images, values include rider lying forward).

REFERENCES

- (1) M. Ehlen, "ANSA as a pre-processor for CFD simulations with Fluent", 1st International ANSA and META Congress, June 2005
- (2) S. di Piazza, D. Nanni, R. Rossi, "Numerical Multiscale Analysis of the Ducati 999 Motorbike Heat Exchangers", Proceedings of the 2nd EACC, Fluent Inc., 2005
- (3) R. Lewis, M. Cross, "Optimization using CFD and Mesh Deformation", Proceedings of the 2nd EACC, Fluent Inc., 2005
- (4) M. Lanfrit, "Best Practice Guidelines for Handling Automotive External Aerodynamics with FLUENT", Version 1.2, <http://www.fluentusers.com>, 2005
- (5) Z. Yang, J. Bozeman, F. Shen, D. Turner, S. Vemuri, "CFRM Concept for Vehicle Thermal System", SAE 2002-01-1207, 2002
- (6) Wolf-Heinrich Hucho, "Aerodynamics of Road Vehicle" Fourth Edition, SAE international, 1998
- (7) J.P. Meijaard, A. A. Popov, "Influences of Aerodynamic Drag, the Suspension System and Rider's Body Position on Instabilities in a Modern Motorcycle" Vehicle System Dynamics, Vol. 44. Supplement pp690-697, 2006
- (8) R. Sharp, S. Evangelou, D. J. N. Limebeer, "Advances in the Modelling of Motorcycle Dynamics", Multibody System Dynamics, Vol. 12, pp251-283, 2004

AUTOMATIC OPTIMISATION OF AUTOMOTIVE DESIGNS USING MESH MORPHING AND CFD

¹Francisco Campos*, ²Paolo Geremia, ³Evangelos Skaperdas

¹ICON, UK, ²ESTECO, UK, ³BETA CAE Systems S.A., Greece

KEYWORDS – aerodynamics, optimisation, modeFRONTIER, ANSA, FLUENT

ABSTRACT - The growing access to extensive computational resources and the introduction of parallelisation methods has facilitated the integration of CFD analysis and optimisation techniques as a way to reduce lead-times from concept to market. This paper describes an example of an automotive application where response surface optimisation methods have been successfully applied to fluid related design problems using a combination of ANSA, FLUENT and the multi-objective optimisation product modeFRONTIER, as part of a proof-of-concept exercise.

TECHNICAL PAPER -

1. INTRODUCTION

The traditional CFD design process is often based on a “trial-and-error” type approach. Starting from an initial geometry, CAD changes are introduced manually based on results from a limited number of design iterations and CFD analyses. The process is usually complex and time-consuming, thus limiting the number of configurations that are verified and reducing the chances of finding an optimum solution.

The introduction of a mathematical framework to find an optimum design through the use of the latest optimisation techniques “standardises” the design procedure and eliminates most of the drawbacks found in the traditional approach. In this sense, designers are exploiting the benefits of parallel execution of CFD analyses by taking full advantage of the most sophisticated IT frameworks available. More precisely, distributed computing based on high-performing CPU technology allows an extensive use of optimisation tools for designs involving large-sized computational fluid domains. As a result, large numbers of configurations can be verified and analysed fully automatically to find an optimum.

In order to reduce the product development time and satisfy the growing design requirements to stay competitive in the market, new design approaches have been introduced. Consequently, designers are giving more and more importance to the quality of their work, complying with the principle of finding the best solution with the minimum effort.

Design parameterisation plays an important role in this context, since the definition of design parameters leads to a very efficient modification of the shape of the fluid domain geometry. Following this approach, the designer can investigate the effects of geometry parameterisation on model performance and find out which is the optimal shape that meets all the requirements needed. This task is normally accomplished by using optimisation software which allows the parametric model to be automatically adjusted in order to achieve the optimal solution. The techniques currently employed for this purpose include a parametric CAD model, topological optimisation and mesh morphing approach.

Parameterisation of CAD models in the optimisation loop is based on the fact that a finite number of design variables can define the geometrical shape of the model by using parametric curves and surfaces, following Bezier and NURBS theory [1]. This approach is widely used by engineers since most of the CAD tools available in the market feature parametric definition of the geometrical model. However, to integrate this process into the CFD optimisation loop requires a fully automatic mesh generation tool, leading to additional time and difficulty in the process. This is especially true in cases involving complex geometries which could result in poor quality meshes, thus affecting the reliability of the CFD analysis stage.

An alternative approach is that of Topological optimisation. The approach is based on the idea that cells with back flow can be retrieved and discarded, thus isolating the “healthy” cells which feature no flow recirculation problems. The overall space available for the fluid can then be shaped by switching off recursively the “bad” cells. The main advantage is that just a single CFD model is required and, most importantly, no parameterisation is required.

Finally, the mesh morphing approach allows for the model shape to be modified with no need for parameterisation of the CAD model or automatic mesh generation. An existing mesh is deformed based on predefined actions, such as stretching or contraction of nodes, thus saving computational time during each optimisation loop. However, a significant number of mesh changing parameters are needed to perform an efficient mesh modification while avoiding issues related to excessive mesh deformation.

In this work, the latter approach was applied in the optimisation of the rear part of a car body using a parametric mesh morphing model. The benefits of employing a Response Surface Methodology were also demonstrated.

2. RESPONSE SURFACE METHODOLOGY

Engineering design optimisation problems typically boil-down to performing the optimisation of a baseline system by evaluating the lowest number of analyses while extracting as much information as possible out of the design space. This approach requires a suitable sampling of the design space by using the most advanced Design of Experiments techniques available.

The traditional approach is to test one factor at a time (OFAT). The first factor is moved while the other factors are held constant, then the next factor is examined, and so on. Design of Experiments (DOE) provides a strong and universal framework to design and analyse all comparative experiments. OFAT usually requires many runs to obtain sufficient information and this is generally prohibitive. The DOE approach is in direct contrast to OFAT because it considers all factors simultaneously. Design of experiments uses the best factor settings to obtain a certain amount of information.

The DOE approach can also be applied for CFD optimisation. A limited number of evaluations exploring different design configurations can be performed by employing a “high-fidelity” CFD model. This is particularly useful when confronted by models with considerable mesh sizes and extensive running times.

After the sampling phase of the design space is completed, statistical analysis can be applied to the database of results in order to assess the response of the system with respect to variation of the factors considered in the analysis. For this purpose, t-Student criterion as well as main effects analysis can be applied in order to investigate existing relationships between the output values (response variables) and the input variables (factors). As a result, the direct/inverse effect of each factor with respect to the response variables can be detected and quantified.

A further step in the design process can be made whenever the need for a better resolution of the response of the design space arises. In practice, the designer would typically like to understand well the behavior of the system under investigation. For this, a suitable fitting of the data available from the numerical computations is therefore needed. A technique known as Response Surfaces Methodology (RSM) is a widely employed approach for building meta-models to approximate the response from experimental data or analysis codes.

RSM is a collection of mathematical and statistical techniques useful for the modelling and analysis of problems in which a response of interest is influenced by several variables. These synthetic models, when found to be satisfactory, effectively replace the simulation in the next steps of optimisation or design space exploration. The important point to note is that these simplified models will calculate a response in near instantaneous time, with obvious advantages over an alternative such a full CFD analysis.

In this paper, the geometrical shape of the rear part of a passenger car body was parameterised according to a mesh-morphing related model, in order to analyse the response of the system with regards to the aerodynamics. The Latin Hypercube Sampling scheme was used to perform the preliminary exploration of the design space through the DOE approach. After the sequence of computations was completed, several RSM algorithms were considered in order to retrieve a proper mapping of the solution under examination. As a result, the most efficient designs were selected from the set of optimal solutions belonging to the so called Pareto frontier.

3. APPLICATION CASE: OPTIMISATION OF CAR AERODYNAMICS

The optimisation case in this example focuses on the external aerodynamics of the Audi A6 Avant shown in Figure 1. The aerodynamics engineer is responsible for enhancing the aerodynamic characteristics of the car so as to reduce drag, reduce wind noise, and prevent undesired lift forces at high speeds.



Figure 1. Audi A6-Avant (www.audi.com – AUDI AG © 2007)

The main objective of the simulations presented here was to find the optimal aerodynamic shape for the rear part of the car body. The optimisation problem was therefore defined by means of the following two objective functions: (i) minimisation of the drag coefficient, and (ii) minimisation of the car balance in terms of aerodynamic lift forces acting on the front and the rear wheels. The latter is defined as the absolute difference between front and rear lift (zero being the optimum).

The optimisation procedure consisted of generating a parametric mesh morphing model of the car geometry, performing a CFD analysis in batch mode and using the multi-objective optimisation product modeFRONTIER to find, screen and select the optimal design layout.

The work to perform the car optimisation can be summarised as follows:

- Generate parametric mesh morphing model in ANSA
- Setup CFD analysis in FLUENT
- Setup optimisation workflow within modeFRONTIER
- Perform statistical analysis
- Response Surface modelling
- Results assessment

3.1 MESH MORPHING WITH ANSA

A watertight model was created in ANSA v12.1.1 by merging a combination of geometrical data for the main aerodynamic surfaces of the vehicle and shell elements for the wrapped suspension and exhaust system.

The variable size surface mesh, shown in Figure 2, was restricted to around 330 thousand triangular elements, while the maximum Fluent skewness was kept below 0.6.

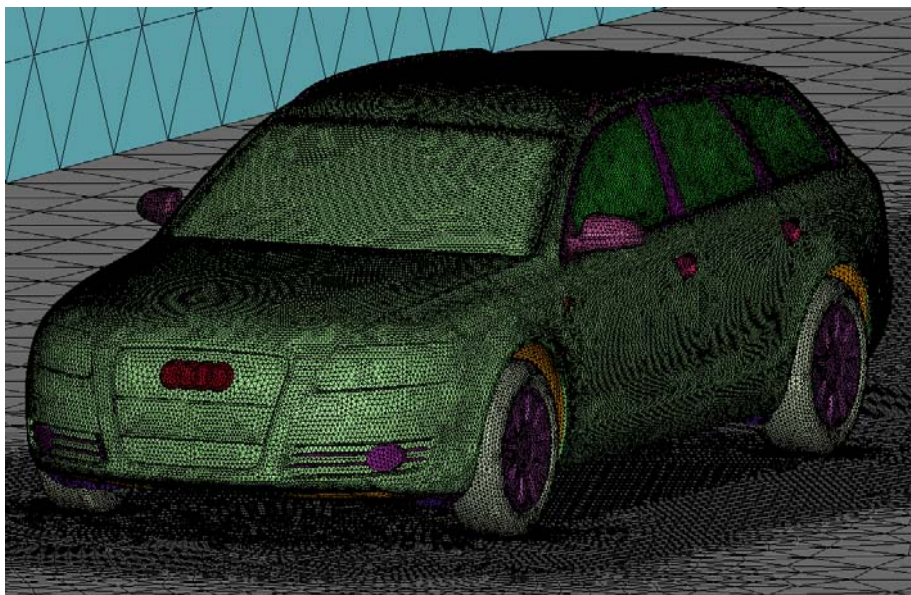


Figure 2. Surface mesh of vehicle and virtual wind tunnel box

The volume mesh consists of around 4.4 million elements. The Hexa-Interior algorithm of ANSA was used to generate variable size hexas in the main volume connected through pyramids and tetras with the surface mesh.

Refinement boxes were placed in the wake of the vehicle and wing mirrors, thus allowing control of the volume element size, as shown in Figure 3. An average Fluent tetra skewness of 0.27 was achieved, with max skewness kept below 0.95.

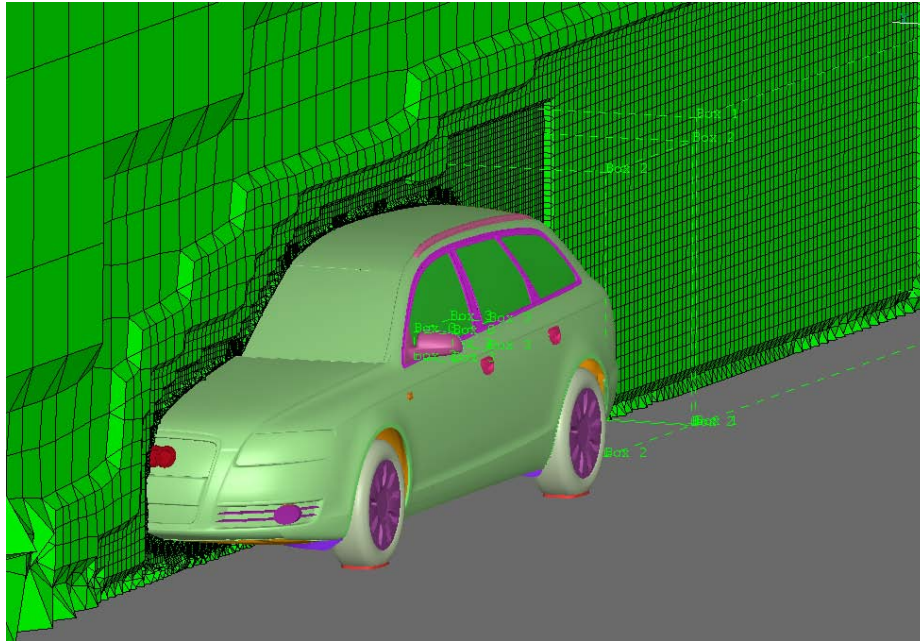


Figure 3. Hexa-Interior volume mesh with refinement Boxes in the vehicle and mirror wakes

After the mesh was built, morphing boxes were created, split and fit exactly onto the main features of the vehicle, as shown in Figure 4. The boxes allow precise control of morphing operations to examine various shapes parametrically. Morphing parameters were specified in predefined degrees of freedom so that the position of the rear spoiler as well as the inclination of the D-pillar could be altered. A total of four design parameters were set to influence the shape of the rear of the car, namely: rear spoiler position in X, Y and Z, and D-pillar angle.

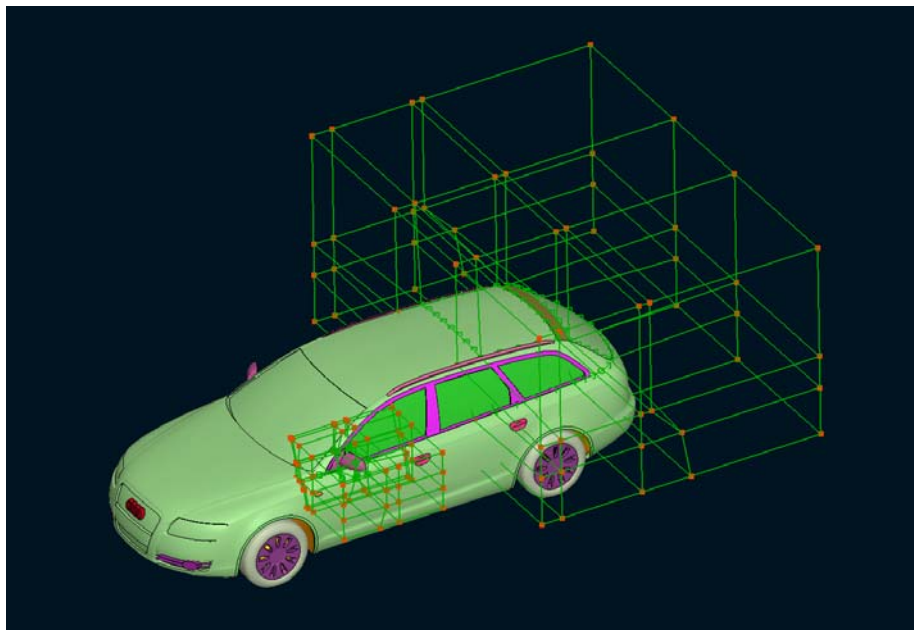


Figure 4. Mesh morphing model within ANSA

A preliminary feasibility study was performed in order to determine a valid range for each of the design parameters described above. Any parameter set causing mesh generation difficulties or excessive mesh deformation was detected and the values for the range of each parameter readjusted accordingly. This task was accomplished in modeFRONTIER by systematically exploring all of the possible combinations of the design parameter sets within the bounding values.

Finally, all mesh morphing operations were automated in modeFRONTIER using the ANSA batch running capabilities. A session file was created to read the morphing parameters from a text file containing the morphing definitions. The process was repeated for each design variation by changing accordingly the values listed in the text file.

3.2 CFD MODELLING WITH FLUENT

The CFD analysis stage was performed in FLUENT 6.3. The air flow was computed as an incompressible-subsonic turbulent gas (i.e. constant density). The Spalart-Allmaras one-equation turbulence model, specifically intended for aerodynamic calculations, was applied in every simulation.

A normal inlet velocity boundary condition was specified at the entry of the virtual wind tunnel with a value of 19.44 m/s (or 70 kph driving speed). The prescribed incoming air temperature was set to 293 K, while the turbulence intensity and length scale were set to 5% and 0.4 m, respectively. Similarly, the static pressure was fixed at 0 Pa relative to a reference pressure of 101,325 Pa at the tunnel outlet. The ground and wheels were assumed to be stationary, while all surfaces representing the car body were defined as adiabatic and no-slip wall boundaries. Finally, the tunnel walls were modelled as symmetry planes.

The SIMPLE solution procedure for pressure-velocity coupling was employed in the calculations with the AMG solver. The default differencing schemes were utilised for all flow variables. An upper limit of 500 iterations was specified in the event that a case would not fully converge.

FLUENT was run in batch mode using a journal file to allow modeFRONTIER to perform the analyses and extract all relevant information fully automatically. The latter was achieved by means of post-processing monitors for drag, lift and moment coefficients.

3.3 modeFRONTIER SETUP

The optimisation software employed in this work was modeFRONTIER. This package allowed the process integration of ANSA and FLUENT with the design study strategy employed. This was achieved by reading a specific set of morphing parameters as input variables for ANSA, and retrieving drag coefficient and aerodynamic lift forces values as output variables from FLUENT.

For every step of the optimisation process ANSA and FLUENT were run in batch mode in order to evaluate each specific design configuration. Furthermore, modeFRONTIER parallelisation capabilities were exploited to allow concurrent FLUENT analyses to be performed in a multi-processor cluster machine.

The whole process, including the data and logic flows, were defined under modeFRONTIER's workflow environment, as shown in Figure 5.

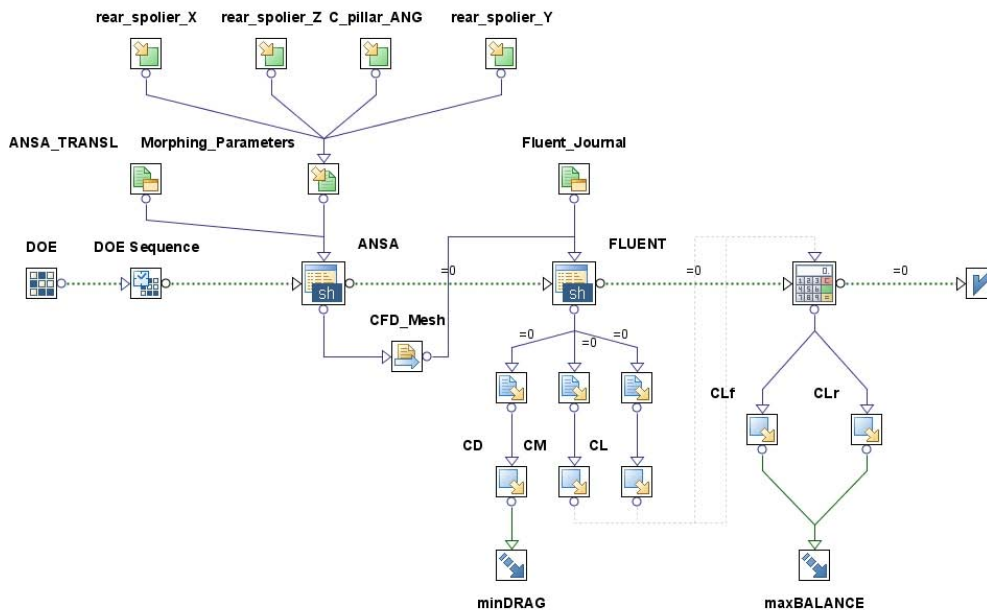


Figure 5. modeFRONTIER Workflow definition

3.4 DESIGN OF EXPERIMENTS AND STATISTICAL ANALYSIS

The Latin Hypercube Sampling (LHS) preliminary exploration sequence was employed [3]. Given a multivariate statistical distribution, LHS technique samples the joint probability distribution (i.e. the statistical distribution of all the variables) independently generating the values of the marginal probability distributions (i.e. the statistical distribution of each single variable). LHS arranges the values of the marginal probability distributions in order to sample the multivariate space in a relatively uniform way. Consequently, the correlation index between the design parameters was drastically reduced to almost nil, as shown in green in Figure 6, thus confirming the fact that LHS distributes efficiently the points around the design space in this particular case.

Following this approach, 40 designs were created and then evaluated using FLUENT according to a uniform distribution applied to each of the four input variables considered.

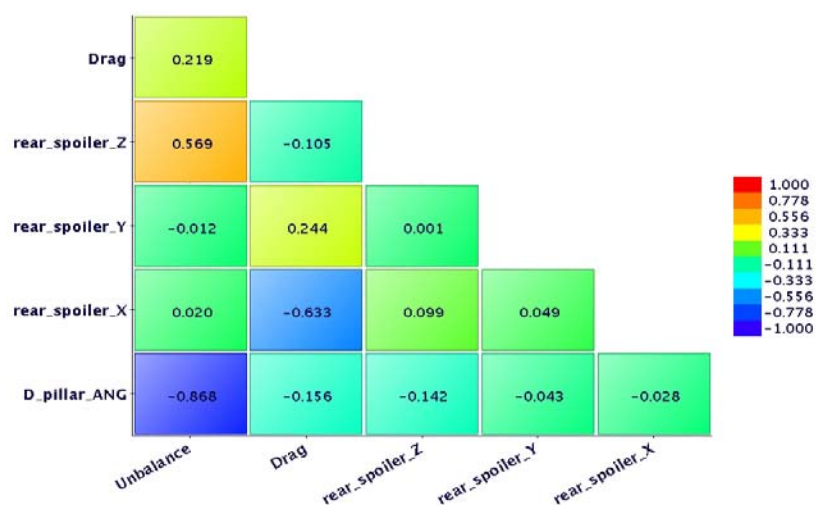


Figure 6. Correlation Matrix of the variables

Figure 6 also depicts the correlation index between the output variables (i.e. drag and unbalance) and the input variables. Thus, the measure of the linear association between each couple of variables was automatically computed and displayed.

Advanced statistical tools were then exploited in order to acquire more information about dependencies between input and output variables. For this purpose, the Student Chart was created for both the output variables in order to assign a precise measure of the influence of each factor (i.e. the input variables). This tool is based on the t-Student test considering the significance of the effect of each factor on a specific response variable. As a result, any direct/inverse effect can be detected and then quantified (see Figure 7).

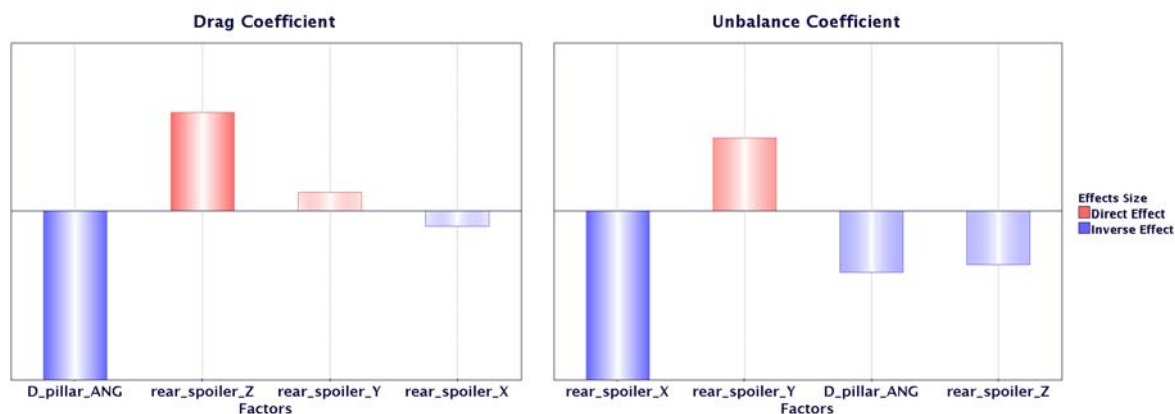


Figure 7. Student Chart – Drag Coefficient (left) and Unbalance (right)

The Student Chart and the Correlation Matrix both reveal a strong inverse relationship between the D-pillar angle and the drag, and also between the rear spoiler variation in X and the unbalance. Similarly, the rear spoiler variation in Z and the rear spoiler variation in Y have significant direct effects on drag and balance, respectively.

3.5 RESPONSE SURFACE MODELLING

The RSM tool featured several algorithms designed for data interpolation. Different techniques were employed to produce a proper fit to the data available from the 40 CFD simulations. Three state-of-the-art algorithms were considered, namely (i) Multivariate Polynomial Interpolation, (ii) Neural Networks and (iii) Radial Basis Functions.

The Multivariate Polynomial Interpolation is based on the Singular Value Decomposition (SVD) algorithm. It is considered to be a very powerful technique for solving a linear system of equations with particular benefits when dealing with numerically difficult situations [4].

Neural Networks (NN) is a very efficient and powerful interpolation tool [5]. Inspired by the brain structure and functions, NN can learn from training data. In this way NN can model any generic non-linear relationship between input and output variables.

Radial Basis Functions (RBF) is another efficient tool for multivariate scattered data interpolation [6]. Scattered data means that the training points do not need to be sampled on a regular grid and in practise this provides a truly meshless method. Since RBF are interpolating response surfaces they pass exactly through training points, whereas both the Polynomial and the NN methods are pure approximating algorithms, since they perform a surface fitting throughout the set of the points available for the training.

In order to evaluate the accuracy of both the Polynomial and NN surfaces the residual quantities were considered. The residual quantities are the differences in terms of relative or absolute error between the value of the points belonging to the training set and the corresponding value predicted by the response surface. More precisely, the mean and the maximum values were considered for each response surface created. Furthermore, the regression index was exploited as a measure of the quality of the response surface. This criterion measured the amount of the overall interpolation error between effective and predicted values of the points belonging to the training set. A regression index value close to 1 indicates a good synthetic model.

For the RBF functions, the “leave-one-out error” criterion was considered. In turn, each point belonging to the training set is excluded from the training procedure. The value predicted in the excluded point by the so created surface is then compared to the known value. A smaller value on average indicates that the response surface is better trained on the whole dataset.

Following this approach, first, second and third-order Polynomial Interpolation functions and a fully automatic NN were exploited. Regarding the RBF surfaces five different radial functions were applied: Gaussians (G), Duchon’s Polyharmonic Splines (PS), Hardy’s Multi Quadrics (MQ), Inverse Multi Quadrics (IMQ), and Wendland’s Compactly Supported C2 (W2). This list represents a complete set of state-of-the-art and widely used radial functions that can be found in literature [6].

Analysis of the RSM interpolation errors on all the nine response surfaces algorithms revealed that the best performer was the RBF algorithm for both of the output variables considered. Furthermore, the Gaussian model was selected for the unbalance, while the Duchon’s Polyharmonic Splines was applied to the drag coefficient.

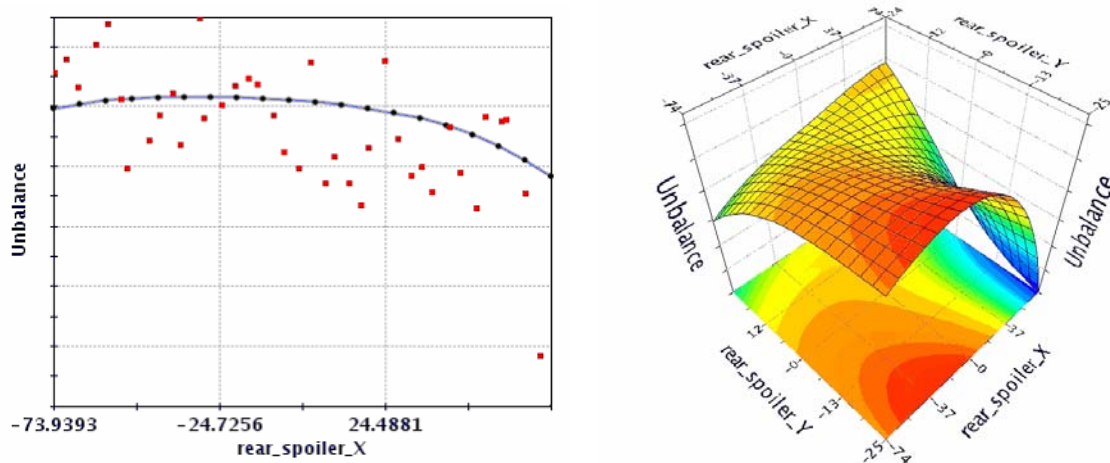


Figure 8. RBF surface for Unbalance

Two-dimensional plot: vs. rear_spoiler_X (left)

Three-dimensional contour plot: vs. rear_spoiler_X and rear_spoiler_Y (right)

Figure 8 shows the matching for the RBF is sufficiently accurate. The smoothness of the resulting function also provides a good fitting of the design space with respect to the points considered in the training set.

3.6 OPTIMISATION PHASE

After the response surfaces were selected for the two output variables, it was possible to re-use the created meta-models instead of using the CFD solver in order to evaluate the performance of the car aerodynamics. Since the design evaluation using the RSM is very fast, a massive optimisation of the design space was carried out using the response surfaces created. The NSGA-II optimisation algorithm [7] was used for the present work as it is based on a fast and elitist multi-objective evolutionary algorithm. At the end of the optimisation phase, the best designs (by definition those belonging to the Pareto frontier) were retrieved.

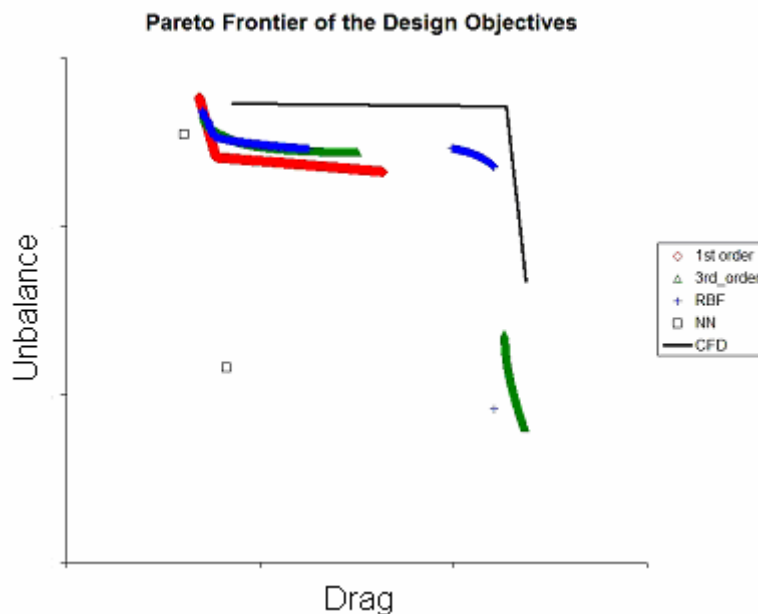


Figure 9. Scatter Chart of the Pareto frontier for the CFD and the RSM results

For each RSM created, an optimisation run was performed and then the Pareto frontier was detected. Apart from the second-order Polynomial Function, all the other response surfaces showed acceptable agreement with the Pareto curve provided by the CFD runs (as shown in Figure 9). Moreover, all of the RBF functions showed a similar behavior in terms of results obtained.

The plot of the Pareto frontier highlights once again the better accuracy of the RBF model in fitting the dataset available. This response surface model was successfully employed to find, screen and select the layout of the optimal shape of the car for enhanced aerodynamics performance.

The use of RSM led to a drastic reduction in analysis time. A full optimisation that would have required hundreds of FLUENT computations (maintaining the same optimisation algorithm design settings) was replaced with only 40 design evaluations using the RSM approach proposed in this work.

4. CONCLUSIONS

The fast and efficient mesh-morphing tools available in ANSA, as well as parallel executions of FLUENT solver capabilities, were successfully coupled with modeFRONTIER in order to manage the whole design process, as well as the RSM strategy applied, as part of a proof-of-concept exercise.

The Latin Hypercube Sampling scheme was used to perform the preliminary exploration of the design space through the DOE approach. After the sequence of computations was completed, several RSM algorithms were considered in order to retrieve a proper mapping of the solution under examination. As a result, the most efficient solutions were selected from among the set of the not dominated solutions belonging to the Pareto frontier.

In order to select the best solution, the results from the RBF response surface were considered. Both performance objective goals were successfully achieved. The optimisation of the RBF response surface model allowed a fast comparison of the results for drag and unbalance for both the baseline design and the optimised configuration (see Figure 10). Overall, the drag coefficient was reduced -2.7%, while the unbalance was reduced -8.3%.

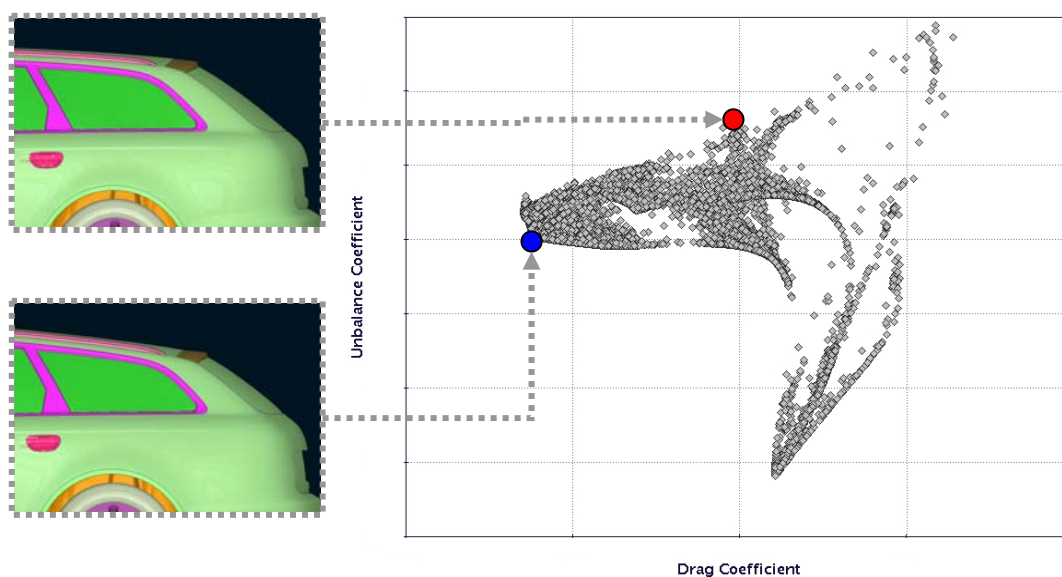


Figure 10. Scatter Chart of the Design Objectives using the RBF model (red dot – baseline design; blue dot– optimised design)

The solutions presented above are restricted by the accuracy of the CFD methods employed. For example, it is well known that RANS turbulence models are sometime unable to predict the on-set of separation, or even whether flow separation occurs at all [8]. This type of situations tends to generate misleading results which could affect the outcome of the optimisation exercise. Consequently, a good knowledge of the limitations of the numerical methods in use is fundamental when selecting the best design from the Pareto frontier. This knowledge is reinforced by extensive experience gathered from widespread wind tunnel testing and systematic validation of selected aerodynamic CFD calculations.

REFERENCES

- (1) Haslinger, J., and Mäkinen, R. A. E., Introduction to Shape Optimization, and Computation, SIAM, ISBN: 0898715369
- (2) Campos, F., Geremia P., Weston, S., and Islam, M., Automatic Optimisation Of Aerodynamic Designs Using CFD-Based Methods, Proceedings of 6th MIRA International Vehicle Aerodynamics Conference
- (3) modeFRONTIER v3 User manual – www.esteco.com
- (4) Press, W. H., Teukolsky, S. A., Vetterling, W. T., & Flannery, B. P., 1992, Numerical Recipes in C. The Art of Scientific Computing, 2nd ed., Cambridge University Press

- (5) Haykin, S., Neural Networks – A Comprehensive Foundation, Prentice Hall International Editions, 1999.
- (6) Buhmann, Martin D., 2003, Radial Basis Functions: Theory and Implementations, Cambridge University Press
- (7) Deb, K., Pratap, A., Agarwal, S., and Meyarivan, T. 2000, A Fast and Elitist Multi-Objective Genetic Algorithm-NSGA-II, KanGAL Report Number 2000001
- (8) Menter, F. Test Case 9.4: Flow around a simplified car body (Ahmed body). Comments (F. Menter), 10th joint ERCOFTAC (SIG-15) -IAHR-QNET/CFD Workshop on Refined Turbulence Modelling, October 2002, viewed on 14/11/2005, <http://labo.univ-poitiers.fr/informations-lea/Workshop-Ercoftac-2002/case9.4/Case9.4_comments.pdf>

ACKNOWLEDGEMENTS

The authors would like to thank Audi AG for providing the data and permission to use the A6 Avant for this work.

CONTACT

For information regarding this paper, please contact s.weston@icon-cg.co.uk



www.icon-cg.co.uk

Icon is an independent provider of confidential CAE simulation services and has had a long association with industry by delivering CFD related projects at both OEM and supplier level since 1992. Close links with academic institutions, and continuous involvement with clients in various industries, has allowed Icon to establish a wide base of knowledge and offer technology transfer to its clients.



www.esteco-uk.com

modeFRONTIER is a multi-objective design optimisation software package developed by ESTECO. It is widely used in automotive and aerospace engineering to find, screen and select the optimal design in an organised fashion. modeFRONTIER can drive your FLUENT tools to explore the design space and iterate towards these improved and/or optimal designs.



www.beta-cae.gr

BETA CAE Systems S.A. is a private engineering software company specialised in the development of state of the art CAE pre- and post-processing software systems.

The company's flagship products, ANSA pre-processor and μETA post-processor package, currently hold a leading position in the CAE software market worldwide.

Session H2.6

DEFINITION AND PARAMETERIZATION OF A TASK MANAGER PROCESS WORKFLOW, APPLIED ON THE GENERATION OF AN ABAQUS LOADCASE

Stelios Seitanis*, Michalis Giannakidis
BETA CAE Systems S. A., Greece

KEYWORDS - Template driven process, parameterization, automation, repeatability, ABAQUS

ABSTRACT - The current trend of template driven CAE analyses imposes the need to define and parameterize flexible and reusable model build-up processes. Within this concept, this presentation will focus on the actions that a CAE analyst should take to achieve this goal.

For any given task of relatively high complexity, the engineer should plan the skeleton of the automated process and continue on to its implementation. Typical aspects in this respect are the recognition of the loadcase being investigated, the respective model and analysis specific data and the organization of all these in a 'data pool'. Regarding the actual implementation, individual task components need to be defined and correlated to each other, to handle model inter-dependencies and allow easy modifications.

This work exploits existing ANSA Task Manager functionality, to demonstrate the generation of a template driven process for an ABAQUS/Standard durability analysis. ANSA, along side ANSA Data Management and Task Manager, promote parameterization and safeguard model quality while keeping the complete process simple and versatile.

TECHNICAL PAPER -

1. INTRODUCTION

The usefulness of a managed organization of a project's data and the parametrized build up of an FE analysis loadcase is widely accepted. This paper is an accumulation of all the considerations an analyst needs to take into account in order to create a reusable CAE process workflow, aiming in the creation of a complete FE analysis model. The work described targets in the planning and implementation of the process, alongside with the definition and parametrization of all the individual entities that are used in the process itself. The possibility of using the same template or components of it in other projects is also considered.

The durability analysis of a vehicle rear Lift Gate is taken as a test case. The tools used to automate the analysis process are the *ANSA Data Manager* and the *ANSA Task Manager*¹.

¹ *ANSA Data Manager* and *ANSA Task Manager* are integrated parts of the ANSA pre-processor. They are commonly referred to as *ANSA DM* and *ANSA TM* respectively.

2. PROCESS REQUIREMENTS

The model to be produced from this work is a Rear Gate durability Analysis model with special interest in the areas of i) the modeling of the hinge connecting the Lift Gate to the Car Frame and ii) variations of loading conditions. This model build-up should be based on a *template workflow* that will promote the parametrization and reusability of the whole model and its individual components.

The actual design and model variations this process needs to consider are:

1. variations of the hinge (both on geometry level and modeling representations),
2. study of different Lift Gate loading scenarios and
3. study of these variations at different Lift Gate positions

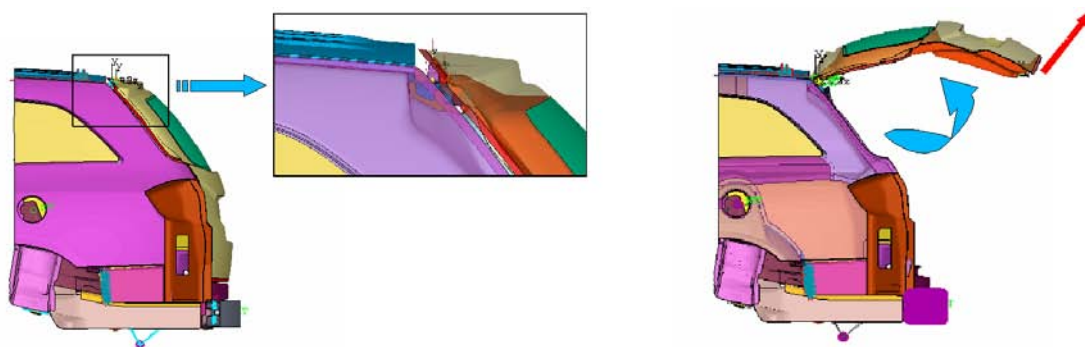


Illustration 1.: Area of interest and position variations of the Lift Gate durability model.

In order to allow easy adaptations to these requirements (Illustration 1), special considerations need to be into account for the general setup and organization of the overall process. These include:

1. Build the Durability model, using a DM configured model
2. Isolate areas of interest for the specific loadcase
3. Position the Lift Gate (open it at a specific angles)
4. Define appropriate connectors, trim items, boundary conditions and loads
5. Parameterize definitions to allow easy adaptations to:
 - (a) geometry changes
 - (b) different vehicle models

3. BASIC PROCESS WORKFLOW WETUP

The durability specific model that is considered in this work is based upon the infrastructure of an already existing and fully configured *ANSA DM/Task model*. This implies that an existing data pool of the model's geometry data is already available. This data pool hosts (among others) the '*common representations*' of all the parts of the vehicle.

Moreover, the 'Common Model' section of the Task Manager is also setup and functional for the specific project. This Task template includes the model's geometry as a hierarchy of parts having the common model representations, connections for the total assembly and abstract definitions of *Connectors and Model Trimming*, all suitable for the Common Model description.

The existence of the ANSA DM data pool and the availability of the TASK Manager template functionalities are important parts of the loadcase build-up process. The ANSA DM functionality binds our workflow to the changes made in the geometry level allowing us to adopt them with minimal effort, handle the data that we produce and also have these shared and reused by other engineers. ANSA TASK Manager functionality completes the aforementioned and gives us the possibility to describe our complete process as a template,

allowing an easy overview of the process and the interdependencies of the items that it consists of.

With the usage of the Connectors, Boundary Conditions and Output Requests definitions available in ANSA alongside the ANSA scripting functionality we are able to proceed to the generation of a parametric ABAQUS Durability Analysis Template.

4. PLANNING OF THE WORKFLOW SKELETON (TEMPLATE CREATION)

As any complete TASK Manager Template, our durability template consists of three top level sections: i) the Common Model (already available in our case), ii) the ABAQUS Common Model, hereon named 'Lift Gate Common Model' and iii) the respective ABAQUS loadcase, hereon the 'Lift Gate Load Case'.

As usual, the groups in the common model section are already available and stripped of any solution scenario dependent entities. They need to be changed to suitable representations or realized for the specific load case. In turn, the Lift Gate Common Model serves two purposes. First, it will transform the Common Model into a form suitable for all the ABAQUS analyses that will follow. Secondly it will add the solution dependent entities for all the loadcases that will follow. Finally, the Lift Gate loadcase will add to the model all loadcase dependent entities and will feed the model to the solver.

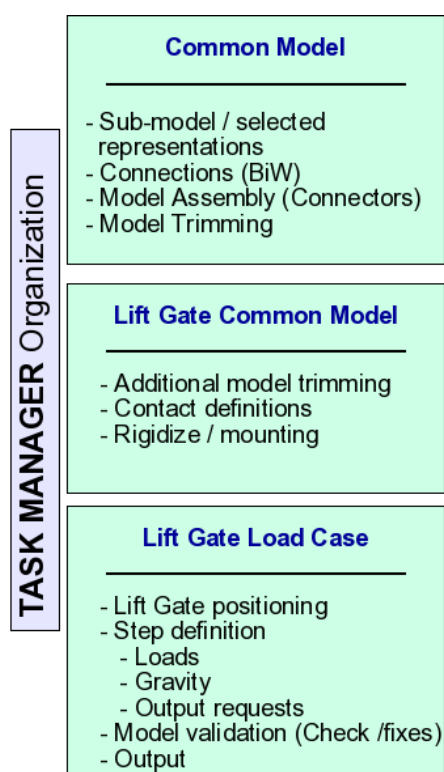


Illustration 2.: Template skeleton of the parametrized ABAQUS durability analysis and its respective sections

5. PREPARING THE DURABILITY REPRESENTATIONS

As previously mentioned, the ABAQUS durability loadcase we prepare is based on the Common Model representation of the complete vehicle. This gives us the complete collection of all the components of the model in the Task Manager Tree (Illustration 3). Here, the representations of these components need to be changed to a form suitable for our analysis. We will call this representation the *Durability Representation*. This is done with the use of the 'Change Representation' functionality of ANSA DM. We may find the Durability versions of parts already available in DM, or we may need to go through the process of creating them. In the latter case, we can then publish these in the central Data Pool, thus making them available for use by other engineers.

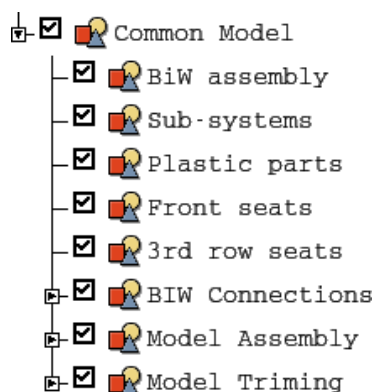


Illustration 3.: Task Manager Common Model section.
Entities in this section need to have their representation changed to '*Durability*'.

After the parts have their representations changed, the model's geometry serves us no other purpose in the model. For this reason, and also in order to simplify the cut of the vehicle according to the loadcase specifications (see Section:7. *The Lift Gate Common MODEL*), the elements are released from the geometry, and the geometry is deleted.

6. ASSEMBLING AND TRIMMING IN THE COMMON MODEL SECTION

The abstract definitions of Connections, Connectors and Body Trimming in the Common Section need to be properly parametrized and also realized as suitable ABAQUS entities. The connectors of the Lift Gate's hinges' that we will review later on in more detail are also found in this section.

7. THE LIFT GATE COMMON MODEL

The Lift Gate Common model, is an abstraction of the Durability Common Model. In this section, specific parts have their representations changed to match the durability analysis requirements or modeling needs. This modifications includes, for example, the removal of the suspension system by changing its representation into 'Don't Use'. This process relieves the model from non relevant parts.

Moreover at this part of the template, the parameter of the cut of the BiW at a position along the vehicle axis (defined in the analysis specs) is applied. After this, the model is ready to be mounted (Illustration 9).

8. THE LIFT GATE LOADCASE

In conjunction with the ABAQUS specific Common Model, the Load Case Group will position the Lift Gate, apply proper loads and define the desired output requests. Finally the model will be validated and checked against errors, in the scope of the current analysis.

9. MODELING OF HINGES – CONNECTOR PARAMETERIZATION

In all the rear lift gate durability projects for which our template is being parameterized, frequent and extensive modifications of the hinge (either geometric or FE) are expected. This calls for special planning on the design stage of the template in order to allow modifications on the modeling of the hinges in a way that is efficient for the engineer.

To make the preparation of the hinges easy, each hinge is modeled separately. This includes all of its geometry and its *internal connectors*. Each hinge model is then saved in DM as a new representation for the *Hinge Group*.

The hinges connectivity to the BiW, is achieved with the *external connectors*. These are saved in the master model and are properly parameterized so as to work with different hinge representations. This set-up allows an automatic realization of the hinge's connectivity to the structure each time a new version of the hinge becomes available (Illustration 4).

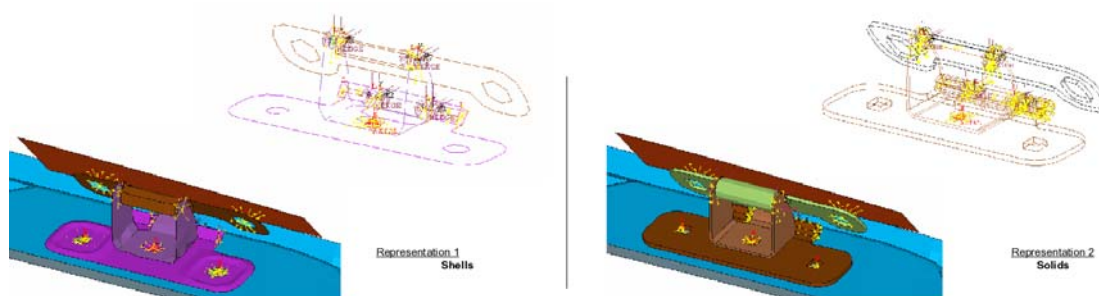


Illustration 4.: Different representations of a hinge (shells and solids), with internal and external connectors realized

10. CONNECTORS' DEFINITION AND PARAMETERIZATION

The requirement to automatically connect with each other different parts of the hinge and also the hinge to the car body through kinematic joints, is achieved with the use of *ANSA Connector* entities. These entities allow the definition of their main part (the body) to reside in the DM as a library item. Moreover, they have the capability to attach on the parts they connect through interfaces based on the results of parametric searches. For more details on defining a Connector entity, refer to the respective section of the ANSA User's Guide (1).

The wise selection of the connectors' parameters is important since all subsequent realization will be based on these values. These parameters need to be chosen in a way that modifications to the geometry of the hinge will not invalidate them.

In order to achieve this, the definition of the connectivity for the connected parts needs to be chosen properly. It can be either the *Module Ids* of *Parts* or the *Property Ids*, depending on which attribute is expected to remain the same when the hinge is changed. In our case the Module Id was chosen, because in case the hinge was modeled with solids, then the Property Ids were expected to change.

Also, when defining the searches for the connectors interfaces, the more specific search patterns should be preferred (when possible) instead of general ones. This means that search for 'NamedEntities' on a given 'Connectivity' should be preferable in most cases. Similarly, searches for circular features (applicable both for shells and solids) should be preferred over searches for Holes (applicable only for shells) or Nodes in a given radius. In cases where Connectors are attached to each other forming chains, the names of the attachment points (e.g. attach_node1, attach_node2) should be used in the search pattern of the next connector.

Finally, if any of the connector's parameters depend on its actual position in space, then the user will need to move it if the corresponding connectivity parts are also moved.

Connectors, after being defined in the Task Template, are realized automatically. Moreover they get updated of model changes that affect them and potentially invalidate them. For this reason they have a status flag to indicate if they are built against the latest model changes (Illustration 5).

Id	Name	search1	search2	interface1	interface2	status
1	Hinge_Lift_Gate_A_Axial_Connector	CircularFeature	Node	Rbe2	Rbe2	ok
2	Hinge_Lift_Gate_A_B5	NamedEntities	NamedEntities	None	None	ok
3	Hinge_Lift_Gate_A_B4	NamedEntities	Node	None	Rbe2	ok
4	Hinge_Lift_Gate_A_B3	Node	Node	Rbe2	Rbe2	ok

Illustration 5.: List of connectors used as internal in the hinge group. Their definition parameters and realization status are shown in the list.

11. SPECIALIZED CONNECTORS

As a complement to the previous connector definitions, the representation and the interface of each connector can be customized through user scripts. A script that creates the connector representation can be invoked and passed on the results of the search patterns. Moreover, a second script can control the creation of the interface.

In our model, we used a specialized realization of the connectors to create contacts among the hinge parts and the connecting frames on the car (Illustration 6).

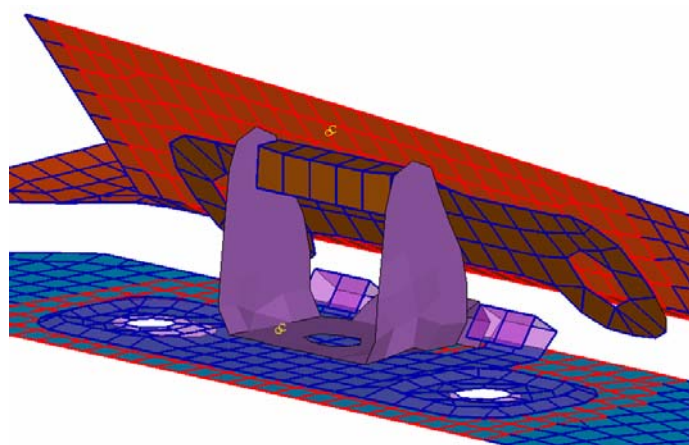


Illustration 6.: Contact Pairs created through connector entities. Search is performed by the Shell_SolidFacet pattern

Even in the case of specialized connectors, ANSA Task manager can track the connector's status, delete and re-apply it when needed.

12. LIFT GATE COMMON MODEL CREATION

Model preparations similar to those of the Common Model are required also in the Lift Gate (analysis specific) common model. In this section all the analysis specific modifications that are needed for the model setup are gathered. In principal these are similar to those in the common section.

The most important part in this section of the template is the cut of the complete vehicle by a plane along its X axis (Illustration 7 and Illustration 8).

13. LOAD CASE SPECIFIC MODEL TRIMMING AND MOUNTING

The cutting position of the model, is given in the analysis specifications. For simplicity reasons, this parameter needs to correspond to a single parameter and action in our template. This will ensure that the model's geometry is modified in a single step and that the proper mountings are defined at the same time.

The cut to the vehicle is performed with the use of an ANSA User Script embedded in the template. This script, given the cut position along the X axis from the specifications as a parameter, removes all model entities that lay in front of the cutting plane. Elements with free nodes after the cut, are attached to an appropriate rigid body. A boundary condition is then defined on the master node of the rigid body, so as to mount the model (Illustration 9).

The script's actions that compose this task are:

1. find entities behind the cutting plane,
2. replace these with an appropriate rigid entity (in our case MPC, TYPE=LINK) and
3. apply the proper mounting/boundary conditions

The actual internal workings of the script are similar to those performed with the Rigidize function.

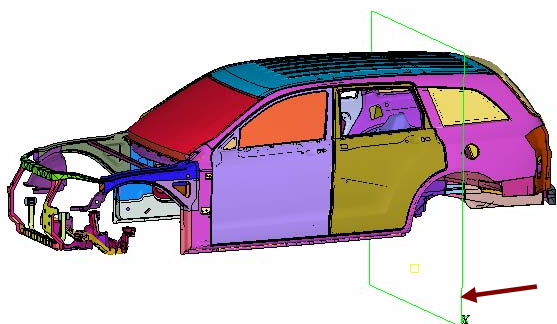


Illustration 7.: BiW and plane indicating the cutting position along the X axis.

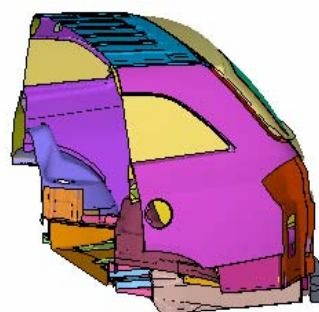


Illustration 8.: BiW after being trimmed at the desired position.

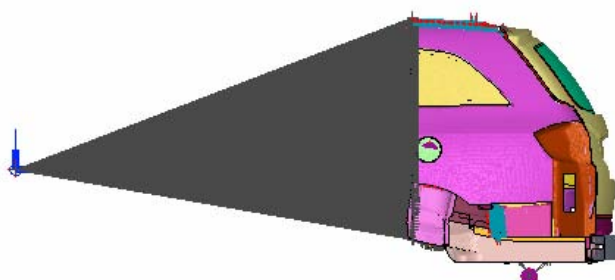


Illustration 9.: Vehicle model, trimmed by the cutting plane and mounted.

14. LIFT GATE LOAD CASE CREATION

The third and final part of the Durability template needs to address the issues of positioning the Lift Gate, applying loads to the structure and creating the required Output Requests. All these actions need to be parametric in definition and application in order to allow the easy creation and modification of the loadcase.

15. LIFT GATE POSITIONING

The Lift Gate needs to be studied at different positions. We handle each of these positions as a parameter to our template workflow. The Lift Gate is positioned and all the related definitions are automatically modified in order to match the new geometry. This behavior is achieved because of the special care that has been taken to define all related connector entities in a parametric way (Illustration 10).

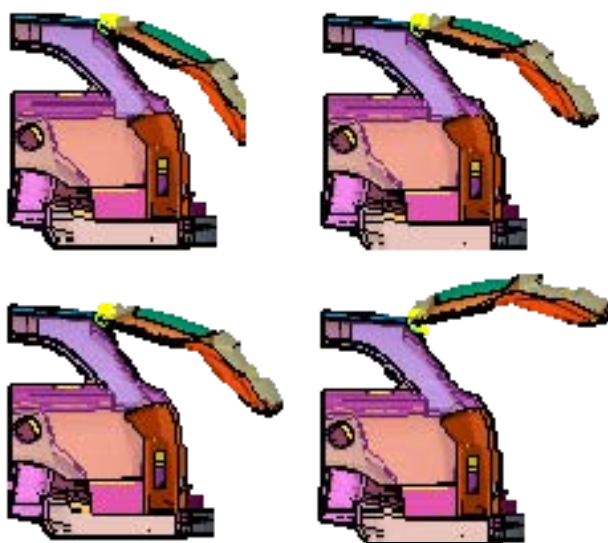


Illustration 10.: Rear Lift Gate at different opening positions

The Gate positioning is done through an *ANSA User Script*. This script is parameterized against the opening angle. It creates a transformation matrix which is applied to the components of the Lift Gate.

The geometrical transformation of the Lift Gate subassembly is simple and requires only the opening angle as a parameter. The axis of rotation is fixed and aligned to the global Y. The components that will be transformed are best defined as a collection of the properties of the Gate. This allows the positioning to succeed even when the model's geometry is modified.

The actual positioning is done through a *NMAP keyword.

16. STEP DEFINITION

The Step definition section of our template needs to consist of two major parts: the application of the loads, and the creation of the Output Requests. These are both predetermined and can be given a parametric definition to allow them to be valid for any model variation our workflow can handle.

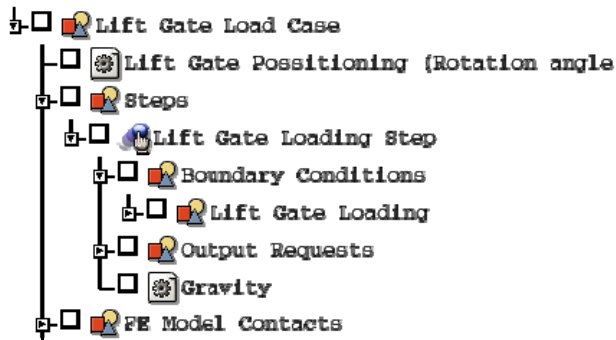


Illustration 11.: Outline of the Lift Gate load case in our Task Manager template

17. LOAD DEFINITION

The loading of the Lift Gate is in itself a parameterized definition combining a) an independent library item (Illustration 12) and b) its application method on the model.

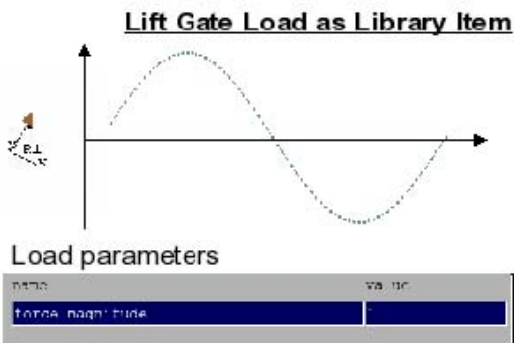


Illustration 12.: Durability analysis load, stored in ANSA DM

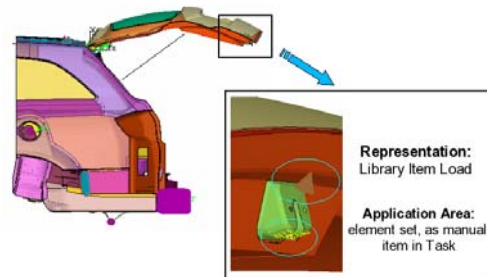


Illustration 13.: Application of the library load on the positioned model.

The loading is saved as a library item in the ANSA DM pool. The load definition is parametrized in the following ways:

1. its magnitude is a model parameter. (given as an A_PARAMETER definition, named 'force_magnitude' – through F3 in the entity's edit card)
2. the load is defined on global axis X at position [0,0,0]

The load application is performed through the use of a '*GEB Boundary Condition*' entity. This allows the possibility to predefine and automatically detect the application area. Also it allows the proper orientation of the load with respect to the position of the Lift Gate. Finally, it utilizes the parametric definition of the library load by modifying its magnitude as needed. The load application is parametric in terms of:

1. Its direction, given from the '*orientation coordinate*' of the GEB entity. In turn, this coordinate is defined with nodes on the Lift Gate, so that it follows its rotation when it is positioned.
2. Its magnitude. The load's value is defined in the GEB entity (through A_PARAMETER).
3. Its attachment position. The load is attached on a predefined area on the structure (an existing set) near the lock, with a rigid element as an interface.

18. DEFINITION OF OUTPUT REQUESTS

In the analysis template we are preparing, areas of interest where results need to be studied during post-processing, are already known (Illustration 14). Moreover, the type of required results are also known as well as the frequency in which these should be written to the solution output database (in our case the ODB).

With this information available, suitable output requests can be applied through the use of generic entities, lying at the Step section of the template.

This approach of defining Output Requests with Generic Entities leads to the automatic creation of the required node and element sets of the *NODE OUTPUT and *ELEMENT OUTPUT keywords (Illustration 15). The respective entities are detected through parameterized searches and assigned to the Output Requests. The usual considerations on the parameterization of Generic entities such as Connectors, apply here as well.

In our example, the nodes of the pin and the elements of the hinge are automatically assigned to node-output and element-output requests respectively. In particular, nodes are searched by name and elements are searched by connectivity.



Illustration 14.: Detail of the hinge. Area of interest where output request are defined.

Output requests:		
OPTION	SET ID	SET NAME
*OUTPUT		
*NODE OUTPUT	17936	Hinge LT: Gate Side Pin
*OUTPUT		
*ELEMENT OUTPUT	17939	Hinge LT: Body Side Elem

Illustration 15.: List of output requests for the durability *STEP

19. VALIDATION OF THE MODEL AND MODEL OUTPUT

The template process that is proposed in this paper ensures that a complete model will be produced and no modeling actions will be missed or left unattended.

Moreover, the template can be expanded to include and automatically perform a wide collection of checks available in ANSA. These checks will be run just before the process workflow completes.

With the completion of the checks, the template can output the complete model. As with everything else, the process can have predefined settings of all the output parameters.

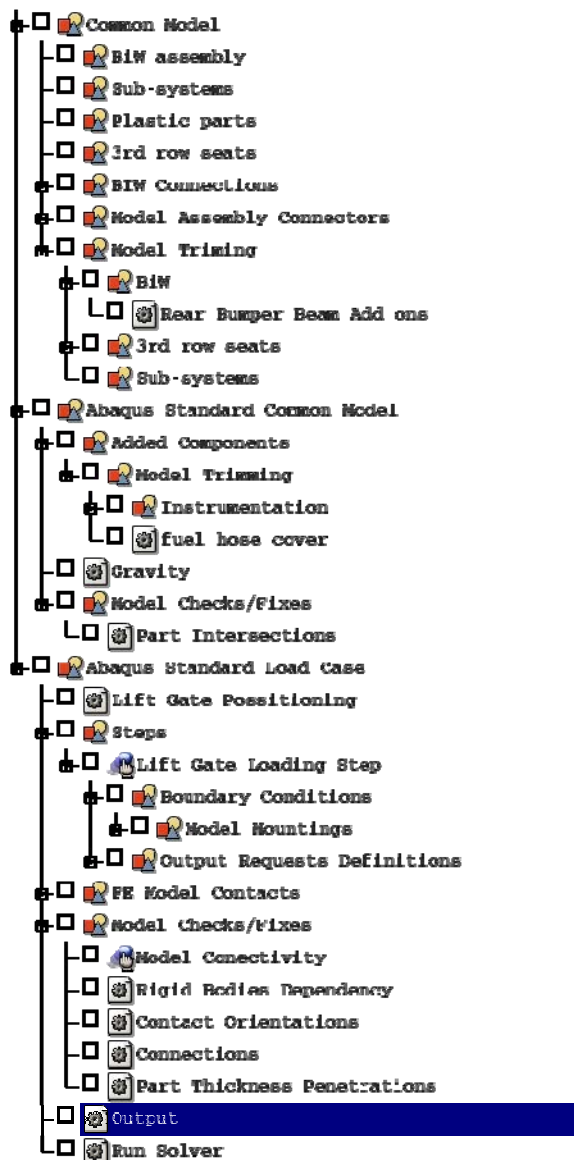


Illustration 16.: Complete TASK Manager template of the durability process workflow.

20. CONCLUSIONS

The creation of a template based process requires investigation and planning. Many of the every day practices and data handling rules of the host CAE environment have a direct affect on it. Moreover, the specific parameters and variations that the given analysis scenario wants to address need to be thoroughly considered.

All the existing model build-up techniques and the projects new requirements need to be incorporated in the newly designed template. Usage on ANSA TM and ANSA DM, as well as the parametrization guidelines described in this paper, help in making the complete process automatic, reusable and extensible (Illustration 16).

The effort spent on creating such a template process pays off. Reasons that make this true are:

1. Changes in analysis parameters are easily applied, while modifications of crucial areas / components are seamlessly imported.
2. The process becomes repeatable and robust: Actions needed to build a model are followed in sequence, considering their inter-dependencies.
3. The template process aims to reduce the overall CAE turnaround time.
4. Association with ANSA DM assists data collection and organization and promotes the use of library items.
5. Model quality becomes inherent in the process and does not depend on user experience/expertise.

REFERENCES

- (1) ANSA v12.1.2 User's Guide, BETA CAE Systems S.A., 2007
- (2) M. Giannakidis, "Outline and features of a multi-disciplinary Finite Element pre-processing system, capable of generating complete and reusable models for the field of mechanical engineering analysis", Engineering Doctorate Thesis, Aristoteles University of Thessaloniki, 2007

USING SUBMODELING TECHNIQUE TO UNDERSTAND PASSIVATION CRACKS IN MICROELECTRONIC DEVICES Pre-processing with ANSA

¹Dr. Endre Barti^{*}, ²Dr. Matthias Stecher

¹Siemens AG, Germany, ²Infineon Technologies AG, Germany

KEYWORDS - passivation cracks, microelectronics, temperature cycling, robust design, submodeling

ABSTRACT - Electronic devices like integrated circuits (IC) are used for automotive applications. The plastic (in the most cases mold compound) encapsulated devices exposed to temperature cycling (TC) undergo an excessive mechanical stress due to different coefficients of thermal expansion (CTE) of the various materials used in the system.

The large difference in the CTE between mold compound (MC) on the one hand and silicon and lead frame on the other hand causes in the metallization layers thermally induced strains and consequently stresses.

An analysis of the strains (or stresses), as they occur after molding, under subsequent tests, e.g. temperature cycling, and under realistic service conditions revealed that plastic encapsulated ICs show two main failure mechanisms, which are thermo-mechanically induced: metal shifts and passivation cracks.

This paper presents the computation of the thermally induced strains and stresses by using the Finite Element Method (FEM). The very small feature size of the passivation layer comparing with the global package size is one of the greatest problems in the application of the mentioned method and was solved by using submodeling.

Submodeling is a finite element technique that can be used to obtain more accurate results in a particular region of a model. A finite element mesh may be too coarse to produce satisfactory results in a given region of interest. The results away from this region, however, may be satisfactory. By using submodeling to generate an independent, more finely meshed model of the region of interest only made in this case the computation of the strains and stresses possible.

The large possibilities provided by the software ANSA (Automatic Net-generation for Structural Analysis) allowed a time saving generation of the 3D geometry and mesh of the submodel.

Results obtained with the FEM show a very good agreement with the location of passivation cracks as detected by Scanning Electron Microscope (SEM). It was possible to understand the mechanism of crack occurrence and to deduce corrective actions in order to develop a robust design.

TECHNICAL PAPER -

INTRODUCTION

The object of our investigation is a chip produced for automotive electronics. It is a micro electronic component having a length of 16 mm, a width of 11 mm and a thickness of 3.25 mm (Figure 11).

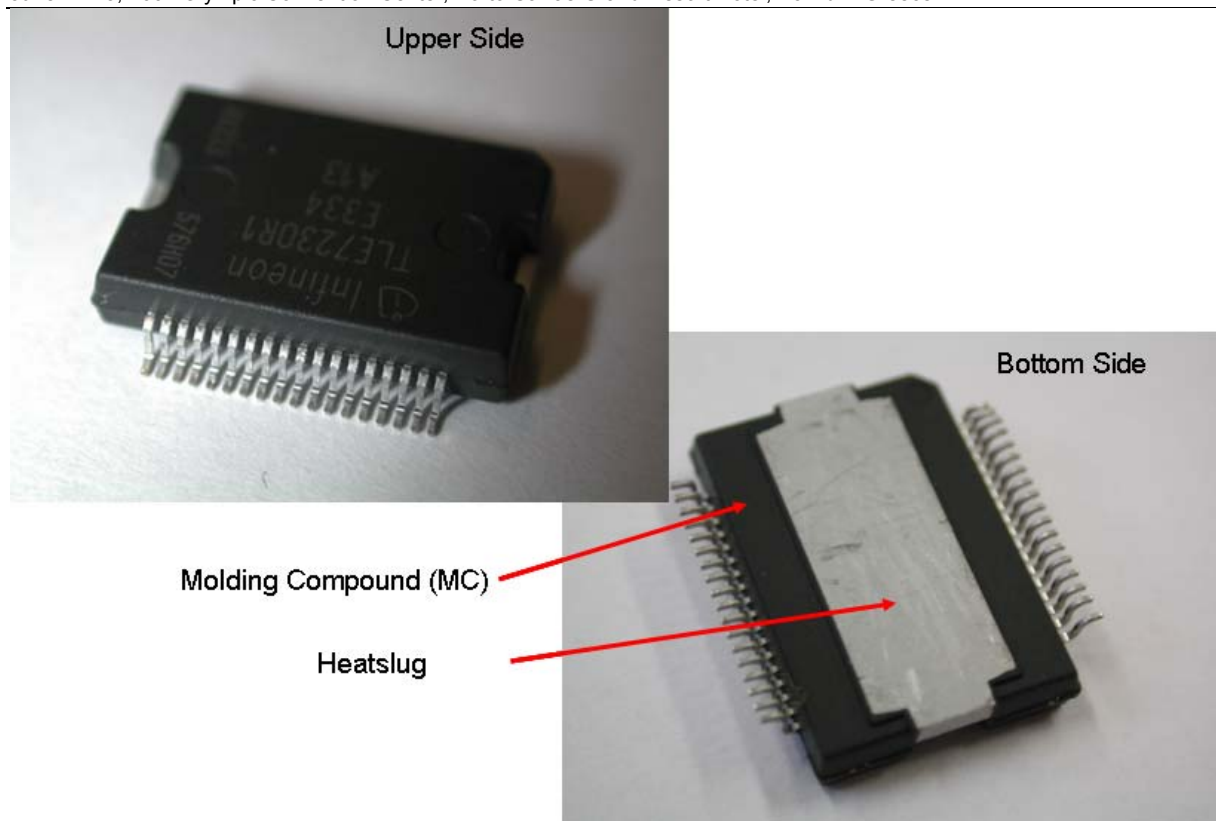


Figure 11: Examined object

This micro electronic component consists of a copper heat slug, the silicon chip, the lead frame and the molding compound. The latest serves for the protection against environmental influences like dust, humidity and chemical pollutants (Figure 12).

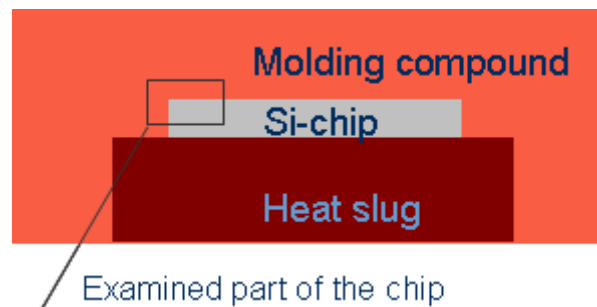


Figure 12: Longitudinal section of the examined object

To allow the contact of the individual electrical elements (i.e. transistors) with the exterior, several metal layers are needed. Isolators made of glass or ceramic are placed between the metal layers. Because the molding compound doesn't offer a 100 per cent protection, the metallization is protected with an additional passivation layer. In the presented example it consists of silicon nitride (Figure 13).

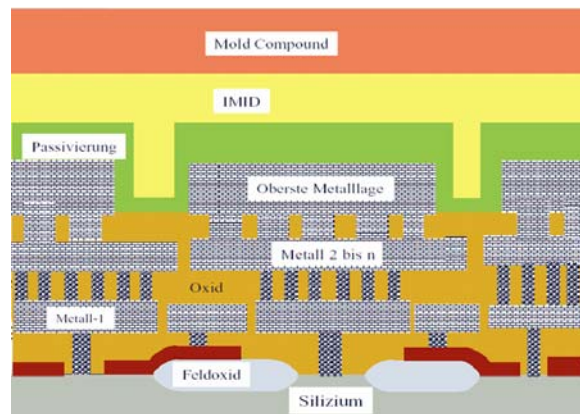


Figure 13: Metallization layers protected with an additional passivation layer

All these layers are applied one by one by chemical vapor deposition and/or sputtering at relatively high temperatures. After the production the wafer is sawed up and the individual chips are transferred to the final assembly.

The final assembly consists also of several steps. In this example the chip became soldered on the heat slug at temperatures over 300°C. After the cooling on ambient temperature the two parts become warmed and then embedded with molding compound at 175°C. After that the molded lead frames are cooled down to ambient temperature, the leads are plated and the trim and form process follows. Finally the devices are stored and delivered to the customer.

Consequently a device consists of different materials. The adhesion of the individual layers is particularly good. Very high shear stresses are induced in the component since the coefficients of thermal expansion of the layers are different. This leads in few cases to passivation cracks (Figure 14) even during the fabrication process.

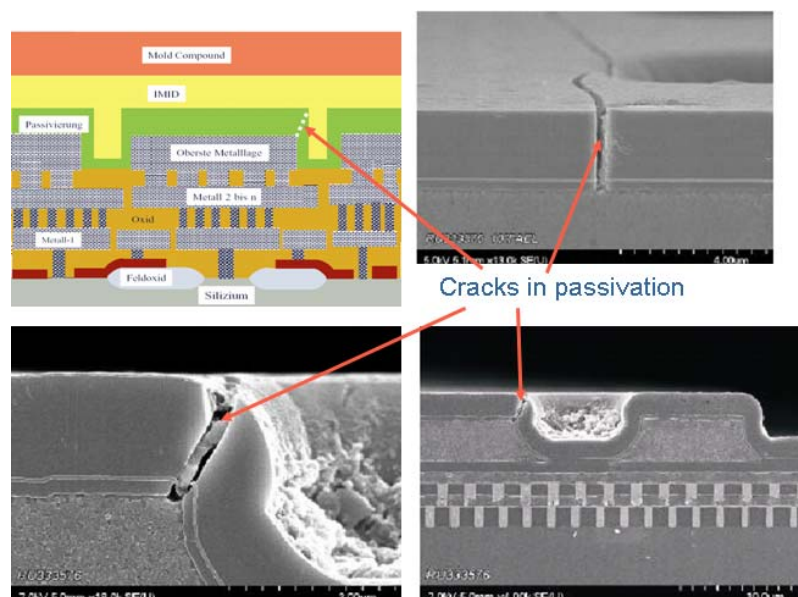


Figure 14: Scanning electron microscopy images of passivation cracks

BOUNDARY CONDITIONS

The majority of cracks occur during reliability tests like temperature cycling tests from -55°C to $+150^{\circ}\text{C}$. This extreme temperature difference causes higher shear stresses and consequently leads to the failure of the passivation layer. Corrosion caused by humidity and chemical pollutants can act now and destroy the device. This leads to the failure of the presented micro electronic component.

The aim of the technology development is to develop robust products which are able to “survive” for e.g. 1000 temperature cycles from -55°C to $+150^{\circ}\text{C}$.

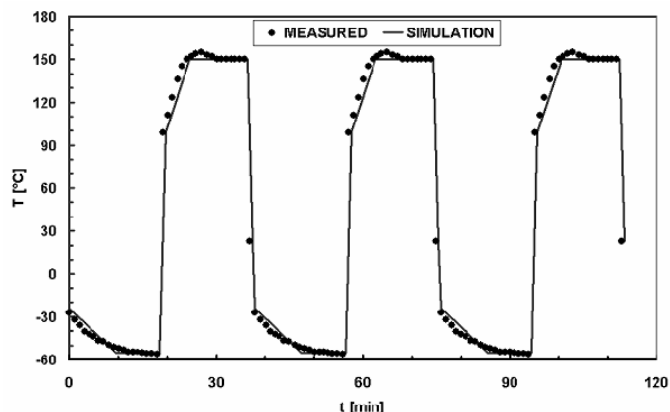


Figure 15: Three temperature cycles are shown exemplarily in this diagram.

The temperature profile during the temperature cycling test was measured in the immediate proximity of the electronic component and is represented in the (Figure 15) by the bulk symbols. A simplified temperature profile was simulated and represented in the diagram by the continuous line. The number of 1000 temperature cycles should correspond approximately to the average service time of a normally used car.

At the beginning of the project the components showed passivation cracks already after 100 temperature cycles (TC) (Figure 16).

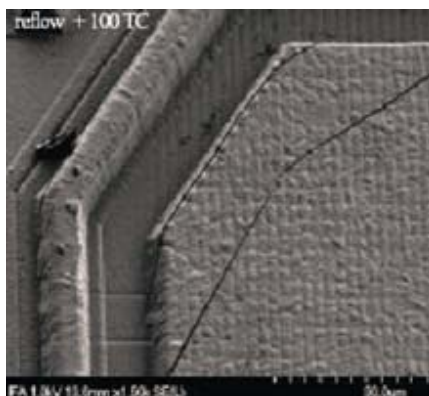


Figure 16: First visible cracks after 100 TC

MORE CRACK EXAMPLES

In Figure 17 and Figure 18 examples of passivation cracks are presented. Each figure shows the respective crack region in three different views. On the right hand side one can see a light microscopy (LM) image. It is hard to observe the cracks because the passivation layer as well as the oxide layers is transparent. In this picture one can recognize the individual metal layers. The cracks are well observable only in the scanning electron microscope (SEM) as shown in the bottom image.

Using these representations one can recognize only with difficulty the origin of the cracks. No suggestions for improvement can be derived from it. Such images can be made only at room temperature. The behavior at higher or lower temperatures can unfortunately not be derived from this representation. A FE simulation is the only possibility for a better understanding of the state of stress both at room temperature as well as at other temperatures.

On the left hand side top picture the FE model of the metal3 layer is shown. The area studied is approximately in the middle of the FE model.

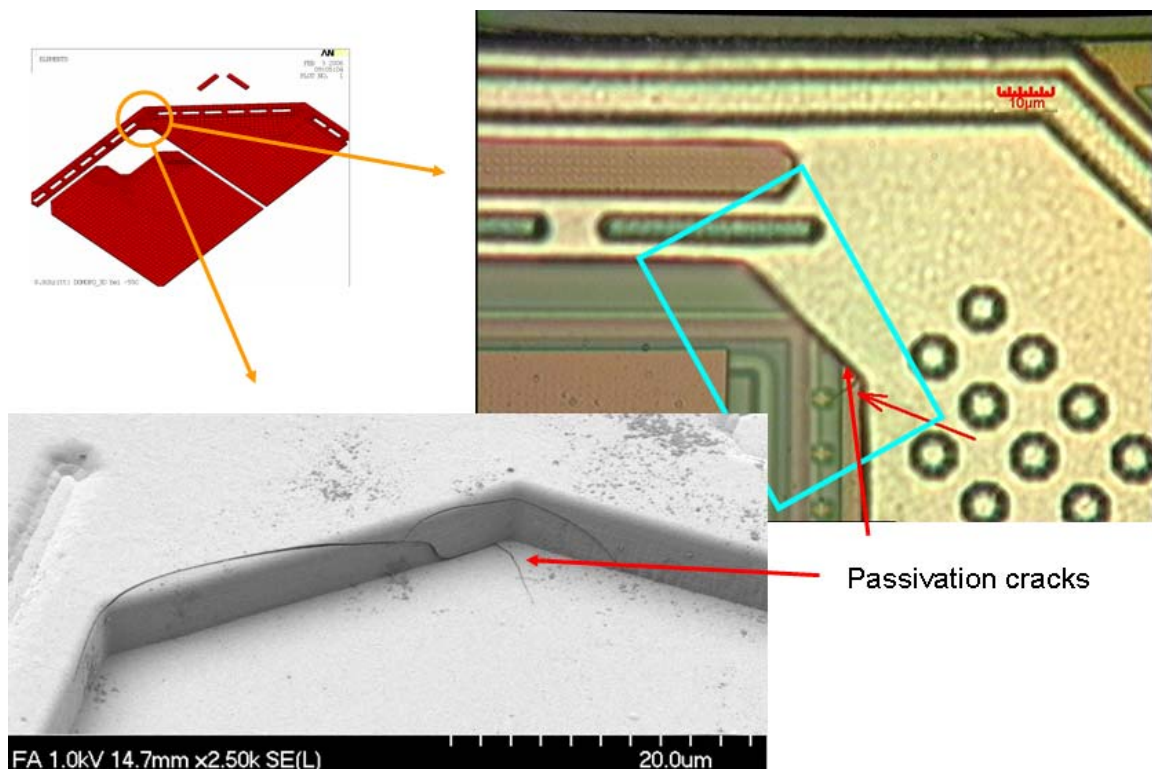


Figure 17: LM and SEM image of a crack region and the corresponding FE-Mesh of the metal 3 layer

The crack regions shown in Figure 17 and Figure 18 have been studied by FE analysis.

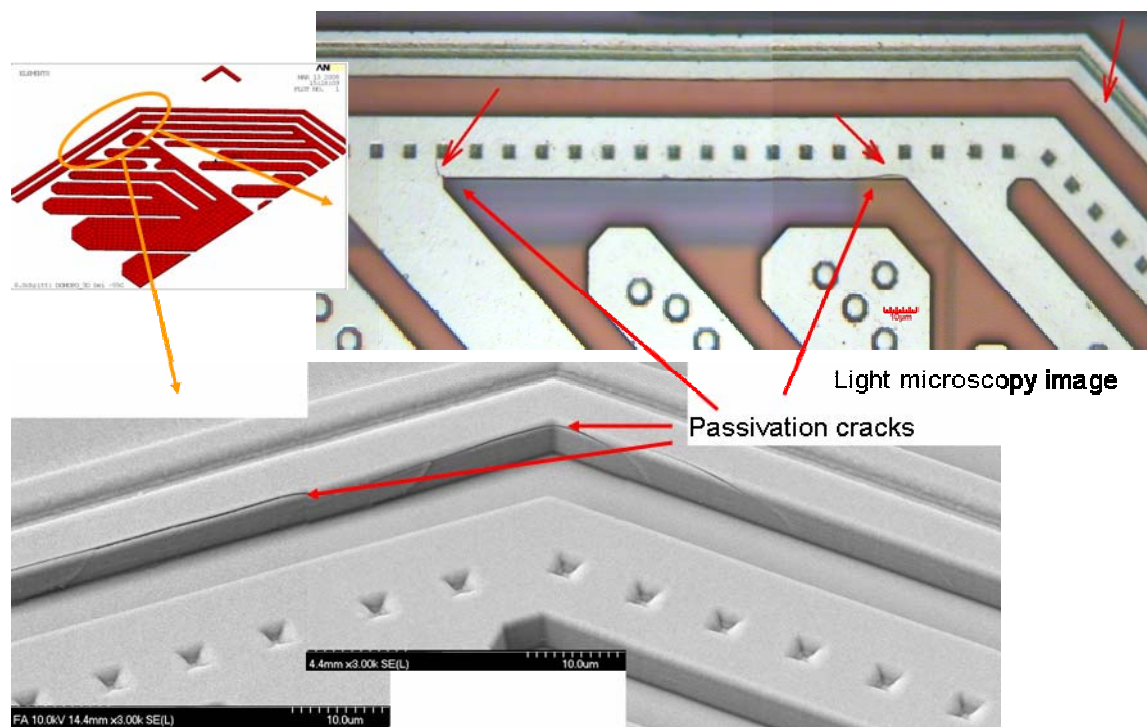


Figure 18: LM and SEM image of a crack region and the corresponding FE-Mesh of the meta 3 layer

In the FE simulation the production steps were considered because materials like solder and molding compound show a high temperature, time and stress dependency. Following production steps were simulated:

1. Wafer fabrication
2. Package fabrication
 - Silicon die (chip) attached at 305°C
 - Storage at room temperature for a few hours (simulating the time before wire bonding and embedding in mold compound)
 - Mold process at 175°C
 - Post mold cure process at 175°C
 - Storage at room temperature for a month (simulates storing at the manufacturer and transport time to the customer)
3. Simulation of one temperature cycle
 - Cooling down to -55°C and storage for 10 minutes
 - Heating up to +150°C and storage for 10 minutes
 - Cooling down to room temperature

Due to the limitation of the computer capacity only one temperature cycle could be simulated in the 3D model.

SUBMODELING

The stresses in the shown crack regions should be calculated as exactly as possible. For this purpose a fine meshing of the structure is required.

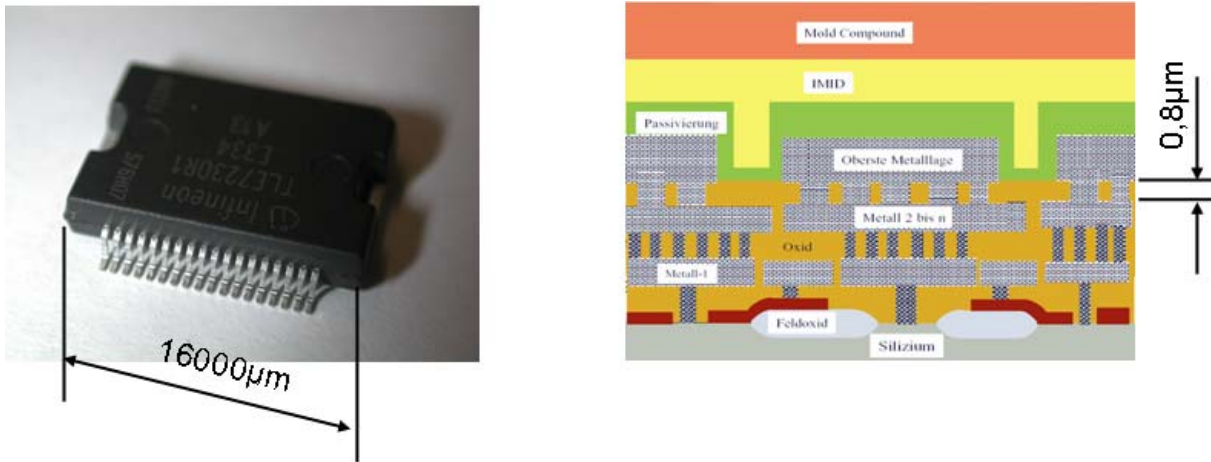


Figure 19: Ratio between longest and shortest line

Because of a ratio between the longest and shortest line of approx. 20000, many elements would be generated during the meshing of this micro electronic component (Figure 19). A simulation would be only possible on a mainframe computer. To avoid this obstacle, in the simulated examples a submodel technique in two steps was used.

Submodeling is a finite element technique (1) that can be used to obtain more accurate results in a particular region of a model (Figure 20).

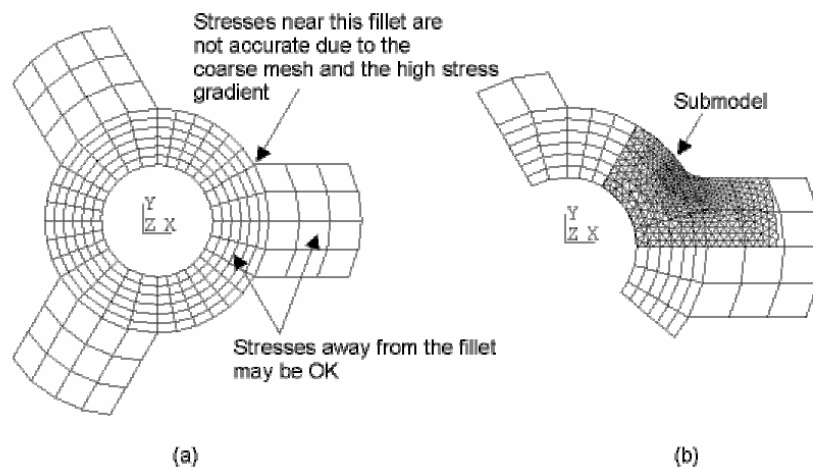


Figure 20: Submodeling technique

- (a) Coarse meshed model
- (b) Fine meshed submodel, superimposed to the coarse model

Submodeling is also known as the **cut-boundary displacement** method or the **specified boundary displacement** method. The cut boundary is the boundary of the submodel which represents a cut through the coarse model. Displacements calculated on the cut boundary of the coarse model are specified as boundary conditions for the submodel. Submodeling is based on **St. Venant's** principle, which states that if an actual distribution of forces is replaced by a statically equivalent system, the distribution of stress and strain is altered only near the regions of load application.

As already mentioned, this micro electronic component consists of several parts (Figure 21).

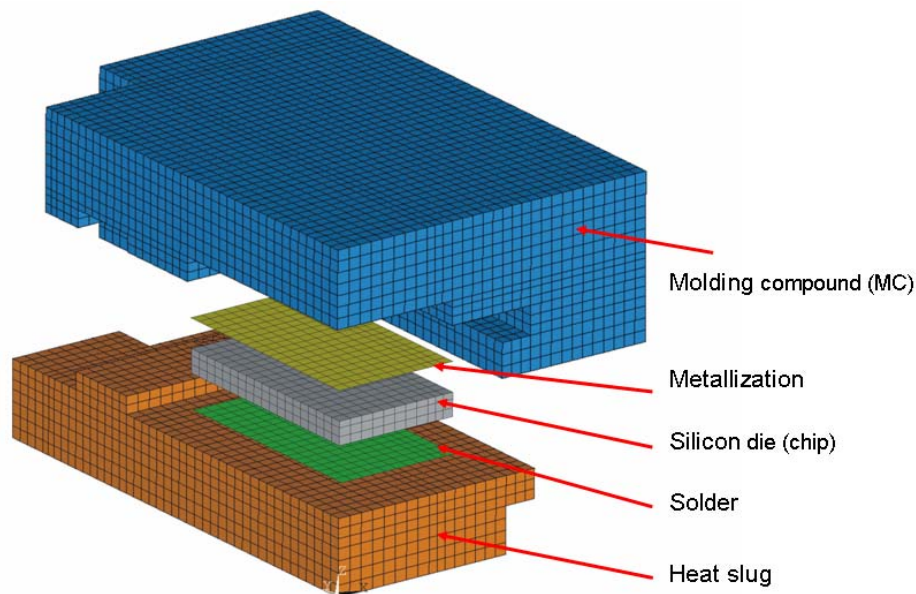


Figure 21: 3D FE coarse model

The stresses in the metallization layers are of special interest, but the modelling of the individual layers is not possible in the coarse model. Subsequently a substitute layer was used instead of this layer structure. The material properties of this substitute layer were derived from the material properties of the layer structure.

Firstly the introduced approach was verified in a 2D example. The 2D model and its position in the 3D model are presented in (Figure 22). The big aspect ratios are pointed out again.

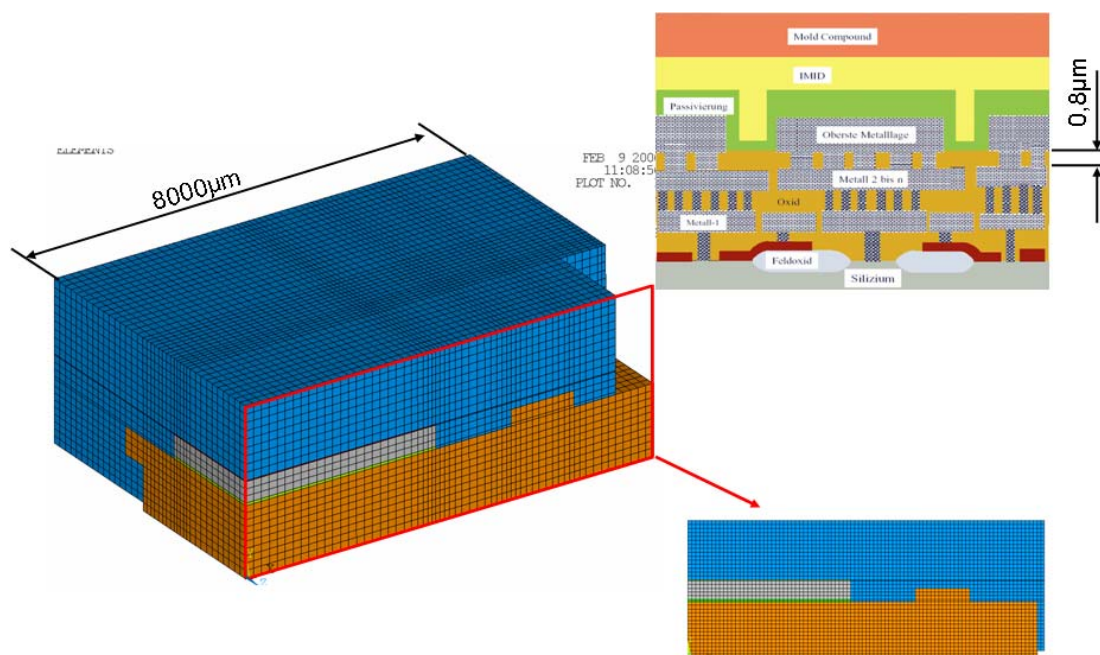


Figure 22: 3D and 2D coarse models

The coarse model, the 1st submodel and the 2nd submodel are shown in the figure below. The relative position of the individual models are pointed out by the rectangles. (Figure 23)

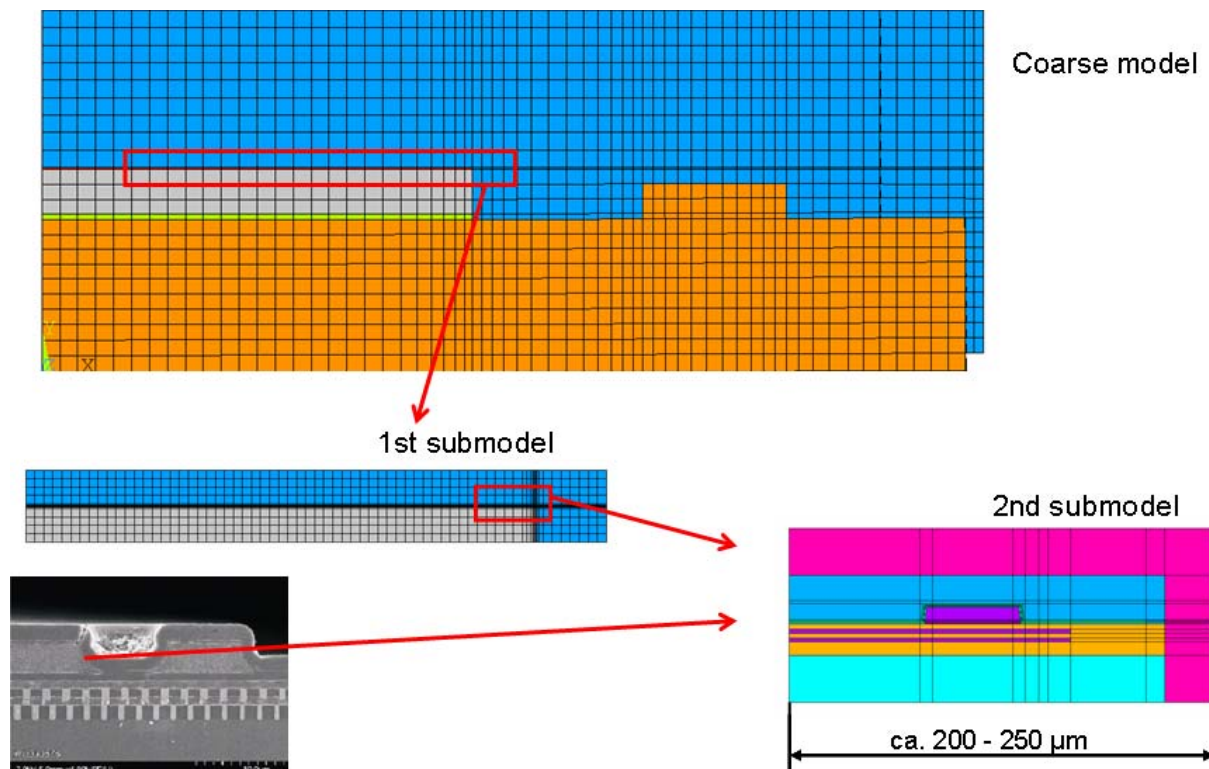


Figure 23: 2D-model of the chip – Coarse model, 1st and 2nd submodel

The 2nd submodel was created starting from the SEM picture presented in Figure 24. With this submodel first conclusions could be drawn regarding crack behavior of the studied cross section. In the submodel the aspect ratio of the longest too shortest edge was at most 250 μm to 0.8 μm. This would correspond to a ratio of at most 312,5. The obtained results allow planning and implementation of the 3D simulation.

The picture in Figure 24 represents a cross section through the 2nd submodel. It is important to include parts of silicon and molding compound in the model.

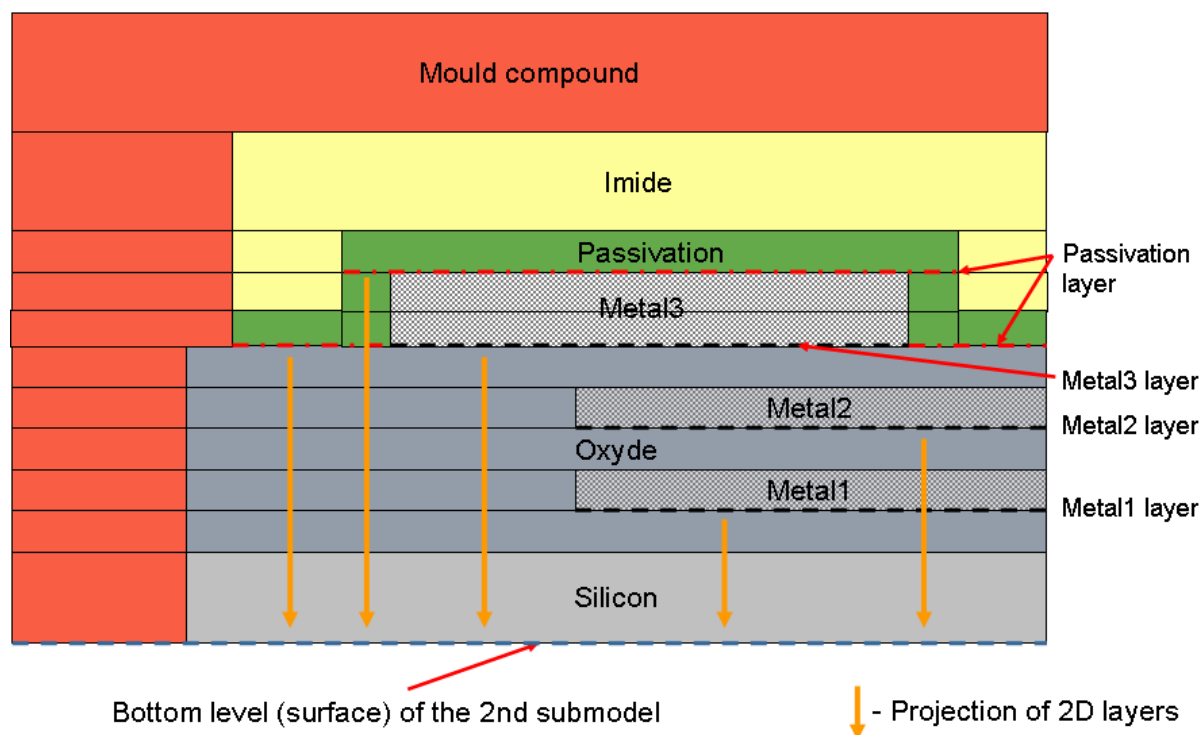


Figure 24: Cross section through the 2nd submodel

Using this cross section, the approach to the construction of the 2nd 3D submodel can be explained.

The information of the 2D representation of the three metal layers has been obtained from the E CAD tool of the layout developer. Unfortunately, only the structure of the conductors and its spatial position could be derived from this data. Consequently the 2nd 3D submodel could be created only by extrusion technique. Before the extrusion, the 2D information obtained from the layout tool had to be projected firstly onto the bottom level of the 2nd submodel. The projection of the 2D-Layers on the bottom surface is represented by the orange arrows.

In the presented example the six layers shown in (Figure 25) on the left hand side were projected onto the base of the 2nd submodel. The upper three layers are taken from the E-CAD tool of our customer. The lower three were generated in ANSA.

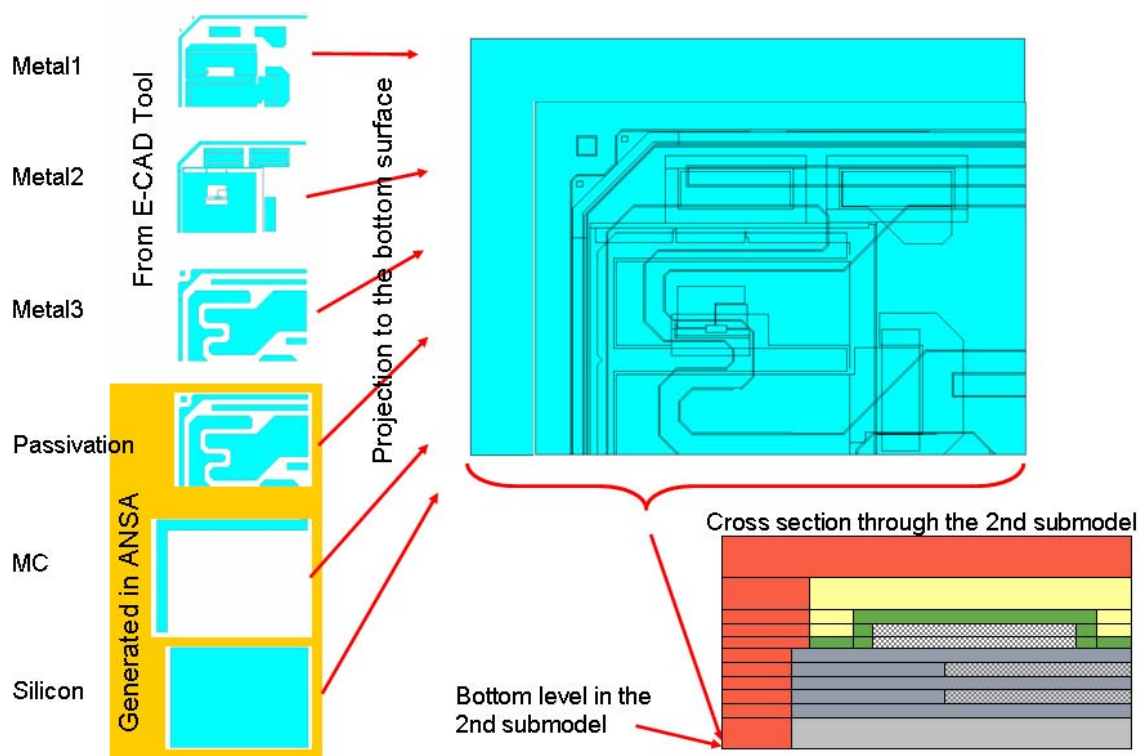


Figure 25: Projection to bottom surface

In the next step the meshing of the base was carried out (Figure 26). It is obvious that the obtained mesh is very sophisticated and it is very hard to assign the elements to the individual layers.

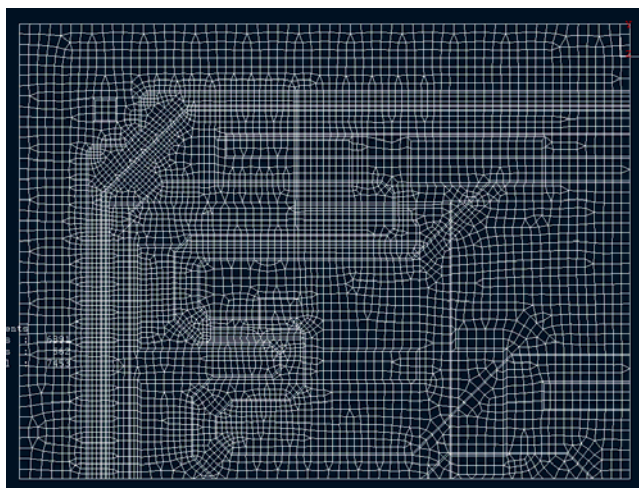


Figure 26: Meshed bottom surface

The topography of the three metal layers and the passivation layer is in the most cases very complex. The selection of the elements for the three metal layers was difficult and time consuming. The problem could be solved with ANSA very simply and very fast with the command `TOPO > RM.DBL`. The possibility of simply selecting the elements was one of the

reasons for the choice of this software. Parallel to the extrusion of the elements, the corresponding material properties were also assigned.

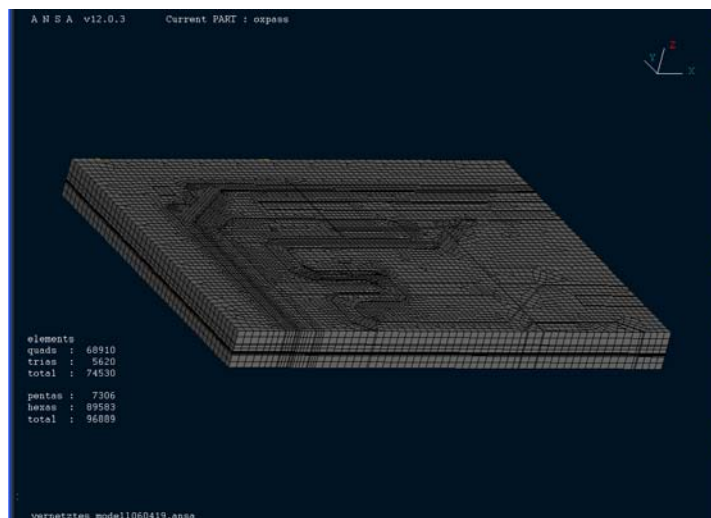


Figure 27: 3D FE-model generated by "step by step" extrusion

The simulated submodel had the size of about 750 μm to 500 μm (Figure 27 and Figure 28). The height was approximately 80 μm. The element size was reduced correspondingly in the areas where higher stress gradients were expected. Elements with midside nodes were chosen.

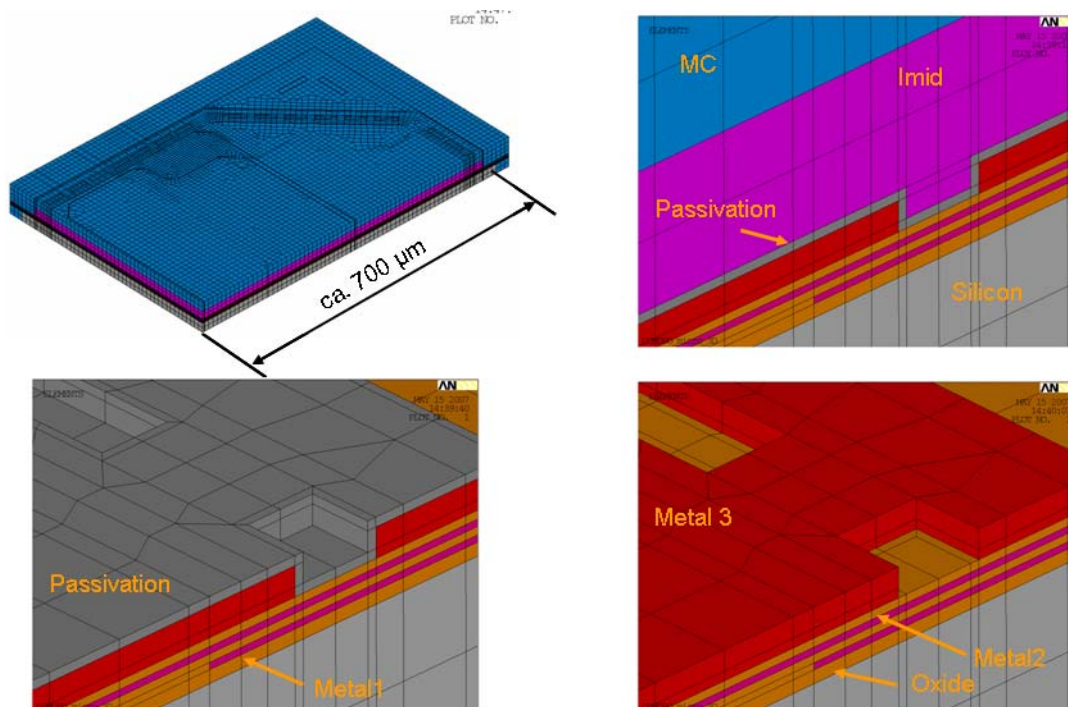


Figure 28: 3D FE-model of the crack region

3D SIMULATION OF THE CRACK REGION

In the next three figures the results of the thermo-mechanic evaluations carried out by ANSYS are presented. Since the studied passivation layer is a very brittle material, the 1st principal stress was evaluated here at -55°C (Figure 29, Figure 30 and Figure 31).

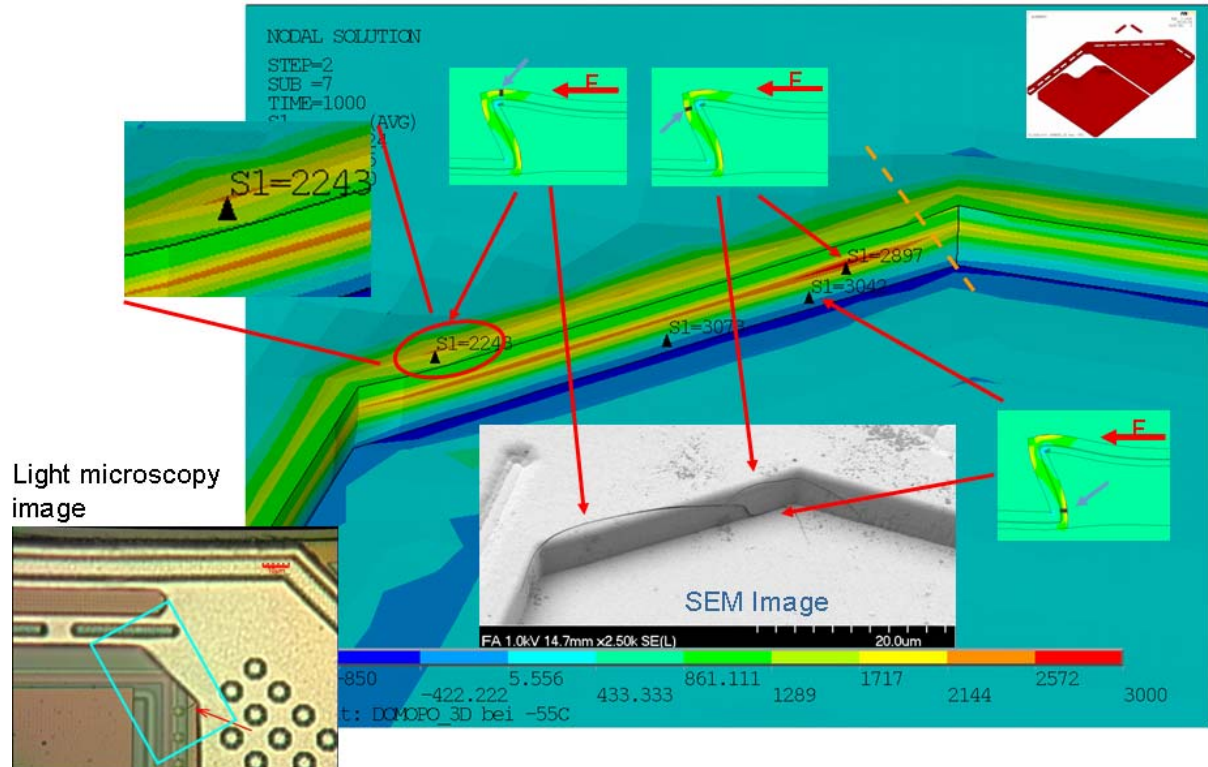


Figure 29: FE Results from 2D and 3D simulations compared with SEM Images

As mentioned above, simulations were conducted firstly in the 2D model. The result of these simulations is represented in the small windows. The simulated 2D cross section lies parallel to the direction of the forces. This corresponds approximately to the direction in the 3D submodel marked with the orange dashed line (Figure 29).

Using the 2D simulations a view into the states of strain and stress of this characteristic cross section could be obtained. With these recognitions the results in the 3D model could be better understood. In the 2D model three areas with very high principal stresses can be identified. We could recognize the stress peaks also in the 3D submodel in similar regions. In addition, the positions of these stress peaks show a very good agreement with the observed crack locations.

A good agreement of the results of simulation could also be observed with the SEM images in the submodel presented on (Figure 30). The stress peaks were compared with the actual crack locations in the region near the edge of the aluminum lines. The agreement is very good.

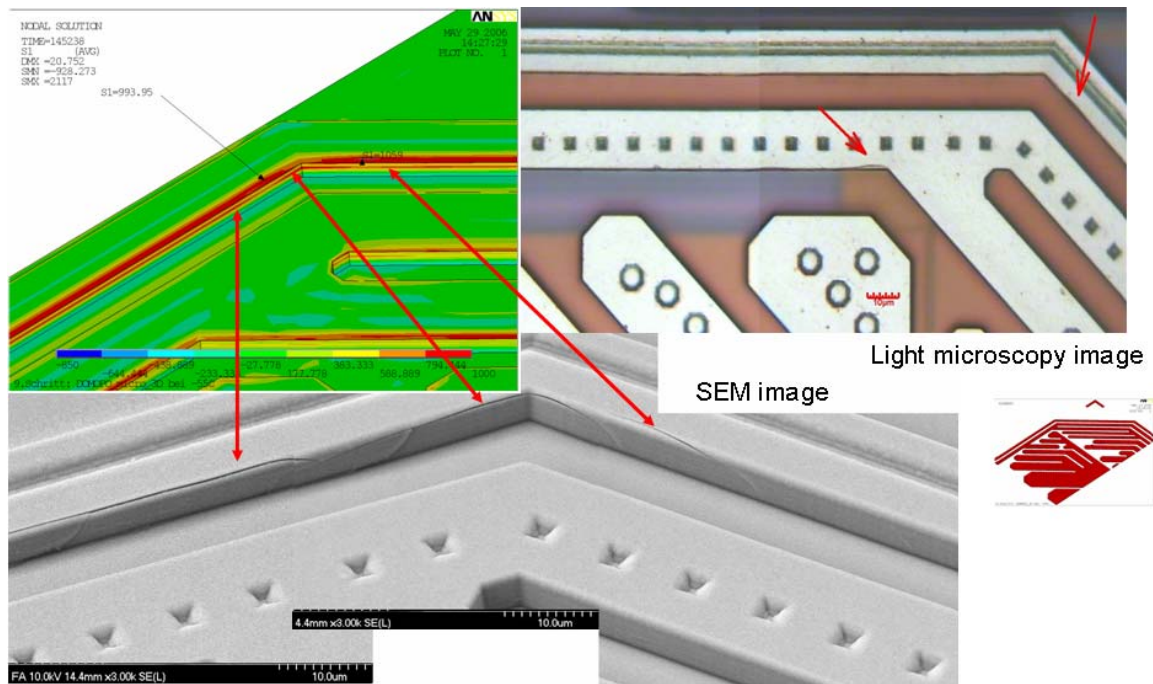


Figure 30: FE Results from 3D simulations compared with SEM Images

In Figure 31 another interesting comparison is presented. The position of the three stress peaks at the conductor edge agrees very well with the position of the three cracks on the SEM image.

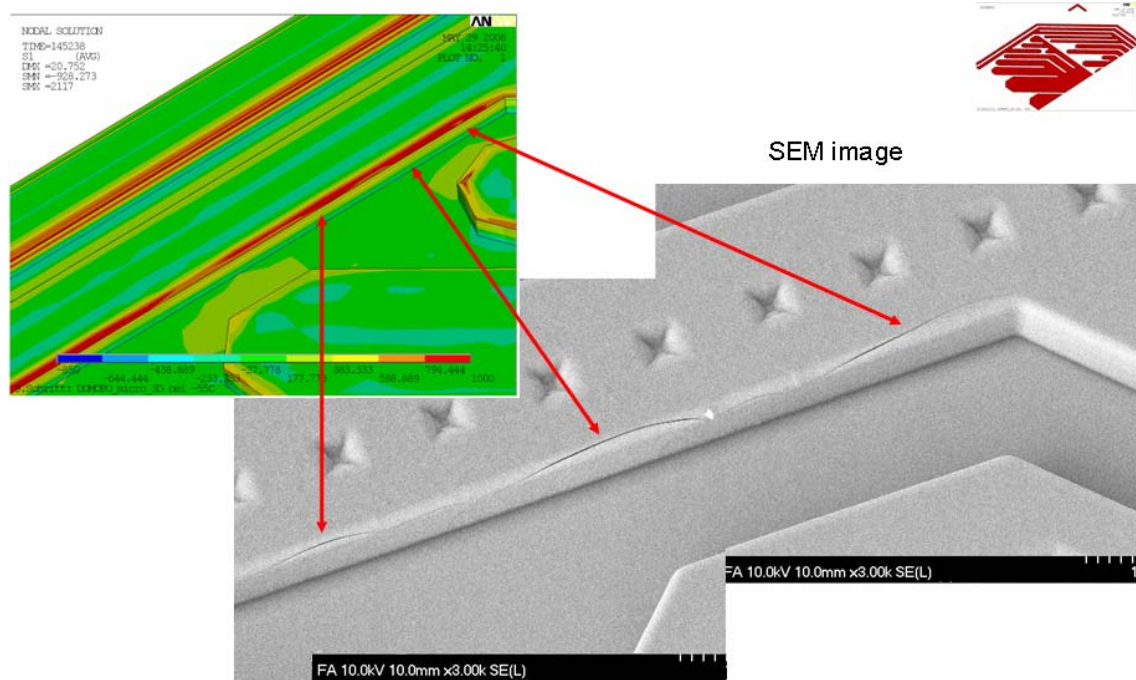


Figure 31: FE Results from 3D simulations compared with SEM Images

CONCLUSIONS

It could be shown that in spite of such extremely small structures, the 3D FE simulation can provide good results.

The location of maximum stresses shows a good correlation to the crack position observed experimentally. Thus the starting point of the passivation cracks can be predicted by FEM simulations. Additionally the influence of passivation topography on the maximum stress could be simulated and recommendations for new "Design Rules" could be deduced.

These results have a substantial contribution to the understanding of the thermo-mechanical behavior of 2 μ m thick passivation layers.

The simulations introduced here were only the top of the iceberg. Basis for these good results was the very thorough examination of the material behavior of the individual layers.

Further simulations and investigations are required to be able to predict the failure of the investigated structures.

The benefits for the device supplier are obvious. The robustness and reliability of micro electronic devices for automotive application could be improved.

REFERENCES

- (1) Ansys, Inc., Canonsburg: "Advanced Guide", ANSYS Documentation, version 10

CRACK PROPAGATION IN VARIOUS 3-D SHELL STRUCTURES, APPLICATION OF SPECIAL SOFTWARE-TOOL USING ANSA/ μ ETA WITH STANDARD ABAQUS SOLVER

Dirk Dreissig, Bernd Weisser*, Dr. Ulrich Hindenlang
LASSO Ingenieurgesellschaft mbH, Germany

KEYWORDS -

ABSTRACT - A modular crack-propagation software-tool is presented using standard Pre- and Post-processing features of ANSA and μ ETA together with ABAQUS-Standard to simulate the load/displacement history of an arbitrary 3D shell structure. In order to efficiently simulate fatigue crack propagation in large finite element models a submodel is extracted from the global model. The submodel is subjected to the probably time-dependent kinematics given in the interface to the global model.

Concerning fracture mechanics theory the stress intensity factor (SIF) concept is applied. Various examples will show the general applicability and accuracy of the developed software-modules.

ORTHOTROPIC MATERIAL OF BONES GENERATED BY MEANS OF CLINICAL CT-DATA, APPLIED TO FE-MODELS FOR THE NONLINEAR SIMULATION OF ONE-LEG STAND WITH PELVIS, FEMUR AND LOWER LEG

Ralf Schneider^{*}, Peter Helwig, Gunter Faust, Dr. Ulrich Hindenlang
LASSO Ingenieurgesellschaft mbH, Germany

KEYWORDS -

ABSTRACT - A realistically modelling of the material of bones on the basis of clinical CT-Data is presented well suited for nonlinear analyses. The determination of the needed independent variables for the orthotropic stiffness was performed using established procedures. The identification of the different directions of orthotropy was carried out with the so called Star-length-distribution.

Using these directions the Youngs-moduli are evaluated by following the method invented by Roh-Hobatho-Ashman interpreting the density distribution of the CT-Data. The determination of the Poissons ratios was ascertained by empirical knowledge and then used for the definition of shear-moduli. The mapping of these sets of data to the realistic FE-model of one-leg-stand is presented, which is built of pelvis, femur and lower leg together with their appropriate muscles and tendons.

The sane skeleton as well as a stabilised trochantric fracture is shown in a one-leg-stand situation, analysed with a nonlinear standard solver to visualize the functionality of the implant with respect to the different distribution of forces.

Session H3.6

PREDICTION OF E-COAT VOIDS AND PUDDLES DURING AUTOMOTIVE PAINTING USING ANSA

¹Prasad Dev Hanumalagutti, ¹Yu-Ning Liu, ²Ramu Mothukuri*

¹Research and Advanced Engineering, Ford Motor Company, Dearborn, Michigan, USA,

²BETA CAE Systems Inc., USA

KEYWORDS - V.Traps, e-Coat void, e-Coat puddle, automotive paint, corrosion resistance

ABSTRACT - In automotive painting, Electro-Coat (e-coat) is applied to the car body sheet metal to increase its corrosion resistance. After e-coat application another three coatings of paint materials, namely prime, basecoat and clearcoat, are applied to provide the final paint finish. E-coat voids and puddles are common issues occurred during e-coat application and this study uses ANSA to identify the potential problem areas.

After the car body is coated with e-coat it is sent through a baking oven for curing. Two of the most common issues that occur during this process are voids and puddles. A void occurs when air is trapped in vehicle cavities. This prevents contact of the e-coat bath with the metal and thereby prevents paint deposition. A puddle occurs when excess e-coat liquid is trapped in the vehicle cavities due to incomplete drainage. This excess e-coat liquid reaches its boiling point while in the oven and can cause poor appearance on the vehicle exterior surface.

ANSA's built-in feature, V.Traps, was utilized in this study to detect the formation of voids and puddles. Combined with ANSA's localized meshing and hole creation features, it is easy to study the effectiveness of drainage hole locations on voids and puddles. Results of the case study are presented along with recommendations to enhance V.Traps features. A comparison between the traditional method for void and puddle prediction and ANSA's V.Traps feature is also included.

TECHNICAL PAPER -

1. INTRODUCTION

Modern automotive painting is a highly complex process that provides corrosion resistance, color, and a glossy finish to the vehicle body. The shell of the vehicle enters the paint shop from the body shop and goes through a pretreatment process. In the pretreatment process, oil and debris are washed off of the vehicle body and phosphate is deposited on the metallic surface. Phosphate is an important part of the paint corrosion protection system and increases the adhesion of e-coat to metallic surfaces. The vehicle body then goes through the e-coat process. E-coat is an epoxy paint layer which is applied using electro-deposition. This paint layer is cured in an e-coat oven to ensure the performance characteristics of the coating. Following e-coat, prime is applied to exterior surfaces and cured, followed by enamel application and cure. The purpose of primer is for chip resistance, protection of the e-coat from UV light, and improved surface smoothness. Two layers of coating are applied in the enamel process, basecoat and clearcoat. Basecoat provides the color, while clearcoat provides the glossy appearance and scratch resistance to the finished vehicle body.

The main purpose of e-coating is for corrosion resistance. The vehicle body is hung from an overhead conveyer with chains and dipped into a tank that is filled with e-coat paint (see Figure 1). Electrodeposition occurs in the tank and builds a layer of e-coat film on interior and exterior surfaces of the vehicle body. E-coat must cover all sheet metal surfaces, including recessed locations such as rocker panels, in order to protect these regions from corrosion. That is part of the reason why e-coat is applied using an immersion process, whereas prime and enamel paint are applied only on exterior surfaces using a spray process.

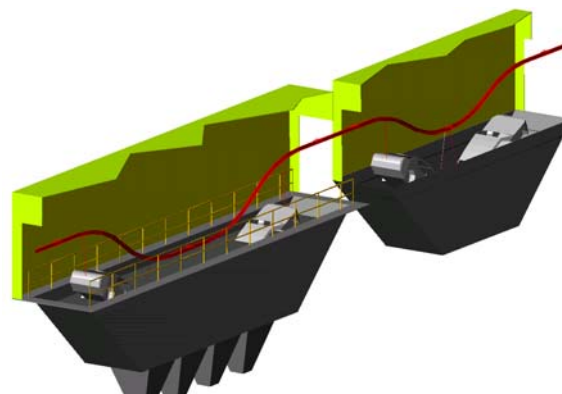


Figure 1: Schematics of a typical e-coat process

Common defects of e-coat include areas of no paint and runout. No paint usually is because of air bubbles trapped under a concave surface where the sheet metal did not have a contact with the e-coat bath and therefore no material was deposited. Runout usually happens when the e-coat liquid stays in a convex surface and forms a puddle. The liquid in the puddle boils during baking and drips on the sheet metal. The drip is usually sanded to provide a smooth surface for further painting. However, sanding results in thin or no e-coat film protection at that location and hence a potential problematic site for corrosion performance. The dust generated during sanding also creates dirt problems in the paint process.

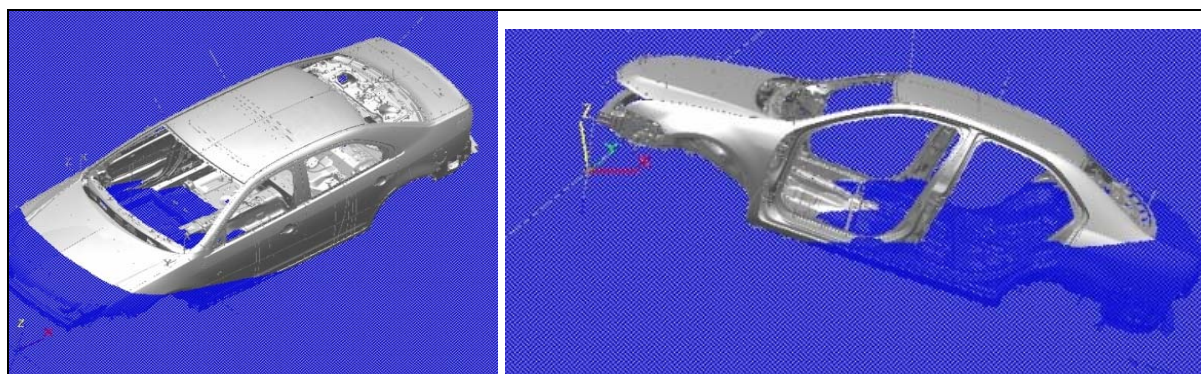
The purpose of this paper is to discuss the techniques used to detect voids and puddles during the e-coat process from the perspective of vehicle body design. A comparison between the traditional processes and the V.TRAPS functionality of ANSA is included. Case studies of sheet metal parts were used to verify the capability of the new tool, followed by an attempt to define and apply the process for a full-vehicle analysis. At the end, a summary of the case studies and recommended next steps are included.

2. TRADITIONAL PROCESSES

Traditionally, in order to identify problem areas of e-coat voids and puddles, prototype vehicles are used. These prototype vehicles are e-coated to observe no-paint and runout problems. Enclosed areas of the vehicle are cut apart and film builds are measured manually to identify regions of no paint or thin paint problems (see Figure 2). This process is very expensive and time consuming. Automotive manufacturers can only afford a limited number of prototypes for each vehicle program using this destructive method.



Figure 2: A prototype is cut open to measure e-coat film build inside the rocker.



(a)

(b)

Figure 3: Using visualization software to find air bubbles and e-coat puddles; (a) when the vehicle enters the tank and (b) when the vehicle leaving the tank.

Thanks to the fast progress of computer technology, engineers can now detect problem using CAD data in the virtual world. This is much cheaper and can be performed earlier in the vehicle development process than the aforementioned destructive method. It also provides engineers the opportunity to improve the design and iterate before physical vehicles are launched. Visualization software is used for the analysis. The analyst tilts the vehicle according to the entrance and exit angle of the e-coat tank, creates a horizontal surface to represent the e-coat liquid surface (see Figure 3), and moves this surface vertically throughout the vehicle to simulate the process of vehicle entering/exiting the tank. The analyst looks for areas of the liquid surface that are isolated by sheet metal, and then look for drainage holes (air escape holes) on the sheet metal. If there is no hole for the liquid/air to escape, it is potentially a problem area for a puddle/void. However, this is a manual process. The accuracy and efficiency totally depends on the experience level of the analyst. An experienced analyst can finish the analysis for a full vehicle body in one working day. This approach can only provide the information of where the potential problem areas are, but cannot predict the size of the e-coat voids or puddles.

3. ANSA V.TRAPS

The V.TRAPS tool of ANSA identifies the regions of resting liquid or air bubble enclosures formed when a complete body-in-white (BIW) or a few parts are positioned to represent the entrance, horizontal and exit positions with respect to the virtual bath. This process is fully automatic and calculates the location as well as volume of air bubbles and e-coat puddles. It also allows the engineers to quickly open holes in the model and evaluate their effectiveness.

In preparation for the use of the V.TRAPS tool, the CAE model must be meshed with triangular elements free from intersections and duplicate elements as shown in the Figure 4. Upon activating the V.TRAPS tool, the model becomes transparent as shown in Figure 5. Using the positioning tool, the model is oriented to match the entrance and exit angles of the actual e-coat tank that the new vehicle will be launched.

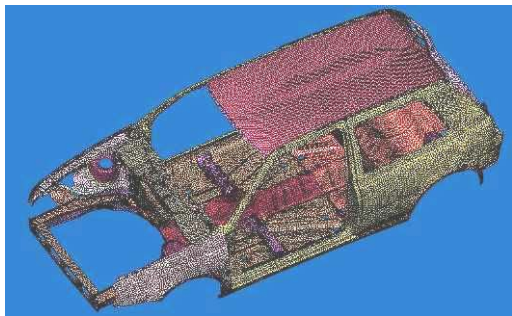


Figure 4: An example of mesh ready for V.TRAPS analysis.

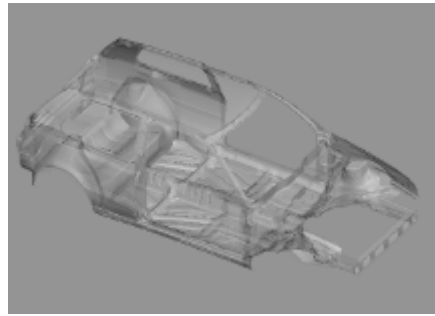


Figure 5: Vehicle model in transparent form after V.TRAPS is activated.

Check for Voids or Bubbles

After the mesh is ready, the vehicle body is first positioned to match the entrance angle of the actual e-coat bath as shown in Figure 6, then the bubble check button is activated and step size is specified. ANSA identifies the air trapped in vehicle cavities and displays the total volume, total metal wetted area, positioning and the step size used for the analysis as shown in Figure 7. The user has an option to specify a minimum significant volume below which the traps are ignored and not shown on the screen. The user also has the option to traverse through all traps to evaluate their significance.

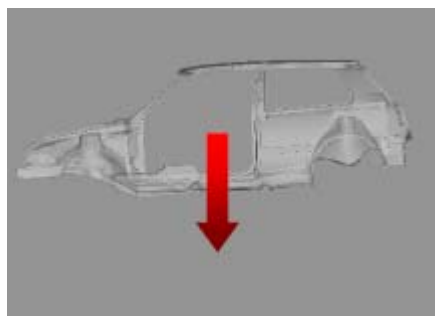


Figure 6: Bubble check in progress

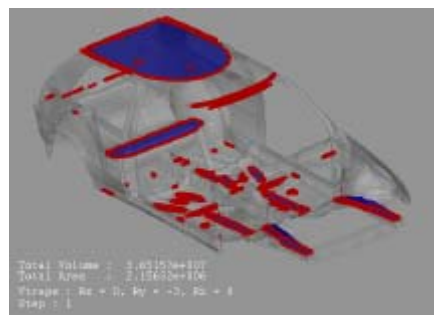


Figure 7: Results of bubble check.

Check for Puddles or Ponds

Regions of excess e-coat liquid trapped in the vehicle cavities due to incomplete drainage are identified using the “Ponds Check” function. The BIW is positioned horizontally or at an angle representing the exit of the vehicle of the e-coat tank as shown in Figure 8 and the pond check button is activated. ANSA identifies the puddles in the model and displays them on the screen along with the total volume, wetted area, positioning and the step size used in the analysis as shown in Figure 9.

After completion of the analysis, ANSA automatically saves the simulation results as shell elements with a separate part and PID for easy filtering and viewing.

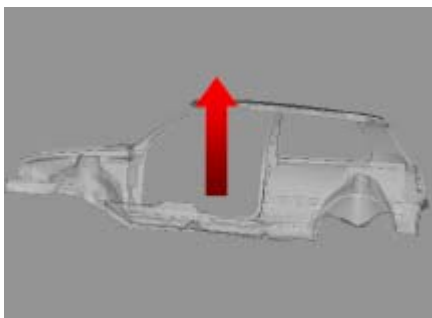


Figure 8: Pond check in progress

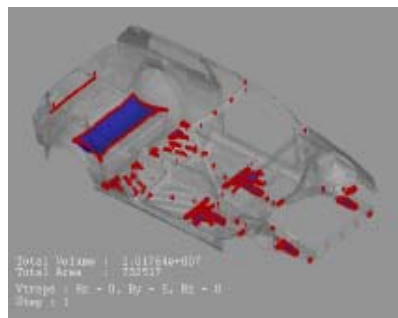


Figure 9: Results of pond

V.TRAPS CAPABILITY VERIFICATION

Two case studies were performed to verify the capability of V.TRAPS. The purpose of these studies was to demonstrate the void/puddle detection capability of V.TRAPS and compare the results with the traditional method using visualization software as well as experiences during vehicle launch.

Case Study 1 – Rear Floor Pan

The traditional method predicted that there would be e-coat accumulation in the highlighted regions of the rear floor pan as shown in Figure 10. But the process could not determine the extent of accumulation.

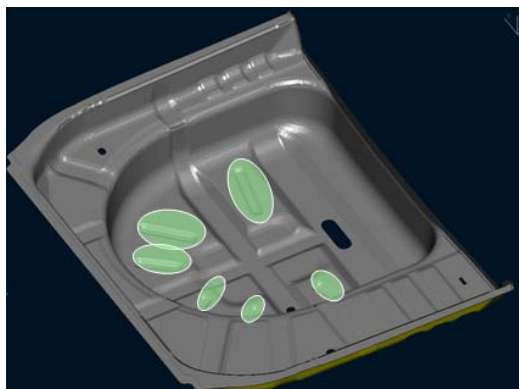


Figure 10: The traditional method predicted e-coat puddles in the indentations.

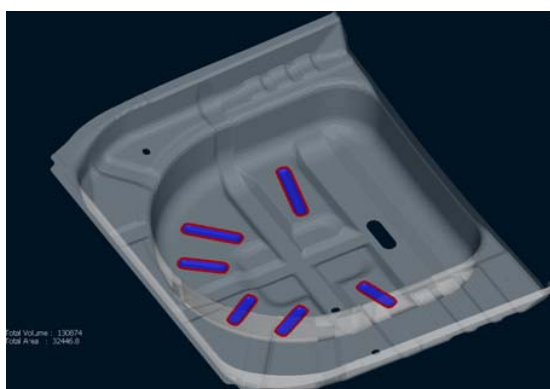


Figure 11: Results of V.TRAPS analysis on the same part.

The same model was prepared and meshed in ANSA and then analyzed using V.TRAPS as shown in Figure 11. The results were verified to match the results obtained by the traditional process. The tool also calculated the total volume of these puddles to be about 1 cc (1083 mm³). This small amount of e-coat accumulation would flatten over the surface of the sheet metal thus increasing the e-coat thickness by just a few microns. Such small volume of accumulation would not pose a big problem when the unit goes through the curing oven. Hence, a design change is not necessary. This case study demonstrated the value of V.TRAPS capability of calculating bubble/puddle volume. The ability of V.TRAPS to quantify the bubble or puddle volume helps in deciding if any design changes are required. Without the knowledge of the volume, unnecessary design changes would be performed and extra cost and time delay would occur.

Case Study 2 – Rear Quarter Panel

In the original study using the traditional process, a problem in the rear quarter panel was undetected and resulting in a significant accumulation of e-coat. This was observed later during physical launch. In order to solve the problem engineers added a hole to drain the accumulation. The same model was prepared and meshed in ANSA and then analyzed using V-TRAPS. The V-TRAPS tool was able to detect the e-coat accumulation and also calculated the volume to be 32 cc (10 oz) as shown by Figure 12.



Figure 12: E-coat accumulation was identified by V.TRAPS.



Figure 13: The capability of evaluating effectiveness of drainage holes was demonstrated

With ANSA’s mesh editing features, an opening was created to represent a drainage hole in the sheet metal. The analysis was re-run and it was observed that the e-coat accumulation reduced to minimal (Figure 13). Hence, ANSA could have detected the issues that the traditional process overlooks early in the design phase. This case study also demonstrated the value of ANSA's mesh editing feature which enables simulation of a drainage hole and evaluate its effectiveness.

4. FULL VEHICLE ANALYSIS

After the bubble/puddle detecting capability of V.TRAPS was verified by the above two case studies on sheet metal parts, the next step was to define the process of analyzing a full vehicle body using V.TRAPS. Model preparation was identified as a potential problem. A full vehicle body consists of a large number of sheet metal parts. These parts are put together in the body shop by seam welding, bonding, or fastening. Sealers are applied to seal off gaps between parts. However, in the virtual world, all parts are separate and gaps exist between them. V.TRAPS sees these gaps as escape channels for air/liquid and no bubble/puddle will be formed. It is necessary to seal the parts at the mesh or CAD level to represent the welds or sealers. Two approaches were evaluated, one begins with raw CAD (IGES, IDEAS, or CATIA format), and the other begins with an existing mesh.

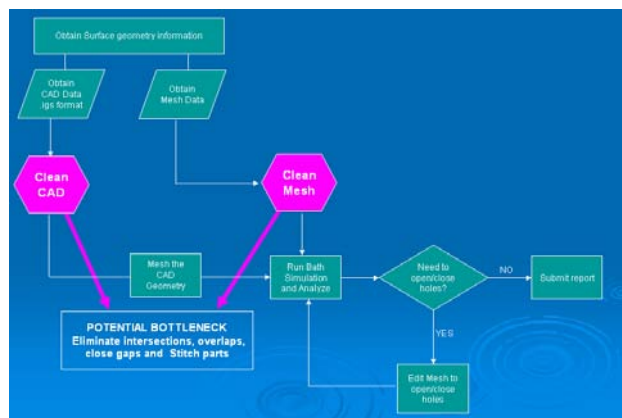


Figure 14: Process of full vehicle analysis

Model Preparation – Raw CAD

To prepare a V.TRAPS model for paint bath analysis, the CAD model of the BIW in the form of IDEAS, CATIA or IGES is used. This CAD is then translated into ANSA either using the CATIA translator or using the IGES reader available within ANSA. The translated CAD is then cleaned using tools available in ANSA under the TOPO menu.

The next step is to stitch/fuse the parts together at the welded flange as shown in the figure 15. To represent the actual welding the flanges has to be “fused” together, otherwise the V.TRAPS detects these as openings and allows air/fluid to leak through the gaps. Fusing is performed preferably at TOPO level using CAD functions, Alternatively, the user can also create shell elements and close the gaps using other function in the MESH menu. Red and Cyan representing free and multiple edges respectively and pose no problem for the V.TRAPS analysis.

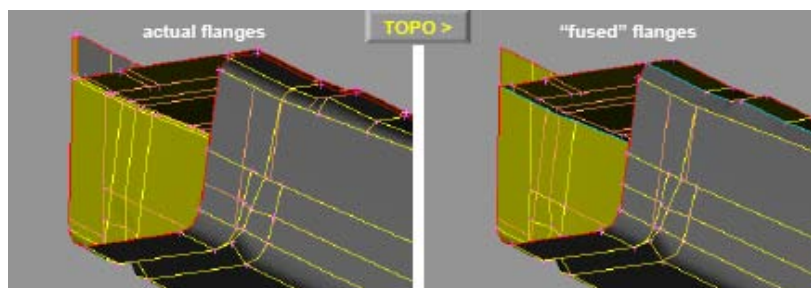


Figure 15: Model preparation for V.TRAPS analysis.

Once the stitching of the parts is done, the model is meshed using triangular elements. Any duplicate elements in the model are identified and deleted. The final step in model preparation is to eliminate intersections in the model. ANSA automatically identifies the intersecting parts and highlights them on the screen. The user then offsets the nearby parts or moves the nearby nodes to clear the penetrations. The model is now ready to be analyzed using V.TRAPS tool. After the analysis, if there is more than acceptable amount of voids and puddles the user can add drainage holes and re-run the analysis to study their effectiveness.

Model Preparation – Existing FE Mesh

Alternatively, an existing finite element mesh can be obtained from other CAE groups for analysis. If the obtained mesh has any quad elements in it they are converted to triangular elements. The mesh is checked for any intersections and fixed if required. The parts are stitched at the welded flanges as described above to represent welds and sealers.

Case Study 3 – Floor Pan

A study was performed to estimate the approximate time needed to clean a finite element mesh before a full vehicle body can be analyzed using V.TRAPS. A previously generated mesh was utilized for this study. The cleanup started with the floor pan. The mesh was converted to triangular elements and the edges were stitched to represent welds and sealers. It took approximately an hour to prepare this module for ANSA's V-TRAPS analysis (as shown in Figure 16).

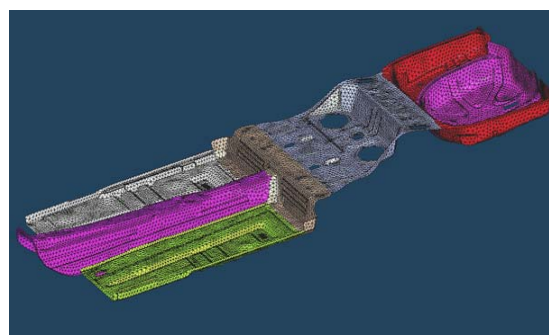


Figure 16: It took one hour to prepare a floor pan with 8 parts. It is estimated to take hundreds of man-hour to prepare a full vehicle model.

At this stage it was estimated that it would take hundreds of man-hours to fix a mesh of a full vehicle body including all the closure panels. The amount of time needed depends on the complexity of the model and the quality of the base mesh. Due to the time limit on this study it is not practical to continue the process to prepare the full vehicle model for V.TRAPS analysis.

5. SUMMARY

ANSA's V.TRAPS functionality of identifying e-coat voids and puddles was evaluated. It is superior to the existing traditional process in several areas. V.TRAPS is an automatic process that eliminates the human factor in the traditional method. It also has the ability to calculate the volume of the bubble/puddle. ANSA is capable of creating a drainage hole in the mesh and evaluate the effectiveness of the hole. It is also useful to evaluate an effective drainage hole design if the void or puddle is above the acceptable size. However, the mesh requirement for V.TRAPS is too strict. The time needed to clean up the geometry for a full vehicle analysis is unacceptable. The use of this tool is recommended only to perform analysis on a single sheet metal part or an isolated module. It is not practical to use this tool for the analysis of a full vehicle body unless there's a dramatic improvement of the geometry data quality or if there are improvements on V.TRAPS functionality that takes into consideration that small gaps between sheet metals to be ignored.

6. NEXT STEPS

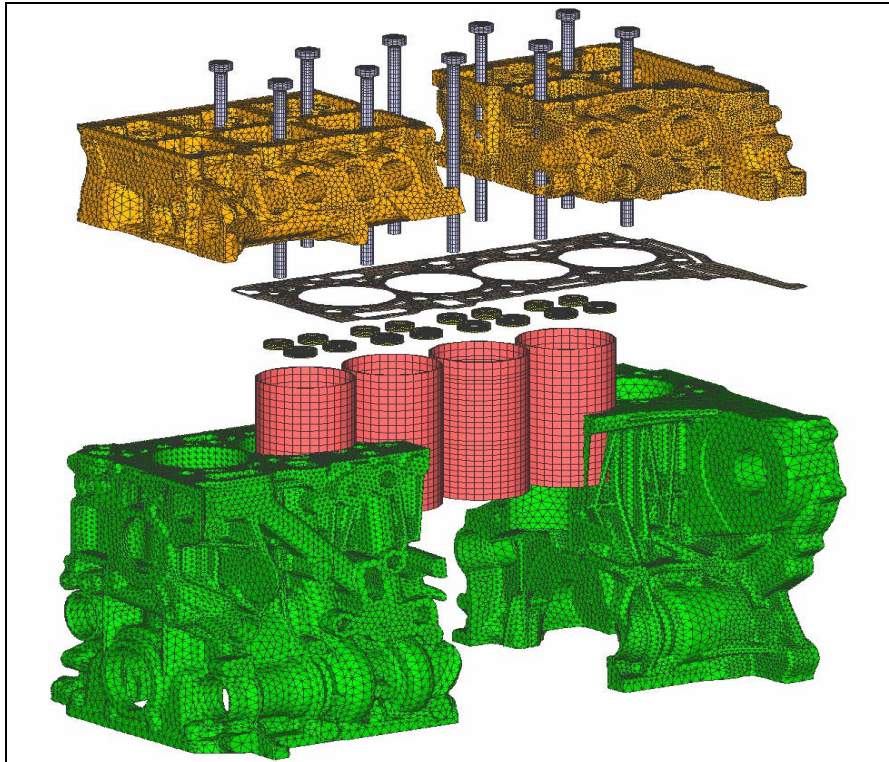
Based on the results of the study, following opportunities for improvement of the V.TRAPS tool are identified:

1. The ability to save the results of the V.TRAPS analyses was unavailable in ANSA v12.0.3 used for the study. This capability is currently added in ANSA version 12.1.0. However, the user should be able to save results in the V.TRAPS menu similar to cross section tool.
2. The bubbles and puddles/ponds identified in the analysis should be displayed in different colors for easy identification.
3. There should be a capability to add the drainage hole within the V.TRAPS menu that would avoid going back into the MESH menu every time the user creates a hole.
4. The capability to consider a welded flange (welded using traditional RBE2 elements) as "sealed" should be added in the future versions of ANSA. Currently, all the welded flanges need to be fused in order to prevent the fluid from passing through.
5. Fluid dynamics should be incorporated to further enhance the tool. For instance, the user should be able to calculate the time required to drain a puddle based on the volume of fluid, viscosity and other parameters. This time required to drain will help engineers to decide on the severity of the puddle and to design a drainage that is large enough to drain the liquid in time without jeopardizing structure integrity of the vehicle body.
6. ANSA V.TRAPS does not take into account the dynamic movement of the BIW through the bath. For example, the user can see the puddles created when the BIW comes out at an angle of 15 degrees. However, the BIW will come back to horizontal position after it comes out of the bath which results in the drainage of some of those puddles identified earlier. The above dynamics is not captured by the V.TRAPS tool and is a potential opportunity for improvement.

USAGE OF ANSA'S AUTOMATED VOLUME MESHING-METHODS IN THE RAPID PRODUCT DEVELOPMENT PROCESS OF DIESEL ENGINES

Günther Pessl*, Dr. Robert Ehart, Gerwin Bumberger
BMW Motoren GmbH, Austria

KEYWORDS - ANSA, CAE-Simulation, automated Volume Meshing, complete engine models, diesel engine



ABSTRACT - In order to stay successful in today's competitive markets, it is necessary to set high end standards in the product development process of diesel engines and it is also essential to reduce the development time of new products.

Despite a further increase of power and torque, the weight of the new 4 and 6-cylinder diesel engines of BMW has been significantly reduced and high quality and low emission standards have been achieved.

In this respect, state of the art CAE-simulation methods play an important role in today's development processes at BMW and therefore "New Automated Volume Meshing Methods of ANSA" are a milestone for rapid and successful application of the virtual product development.

Some years ago, it was not possible to create complete engine FE-volume models within a reasonable time range. Hand made meshes took up to 10 weeks of pure meshing time and thus model changes, design variants or optimization loops were nearly impossible to handle, because of the enormous time consumption. ANSA's new automated meshing methods allow an effective creation of complex volume meshes, e.g. for complete cylinder heads or crankcases models, within one or two days and so give a benefit of weeks to build up complete engine models.

As a result of this fast possibility to build up not only segment models but also complete simulation models, effects like global bending, non-uniform temperature distributions, a.s.o. could be taken into account for the numerical optimization of engine parts.

Finally these “New Automated Volume Meshing Methods” allow an effective and rapid virtual product development and guarantee excellent results in component durability calculation and quality despite of increasing engine power and weight reduction.

TECHNICAL PAPER -

1. INTRODUCTION

In order to stay successful in today’s competitive markets, it is necessary to set high end standards in the product development process of diesel engines and it is also essential to reduce the development time of new products.

Despite a further increase of power and torque, the weight of the new 4 and 6-cylinder diesel engines of BMW has been significantly reduced and high quality and low emissions standards have been achieved.

On the example of the New BMW 4 Cylinder Diesel Engine the usage of ANSA’S automated volume meshing-methods is shown on a overview of special applications. The experiences, advantages and benefits of the meshing functionalities in the rapid product development of our new diesel engines are presented on examples out of the complete range of FEM-simulation, like structural and fatigue analysis, optimization / morphing, dynamic & acoustic analysis and also CFD-analysis and CFD-optimization.

Usage of ANSA’S automated volume meshing-methods:

State of the art CAE-simulation methods play an important role in today’s development processes at BMW and therefore “New Automated Volume Meshing Methods of ANSA” are a milestone for a rapid and successful application of virtual product development. Some years ago, it was not possible to create complete engine FE-volume models within a reasonable time range. The former 2,5 cylinder models had a low level of details and discretisation:

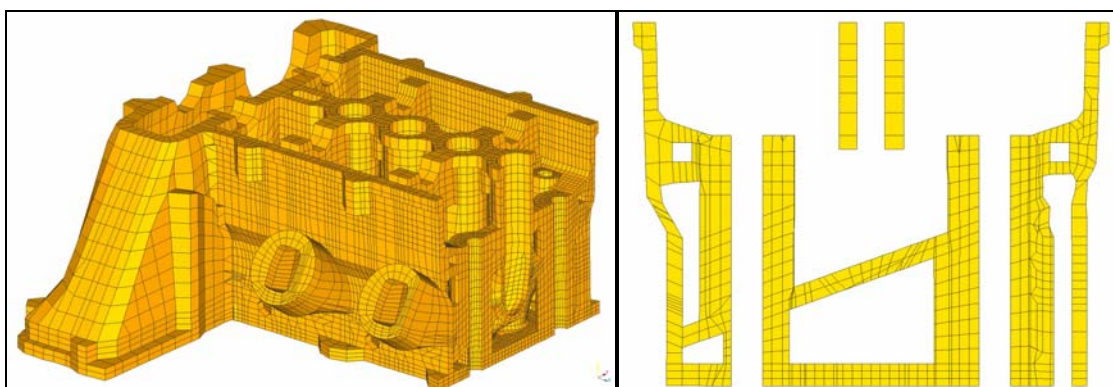


Figure 1: „manually“ created solid mesh

Hand made meshes took up to 10 weeks of pure meshing time and thus model changes, design variants or optimization loops were nearly impossible to handle, because of the enormous modelling time.

ANSA’s new automated meshing methods allow for an effective creation of complex volume meshes, e.g. for a complete cylinder head or crankcase model, within one or two days and give a benefit of weeks to build up complete engine models.

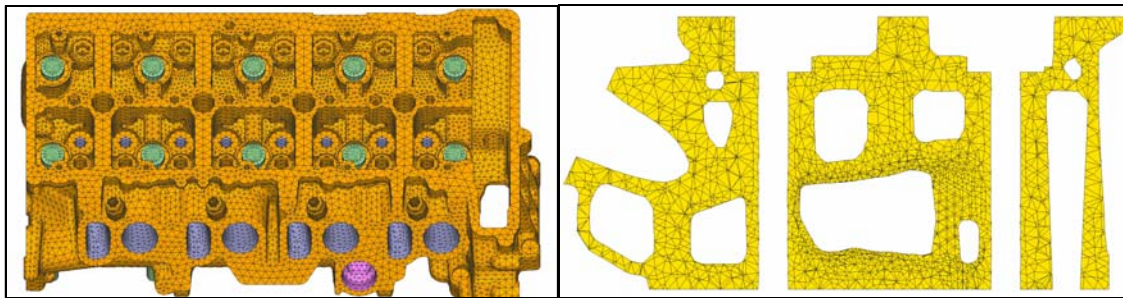


Figure 2: "automatically" created ANSA mesh

Using of ANSA's functionalities for the meshing process like, direct and part structured CAD import, geometry cleanup and surface improvement using macro create, element quality improvement using "RESHAPE" (with optimized reshape parameters), the local mesh refinement for critical areas and a finish element quality check of the volume mesh, gives us high quality meshes with a high level of details and discretisation within some hours or at maximum within some days.

As a result of this fast possibility to build up not only segment models but also complete simulation models, effects like global bending, non-uniform temperature distributions, a.s.o. could be taken into account for the numerical optimization of engine parts.

Complete engine model:

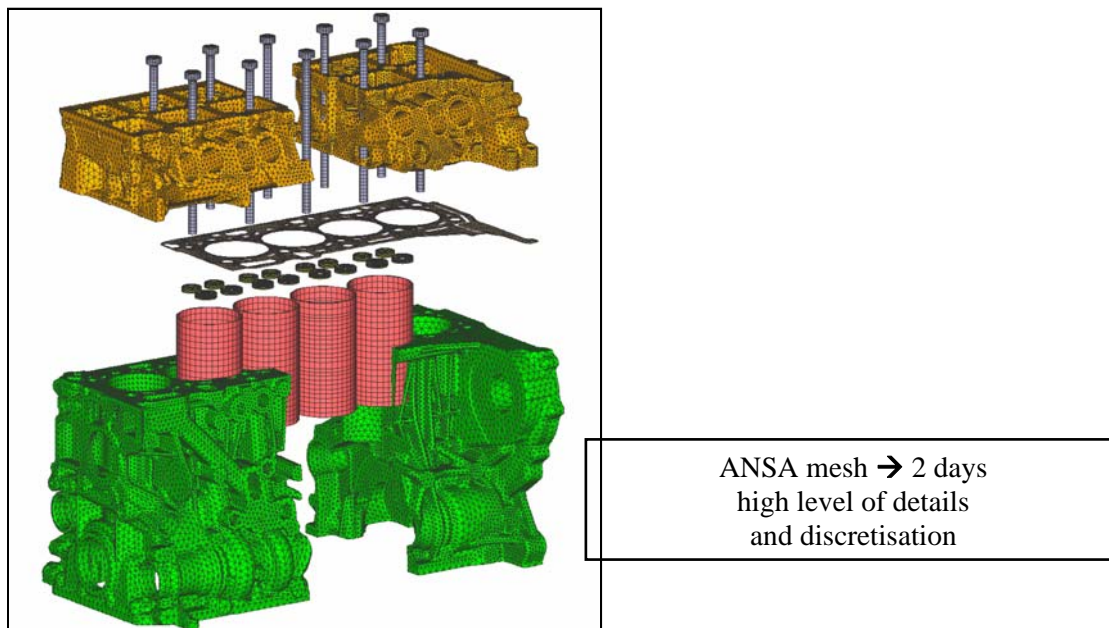


Figure 3 complete engine model:

One example of the big benefit of using complete engine models is the cooling flow optimization. A loop between 3D-coolant simulation in STAR CD and resulting heat transfer coefficients which are used for the thermal calculation in ABAQUS, provide us a non-uniform temperature field of the engine as basis for a cooling flow optimization with the target of reduction of the maximum engine part temperatures.

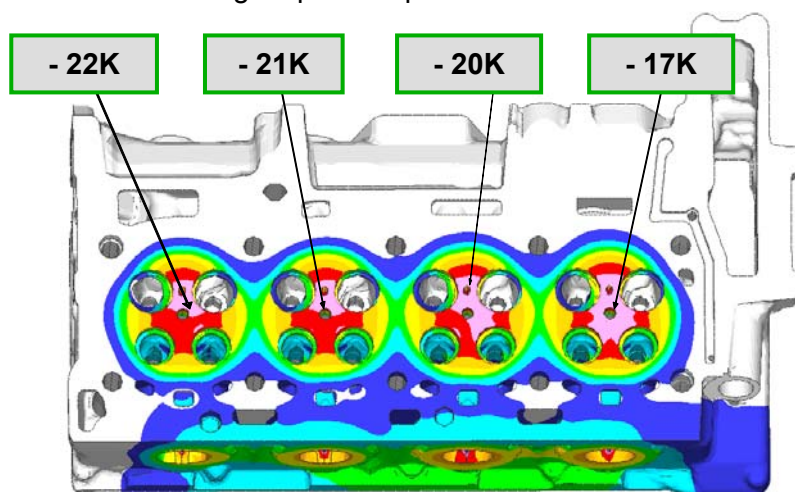


Figure 4: temperature optimization result

Using ANSA's new automated meshing methods more than 20 cylinder head optimization variants could be evaluated in the optimization process and the optimal design gives us an increased heat transfer coefficient of factor 3.5 in the critical areas and a benefit of more than -20K in the hot areas of the cylinder head. This optimized cylinder head water-jacket geometry is verified and measured in a lot of engine test runs and is now the basis for the New BMW-4 Cylinder Diesel Engine.

Submodel technique-fatigue analysis-optimization:

The complete engine model calculation, takes into account non-uniform temperature field, mounting loads (set rings, liners, pre-tension of the bolts) and the combustion load cases of each cylinder.

However, despite the excellent possibilities of ANSA to create highly efficient meshes with strong variations of mesh size dependent on the curvature, the global meshes are sometimes still have to be too coarse for a high precision fatigue analysis. In this case the sub-model technique of ABAQUS is an effective way to use very fine meshes for best discretisation to detect the critical areas of all engine parts.

Based on the global results of the whole engine model, which do not contain unrealistic boundary effects at cutting planes or symmetry faces (typical for only partial engine models), a submodel analysis can now be performed at any position of the analyzed engine. It is carried out by transferring the already accurate deformation-results of the global model to the boundary faces of the submodel. Similarly the temperatures are mapped to the complete submodel.

Based on the accurate stress distribution of the submodel mean-stress and stress amplitude are calculated and used for the fatigue analysis with FEMFAT (MAGNA). If critical areas are detected, use can be made of another feature of the submodel technique: providing a sufficient submodel size and as long as the global stiffness does not change too much, an optimization with TOSCA (FE-DESIGN) including several loops can be carried out purely on the submodel. As a consequence, no contacts and major nonlinearities like gaskets are contained in the model, which leads to a dramatic speedup in the FE analyses. For instance also the whole cylinder head can be used as a submodel with a very exact discretisation (extremely fine mesh for the water jacket) for fast, but highly accurate results. Of course, the final design has to be verified by a global analysis to get safe and robust engine parts.

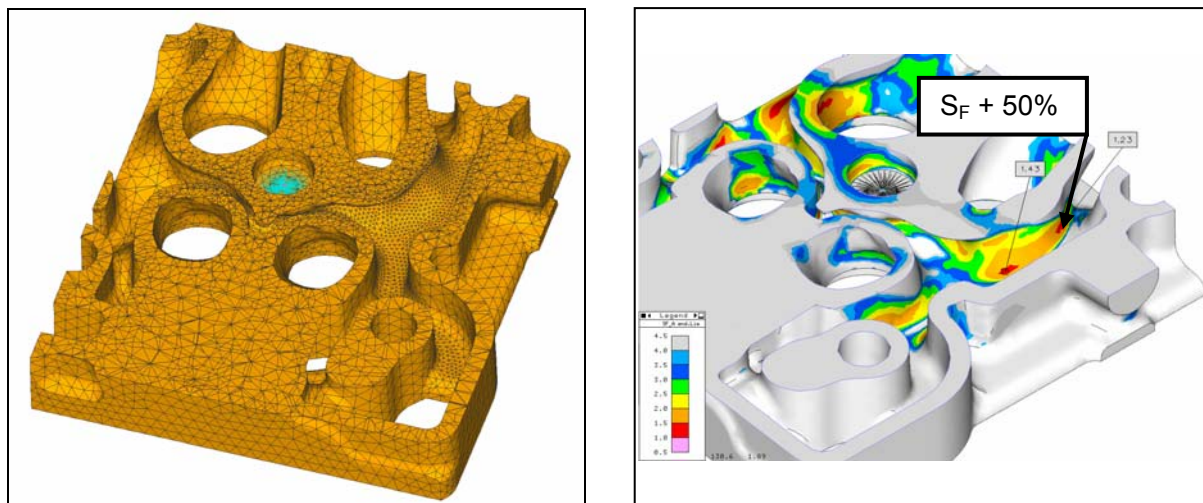


Figure 5: Submodel technique, TOSCA shape-optimization

Structural dynamics and acoustics:

In the years before "manually" created shell / solid meshes take an of the enormous time consumption of up to 12 weeks to get an acceptable dynamic-model of a power train-unit. Special transition elements between shell an solids had to be used for the connection and also the flexibility for changing engine parts or variants was low and spent a lot of time.

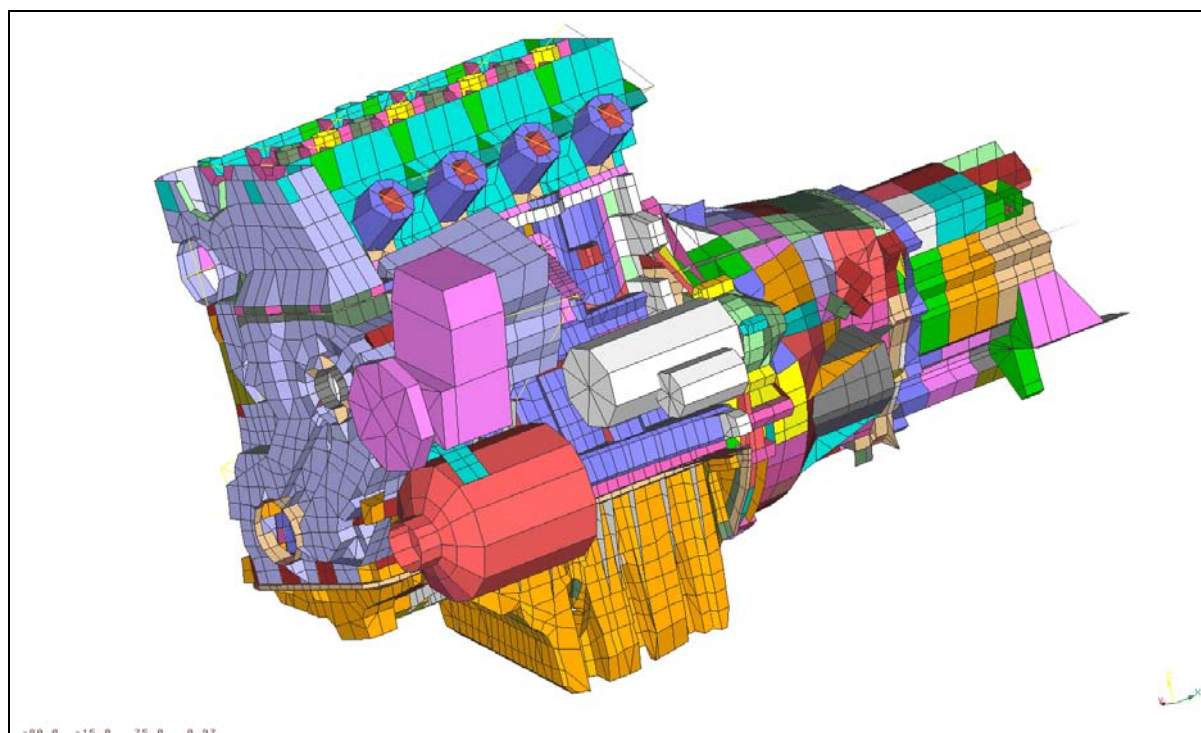


Figure 6: "manually" created shell / solid meshes

ANSA's new automated meshing methods gives an effective creation of all complex volume engine parts, a high flexibility for model changes, variants and optimizations. The complete meshing time for the a power train-unit will be reduced per factor 10!

To obtain a power train-unit model a lot of engine parts need to be modelled. When all the necessary machine elements are meshed with ANSA they are assembled using a separate Tool which allows a detailed modelling of all the screw connections which are holding the engine together. An according model of a 4 cylinder diesel engine is shown in the following figure.

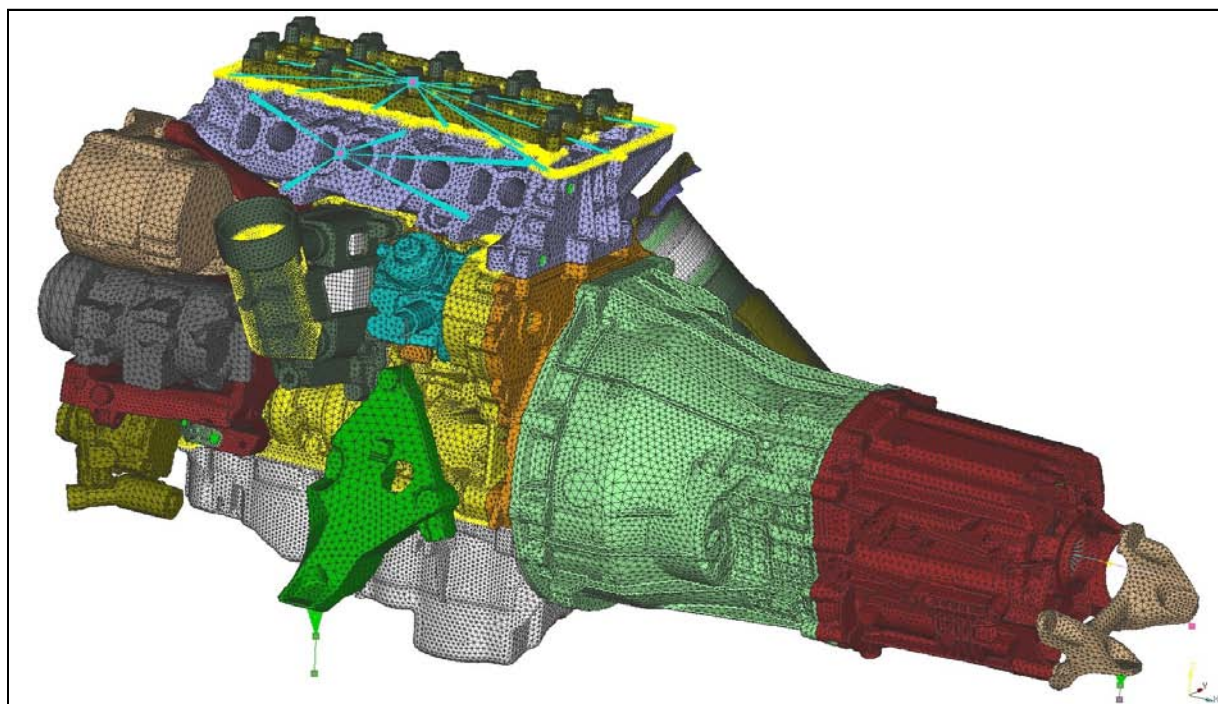


Figure 7: "automatically" created ANSA mesh

At the outset a normal mode analysis is performed. The global modes are of great interest in this respect to acquire the dynamic behaviour of the model. Based on the modal basis an engine speed-up run simulation is performed where the complete power train-Unit model is passed through the hole engine speed array.

The result of such investigations are Campbell-Plots which are a useful assistance to specify engine speeds where the acoustic behaviour of the corresponding engine is worth to be investigated more precisely. Finally a modal frequency response analysis for the selected engine speeds is conducted to get for instance, amongst others, the surface distribution of the structure-borne noise indicators.

ANSA-meshing methods for CFD analysis

Low meshing time and a high level of discretisation is necessary for accurate and fast results in the 3D-CFD-analysis. ANSA's CFD-mesh algorithm are used to define boundary layers on the surfaces for better discretisation, mixed elements (prism, tets, pyramids) for transition layer and quads (hexahedral elements) to fill the rest of the volume to decrease the degree of freedoms and to increase the calculation speed.

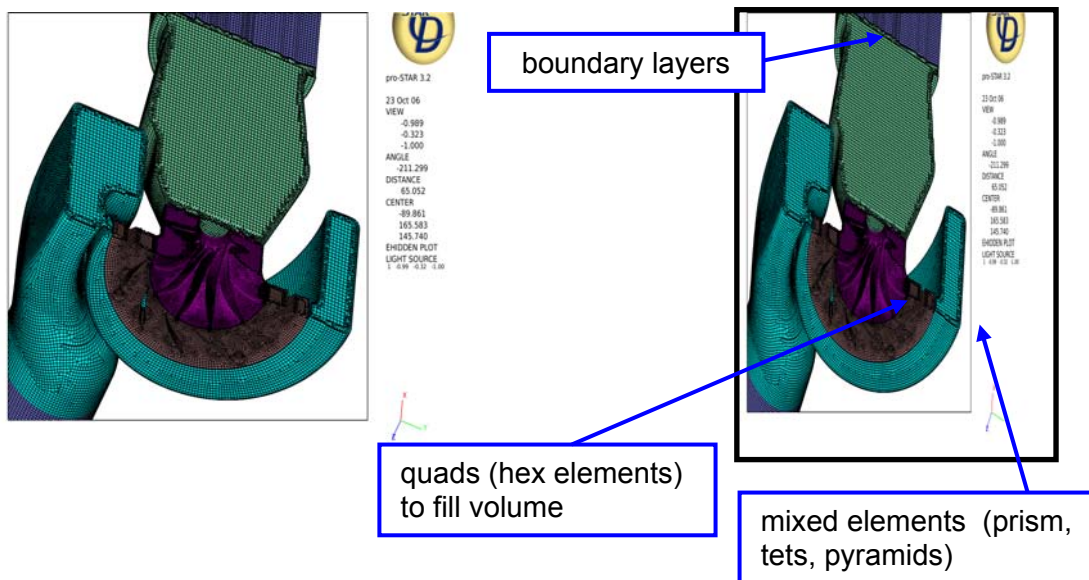


Figure 8: ANSA CFD -model

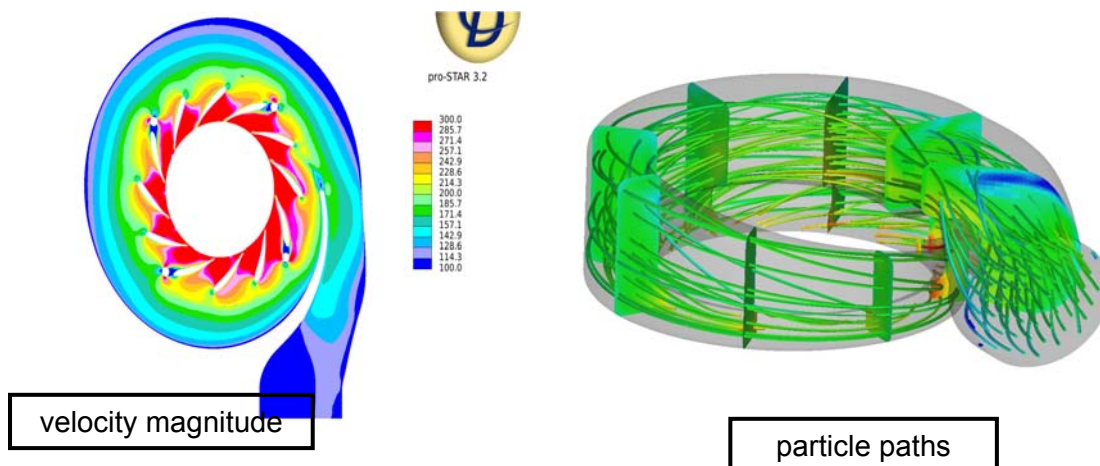


Figure 9: 3D-CFD analysis StarCD

Optimization using ANSA-Morphing:

Highly three dimensional effects of fluid dynamics leads the simulation engineer to the problem of a huge number of influence variations. An effective method of shape improvement is using the morph option in combination with an automatic optimization, e.g. modeFRONTIER. The ANSA morphing creates based on the parameterizes CFD-mesh (parameters are set on the edges of the morphing boxes) a huge amount of meshes with different geometries. All these geometries are automatically calculated in STAR CD and parallel evaluated by the free optimization algorithm in modeFRONTIER to reach the optimum target option.

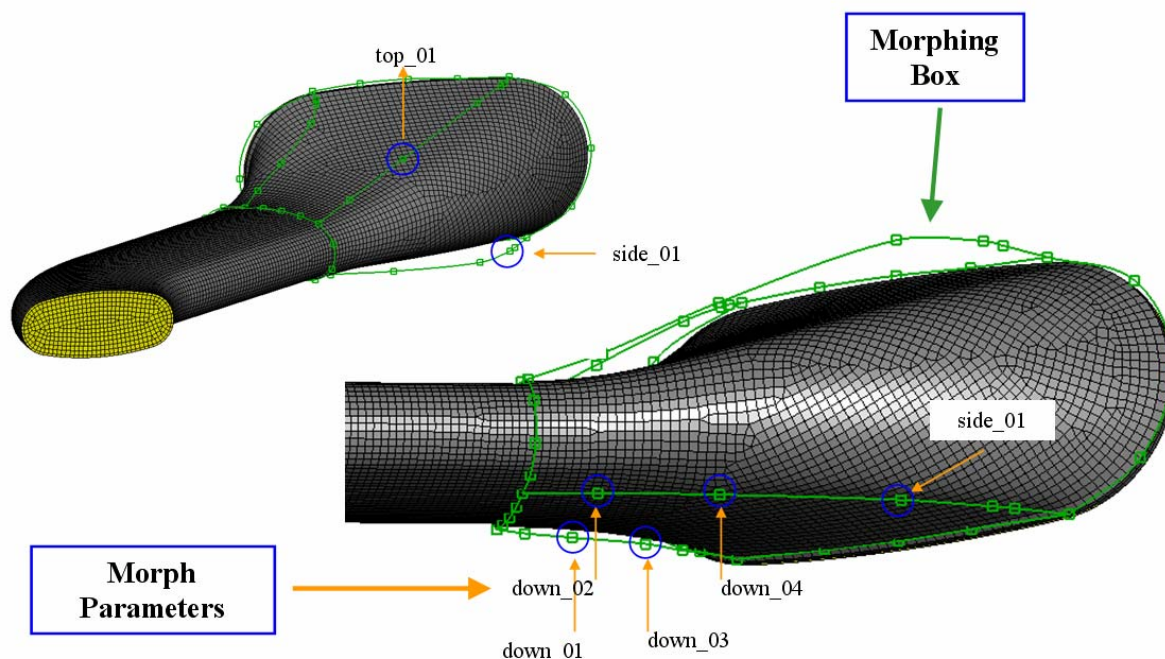


Figure 10: ANSA Morphing

In the current example an inlet to a catalyst is object of an optimizing, see figure above. For that purpose six morph parameters have been defined in ANSA, which can be modified in batch mode. Therefore you need an ANSA translation respectively a Session File. Important is of course to check quality of mesh, because there is a limit of morphing range. In modeFRONTIER a UNIX script in processing the necessary steps as follows:

- ANSA mesh loading
- Morphing with Output Parameters of Optimization (Target Options are Reduction of Pressure Drop and Improvement of Velocity Uniformity Index)
- CFD Simulation in STAR CD
- Determination of Input values for modeFRONTIER
- Definition of Output Parameters for ANSA Morphing

Mesh size is 250 000 cells and one optimization loop needs about 30 minutes (4 processors parallel). After 250 loops the run have been stopped and as result pressure drop and uniformity index were improved.

2. SUMMARY

ANSA is an effective tool for a rapid virtual product development process. Using the functionalities of ANSA gives a maximum reduction of meshing time and complex meshes with a high level of discretisation as guaranty for accurate and fast results. Model changes, design variants and optimization loops can be done in a rational time range of some hours or days. ANSA can be used in the complete range of FEM, like structural and fatigue analysis, optimization / morphing, dynamic & acoustic analysis and also CFD-analysis and CFD-optimization.

Finally these “New Automated Volume Meshing Methods” allow an efficient and rapid virtual product development and guarantee excellent results in component durability and quality despite increasing engine power and weight reduction.

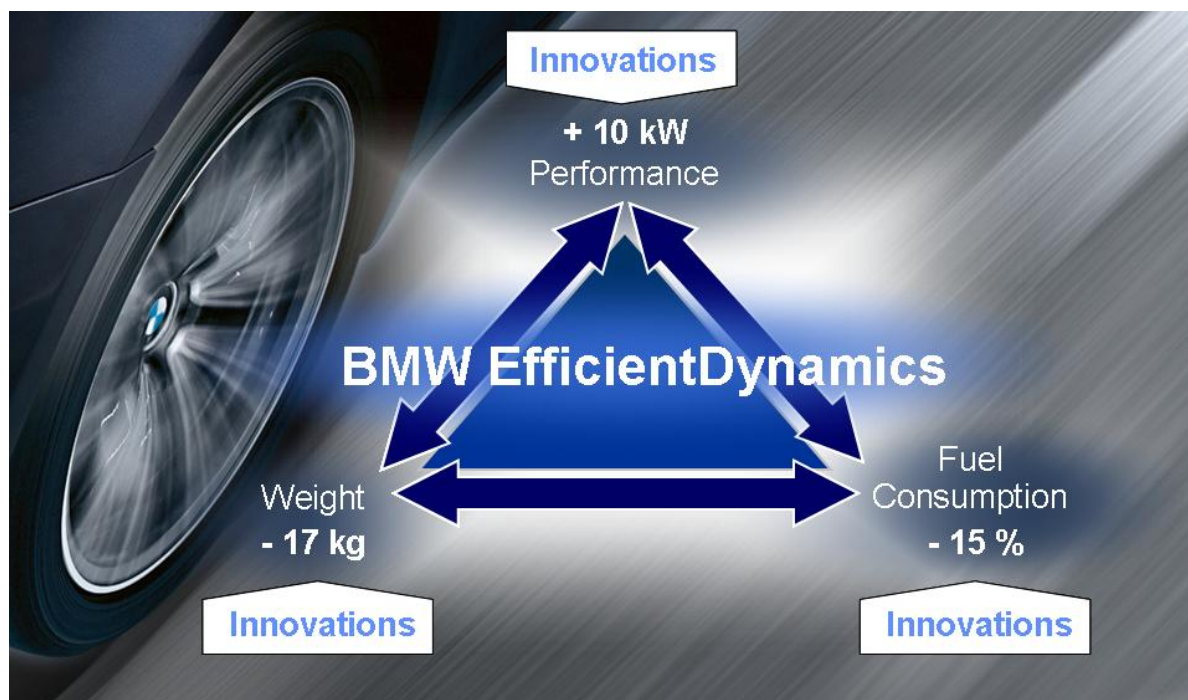


Figure 11: BMW efficient dynamics-The New BMW 4-Cylinder DIESEL Engine

REFERENCES

- (1) Ing. F. Steinparzer, Dipl.-Ing. W. Mattes, Dr. P. Nefischer, Dipl.-Ing. R. Wichtl, “The New BMW 2.0l 4-Cylinder Diesel Engine”, BMW Motoren GmbH Steyr, 2007
- (2) Dr. P. Nefischer, R. Kroiss, G. Winter, “Computer Aided Optimisation (CAO) for Spray and Combustion Simulation”, BMW Motoren GmbH Steyr, 2006

PRE-PROCESSING OF LIGHTING HEAT ANALYSIS AT VISTEON-AUTOPAL

Tomas Havlik*, **Roman Malucha**
Visteon-Autopal, Czech Republic

KEYWORDS - heat analysis, lighting, ANSA, script, I-Deas TMG/ESC

ABSTRACT - Software I-Deas TMG/ESC (hereinafter TMG) is used by Visteon-Autopal for the heat analysis of lighting. Ansa is used for pre-processing and TMG is used for following solving and post-processing. Script for acceleration work created in the TMG (hereinafter TMGscript) allows the fast setting of the complete process but it requires modifications of the script for each analysis, therefore Ansa scripting language (hereinafter Anscript) was chosen in preference.

The main function of Anscript is to transfer the FE model from Ansa to TMG and to pre-process the analysis. Anscript recognizes element property names which contain keywords for part names, materials, boundary conditions, etc., and accordingly, creates sets in Nastran deck and TMGscripts which use these sets. The transferring process is to run the TMGscripts created by Anscript which work with the FE model saved by Anscript as a TMG universal file.

The reason we use ANSA scripting language and not TMG scripting language is that Anscript is easier and based on language "C" which is found in most manuals. The process of transferring using Anscript, reduces the pre-processing time, simplifies model modification and eliminates mistakes made when setting boundary conditions and materials, manually. This procedure can be applied to any other software.

TECHNICAL PAPER -

1. INTRODUCTION

Visteon-Autopal is one of the leader automotive lighting companies. During development of last 10-15 years we could have seen quite significant changes – plastic materials mostly removed metal and glass material from lighting product by increasing of their heat resistance. And escalation of competition between lighting suppliers decreased time and cost for development as much as possible. Simulations happened important and necessary tool in supplier contest.



Figure 1 – History and present

2. HEAT ANALYSES

Heat simulation plays significant role in lighting product development. Components are under quite big heat load from operated bulbs. The trend in design points to using the smallest dimensions of lamp chambers with the highest wattage source because of more original appearance. More heat resistant but more expensive materials do not meet low cost requests. A few heat simulations have to be performed to find a compromise - optimal design and material in short time.

Heat simulation is necessary to perform during concept phase, when changes are easy to do. Bad concept could lead to the lamp that need not to meet customer requests (tests) and could increase overall cost. Lamp design is complicated and consist many design features and components that are not important from point of view heat simulation. So CAD data has to be simplified. ANSA provides us the performance that we need to build a high quality FE-Model in short time.

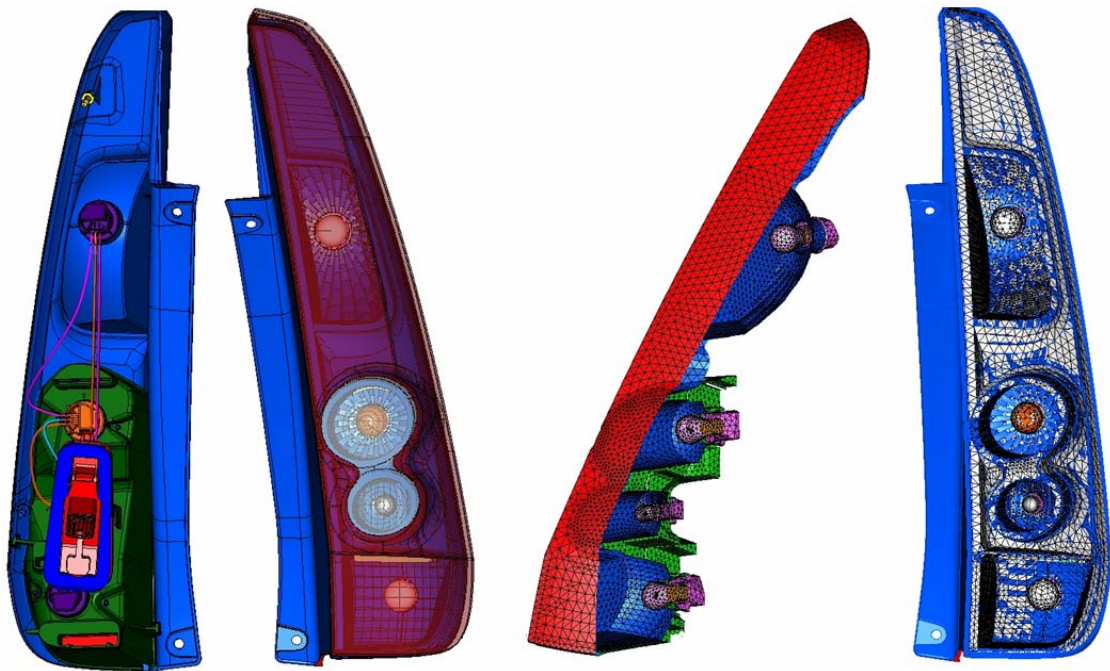


Figure 2 – CAD data to FE-Model transfer

TMG heat transfer solver can solve all three principles of heat transfer in automotive lighting – radiation, convection and conduction.

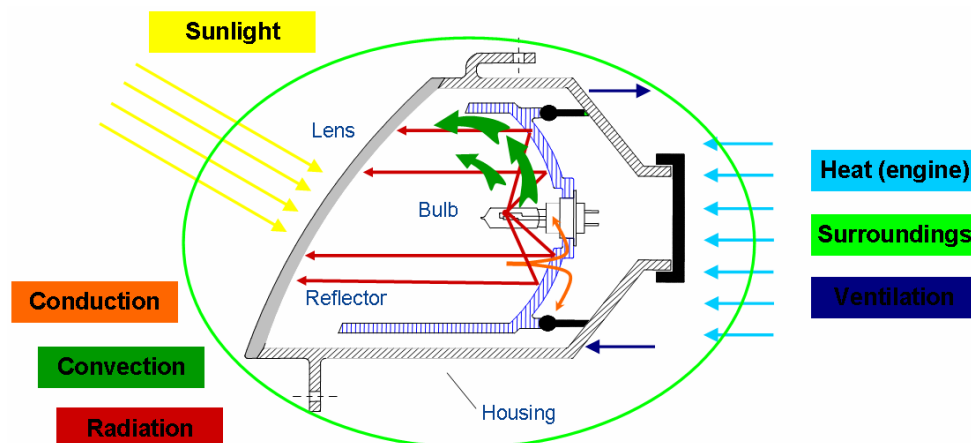


Figure 3 – Three principles of heat transfer in automotive lighting

3. PRE-PROCESSING

Ansa supports output of FE-Model to I-Deas universal format. Boundary conditions can be set in DECK>NASTRAN but TMG boundary conditions and materials are not supported. After FE-Model is done in Ansa, setting of boundary conditions and materials is made in TMG. This hand work can cause a lot of mistakes. For example you can spend time by setting materials in TMG and in the end of your work you find mistake so you repair the model in Ansa and set it again in TMG or you want do some modification. The same situation, you have to do settings all again. For that reason some automation is required.

First automation was made using the TMGscript. It used numbers of group (set in Ansa) and it was not user friendly language. When we wanted set TMG it took lots of time to change syntax of the TMGscript, but it allowed us further modifications of the model and eliminated mistakes. It was great start and useful for next automation process.

As a second automation we needed universal script which we didn't have to change for each calculation. As the best was Anscript. There is shown how we use Anscript in figure 4.

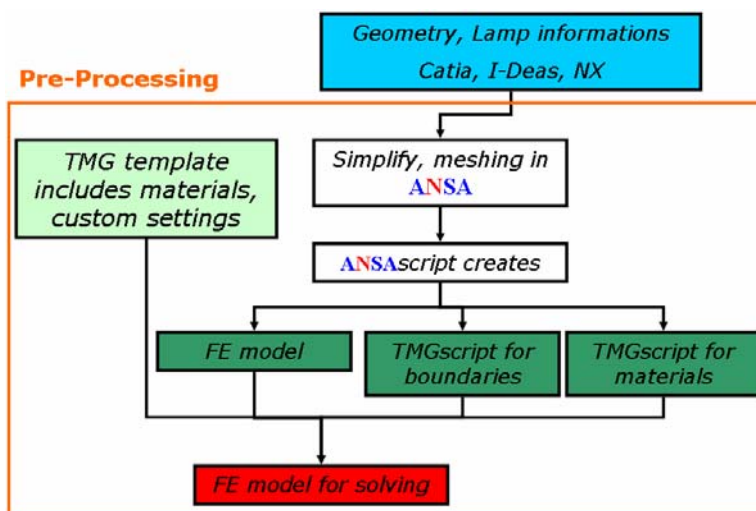


Figure 4 – Pre-Processing Heat Analysis

We have predefined template file with material library and custom settings. We start from that template and load FE model (File 1) which includes groups. After loading we execute two TMGscripts (Files 2, 3) for setting boundary conditions and materials. These three files are made by AnsaScript. AnsaScript works with property names (Figure 5).

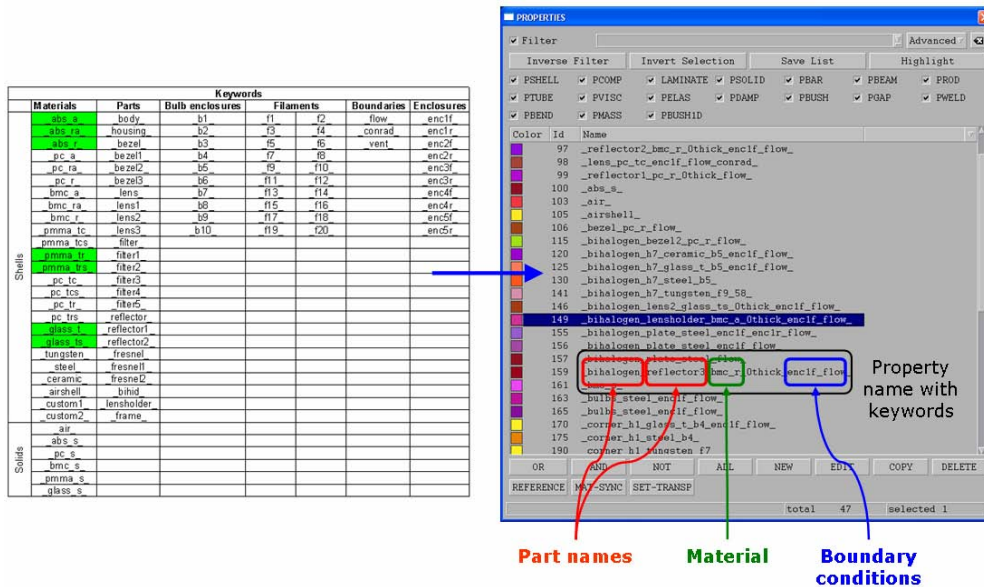


Figure 5 – Defined keywords

We defined keywords that we use for element property (PIDs) names. AnsaScript seeks for a keyword in PID name and creates set from all PIDs which includes this keyword in PID name. Simultaneously AnsaScript writes to TMGscript needed syntax. After AnsaScript seeks all keywords, TMGscripts are saved and FE-Model is saved to TMG universal file. For better orientation we separated material and boundary conditions settings to two TMGscripts. Function which creates set from all PIDs include keyword is in figure 6.

```

//Function for making groups according to parameters
-----
def MakeSetFromPid (string name,int id,string TypeOfElement)
{
    search_type[0] = "P" * TypeOfElement;
    pelements = CollectEntities(NASTRAN,0,search_type,0); //Collect all PSHELLS

    matrix wattages = {"3.0", "3.8", "5.5", "6.6", "8.26", "8.8",
                      "14.6", "17.8", "18.55", "18.8", "19.2", "19.4",
                      "21.24", "23.6", "23.9", "26.25", "26.5", "30",
                      "43", "58", "68"};

    k=0;
    watt = 1;

    foreach pelement in pelements
    {
        GetEntityCardValues(NASTRAN,pelement,"Name",prop_name); //get the name of each PSHELL
        ind = MatchString(prop_name,name); //check for the name that it was given as input
        if(ind)
        {
            foreach wattage in wattages
            {
                if (MatchString(prop_name, wattage))
                {
                    watt = wattage;
                }
            }

            to_set[k]=pelement; //Store the PSHELLS that contain the name
            k++;
        }
    }
    if(k==0)
    {
        Print("None");
        return 0;
    }
    search_type[0] = TypeOfElement;
    if (TypeOfElement == "CBEAM")
    {
        search_type[0] = "CBEAM";
    }
    elements = CollectEntities(NASTRAN,to_set,search_type,1); //Collect the shells that use the PSHELLS that were found
    set = CreateEntityVa(NASTRAN,"SET",name,"SID",id); //create a set
    AddToSet(set,elements); //Add to the created set the shells
    Print("Done");
    return watt;
}
-----

```

Figure 6 – Main function of AnsaScript

4. CONCLUSION

This process can be applied to any other software so in future we will use it for NX 5. Advantage of the Anascript is that it is based on language “C” which is found in most manuals. Using of the Anascript reduces time of Pre-Processing, reduces mistakes made by human and lets easy modifications and makes Pre-Processing more funny.

THERMAL JUDDER ON DRUM BRAKES DUE TO MOUNTED RADIAL RUN OUT

Danet Suryatama*, Robert P. Uhlig, , Satya Vallurupalli, , Robert M. Lundgren,
Frederick J. Zweng
DaimlerChrysler NA, USA

KEYWORDS - Judder, Drum, Brake, Thermal, Vibration

ABSTRACT - Brake torque variation is a phenomenon which induces seat, steering and body vibration on passenger vehicles these days. One form of the phenomenon is popularly known as brake judder. One root cause of the brake judder is the non-uniform radial thermal expansion of rear brake drums due to localized temperature increase, or known as hot spots. Non-uniform temperature distribution causes ovality which is a deformed oval shape of the circular drum rubbing surface. The ovality is measured as the Mounted Radial Run Out (MRRO) which is the difference between the longest and shortest drum expanding radii. The objective of this paper is to study analytically the generation and reduction of drum MRRO. ABAQUS code is used to analyze the MRRO finite element simulations while ANSA and μETAPOST are used to pre- and post-process simulation results. Explicit heat transient analyses will be selected to correctly predict the phenomenon. Simulation results will be plotted as graphs to illustrate the MRRO and probable deformation scenarios of brake drums. Various design parameters which are significant to reduce MRRO will be outlined. Dynamometer and on-board vehicle tests were conducted to verify the recommendations and benchmark the CAE results.

TECHNICAL PAPER -

1. INTRODUCTION

Frictional contacts between brake linings and rotors/drums will initiate temperature increase to cause thermal deformation. These deformations may induce the generation of disc/drum thickness variation (DTV) which in turn creates localized high temperature areas commonly known as hot spots. Various studies have been conducted to investigate hot spot generation. Experimental and analytical studies by Barber et al. (3) indicated that pressure variations could lead to localized contacts and hot spot generation that is commonly known as thermo elastic instability (TEI). TEI may cause material degradation, thermal cracking and unacceptable brake performance.

Analytical studies on the disk brake temperature prediction due to friction have been conducted as well. Barber et al. (4) studied thermo elastic stability problems and their implications to the design of brakes. Approximate solutions for transient thermo elastic contacts for uniform brake deceleration have been derived and presented. It was observed that depending on the speed of the deceleration, the time to develop hot spots could be different.

Numerically, hot spot investigation is more difficult to undertake. The analysis requires powerful computers and accurate numerical methods to simulate mechanical contacts between fast moving solids. To overcome the need for powerful computers, a combined analytical and numerical computation has been studied by Floquet and Dubourg (5,6). Their work combined fast fourier transform with the finite element method in order to predict transient temperature distribution during braking. The method basically predicted temperature fields on the disk brake and then applied the temperature loads to the rotor finite element model. The method predicted temperature distribution of a moving solid (i.e. the disk brake) under transient heat condition on a physically fixed disc brake finite element model. The temperature loads were then obtained by solving the boundary value problem using the

fast fourier transform technique (FFT). In this process, the thermal and stress analyses were uncoupled and thus, the effects of thermal deformation on the contact, which could affect the heat generation, were not taken into consideration.

To conduct numerical analysis studies on fast moving solids are very challenging and time consuming, requiring the use of high powered computational resources. The computation requires the use of non-linear mechanical approach that simulates non-linear contacts between finite element parts. The fast moving body contacts necessitate the implementation of small incremental iterations in order to guarantee a converged solution and thus, increase computational time considerably.

The scope of this paper is to give a close-up look on the development of brake judder prevention methodologies applied to brake drums. An overview of related brake judder analysis projects, conducted by the author at the Brake CAE and Brake Center of Competence of DaimlerChrysler, will be given. The project spans over a period of ten years which are divided into several stages. The first stage is the development of numerical methodologies to study brake thermal judder phenomena that cause hot spots. The next stage is the development of guidelines to reduce the sensitivity of mounted lateral run out (MLRO) on disc brakes under imbalanced brake bolt torques. The focus of this paper, which is the latest stage of brake judder study, is the development of methodologies to reduce thermal judder due to drum mounted radial run out (MRRO).

Computer simulation techniques derived from ABAQUS applications have been developed since 1997. These techniques implement 3-D brick, hexa finite elements to simulate - more accurately than the tetra or tria elements - frictional contact between discs, drums and their lining pads. The use of fully coupled, simultaneous heat transfer and stress analysis was incorporated. Both implicit and explicit procedures of ABAQUS/Standard and ABAQUS/Explicit were used to solve varieties of brake judder problems (7).

2. HOT SPOT AND THERMAL JUDDER MODELING

Finite element models of a disc brake and two lining pads were developed for this study. The FE models have boundary conditions to simulate fast moving bodies contacting each other. 8-noded solid elements with coupled thermal and stress characteristics were used. Boundary conditions were set up to model the spinning rotor as well as to allow deflection in the axial direction caused by bolt clamping forces. Localized bolt forces produced initial mounted disk run outs on the disk surface. Initial run out could also be generated by the presence of bolt torque variations.

Since the real brake system will undergo thermal and displacement loads simultaneously, coupled temperature-displacement solution was used. In this application, creep and swelling (i.e. structural thermal expansion) response can also be considered. However for our cases, the creep and swelling were negligible since braking only lasts for short period of time.

Four our case studies, the rotor and the pads were modeled realistically with the presence of fins. Thermal film coefficients, defined as the convection rate on certain surfaces, were used as well. The heat convection rates were obtained from the results of computational fluid dynamics (CFD) analyses, after simulating a similar disk brake subjected to certain braking conditions. By using thermal convection rates for the finite element analysis, a link-up between CFD and thermal conduction simulations were developed. The thermal convection rates were difficult to determine or measure.

Realistic braking speed and conditions were also simulated. The brake spinning speed was calculated by taking into account tire and disk brake/rotor radii. The pad pressure loads were applied to the brake by applying the piston into the backing plate of the pads. In turn, the pads clamped the rotor to generate friction. By modifying the pad pressure, several braking

scenarios could be simulated. Constant pad pressures reflected drag braking conditions while variable pad pressure may reflect deceleration, brake fading or snub braking scenarios.

3. CASE STUDIES FOR DISC THERMAL JUDDER

Various case studies were performed for our brake thermal judder models. A model consisting of brake disc and lining assemblies is shown in Figure 1. These models were run to simulate actual disc spinning and braking with a constant speed of 30mph. Correlation runs were conducted to see the accuracy of the temperature increase with dynamometer tests. Figure 2 shows the temperature increase prediction of FEA models with dynamometer results.

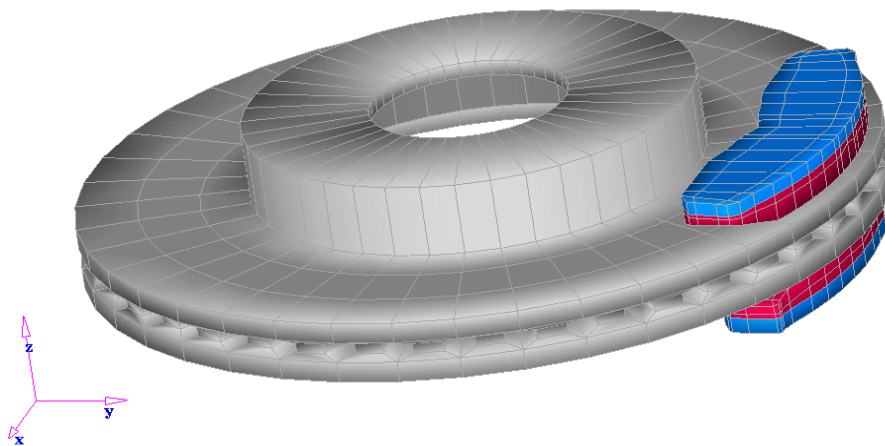


Figure 1. A 15-inch rotor/disc drag braking/correlation study

The following scenarios were applied to the brake model shown in Figure 1. The discs were subjected to a drag braking with constant speed of 60mph for 0.825 sec with a 100psi pad pressure. The lining pad coefficient of friction was 0.34 and the disc initial temperature was 93°F. The temperature plot after the simulation is shown in Figure 3. As expected, the disc rub track surface does not show any hot spot generation as the disc rub track surface was modeled to be flat and smooth.

Temperature (°F)

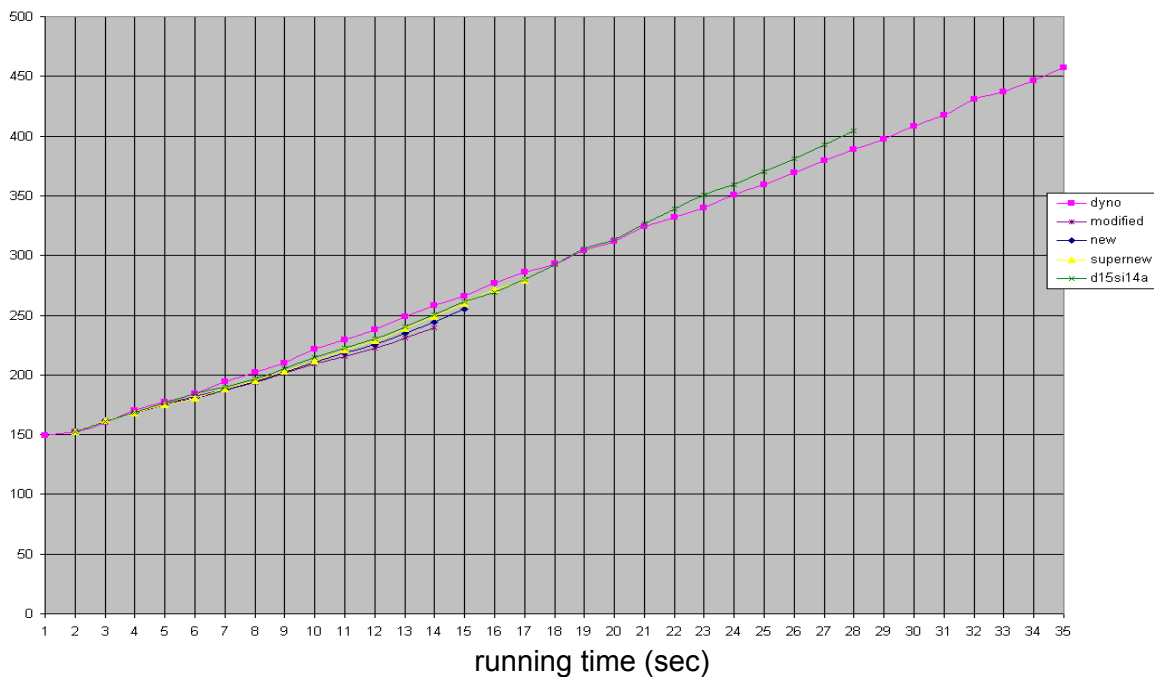


Figure 2. Correlation Results between FEA Models with Dynamometer Tests

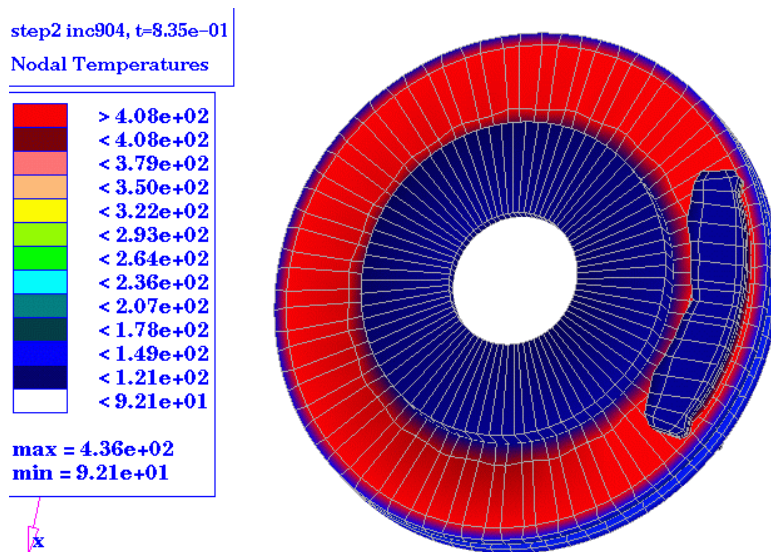


Figure 3. Final Temperature Plot for Smooth Rub Track Surface

To show the presence of DTV, a similar model was modified to include disc thickness variations (DTV) on its rub track. The disc was subjected to a constant drag braking of 60mph speed with less than 100psi lining pad pressure. The following Figure 4 shows the final temperature plot of the disc with hot spots are shown on the disc rub track.

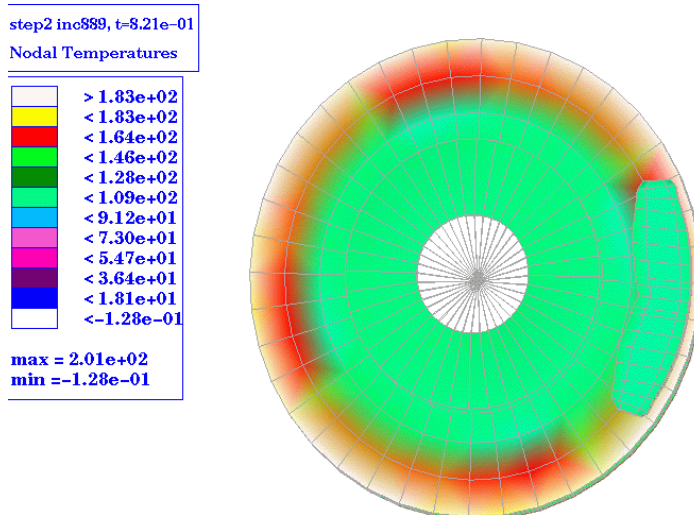


Figure 4. Final Temperature Plot with Hot Spots Shown on the Disc Rub Track

To realistically model brake mounted conditions on vehicles, several runs that showed the presence of imbalanced brake torque were performed. A model that includes a wheel, disc, lining assembly and hub is shown in Figure 5. The model was subjected to bolt torque variation due to un-tightened bolts or imbalance bolt torque. In this case, there were two loose bolts located next to each other. The plot with the presence of hot spot is shown in Figure 6.

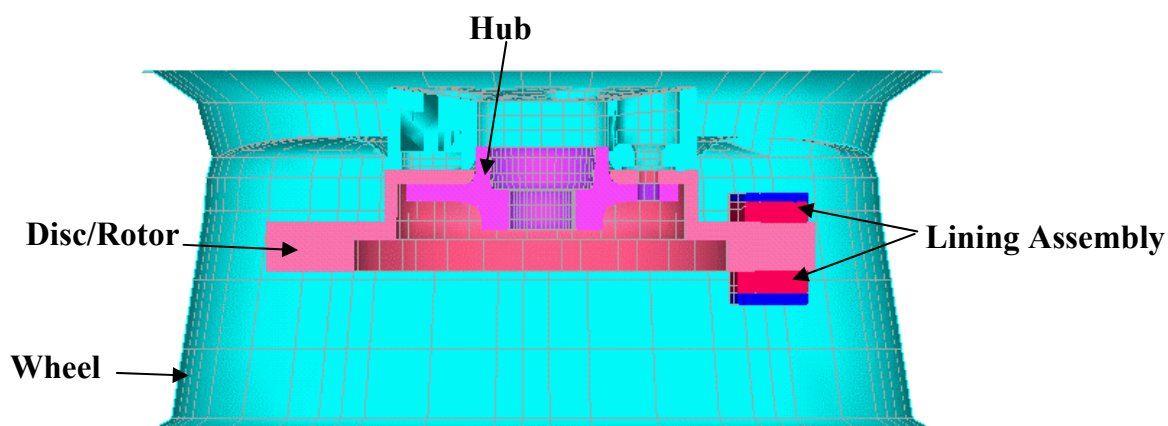


Figure 5. A Wheel, Disc, Hub and Lining Pad Assembly for Hot Spot Modeling

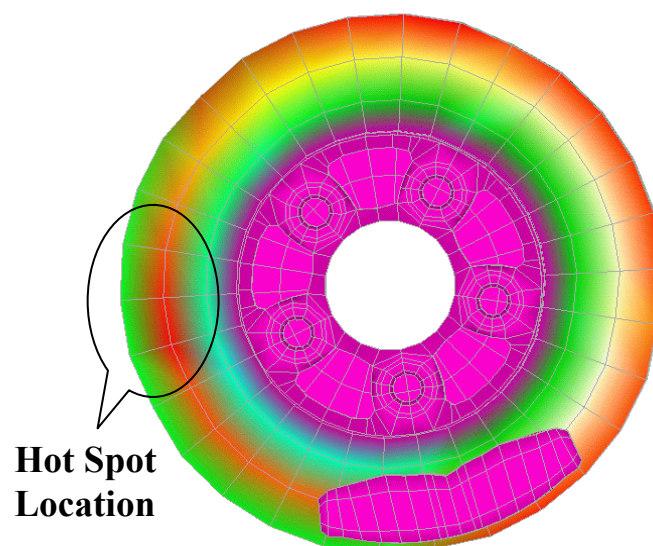


Figure 6. DTV on the Disc Rub Track Showing Hot Spots due to Imbalanced Bolt Torques

In summary, there is a significant correlation between DTV and the generation of hot spots. DTV induces hot spots and the resulting vibration is translated to the driver as the brake pedal pulsation, steering shake, seat or body vibration. Factors that initiate DTV were identified in this study as the initial run out or mounted lateral run out (MLRO) of the disc brake. Lateral run out (LRO) can be triggered by several parameters which are shown in the next stage of our study.

4. MOUNTED LATERAL RUN OUT (MLRO)

In this study (1), a phenomenon - identified as the primary contributor of disc thickness variation (DTV) - was explored. Mounted Lateral Run Out (MLRO) is the main generator of DTV which may cause hot spots and subsequently brake judder. Brake judder is a complex phenomenon in which factors such as, vehicle sensitivity, brake torque variation, caliper slide force, running clearance/rollback, lining material and primarily MLRO sensitivity play significant role in DTV build up which causes brake judder.

A wheel joint configuration, consisting of a wheel, rotor/disc and hub, is shown in Figure 7. When the parts were mounted on a vehicle before wheel lug nuts were tightened, the wheel joint showed no deformations as shown in the figure. Subsequently, once the lug nuts were tightened, the clamping forces exerted on wheel joint parts and especially on the disc would create waviness as shown (as an exaggerated FEA deformation plot) in Figure 8. Mounted Lateral Run Out is measured in μm as a distance between the highest to the lowest point of the disc rub track surface or, as can be seen on the plotted graph of Figure 8, as the distance between the crest and the bottom of the curve.

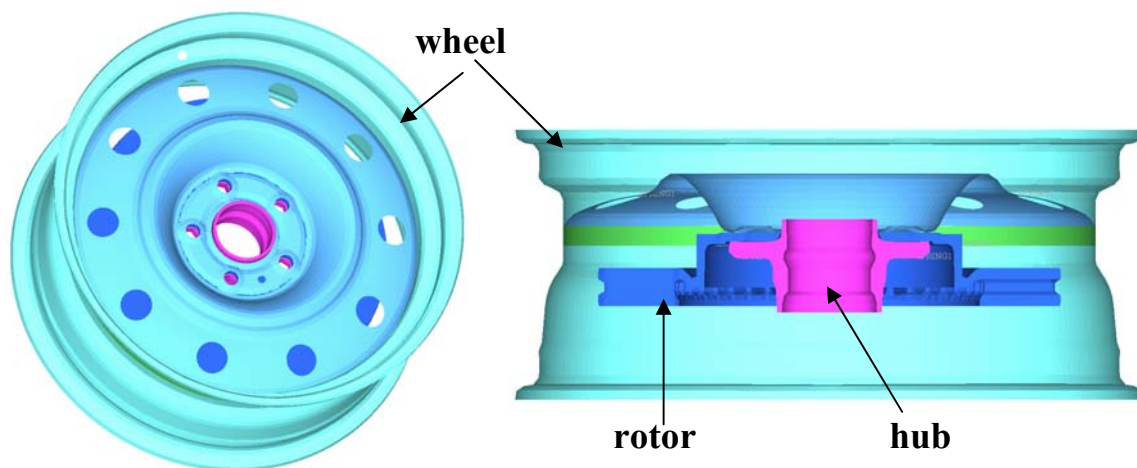


Figure 7. Wheel Joint Configuration

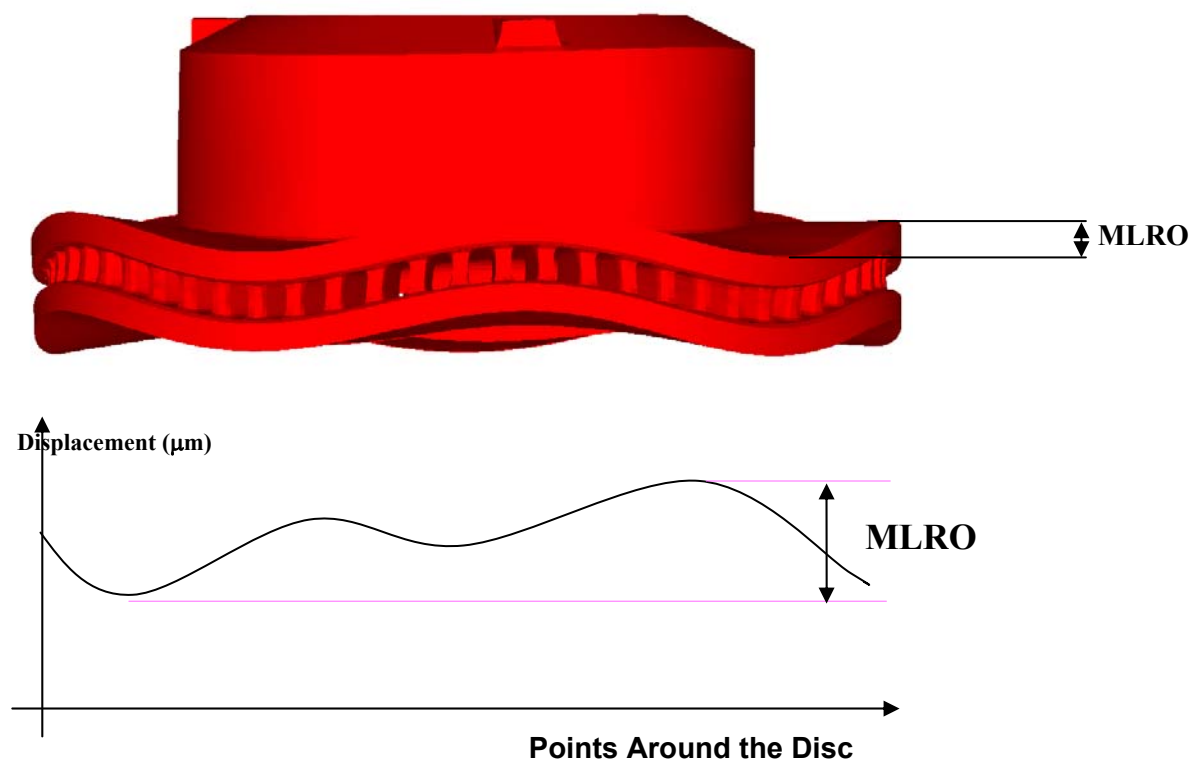


Figure 8. Mounted Lateral Run Out (MLRO) Measurement

Several wheel joint design parameters were investigated to understand their effects to induce MLRO. Wheel step height, wheel mounting pad styles, bearing hub flange thickness, annular groove in the bearing hub flange, wheel to hub flange load path and wheel stiffness were the design parameters identified to be investigated.

A detailed discussion on CAE methods and results of this study can be seen in reference (1). A conclusion was inferred that the most dominant parameters were the wheel step height and the wheel mounting pad styles. Other parameters may still give certain effects on MLRO, however their significance were less dominant than the first two parameters. These design

parameters may be balanced with other performance objectives to give an improved wheel joint overall system characteristic beyond LRO sensitivity.

5. MOUNTED RADIAL RUN OUT (MRRO) ON BRAKE DRUMS

Brake drums, now commonly used as rear brakes (see Figure 9), may experience several performance issues with regards to groan, moan, squeal noise, and roughness/judder. Comprehensive design considerations taking into account the generation of the above performance issues will satisfy the required brake service requirements during brake operational life. In this study, the issue of drum thermal judder due to the roughness on its rub track was investigated. These issues are very common due to the characteristics of a relatively thin rub track sectional width on brake drums (see Figure 10).

To get a clear understanding, drum mounted run outs are measured in the radial direction of the axis or perpendicular to the brake/vehicle axis direction, as shown in Figure 11. It is called the mounted radial run out (MRRO) as compared with the brake disc MLRO. The MRRO is measured as the difference between the deformed maximum (R_{max}) and minimum radii (R_{min}).

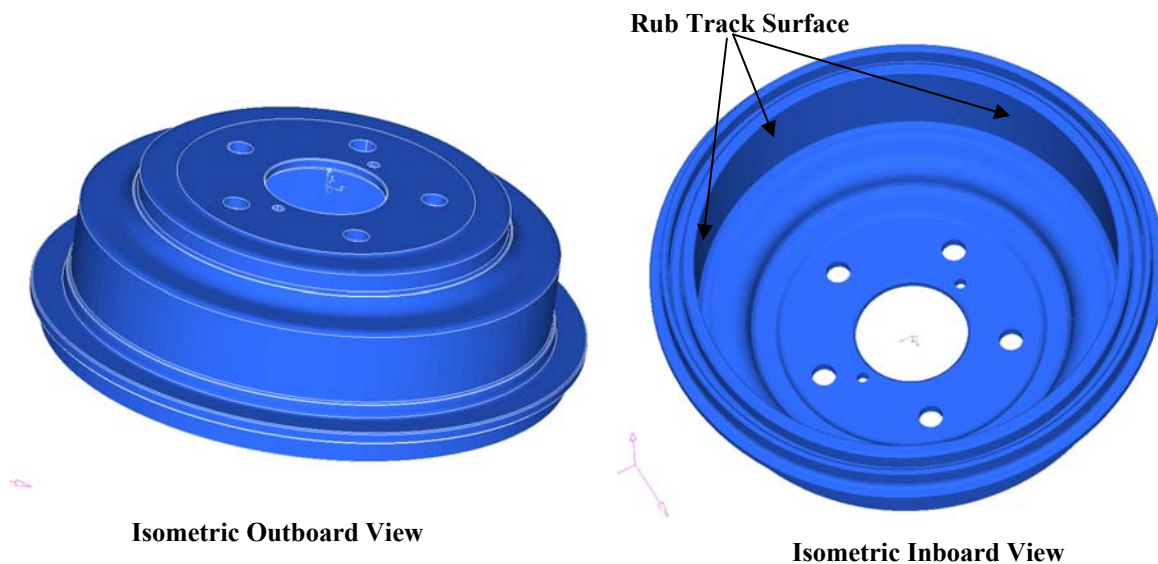


Figure 9. Outboard and Inboard Views of Brake Drums



Figure 10. Sectional View of a Brake Drum

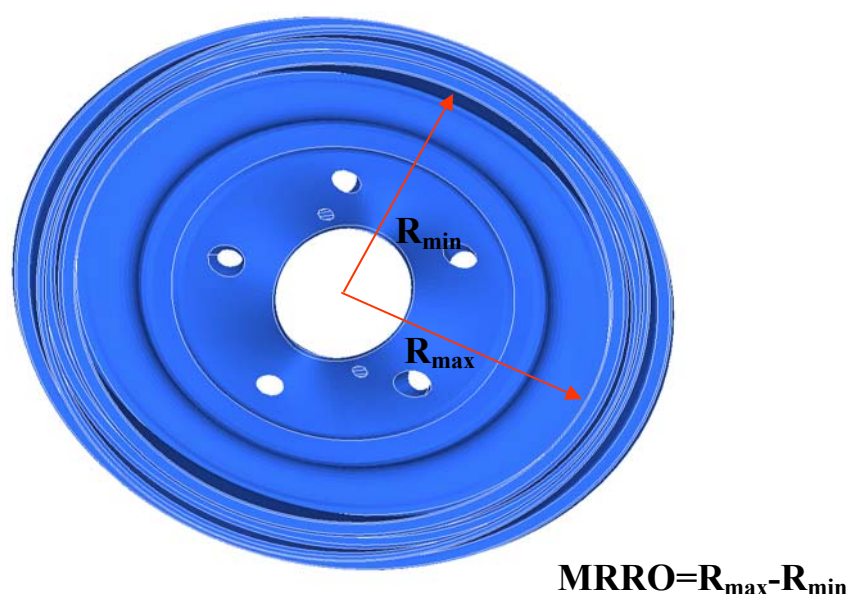


Figure 11. Ovality and Mounted Radial Run Out (MRRO) Measurement

In the case of disc brakes, the lateral run out, i.e. the mounted lateral run out (MLRO) will have to induce disc thickness variation (DTV) before causing hot spots to trigger brake judder. For drum brakes however, uneven temperature increase does not need to cause drum thickness variation (DTV) before causing hot spots and brake judder. The frictional temperature increase can directly cause radial run out and trigger brake roughness/judder.

6. DRUM JUDDER MODELING

The coupled transient temperature and displacement environment in ABAQUS/Explicit (7) was selected for our CAE cases. The consideration was based on the capability to couple stress/displacement and thermal analyses as well as to create efficient runs for our models. Temperature loads were non uniform temperature variations distributed along the drum's rub track section. MRRO's were then measured from the deformed/displaced position of nodal points along the rub track section. Our solutions rely primarily on optimizing brake drum geometrical, dimensional and material properties in order to reduce MRRO's. ANSA and μETAPOST, due to their capabilities to analyze ABAQUS/Explicit problems, were used as the primary pre- and post-processor tools for these applications.

Design Type	Damped Iron (μm)		Gray Iron, 30 (μm)	
	Edge	middle	Edge	middle
Baseline	39.1	22.8	29.98	20.92
Iteration 1	18	11.3	20.23	10.8
Iteration n+1	36.2	17.8	28.3	18.4
Final Design			12.8	6.1

Table 1. MRRO Results of Brake Drum Thermal Judder Analyses

The focus of the study was to reduce MRRO's on both the opening and the middle section of the rub track. Two material properties were considered, damped and gray iron materials. From Table 1, the baseline designs which create thermal judder issues have relatively unacceptable MRRO values of 29.98 μm on the rub track's edge/opening and 20.92 μm on the middle of the rub track for gray iron drums. After various iterations, the final design could reduce the edge and middle section MRRO by more than 50%. The edge section MRRO went down to 12.8 μm (53% reduction) and the middle MRRO was 6.1 μm (71% reduction). The optimized design had a mass increase of 29% over the baseline design. It was the smallest mass increase compared with other design iterations.

7. CORRELATION TESTS

Several brake dynamometer and on-board vehicle tests were conducted by our supplier TRW to verify the CAE findings. The drums with our final design were tested to investigate any reductions or increases in vehicle responses due to judder or torque variation inputs. Dynamometer test results showed 300% lower 2nd order torque variation of the optimized final design drum compared with the baseline/production drums. The 1st order torque variation was also lowered for the final design even though it was not as significant. The final design also showed lower brake accelerations in vertical and fore-aft directions. TRW also conducted on-board vehicle tests to one of the proposed designs and showed significant reduction of steering nibble, vertical seat, vertical axle and fore-aft accelerations.

8. CONCLUDING REMARKS

A review of a ten year project to investigate the generation of thermal judder and its influence to vehicle shake and vibrations was presented. The findings identified that thermal judder on the brake discs and drums were significantly influenced by run outs. For disc brakes, the run out (MLRO) indirectly affects thermal judder through DTV and hot spots generation. For the drum brakes however, the run out induces MRRO directly (without the need to create thickness variation) due to the relatively large oval deformations of the brake drum rub tracks.

Thermal judder is a major contributor to vehicle torque variations which can translate into seat, steering and axle accelerations. A comprehensive design approach should be conducted for vehicle design and engineering to account for the generation and translations of brake judder as well as for the response to the vehicle body or chassis.

REFERENCES

- (1) Burns, R., D. Suryatama, P. McCormick, P. Stoloff, "Wheel Joint Analytical System Approach to Evaluate Brake Rotor LRO Sensitivity Effects", Brake Colloquium, SAE International, October, 2007.
- (2) Suryatama, D., D.J. Stewart, S.C. Meyland, L.J. Hou, "Contact Mechanics Simulation for Hot Spots Investigation", SAE 2001 World Congress, Detroit, MI, March 5-8, 2001.
- (3) Lee, K., and J.R. Barber, "An Experimental Investigation of Frictionally-Excited Thermoelastic Instability in Automotive Disk Brakes Under a Drag Brake Application", Journal of Tribology, Vol. 116, pp. 409-414, 1994.
- (4) Barber, J.R., T.W., Beamond, J.R. Waring, C. Pritchard, "Implications of Thermoelastic Instability for the Design of Brakes", Transactions of the ASME, Vol. 107, pp. 206-210, 1985.
- (5) Floquet, A. and M.C. Dubourg, "Nonaxisymmetric Effects for Three-Dimensional Analysis of a Brake", Journal of Tribology, Vol. 116, pp. 401-408., 1994.
- (6) Floquet, A. and M.C. Dubourg, (1996), "Realistic Braking Operation Simulation of Ventilated Disk Brakes", Journal of Tribology, Vol. 118, pp. 466-472, 1996.
- (7) Anonymous, ABAQUS Version 6.5 Online Documentation, Abaqus, 2005

Session H2.7

THE DEVELOPMENT OF THE 2007 FORMULA SAE BY THE ART-7 TEAM

Dimitrios Perperidis*

Prepared by the ART-7 team members¹

KEYWORDS -

ABSTRACT - In September 2007 a formula student team, named ART-7, has been established by students of the Department of Mechanical Engineering of the Aristotle University of Thessaloniki. The main goal of this team is to design and build a formula SAE type race car and to participate in the Italian event that is going to take place in 21-23 September 2007 in the Fiorano Ferrari race track.

In this presentation the Formula SAE event, the scope and procedure of the race and finally the criteria that have to be met are outlined at first.

Next, the choice of the basic design parameters is shown. Suspension, steering and braking systems are described. The analysis of the chassis space frame and the heavily loaded components, such as the wheel uprights, the wheel hubs and the differential arms has been carried out under several driving conditions. Pre- and post-processing have been carried out using the ANSA and μETA software of BETA CAE Systems S.A..

The presentation concludes with an update of the current preparation status.

¹. The ART-7 team consists of : Assoc. Prof. A. Mihailidis (faculty advisor) and the following members: G. Fontaras, G. Karaoglanidis, I. Nerantzis, (PhD students) and I. Aslanidou, V. Bitsanis, I. Bosdas, L. Kozas, I. Nasiopoulos, G. Pappas, D. Perperidis, G. Simos and N. Tsoukala (undergraduate students).

